Higher-Order QCD Corrections to Jet Production in Deep Inelastic Scattering

---

Dissertation

zur

Erlangung der naturwissenschaftlichen Doktorwürde
(Dr. sc. nat.)

vorgelegt der

Mathematisch-naturwissenschaftlichen Fakultät

der

Universität Zürich

von

Jan Moritz Niehues

aus

Deutschland

Promotionskommission

Prof. Dr. Thomas Gehrmann (Leitung der Dissertation)
Prof. Dr. Massimiliano Grazzini
Prof. Dr. Ueli Straumann
Dr. Katharina Müller

Zürich, 2017

Contents

1 Introduction

At the lepton-proton collider HERA formerly based at DESY in Hamburg, two experiments, H1 and ZEUS, collected a very precise data set on deep inelastic scattering (DIS) events for a variety of final states [1, 2]. Lepton-proton collisions provide a clean probe of the proton and allow the proton's substructure to be studied precisely in high-energy experiments. To this end, information on the distribution of partons inside the proton and the value of the strong coupling constant α_s can be readily extracted from final states containing jets. Precise knowledge of both quantities is crucial for theoretical predictions used to perform consistency tests of the Standard Model or in searches for physics beyond the Standard Model at the LHC or any future collider. Currently, the value of $\alpha_s(M_Z)$, however, is one of the least known Standard Model parameters. Single-jet and di-jet cross sections have been precisely measured by the H1 and ZEUS collaborations in the Breit frame [3–14], where jet cross sections are sensitive to the value of α_s and to the proton's gluon distribution already at leading order. Jet production cross sections are thereby less sensitive to multiple radiation effects than other observables and can be well described by fixed-order predictions in QCD. The importance of jet production processes has long been known, but confronting the data with relevant hard coefficients evaluated only to next-to-leading (NLO) order in the coupling constant [15–18] could not exploit the full physics potential of the precision measurements. The H1 and ZEUS experiments also measured jet production in diffractive scattering [19–24] that form a subset of the recorded jet events. In diffractive scattering, the proton remains intact after the collision and a theoretical description of diffractive collisions requires the knowledge of quark singlet and gluon distributions with vacuum quantum number inside the proton [25]. Currently, these distributions are only determined to NLO QCD accuracy. In the past, the recorded diffractive events have also been confronted with predictions to extract the value of the strong coupling $\alpha_s(M_Z)$ to NLO QCD accuracy in the strong coupling constant [26].

Electron-positron colliders provide yet another class of high energy experiments. One such experiment, LEP, was based at CERN and another one, SLD, at the Stanford Linear Collider (SLC). Both experiments collected a wealth of precision data on jet cross sections and event shape distributions [29–33]. Precision studies of these data included establishing the gauge group structure of QCD, measurements of the strong coupling constant and investigations of the all-order structure of large logarithmic effects in QCD [34]. Similar to jet cross sections in DIS, most of the original LEP and SLD studies were based on the then available NLO theory predictions for event shapes and cross sections [35–37].

In recent years, owing to the methodological advances in the calculation of two loop amplitudes [38–40] and in the treatment of infrared singular real radiation [41–47], an increasing number of collider processes have been computed in fully differential form to NNLO QCD accuracy.

Following earlier results on the Drell-Yan process [48, 49], on Higgs production [50, 51] and on $e^+e^- \to 3j$ [52, 53], NNLO results have been obtained for $pp \to \gamma\gamma$ [54], $pp \to VH$ [55], $pp \to V\gamma$ [56], $pp \to t\bar{t}$ [57, 58], $pp \to H + j$ [59, 60], $pp \to W + j$ [61], $pp \to Z + j$ [62, 63], $pp \to \gamma + X$ [64], $pp \to ZZ$ [65], $pp \to WW$ [66], $pp \to ZW$ [67],

$ep \to 1j$ [68] and $pp \to 2j$ [69]. All these calculations were implemented in the form of parton-level event generators (some of the lower-multiplicity processes have also become part of the latest version of the MCFM code [70]), which provide full kinematic information on all final-state particles, and consequently allow the precise definition (jet algorithm, kinematic acceptance cuts) of observables used in the experimental analyses.

Calculations of collider observables to NNLO require three types of parton-level contributions, which are individually infrared divergent: double-real radiation, single-real radiation at the one-loop level and two-loop virtual contributions. To implement these contributions into a parton-level event generator, a method to extract and recombine their infrared (IR) singular parts is required. Our group has developed the antenna subtraction method [43, 44] for this purpose. This method forms the basis of the NNLOJET code, which provides the necessary infrastructure and building blocks to implement NNLO corrections to different collider processes. Up to now, $pp \to Z + j$ [62], $pp \to H + j$ [60] and $pp \to 2j$ [69] have been implemented in NNLOJET.

The same framework is used in the calculation of NNLO corrections to jet production. For DIS, results have already been reported in Refs. [71, 152] and will be recapitulated in this thesis. In addition, we also report on new di-jet production results in diffractive scattering, a fit of $\alpha_s(M_Z)$ from H1 data as well as predictions for event orientation distributions in electron-positron annihilation. Finally, combining the method of Projection-To-Born [72] with our DIS di-jet calculation to NNLO and the inclusive structure function to next-to-next-to-next-to-leading order (N3LO) QCD accuracy [73, 74], we calculated single-jet production in the laboratory frame to N3LO QCD accuracy.

In Section 2, we give a short overview on aspects of QCD relevant for our calculations. Sections 3 and 4 give details on the antenna subtraction formalism and its implementation into the NNLOJET program. We then establish the notation and description pertinent to jet production in DIS kinematics in Section 5. In Sections 6 and 7, we give the explicit antenna subtraction terms for single-jet production in the laboratory and for di-jet production in the Breit frame, before moving on to their phenomenological applications. Phenomenological results on single-jet and di-jet production in the Breit frame and their comparison to HERA measurements are given in Sections 8 and 9, respectively. Theoretical predictions for di-jet production in diffractive scattering and a fit of $\alpha_s(M_Z)$ are presented in Sections 10 and 11. Phenomenological results on single-jet production in the laboratory frame to N3LO are given in Section 12. Finally, results on event orientations in electron-positron annihilation are presented in Section 13 and we conclude with Section 14.

2 Aspects of QCD

2.1 The QCD Lagrangian and $SU(3)$

The fundamental mathematical quantity of any quantum field theory is the action, defined as

$$S = \int dtL = \int \mathcal{L}(\phi(x), \partial_\mu \phi(x)) \mathrm{d}^4 x \,, \tag{2.1}$$

where $\mathcal{L}$ is the Lagrangian density, dependent on one or more fields ϕ and their derivatives $\partial_\mu \phi$. Using functional differentiation, one can derive the equations of motion of a particular Lagrangian by finding solutions to

$$\delta S = 0 \,, \tag{2.2}$$

and the values of the fields are determined by the quantised solutions to these equations. The "classical" QCD Lagrangian, in the sense that it is invariant under $SU(3)$ gauge transformations, CP conserving and renormalisable, is given by

$$\mathcal{L}_{classical} = \bar{q_j}(i \not{D} - m_q) q_j - \frac{1}{4} F^a_{\mu\nu} F^{a\mu\nu} \,, \tag{2.3}$$

where it is assumed that any index that appears twice is summed over. Here q and $\bar{q}$'s are the Dirac four-spinors of the quark and antiquarks, respectively, F is the gluonic field strength tensor and $\not{D} = \gamma_\mu D^\mu$ the covariant derivative contracted with the Dirac γ matrices that fulfill the Clifford algebra. In terms of the gluonic fields $A^\mu_{ij} = T^a_{ij} A^{a\mu}$, F and D are given by

$$F^a_{\mu\nu} = \partial_\mu A^a_\nu - \partial_\nu A^a_\mu - g_s f^{abc} A^b_\mu A^c_\nu \,, \tag{2.4}$$

$$D^\mu_{ij} = \partial_\mu \delta_{ij} - i g_s A^\mu_{ij} \,, \tag{2.5}$$

where i and j are fundamental indices and f^{abc} are the structure constants of $SU(3)$, the group of special 3×3 unitary matrices. In Eq. (2.4), g_s is the QCD coupling constant that determines the strength of interactions and relevance of higher-order corrections. Any representation of $SU(3)$ has to fulfill the Lie-algebra

$$[T^a, T^b] = i f^{abc} T^c \,. \tag{2.6}$$

In total, $SU(3)$ has 8 hermitian generators which in the fundamental representation are given by the Gell-Mann matrices. Their normalisation can be chosen such that $\mathrm{Tr}\{T^a T^b\} = \delta_{ab}/2$. Another representation is furnished by the structure constants themselves. This representation is called the adjoint representation. Quark fields transform under the fundamental, gluons under the adjoint representation of $SU(3)$. Under a local $SU(3)$ gauge transformation

$$U(x) = e^{i g_s \theta^a(x) T^a} \tag{2.7}$$

the fields transform in the following way

$$q(x) \to U(x) q(x) \,, \tag{2.8}$$

$$\bar{q}(x) \to \bar{q}(x) U^\dagger(x) \,, \tag{2.9}$$

$$A(x) \to U(x)A_\mu U^\dagger(x) + \frac{i}{g_s}U(x)\partial_\mu U^\dagger(x)\,. \tag{2.10}$$

From the transformation properties in Eq. (2.10) one can deduce that the covariant derivative transforms as

$$D_\mu \to U(x)D^\mu U^\dagger(x)\,, \tag{2.11}$$

such that the Lagrangian defined in Eq. (2.3) is invariant under local gauge transformations.

To determine the values of the fields appearing in the Lagrangian in a perturbative approach, one first solves the equation of motion in the free field approximation taking $g_s = 0$ and quantises the result by imposing canonical commutation relations between the fields and their canonical momenta. Assuming the strong coupling g_s to be small, one can then calculate corrections to these so-called free field solutions as a power expansion in g_s to approximate the result of the full theory. Upon quantisation of the gluonic fields, the physical equivalence of different field configurations that can be transformed into each other via a local gauge transformation poses a problem. The Faddeev Popov procedure solves this issue by introducing new fields, so-called ghosts fields η and gauge fixing terms, into the Lagrangian [75]. In the covariant Lorenz gauge $\partial^\mu A_\mu = 0$ these additional terms read

$$\mathcal{L}_{fix+ghost} = -\frac{1}{2\xi}\partial^\mu A^a \partial_\mu A_a + \partial^\mu \eta^{a\dagger}\left(\partial_\mu g_s f_{abc} A^{c\mu}\right)\eta^b. \tag{2.12}$$

The ghosts are fermionic fields with spin zero and are hence unphysical. The full Lagrangian $\mathcal{L}_{QCD} = \mathcal{L}_{classical} + \mathcal{L}_{fix+ghost}$ is no longer locally gauge invariant, but invariant under the BRST symmetry [76]. From this BRST symmetry, one can derive Slavnov-Taylor identities and together they play a crucial role in proving renormalisability of $\mathcal{L}_{QCD}$ to all orders in perturbation theory [77]. Ghosts do not appear in any physical final state of a scattering process, but cancel propagating non-transverse polarisations of gluons. Similarly the gauge parameter ξ is reminiscent of the gauge degeneracy of the gluonic fields in $\mathcal{L}_{classical}$. Physical amplitudes and states should be ξ-independent and invariant under local gauge transformations. Another possible gauge fixing condition is the axial gauge where, for some unit vector n, $n \cdot A^a = 0$. In this gauge, the ghost fields decouple from any interaction such that only physical fields contribute in any scattering. The gluon propagator, however, is more complicated in this case. For the full Lagrangian $\mathcal{L}_{QCD}$, one can derive Feynman rules that give a pictorial representation of perturbative interactions. Apart from possible ghost-gluon interactions, these include three- and four-gluon vertices and quark-gluon couplings. A complete list of QCD Feynman rules can be found in Ref. [78].

2.2 Renormalisation and asymptotic freedom

The calculation of perturbative corrections in QCD requires the evaluation of loop integrals that are in general divergent, ill-defined quantities. Most commonly one uses dimensional regularisation, introduced by 't Hooft and Veltman [79], to circumvent this problem. In dimensional regularisation, one analytically continues the space-time dimensions to $d = 4 - 2\epsilon$ such that divergences are given by a Laurent series as poles in $1/\epsilon$ and the action is made dimensionless by assigning a mass dimension to the strong coupling constant, $\dim[g_s] = \epsilon$.

Dimensional regularisation can thereby be performed in different ways and consistency of different methods has recently been shown up to NNLO in the strong coupling [80]. Loop integrals have ultraviolet and infrared divergences which occur when loop momenta tend to infinity and when a loop momentum becomes collinear to some other particle momentum or vanishes altogether, respectively. For results given in this thesis conventional dimensional regularisation is used and only ultraviolet divergences will be discussed in this section.

To deal with ultraviolet divergences, one postulates that the bare Lagrangian can be written in terms of renormalised fields and couplings multiplied by rescaling factors. Adapting the Lorenz gauge and assuming quarks to be massless this can be written as

$$\begin{aligned}\mathcal{L}_{bare} = & -\frac{Z_3}{4}\left(\partial^\mu A^a_{r,\nu} - \partial^\nu A^a_{r,\mu}\right)^2 + iZ_2\bar{q}_{r,j}\partial\!\!\!/ q_{r,j} \\ & - \bar{\eta}^a_r\partial^2\eta^a_r Z_2^\eta + Z_1 g_{r,s}A^a_{r,\mu}\bar{q}_{r,j}\gamma^\mu T^a q_{r,j} - Z_1^{3g} g_{r,s} f^{abc}\left(\partial_\mu A^a_{r,\nu}\right)A^{b\mu}_r A^{c\nu}_r \\ & - g^2_{r,s}\frac{Z_1^{4g}}{4}\left(f^{eab}A^a_{r,\mu}A^b_{r,\nu}\right)\left(f^{ecd}A^{c\mu}_r A^{d\nu}_r\right) - g_{r,s}Z_1^\eta\bar{\eta}^a f^{abc}\partial^\mu A^b_{r,\mu}\eta^c_r\,. \end{aligned} \tag{2.13}$$

Here $\xi = \infty$ as it can be proven that the gauge fixing term is invariant under addition of higher-order corrections [77]. The fields and couplings are then rescaled in the following way:

$$\begin{aligned} A^a_\mu &= Z_3^{\frac{1}{2}} A^a_{r,\mu}\,, \\ \eta^a &= Z_2^{\eta\,\frac{1}{2}}\eta^a_r\,, \\ q_j &= Z_2^{\frac{1}{2}} q_{r,j}\,, \\ g_s &= Z_g g_{r,s}\,. \end{aligned} \tag{2.14}$$

Comparing Eq. (2.13) to the relations in Eqs. (2.14), the following relations among the scaling factors can be deduced:

$$\begin{aligned} Z_1 &= Z_g Z_3^{\frac{1}{2}} Z_2\,, \\ Z_1^{3g} &= Z_g Z_3^{\frac{3}{2}}\,, \\ Z_1^{4g} &= Z_g^2 Z_3^2\,, \\ Z_1^\eta &= Z_g Z_2^\eta Z_3^{\frac{1}{2}}\,. \end{aligned} \tag{2.15}$$

It is reasonable to assume, based on the gauge symmetry of the Lagrangian, that the Z_gs in the expressions should be the same, independent of the vertex they multiply. Relying on the BRST invariance of the Lagrangian, a more rigorous proof can be obtained from generalised Ward-Takahashi identities, guaranteeing the universality of the renormalised coupling constant $g_{r,s}$ [81]. The result is

$$\frac{Z_1^{3g}}{Z_3} = \frac{Z_1^\eta}{Z_3^\eta} = \frac{Z_1}{Z_2} = \frac{Z_1^{4g}}{Z_1}\,, \tag{2.16}$$

such that all renormalisation constants in QCD are fixed by renormalisation of only four Green's functions. By writing each rescaling factor as $Z_i = 1 + \delta_i$, the bare Lagrangian can

be split into a Lagrangian $\mathcal{L}_r$ that depends only on renormalised fields and coupling and a Lagrangian containing the counterterms

$$\mathcal{L}_{bare} = \mathcal{L}_r + \mathcal{L}_{c.t.}\,. \tag{2.17}$$

The counterterms absorb the ultraviolet divergences order by order in the perturbation series and can also be represented in terms of Feynman rules. $\mathcal{L}_r$ is the same as $\mathcal{L}_{bare}$ only with bare quantities replaced by their renormalised counterparts. The value of the renormalised coupling is a physical observable and must be determined from experiment. However, a freedom remains in the definition of the finite parts of the counterterms. This freedom is expressed in terms of different renormalisation schemes and calculated observables should be independent of the renormalisation scheme used. A residual difference of $\mathcal{O}(\alpha_s^{n+1})$, where $\alpha_s = 4\pi g_s$, remains when the perturbation series is truncated at order n in α_s and this can be interpreted as a higher-order effect. In the minimal subtraction (MS) scheme, only the divergence is subtracted by the counterterms leaving the finite parts untouched. Using dimensional regularisation in $4-2\epsilon$ dimensions, the poles always appear in the combination [78]

$$\frac{\Gamma(1+\epsilon)}{\epsilon}(4\pi)^{\epsilon} = \frac{1}{\epsilon} + \ln(4\pi) - \gamma_E + \mathcal{O}(\epsilon)\,, \tag{2.18}$$

where the Euler-Mascheroni constant is given by

$$\gamma_E = 0.57721\ldots\,. \tag{2.19}$$

In the modified minimal subtraction ($\overline{\text{MS}}$) scheme, the pole and additional terms appearing in Eq. (2.18) are subtracted and this is the scheme we applied in our NNLO calculations throughout. Results in the ($\overline{\text{MS}}$) and (MS) scheme are related by replacing ϵ with $\epsilon \to \epsilon e^{-\gamma\epsilon}(4\pi)^{\epsilon}$ in the (MS) scheme to obtain results in the ($\overline{\text{MS}}$) scheme.

Bare amputated Green's functions $\Gamma_0^{N_A N_q}(p)$, with N_A and N_q external gluon and quark fields and an aggregate of external momenta p, are given in terms of their non-amputated counterparts $G^{N_A N_q}(p)$ by

$$\Gamma_0^{N_A N_q} = \frac{G^{N_A N_q}}{\prod_G G^{2,0}(p_A)\prod_q G^{0,2}(p_q)}\,. \tag{2.20}$$

It can be shown that bare and renormalised amputated Green's functions, when renormalised at a renormalisation scale μ_r, are related via

$$\Gamma_0^{N_A N_q}(p; g_s) = Z_3^{-N_A/2}(g_{r,s}(\mu_r))Z_2^{-N_q/2}(g_{r,s}(\mu_r))\Gamma_r^{N_A N_q}(p; g_{r,s}, \mu_r)\,, \tag{2.21}$$

where it has been used that in the ($\overline{\text{MS}}$) scheme the field renormalisation factors only depend on μ_r through an explicit dependence on $g_{r,s}$ [81]. Unique physical predictions require the bare Lagrangian to be independent of μ_r, i.e. μ_r dependence is only an artefact of the renormalisation procedure. This leads to the well-known renormalisation group equations (RGEs)

$$\mu_r \frac{\mathrm{d}}{\mathrm{d}\mu_r}\Gamma_0 = 0\,, \tag{2.22}$$

and explicitly, they can be written as

$$\left[\mu_r \frac{\partial}{\partial \mu_r} + \beta(g_{r,s}(\mu_r)) \frac{\partial}{\partial g_{r,s}} - N_A \gamma_A(g_{r,s}(\mu_r)) - N_q \gamma_q(g_{r,s}(\mu_r))\right] \Gamma_r^{N_A N_q}(p; g_{r,s}(\mu_r), \mu_r) = 0\,. \tag{2.23}$$

Here $\gamma_{q/A} = \frac{1}{2}\mu_r \frac{\partial}{\partial_{\mu_r}} Z_{q/A}$ is the anomalous dimension of the quark/gluon field and β is the QCD β-function, which can be shown to be gauge-independent in the ($\overline{\text{MS}}$) scheme [81]. The effect on the amputated Green's function of changing the renormalisation scale from μ_r to some physical scale Q, implying a rescaling of the momenta by a factor Q/μ_r on dimensional grounds, is then given by

$$\Gamma_r^{N_G N_q}(e^t p, g_{r,s}) = \Gamma_r^{N_G N_q}(e^t p, \bar{g}_{r,s}) \exp\left[Dt - \int_0^t \mathrm{d}t' N_A \gamma_A(\bar{g}_{r,s}) + N_q \gamma_q(\bar{g}_{r,s})\right]\,, \tag{2.24}$$

where D is the physical mass dimension of $\Gamma^{N_G N_q}$ and $t = \log \frac{Q}{\mu_r}$. The running coupling $\bar{g}_{r,s} \equiv \bar{g}_{r,s}(g_{r,s}, t)$ satisfies the differential equation

$$\beta(\bar{g}_{r,s}) = \frac{\partial \bar{g}_{r,s}}{\partial t},\ \bar{g}_{r,s}(g_{r,s}, 0) = g_{r,s}\,, \tag{2.25}$$

which can alternatively be written in terms of a running coupling $\alpha_s(\mu_r^2)$ as

$$\mu_r^2 \frac{\partial \alpha_s(\mu_r^2)}{\partial \mu_r^2} = \beta(\mu_r^2)\,, \tag{2.26}$$

with boundary condition

$$\alpha_s(Q^2) = \alpha_s^{\text{ref}}\,, \tag{2.27}$$

where the reference value α_s^{ref} has to be determined experimentally. Eq. (2.24) implies that the strong coupling changes according to the solutions to Eqs. (2.25) when a physical scale in a scattering process is changed. Expressed in terms of a power expansion in α_s, β can be expanded to NLO as

$$\beta(\alpha_s(\mu_r^2)) = -\alpha_s(\mu_r^2)\left(\beta_0 \left(\frac{\alpha_s(\mu_r^2)}{2\pi}\right) + \beta_1 \left(\frac{\alpha_s(\mu_r^2)}{2\pi}\right)^2 + \mathcal{O}(\alpha_s^3)\right)\,, \tag{2.28}$$

with

$$\begin{aligned} \beta_0 &= \frac{11 C_A - 4 T_R N_F}{6}\,, \\ \beta_1 &= \frac{17 C_A^2 - 10 C_A T_R N_F - 6 C_F T_R N_F}{6} \end{aligned} \tag{2.29}$$

for QCD, where $C_F = \frac{N^2-1}{2N}$ and $C_A = N$ are the $SU(3)$ Casimir operators in the fundamental and adjoint representation, respectively, and $T_R = 1/2$. As long as the number of quark flavours N_F does not exceed 16, $\beta_0 > 0$ and the strong coupling parameter will decrease with increasing t and eventually vanishes in the limit $t \to \infty$. This phenomenon is called **asymptotic** freedom and justifies the use of perturbation theory at high energies. To leading order in α_s, Eq. (2.25) can be solved exactly for α_s

$$\alpha_s(Q^2) = \frac{\alpha_s(\mu_r^2)}{1 + \beta_0 \frac{\alpha_s(\mu_r^2)}{4\pi} \log \frac{Q^2}{\mu_r^2}} = \frac{12\pi}{(33 - 2N_F) \log \frac{Q^2}{\Lambda^2}}\,, \tag{2.30}$$

where the integration constant Λ gives the scale at which α_s diverges and truncation of a power series in α_s is no longer justified. For QCD, this scale lies around $100 \sim 300$ MeV. In this sense Eq. (2.30) can only describe the high energy behaviour of the strong coupling constant and indicates that the solutions to Eq. (2.30) are no longer valid at scales $\sim \Lambda$. The solution given in Eq. (2.30) shows that using running couplings, terms of the form $\alpha_s(\mu_r^2) \log \frac{Q^2}{\mu_r^2}$ are resummed to all orders in $\alpha_s(Q^2)$. For fixed-order predictions, that are predictions calculated to a finite power in α_s only, it should be noted that the scale μ_r should be chosen close to the physical scale Q such that large logarithms of Q^2/μ_r^2 are avoided. Going beyond the leading order, solutions to Eq. (2.25) can only be obtained implicitly and have to be evaluated numerically. However, a solution as a power expansion in α_s, that is the fixed-order result, can be obtained

$$\alpha_s(\mu_0^2) = \alpha_s(\mu_r^2) \left[1 + \beta_0 L \frac{\alpha_s(\mu_r^2)}{2\pi} + \left[\beta_0^2 L^2 + \beta_1 L \right] \left(\frac{\alpha_s(\mu_r^2)}{2\pi} \right)^2 + \mathcal{O}(\alpha_s^2) \right] , \tag{2.31}$$

with

$$L = \log \frac{\mu_r^2}{\mu_0^2} , \tag{2.32}$$

relating values of α_s for different choices of renormalisation scales μ_0 and μ_r. Finally, by solving Eq. (2.24) to leading order in α_s, it can be shown that Green's functions vary logarithmically with Q^2 in asymptotically free theories in the limit $Q^2 \to \infty$, according to

$$\Gamma_r \propto Q^D \left(\log Q \right)^{\frac{39/4 - N_F}{33 - 2N_F}} . \tag{2.33}$$

2.3 The parton model

The proton is not a fundamental particle, but is made up of quarks and gluons which are collectively called partons. Evidence for this comes from lepton-proton scattering via the exchange of a virtual vector boson with momentum q and virtuality $Q^2 = -q^2$, by comparing results of measured cross sections to expectations for scatterings off point charges. The cross section for scattering off a composite particle rather than a point-like object are related via

$$\frac{\mathrm{d}\sigma}{\mathrm{d}\Omega} = \left(\frac{\mathrm{d}\sigma}{\mathrm{d}\Omega} \right)_{point} |F(q)|^2 , \tag{2.34}$$

where Ω is the solid angle and the form factor $F(q)$ depends on the composition of the compound particle participating in the scattering. As the virtuality of the vector boson in the collision increases, more of the proton's substructure is resolved such that the vector boson at high enough energies, $Q^2 \to \infty$, scatters off individual partons inside the proton. In this case and to a first approximation, one would expect the form factor to show no Q^2 dependence, but to be rather only dependent on the fraction x of the proton's longitudinal momentum carried by the parton. The variable x is also called Bjorken's x, defined as

$$x = \frac{Q^2}{2P \cdot q} , \tag{2.35}$$

where P is the incoming proton's momentum. In the high energy limit, the cross section factorises into a leptonic and a hadronic piece and can be written as

$$\sigma \sim L_{\mu\nu} W^{\mu\nu} \,, \tag{2.36}$$

where L is the leptonic and W the hadronic tensor. Imposing current and CP conservation, the hadronic tensor can be written in its most general form as

$$W^{\mu\nu} = F_1(x, Q^2) \left[g^{\mu\nu} - \frac{q^\mu q^\nu}{q^2} \right] + \frac{2x}{Q^2} F_2(x, Q^2) \left(p^\mu + \frac{q^\mu}{2x} \right) \left(p^\nu + \frac{q^\nu}{2x} \right) \,, \tag{2.37}$$

in which the energy transferred to the proton by the lepton is given by

$$y = \frac{P \cdot q}{P \cdot k_i} \tag{2.38}$$

for an incoming lepton with momentum k_i. In Eq. (2.37), F_1 and F_2 are known as structure functions and ignoring higher-order corrections on the lepton line, the lepton tensor evaluates to

$$L_{\mu\nu} = e^2 \mathrm{Tr} \left[\not{k}' \gamma_\mu \not{k} \gamma_\nu \right] \,, \tag{2.39}$$

with e being the unit electric charge. Using the above, the differential cross section can then be written as

$$\frac{\mathrm{d}^2\sigma}{\mathrm{d}x \mathrm{d}Q^2} = \frac{4\pi\alpha^2}{Q^4} \left[\left[1 + (1-y)^2 \right] F_1(x, Q^2) + \frac{(1-y)}{x} (F_2(x, Q^2) - 2x F_1(x, Q^2)) \right] \,, \tag{2.40}$$

where α is the fine structure constant. Independence of the form factor from Q^2 in the high energy limit is called Bjorken scaling, postulating that inelastic lepton-proton scattering can be written as an incoherent sum of elastic scatterings from point-like objects within the proton that each carry a momentum fraction x of the proton's momentum

$$\frac{\mathrm{d}\sigma}{\mathrm{d}x \mathrm{d}y} = \sum_{i=q,\bar{q},g} \int_0^1 \mathrm{d}\xi f_i(\xi) \mathrm{d}\hat{\sigma}_i(\xi, Q^2, \mu_r) \,, \tag{2.41}$$

where $\hat{\sigma}$ is the partonic matrix element describing the short distance physics with parton i in the initial state. For DIS to $\mathcal{O}(\alpha_s^0)$, $\hat{\sigma}$ is given by

$$\frac{\mathrm{d}\hat{\sigma}_i}{\mathrm{d}x \mathrm{d}Q^2}(\xi, Q^2) = \frac{2\pi\alpha^2}{Q^4} \xi e_i^2 \left[1 + (1-y)^2 \right] \delta(x - \xi) \,, \tag{2.42}$$

where e_i is the fractional electromagnetic charge of parton i. In particular this means that in the high energy limit,

$$F_2(x, Q^2) \overset{Q^2 \to \infty}{=} F_2(x) = \sum_i e_i^2 x f_i(x), \quad F_1(x, Q^2) = F_1(x) = \frac{1}{2x} F_2(x) \tag{2.43}$$

to $\mathcal{O}(\alpha_s^0)$. A heuristic justification of Eq. (2.41) is as follows [34]: for the proton to remain intact, individual partons cannot have transverse momenta significantly above $p_T \sim M_P$, however, $Q^2 \gg M_P$ such that the life-time of the partons is much longer than the time of interactions. To the interacting vector boson, therefore, the partons appear to be "frozen". The only unknown to be considered is the number of partons that carry a certain momentum fraction x of the proton's momentum at the instant of the interaction. How radiative corrections influence this rather naive picture will be discussed in Section 2.9.

2.4 From partons to jets

Once a parton is created in a hard interaction it hadronises and fragments to form colourless final states due to confinement, stating that coloured particles are never observed in isolation. Hadronisation results in the formation of collimated beams of energetic particles that are called jets and it is these jets that can be measured in experiments. Hadronisation, being a long distance effect, takes place at a much longer time scale than the production of "hard" partons such that hadronisation effects can, to a first approximation, be treated separately to QCD corrections at the parton level. A generic procedure to relate measured jets at the hadron level to theoretical predictions at the parton level is provided by the so-called jet algorithm. The jet algorithm is therefore required to be infrared-safe, that is partons have to be combined in such a way that the jet remains invariant under the emission of multiple soft or collinear particles and must yield finite cross sections to any order in perturbation theory [82]. Many different jet algorithms exist and a detailed description for the majority of them can be found in Ref. [83]. Now two algorithms, that were applied in the calculations presented in this thesis, will be discussed. In the JADE algorithm, suitable for electron-positron annihilation, jets are found in the following way:

1. The distance measure
$$y_{ij} = \frac{2E_jE_i(1-\cos(\theta_{ij}))}{W^2} \tag{2.44}$$
is calculated between all pairs of final-state particles i and j, where W^2 is the square of the total energy in the event.

2. The smallest $y_{min} = y_{ij}$ is determined.

   If $y_{min} > y_{cut}$, the algorithm terminates and all remaining particles are declared as jets, where y_{cut} is some resolution parameter.

   If $y_{min} < y_{cut}$, particles i and j are combined into a single new particle and the procedure is repeated from step one until all pairs of particles fulfill $y_{min} > y_{cut}$.

For lepton-proton collisions via vector boson exchange, we must also introduce a pseudo-particle that represents the beam jet, i.e. to account for hadronisation of the proton remnant. Initially, the beam jet is massless with momentum equal to the missing longitudinal momentum of the event (which is the momentum associated with the partons inside the proton that do not participate in the hard interaction). This pseudo-particle is treated in the same way by the jet algorithm as other final-state partons and all particles that end up in the jet with this pseudo-particle are associated with the beam. Finally, the energy measure W^2 has to be modified and is given by the invariant mass of the vector boson and the incoming proton.

The second algorithm that is considered is the inclusive k_t algorithm. The k_t algorithm is defined in the following way:

1. The quantities
$$d_{ij} = \min(p_{T,i}^2, p_{T,j}^2)\frac{\Delta R_{ij}^2}{R^2} \quad \text{and} \quad d_{iB} = p_{T,i}^2 \tag{2.45}$$

are evaluated for each final-state particle i and every final-state pair ij. In Eq. (2.45), the parameter R is the cone size and similar to y_{cut} a resolution parameter. The value of ΔR_{ij} is given by

$$\Delta R_{ij} = \sqrt{(y_i - y_j)^2 + (\phi_i - \phi_j)^2}\,, \tag{2.46}$$

where ϕ and y are the particle's azimuthal angle and rapidity relative to the beam axis, respectively, and the rapidity is defined as

$$y \equiv \frac{1}{2} \ln \frac{E + p_z}{E - p_z}\,, \tag{2.47}$$

and for massless particles one has $y = \eta$.

2. The minimum value of all d's is determined.

   If d_{iB} is smallest, then particle i is declared as a jet and removed from the particle list.

   If d_{ij} is smallest, particle i and j are merged and the procedure repeated from step one.

3. Once all particles are merged into jets, the algorithm terminates and a cut on the transverse momentum p_T of the jets is applied to separate final-state jets from the beam jet.

The combination of two particles can be defined in different ways and the relevant recombination schemes for our work are

- The 4-vector-scheme:
  The momentum of the new composite particle k is given by the sum of the individual momenta of particles i and j, $p_k = p_i + p_j$.

- The massless E_T-weighted scheme:
  Here the resultant particle is massless with pseudo-rapidity η, azimuthal angle ϕ and energy E given by

$$E_T = \sum_i E_{T,i}\,, \quad \eta = \frac{1}{E_T} \sum_i E_{T,i}\eta_i\,, \quad \phi = \frac{1}{E_T} \sum_i E_{T,i}\phi_i\,, \tag{2.48}$$

  where the sum i is over all the particles in the jet and the pseudo-rapidity η is defined in terms of the particle's polar angle θ as

$$\eta \equiv -\ln\left[\tan\left(\frac{\theta}{2}\right)\right]\,. \tag{2.49}$$

2.5 Colour-ordered squared partial amplitudes

The fundamental building blocks in the evaluation of cross sections are scattering amplitudes that give the probabilistic amplitude for a particular process to occur. Amplitudes are closely related to amputated Green's functions and this relation is expressed in terms

of the LSZ reduction formula [84, 85]. A general QCD amplitude may thereby be decomposed into sub-amplitudes according to the dependence of individual Feynman diagrams on $SU(3)$ generators, that is

$$\mathcal{M}_{\text{full}}(\vec{c},\vec{p}) = \sum_i \mathcal{M}_i(\vec{c}_i,\vec{p}_i)\,, \tag{2.50}$$

where $\vec{c}$ and $\vec{p}$ are vectors in colour and momentum space, respectively. Each sub-amplitude further factorises into a part that only depends on the kinematics of the process and one that only depends on the process' colour structure. For the i^{th} sub-amplitude this can be written as

$$\mathcal{M}_i(\vec{c},\vec{p}) = \mathcal{T}_i(\vec{c})\mathcal{M}_i(\vec{p})\,, \tag{2.51}$$

where $\mathcal{T}_i(\vec{c})$ gives the colour and $\mathcal{M}_i(\vec{p})$ the kinematic dependence of the amplitude. The full amplitude can then be written as

$$\mathcal{M}_{\text{full}} = \sum_i \mathcal{T}_i(\vec{c})\mathcal{M}_i(\vec{p})\,. \tag{2.52}$$

The colour-dependent factors $\mathcal{T}_i$ may be manipulated using the $SU(3)$ relation

$$f_{abc} = -2i\text{Tr}([T^a,T^b]T^c) \tag{2.53}$$

to substitute structure constants in the adjoint with ones in the fundamental representation. Contracted adjoint indices can further be simplified using the $SU(3)$ Fierz identity

$$T^a_{ij}T^a_{kl} = \delta_{il}\delta_{jk} - \frac{1}{N}\delta_{ij}\delta_{kl}\,, \tag{2.54}$$

where $N = 3$ is the number of colours. Upon squaring the full amplitude, the remaining free colour indices in Eq. (2.52) contract. Results for the squared amplitude in terms of partial squared amplitudes that each come with different powers of N can then be obtained by repeated application of Eq. (2.53) and Eq. (2.54). In general, individual amplitudes that make up the N-ordered partial squared amplitudes are thereby linear combinations of sub-amplitudes from Eq. (2.52). For amplitudes relevant to calculations considered in this thesis, it turns out that some to all gluon-vertices cancel in partial squared amplitudes that come with subleading powers of N. A gluon for which all gluon-vertices cancel in a squared partial amplitude is only colour-neighbouring quarks and is referred to as an abelian gluon. In addition, partial squared colour-ordered amplitudes only have divergences in unresolved limits between colour-neighbouring partons. More details of how this works in specific examples can be found in Ref. [86] or [87]. The above discussion of colour-ordered amplitudes carries through to one- and two-loop amplitudes [87].

2.6 Infrared divergences in real radiation

2.6.1 Single-unresolved radiation at tree level

Infrared divergences in colour-ordered squared matrix elements only exist between colour-neighbouring partons. Two types of divergences for single-unresolved radiation exist,

namely soft (particle's momentum vanishes) and collinear (two or more particle momenta are parallel) divergences, with only gluons developing soft divergences due to quark number conservation at NLO. For a gluon j colour-neighbouring partons i and k being soft, a squared colour-ordered tree level matrix element $|\mathcal{M}^0_{n+1}|^2$ factorises in the following way [88]:

$$M^0_{n+1}(\cdots, i, j, k, \cdots) \xrightarrow{j\to 0} S_{ijk} M^0_n(\cdots, i, k, \cdots), \tag{2.55}$$

where we have adopted the short hand notation $|\mathcal{M}^0_n(\cdots)|^2 = M^0_n(\cdots)$ to abbreviate any squared tree level matrix element and this notation will be applied throughout the rest of this thesis. The soft eikonal function is defined as

$$S_{ijk} = \frac{2s_{ik}}{s_{ij}s_{jk}}, \tag{2.56}$$

where $s_{lm} = (p_l + p_m)^2$ is the Lorentz invariant squared mass of partons l and m, and n denotes the number of partons in the squared matrix element M. The soft eikonal function is universal and independent of the particle species of partons i and k. If parton j is collinear to its colour-neighbouring parton k, the colour-ordered tree-level matrix elements factorises according to [89]

$$M^0_{n+1}(\cdots, j, k, \cdots) \xrightarrow{j\|k} \frac{P^{(0)}_{jk\to K}(z)}{s_{jk}} M^0_n(\cdots, K, \cdots) + \text{angular terms}, \tag{2.57}$$

where z is the fraction of K's momentum carried by parton i. As a result of the splitting, parton K carries the combined quantum numbers of j and k, and $p_K = p_j + p_k$. The spin-averaged splitting functions $P_{jk\to K}$ depend on the particle species of the partons involved in the splitting and whether any of the involved particles are in the initial state. A full list of NLO splitting kernels can be found in Ref. [89]. The angular terms arise due to spin correlations between the partons in the splitting process and the spin of the parent parton in the reduced matrix element [90]. Non-trivial spin correlations only arise when the parent parton is a gluon and only then are the angular terms non-vanishing. Angular terms are in general a homogeneous function linear in $\cos 2\phi$, where ϕ is the azimuthal angle of partons j and k about their collinear axis. Hence angular terms can be removed by integrating analytically over ϕ or by generating pairs of phase space points separated by $\Delta\phi = \pi/2$. In our calculations the latter method has been implemented.

2.6.2 Double-unresolved radiation at tree level

Two different scenarios arise when examining double-unresolved radiation in colour-ordered squared tree-level matrix elements. Formulae for infrared factorisations of configurations in which two unresolved partons are not colour-neighbouring each other are given by an iteration of infrared factorisations in single-unresolved limits. In cases where the unresolved particles are colour-neighbours the following unresolved configurations can arise:

- Triple-collinear:
  Momenta of three colour-connected particles become collinear and this results in an

infrared factorisation according to [91]

$$M^0_{n+2}(\cdots, i, j, k, \cdots) \xrightarrow{i||j||k} P^{(0)}_{ijk\to K}(x, y, z) M^0_n(\cdots, K, \cdots) + \text{angular terms}\,, \quad (2.58)$$

where K carries the combined momentum and quantum numbers of partons i, j and k that each carry a momentum fraction x, y and z of K's momentum, respectively. The spin-averaged triple-collinear splitting kernels P depend on the particle species involved in the splitting. A full set of triple-collinear splitting kernels can be found in Ref. [92]. As in the single-unresolved case, the angular terms only arise if the parent parton is a gluon and can be removed by generating phase space points in appropriate pairs.

- Double-collinear:
  Two separate pairs of particles become collinear. In this case the infrared factorisation formula is given by an iteration of NLO collinear factorisation.

- Double-soft:
  For two colour-neighbouring gluons, each with vanishing energy, the infrared factorisation is given by [93]

$$M^0_{n+2}(\cdots, i, j_g, k_g, l, \cdots) \xrightarrow{j,k\to 0} S_{ijkl} M^0_n(\cdots, i, l, \cdots)\,, \quad (2.59)$$

  where S_{ijkl} is the double-soft eikonal factor and as in the NLO case, the factorisation is independent of the particle species of partons i and j. Quark number can still be conserved if a quark and an antiquark are soft simultaneously and this results in a new singularity structure according to [92]

$$M^0_{n+2}(\cdots, i, j_q, k_{\bar{q}}, l, \cdots) \xrightarrow{j,k\to 0} S_{il}(j_q, k_{\bar{q}}) M^0_n(\cdots, i, l, \cdots)\,, \quad (2.60)$$

  where S_{il} is a new singular function independent of the particle species of partons i and l.

- Soft-collinear:
  A pair of colour-neighbouring partons are collinear and another parton, colour-neighbouring either of the two partons, has vanishing energy. In this case the factorisation is given by [91]

$$M^0_{n+2}(\cdots, i, j_g, k, l, \cdots) \xrightarrow{j\to 0, k||l} S_{i,jkl} \frac{P^{(0)}_{kl\to K}(z)}{s_{kl}} M^0_n(\cdots, i, K, \cdots)\,, \quad (2.61)$$

  with new singular function $S_{i,jkl}$ and the other variables follow their definitions given in the description of splittings at NLO.

2.6.3 Single-unresolved radiation at one-loop level

Infrared factorisation at loop level exists in a similar way as for tree-level amplitudes. In a limit with a vanishing gluon momentum the matrix element factorises according to [94]

$$M^1_{n+1}(\cdots, i, j_g, k, \cdots) \xrightarrow{j\to 0} S^{(1)}_{ijk}(\epsilon) M^0_n(\cdots, i, k, \cdots) + S_{ijk} M^1_n(\cdots, i, k, \cdots)\,, \quad (2.62)$$

where M^1 denotes the squared matrix element for the one-loop correction that is the interference between the one-loop and the corresponding tree-level amplitude, S_{ijk} is the aforementioned soft eikonal factor and $S^{(1)}$ is the universal one-loop soft eikonal factor. In analogy to the tree level factorisation, the following formula gives the fatorisation for collinear divergences at the one-loop level [95]:

$$M^{(1)}_{n+1}(\cdots, j, k, \cdots) \xrightarrow{j\|k} \frac{P^{(1)}_{jk\to K}}{s_{jk}} M^0_n(\cdots, K, \cdots) + \frac{P^{(0)}_{jk\to K}}{s_{jk}} M^{(1)}_n(\cdots, i, k, \cdots)\,, \tag{2.63}$$

where $P^{(1)}$ is the analogous function to $P^{(0)}$ at loop level. A list of splitting functions at one loop can be found in Ref. [96].

2.7 Infrared divergences in loop integrals

After calculating loop integrals in dimensional regularisation, ultraviolet poles in $1/\epsilon$ can be absorbed into the redefinition of physical parameters. The poles that still remain after renormalisation are associated with the infrared divergences of the loop integral. Such infrared poles at one- and two-loop order are systematically catalogued by Catani [97] and his description will be followed below.

2.7.1 One loop

At one loop, the infrared singularity structure of an amplitude $\mathcal{M}^1_n$ can be written in the following way

$$\mathcal{M}^1_n = \mathbf{I}^{(1)}_n(\epsilon, \mu^2)\mathcal{M}^0_n + \mathcal{M}^1_{n,\text{finite}}\,, \tag{2.64}$$

where $\mathcal{M}^1_{\text{finite}}$ is the infrared finite part of the virtual amplitude and $\mathcal{M}^0$ is an appropriate tree-level amplitude, such that the right- and left-hand side appear at the same level in the colour decomposition. The operator $\mathbf{I}^{(1)}$ encodes the divergent infrared structure of $\mathcal{M}^1$ and is given by

$$\mathbf{I}^{(1)}_n(\epsilon, \mu^2) = \frac{1}{2}\frac{e^{-\epsilon\gamma}}{\Gamma(1-\epsilon)} \sum_i^n \frac{1}{\mathbf{T}_i^2} \mathcal{V}_i^{sing}(\epsilon) \sum_{j\neq i} \mathbf{T}_i \cdot \mathbf{T}_j \left(\frac{\mu^2 e^{-i\lambda_{ij}\pi}}{2p_i \cdot p_j}\right)^{\epsilon}\,. \tag{2.65}$$

The constant λ_{ij} is $+1$ if partons i and j are both in the initial or both in the final state and 0 otherwise. Poles at NLO are maximally of order $1/\epsilon^2$ and explicit singularities are given by

$$\mathcal{V}_i^{sing}(\epsilon) = \mathbf{T}_i^2 \frac{1}{\epsilon^2} + \gamma_i \frac{1}{\epsilon}\,, \tag{2.66}$$

with

$$\gamma_q = \gamma_{\bar{q}} = \frac{3}{2} C_F, \quad \gamma_g = \frac{11}{6} C_A - \frac{2}{3} T_R N_F\,. \tag{2.67}$$

The colour charge $\mathbf{T}_i$ is a vector in the adjoint representation and projects out parton i's colour charge matrix when acting on an amplitude. The colour-charge matrix is given by $T^a_{bc} \equiv i f_{bac}$ if parton i is a gluon or equal to the $SU(3)$ generator in the fundamental representation if i is a quark in the final state. For antiquarks or quarks in the initial

state the colour-charge matrix is the negative of the corresponding generator. Further, the following relations hold:

$$\mathbf{T}_q^2 = \mathbf{T}_{\bar{q}}^2 = C_F\,, \quad \mathbf{T}_g^2 = C_A\,. \tag{2.68}$$

Finally, due to colour conservation one has

$$\sum_{j\neq i} \mathbf{T}_j = \mathbf{T}_i\,. \tag{2.69}$$

The virtual correction is given by an interference between the loop- and tree-level amplitude

$$M_n^1 = \langle \mathcal{M}_n^1 | \mathcal{M}_n^0 \rangle + \langle \mathcal{M}_n^0 | \mathcal{M}_n^1 \rangle\,, \tag{2.70}$$

such that

$$Poles\left(M_n^1\right) = 2\mathrm{Re}\left[\mathbf{I}_n^{(1)}\right] M_n^0\,. \tag{2.71}$$

It can be shown that in colour-ordered amplitudes the operator $\mathbf{I}_n^{(1)}$ can be decomposed into a sum over the $\mathbf{I}$-operators formed by all colour-neighbouring particle pairs, $\mathbf{I}_2^{(1)}$, in the amplitude,

$$Poles\left(M_n^1\right) = \sum_{\{i,j\}\in 1,\cdots,n} 2\mathrm{Re}\left[\mathbf{I}_{ij}^{(1)}\right] M_n^0\,. \tag{2.72}$$

The operator $\mathbf{I}_{ij}^{(1)}$ depends on the particle species of partons i and j. A full list of these so-called Catani operators at one loop can be found in Ref. [92]

2.7.2 Two loop

The singularity structure for a two-loop amplitude is given by [97]

$$\mathcal{M}_n^2 = \mathbf{I}^{(2)}(\epsilon,\mu^2)\mathcal{M}_n^0 + \mathbf{I}^{(1)}(\epsilon,\mu^2)\mathcal{M}_n^1 + \mathcal{M}_{n,\text{finite}}^2\,. \tag{2.73}$$

At the level of the two-loop correction

$$M_n^2 = \langle \mathcal{M}_n^2 | \mathcal{M}_n^0 \rangle + \langle \mathcal{M}_n^0 | \mathcal{M}_n^2 \rangle + \langle \mathcal{M}_n^1 | \mathcal{M}_n^1 \rangle\,, \tag{2.74}$$

the pole structure is given by [98]

$$\begin{aligned} Poles\left(M_n^2\right) \;=\; & 2\mathrm{Re}\left[\mathbf{I}_n^{(1)}(\epsilon,\mu^2)\right]\left(M_n^1 - \frac{\beta_0}{\epsilon}M_n^0\right) \\ & - 2\mathrm{Re}\left[\left(\mathbf{I}_n^{(1)}(\epsilon,\mu^2)\right)^2\right] M_n^0 \\ & + 2e^{-\gamma\epsilon}\frac{\Gamma(1-2\epsilon)}{\Gamma(1-\epsilon)}\left(\frac{\beta_0}{\epsilon}+K\right)\mathrm{Re}\left[\mathbf{I}_n^{(1)}(2\epsilon,\mu^2)\right] M_n^0 \\ & + 2\mathrm{Re}\left[\mathbf{H}^{(2)}(\epsilon)\right] M_n^0\,. \end{aligned} \tag{2.75}$$

The coefficient K is given by

$$K = \left(\frac{67}{18} - \frac{\pi^2}{6}\right) C_A - \frac{10}{9} T_R N_f\,. \tag{2.76}$$

The $\mathbf{H}^{(2)}$ is dependent on the partonic content of the matrix element, but contains at most single poles in ϵ such that leading poles are of order $1/\epsilon^4$ for NNLO corrections. From the above, the pole structure of any two-loop correction for colour-ordered amplitudes can be inferred.

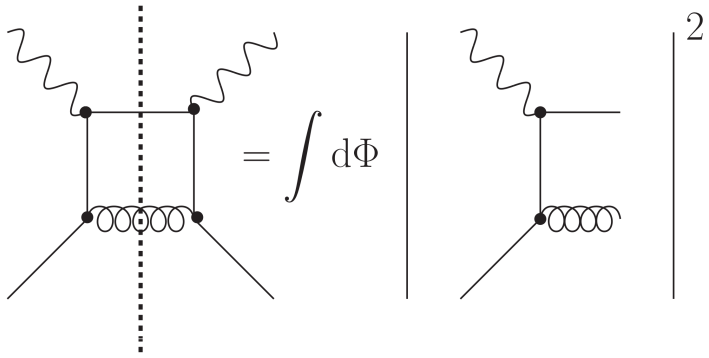

Figure 1. Pictorial description of the optical theorem in DIS, where quarks are shown by solid, gluons by curly and photons by wavy lines and $\mathrm{d}\Phi$ is the space measure of the final-state quark and gluon.

2.8 Infrared cancellation

Infrared singularities originating from loop integrals and integrals over the final-state phase space are related by the optical theorem. It is a result of imposing unitarity, that is probability conservation, on scattering amplitudes. To make use of the optical theorem, discontinuities across branch cuts of loop-containing amplitudes have to be calculated. Cutkosky proved that this can be achieved by "cutting" through the loops and by putting the propagators of cut lines on their mass-shell to all orders in perturbation theory [100]. The so calculated discontinuity is then equal to the interference of the two diagrams that resulted from the cut, integrated over the final-state phase space integral of the cut particles. A diagrammatic visualisation of this for a single cut is shown in Fig. 1. From the above discussion it should be clear that there exists an intimate relation between infrared divergences from loops and the ones resulting from phase space integration over real radiation. In fact, the singularities produced from final-state radiation exactly cancel the singularities appearing in the virtual corrections. This was proven by Kinoshita, Lee and Nauenberg and goes under the name of KLN theorem [101, 102]. To make this cancellation possible, measured observables need to be insensitive to soft or collinear particle splittings in the infrared region. Observables that fulfill this criterion are called infrared-safe. An explicit example of an infrared **un**safe observable would be the number of produced partons in a collision. For initial-state radiation however, this singularity cancellation only works for soft singularities, collinear singularities have to be absorbed into the PDFs and this leads to the QCD improved formulation of the parton model.

2.9 The QCD improved parton model

Cancellation of infrared divergences originating from initial-state radiation can be studied by calculating $\mathcal{O}(\alpha^2\alpha_s^1)$ corrections to DIS. For simplicity, QED corrections to the electron line are ignored and only photon-parton scattering is considered. In massless QCD, loop corrections to external propagators are zero such that only Feynman diagrams as those in Fig. 2 contribute to the $\mathcal{O}(\alpha^2\alpha_s^1)$ corrections. Anticipating a violation of Bjorken scaling

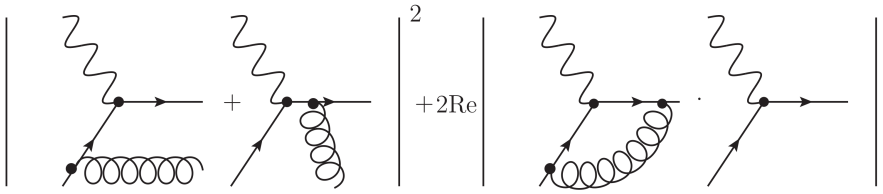

Figure 2. Diagrams contributing to quark-initiated DIS at $\mathcal{O}(\alpha_s)$.

when higher-order corrections are included, the hadronic tensor in Eq. (2.37) is promoted to a partonic tensor such that the partonic structure functions can be extracted via

$$\begin{aligned} p^\mu p^\nu \hat{W}_{\mu\nu} &= \frac{Q^2}{4z^2}\left(\frac{\hat{F}_2}{2z} - \hat{F}_1\right) \equiv \frac{Q^2}{4z^2}\frac{\hat{F}_L}{2z}\,, \\ -g^{\mu\nu}\hat{W}_{\mu\nu} &= (1-\epsilon)\frac{\hat{F}_2}{z} - \frac{3-2\epsilon}{2z}\hat{F}_L\,, \end{aligned} \tag{2.77}$$

where z is defined analogously to Bjorken's x in Eq. (2.35) with the incoming proton's replaced by the incoming parton's momentum. The proton structure functions are related to the quark structure functions via

$$F_2^q(x,Q^2) = 2x\sum_{q,\bar{q}} e_q^2 \int_0^1\int_0^1 \mathrm{d}\xi \mathrm{d}z \hat{\mathcal{F}}_2^q(z,Q^2) f(\xi,Q^2)\delta(x-\xi z)\,, \tag{2.78}$$

where

$$\hat{\mathcal{F}}_2^q(z,Q^2) = \frac{\hat{F}_2^q(z,Q^2)}{2z}\,. \tag{2.79}$$

Then the parton tensor can be calculated to NLO by

$$\hat{W}^{\mu\nu} = \frac{1}{N}\sum_{i=q}\int\left[\mathcal{M}^\mu_{q,LO}\mathcal{M}^{*\nu}_{q,LO}\frac{\mathrm{d}\Phi_1}{8\pi\sigma_{i,0}} + 2\mathrm{Re}\left[\mathcal{M}^{1,\mu}_{q,V}\mathcal{M}^{*\nu}_{q,LO}\right]\frac{\mathrm{d}\Phi_1}{8\pi\sigma_{i,0}} + \mathcal{M}^\mu_{q,R}\mathcal{M}^{*\nu}_{q,R}\frac{\mathrm{d}\Phi_2}{8\pi\sigma_{i,0}}\right], \tag{2.80}$$

where $\sigma_0 = 2\pi\alpha e_i^2$, M_R is the sum of amplitudes for the real correction, M_{LO} is the tree-level, M_V is the one-loop amplitude and the subscript q indicates that the process is quark-initiated. The phase space measure $\mathrm{d}\Phi_n$ for n final-state partons is given by

$$\mathrm{d}\Phi_n(p_{\hat{1}},p_{\hat{2}};p_3,\cdots,p_{n+2}) = \frac{\mathrm{d}^{d-1}p_3}{2E_3(2\pi)^{d-1}}\cdots\frac{\mathrm{d}^{d-1}p_{n+2}}{2E_{n+2}(2\pi)^{d-1}}(2\pi)^d\delta^d(p_{\hat{1}}+p_{\hat{2}}-p_3\cdots-p_{n+2})\,, \tag{2.81}$$

and the notation used above is that a hat over a particle's label indicates an initial-state particle.

Evaluating the corrections in conventional dimensional regularisation, one finds that the quark-initiated structure function receives a correction of the form [103]

$$\delta\hat{\mathcal{F}}_2^q(z,Q^2) = \left(\frac{\alpha_s}{2\pi}\right)\left(\frac{\mu^2}{Q^2}\right)^\epsilon \bar{C}(\epsilon)\left[-\frac{1}{\epsilon}\right]P_{qq}(z) + \text{finite terms}\,, \tag{2.82}$$

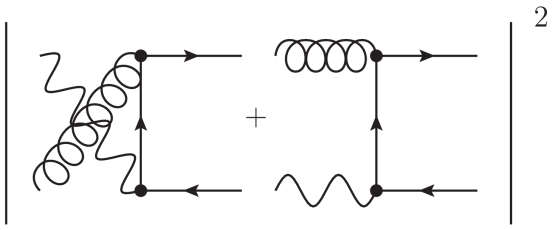

Figure 3. Diagrams contributing to gluon-initiated DIS at $\mathcal{O}(\alpha_s)$.

where the spherical factor $\bar{C}$ is defined as

$$\bar{C}(\epsilon) = (4\pi)^{\epsilon}\, e^{-\epsilon\gamma}. \tag{2.83}$$

The same result holds for the antiquark-initiated processes with $P_{qq} = P_{\bar{q}\bar{q}}$ such that $\delta\hat{\mathcal{F}}_2^q = \delta\hat{\mathcal{F}}_2^{\bar{q}}$ [103]. The quark-quark splitting kernel $P_{qq} = C_F \left(\frac{1+z^2}{1-z}\right)_+$ is an explicit example of a NLO splitting kernel from Section 2.6.1, where the +-distribution of a function $f(z)$ that develops a singularity at $z \to 1$ is defined as

$$\int_x^1 \mathrm{d}z\; g(z) f_+(z) = \int_x^1 \mathrm{d}z\; g(z) f(z) - g(1) \int_0^1 \mathrm{d}z\; f(z)\,, \tag{2.84}$$

for a regular test function $g(z)$. As the photon-quark vertex does not receive any renormalisation due to the QED Ward identity, the left-over pole appearing in Eq. (2.82) has an infrared character and gives an explicit example for non-cancellation of collinear divergences for initial-state radiation.

Evaluating the diagrams in Fig. 3, the gluon structure function receives corrections of the form

$$\delta\hat{\mathcal{F}}_2^g = \left(\frac{\alpha_s}{2\pi}\right)\left(\frac{\mu^2}{Q^2}\right)^{\epsilon} \bar{C}(\epsilon)\left[-\frac{1}{\epsilon}\right] P_{qg}(z) + \text{finite terms}\,, \tag{2.85}$$

with $P_{qg}(z) = \frac{1}{2}(z^2 + (1-z)^2)$. Using the above results, the DIS structure function can be written as

$$F_2(x, Q^2) = 2x \sum_{i=q,\bar{q}} e_i^2 \left((f_{0,q} + f_{0,\bar{q}}) \otimes \hat{\mathcal{F}}_2^q + f_{0,g} \otimes \hat{\mathcal{F}}_2^g \right)\,, \tag{2.86}$$

with the convolution $\otimes$ defined by

$$f \otimes g(x) = \int_0^1 \mathrm{d}y \int_0^1 \mathrm{d}z f(y) g(z) \delta(x - yz) = \int_x^1 \frac{\mathrm{d}z}{z} f\left(\frac{x}{z}\right) g(z)\,. \tag{2.87}$$

The infrared divergences on the right-hand side of Eq. (2.86) can be absorbed into the bare parton distribution functions to give renormalised parton distribution functions and this renormalisation of the PDFs is called mass factorisation. Similarly to ultraviolet renormalisation that was discussed previously, there is a freedom (scheme dependence) to move some of the finite parts from the physical to the bare PDFs upon absorption of the divergence. Two schemes commonly used for this purpose are the modified minimal subtraction

scheme ($\overline{\text{MS}}$) and the DIS scheme. The modified minimal subtraction scheme subtracts the divergence and generic factors that come with the pole, whereas in the DIS scheme all finite parts are subtracted from the bare PDF such that the DIS structure function F_2 remains form-invariant with respect to the leading-order expression. The freedom in this choice makes it clear that the PDF itself should not be regarded as a physical quantity on its own, but only when convoluted with a hard matrix element. The mass renormalisation has to be performed at some scale μ which can in general be different from the scale of ultraviolet renormalisation. Henceforth, scales related to the ultraviolet renormalisation and mass renormalisation will be referred to as μ_r, the renormalisation scale, and as μ_f, the factorisation scale, respectively.

Bare and physical PDFs can be related via

$$\mathbf{f}_0 = \mathbf{\Gamma}^{-1} \otimes \mathbf{f}\,, \tag{2.88}$$

where $\mathbf{\Gamma}$ is the mass factorisation tensor [98] and for the quark PDF this explicitly reads

$$f_{0,q}(x) = \Gamma^{-1}_{qq} \otimes f_q(x,\mu_f^2) + \Gamma^{-1}_{qg} \otimes f_g(x,\mu_f^2)\,. \tag{2.89}$$

To leading order in α_s, the Γ_{ij} functions in the ($\overline{\text{MS}}$) factorisation scheme [34] are, for $\mu_f = \mu_r$, given by

$$\begin{aligned}\mathbf{\Gamma^{-1}}_{ij}(x,\alpha_s(\mu_f^2)) &= \delta_{ij}\delta(1-x) - \frac{\alpha_s(\mu_f^2)}{2\pi}\bar{C}(\epsilon)\mathbf{\Gamma}^{(1)}_{ij}(x) + \mathcal{O}(\alpha_s^2) \\ &= \delta_{ij}\delta(1-x) + \frac{\alpha_s(\mu_f)}{2\pi}\bar{C}(\epsilon)\left[\frac{1}{\epsilon}\right]\mathbf{P}^{(0)}_{ij}(x) + \mathcal{O}(\alpha_s^2)\,,\end{aligned} \tag{2.90}$$

with $\mathbf{\Gamma}^{(1)}$ denoting the leading-order mass factorisation tensor. To leading order, individual elements of the mass factorisation and splitting tensor are related via

$$\mathbf{\Gamma}^{(1)}_{ij}(x) = -\frac{1}{\epsilon}\mathbf{P}^{(0)}_{ij}(x)\,, \tag{2.91}$$

where the individual elements of the tensors on the left- and right-hand side are still bold faced as they may contain colour. The colour decomposition of the leading-order mass factorisation kernels is given by [98]

$$\begin{aligned}\mathbf{\Gamma}^{(1)}_{qq}(x) &= \frac{N^2-1}{N^2}\Gamma^{(1)}_{qq}(x)\,,\\ \mathbf{\Gamma}^{(1)}_{gq}(x) &= \frac{N^2-1}{N^2}\Gamma^{(1)}_{gq}(x)\,,\\ \mathbf{\Gamma}^{(1)}_{qg}(x) &= \Gamma^{(1)}_{qg}(x)\,,\\ \mathbf{\Gamma}^{(1)}_{gg}(x) &= N\Gamma^{(1)}_{gg}(x) + N_F\Gamma^{(1)}_{gg,F}(x)\,.\end{aligned} \tag{2.92}$$

Going beyond the leading order, the expansion of $\mathbf{\Gamma}^{-1}(x,\alpha_s)$ is given by

$$\mathbf{\Gamma}^{(-1)}(x,\alpha_s) = \delta(1-x)\mathbf{I} - \frac{\alpha_s}{2\pi}\mathbf{\Gamma}^{(1)}(x) - \left(\frac{\alpha_s}{2\pi}\right)^2\left[\mathbf{\Gamma}^{(2)}(x) - \left[\mathbf{\Gamma}^{(1)}\otimes\mathbf{\Gamma}^{(1)}\right](x)\right] + \mathcal{O}(\alpha_s^3)\,, \tag{2.93}$$

where $\mathbf{\Gamma}^{(1)}$ and $\mathbf{\Gamma}^{(2)}$ are the one- and two-loop mass factorisation kernels, respectively, and the two-loop kernel $\mathbf{\Gamma}^{(2)}$ may be further decomposed into

$$\mathbf{\Gamma}^{(2)}_{ij}(x) = \bar{\mathbf{\Gamma}}^{(2)}_{ij}(x) - \frac{\beta_0}{\epsilon}\mathbf{\Gamma}^{(1)}_{ij}(x) + \frac{1}{2}\left[\mathbf{\Gamma}^{(1)}_{ik} \otimes \mathbf{\Gamma}^{(1)}_{kj}\right](x)\,. \tag{2.94}$$

Written out in colour-decomposed form, the $\bar{\mathbf{\Gamma}}^{(2)}_{ij}$ are given by

$$\begin{aligned}
\overline{\mathbf{\Gamma}}^{(2)}_{qq}(x) &= \left(\frac{N^2-1}{N}\right)\left[N\overline{\Gamma}^{(2)}_{qq}(x) + \tilde{\overline{\Gamma}}^{(2)}_{qq}(x) + \frac{1}{N}\tilde{\tilde{\overline{\Gamma}}}^{(2)}_{qq}(x) + N_F\overline{\Gamma}^{(2)}_{qq,F}(x)\right],\\
\overline{\mathbf{\Gamma}}^{(2)}_{q\bar{q}}(x) &= \left(\frac{N^2-1}{N}\right)\left[\overline{\Gamma}^{(2)}_{q\bar{q}}(x) + \frac{1}{N}\tilde{\overline{\Gamma}}^{(2)}_{q\bar{q}}(x)\right],\\
\overline{\mathbf{\Gamma}}^{(2)}_{qQ}(x) &= \left(\frac{N^2-1}{N}\right)\overline{\Gamma}^{(2)}_{qQ}(x)\,,\\
\overline{\mathbf{\Gamma}}^{(2)}_{q\bar{Q}}(x) &= \left(\frac{N^2-1}{N}\right)\overline{\Gamma}^{(2)}_{q\bar{Q}}(x)\,,\\
\overline{\mathbf{\Gamma}}^{(2)}_{gq}(x) &= \left(\frac{N^2-1}{N}\right)\left[N\overline{\Gamma}^{(2)}_{gq}(x) + \frac{1}{N}\tilde{\overline{\Gamma}}^{(2)}_{gq}(x) + N_F\overline{\Gamma}^{(2)}_{gq,F}(x)\right],\\
\overline{\mathbf{\Gamma}}^{(2)}_{qg}(x) &= \left[N\overline{\Gamma}^{(2)}_{qg}(x) + \frac{1}{N}\tilde{\overline{\Gamma}}^{(2)}_{qg}(x) + N_F\overline{\Gamma}^{(2)}_{qg,F}(x)\right],\\
\overline{\mathbf{\Gamma}}^{(2)}_{gg}(x) &= \left[N^2\overline{\Gamma}^{(2)}_{gg}(x) + NN_F\overline{\Gamma}^{(2)}_{gg,F}(x) + \frac{N_F}{N}\tilde{\overline{\Gamma}}^{(2)}_{gg,F}(x) + N_F^2\overline{\Gamma}^{(2)}_{gg,F^2}(x)\right],
\end{aligned} \tag{2.95}$$

where the above and a complete list of explicit analytic expressions for mass factorisation kernels at NLO, appearing on the right, can be found in Ref. [98].

The dependence on μ_f vanishes for observables that are calculated to all orders in α_s, but a truncation of the perturbation series at some finite order results in a residual dependence on this artificial scale. Imposing independence of the bare PDFs on μ_f, similarly to what was done in the formulation of the RGEs, leads to the Altarelli-Parisi equation [89, 99]

$$\begin{aligned}
\mu_f^2\frac{\partial \mathbf{f}_0(x)}{\partial\mu_f^2} &= 0\,,\\
\mu_f^2\frac{\partial \mathbf{f}(x,\mu_f^2,\mu_r^2)}{\partial\mu_f^2} &= \left[\mathbf{P}(\alpha_s(\mu_r^2),\mu_f^2,\mu_r^2)\otimes\mathbf{f}(\mu_f^2,\mu_r^2)\right](x)\,.
\end{aligned} \tag{2.96}$$

The splitting function $\mathbf{P}$ to third order in α_s is given by

$$\begin{aligned}
\mathbf{P}_{ij}(\alpha_s(\mu_r),\mu_f,\mu_r,x) = {}& \frac{\alpha_s(\mu_r^2)}{2\pi}\mathbf{P}^{(0)}_{ij}(x) + \left(\frac{\alpha_s(\mu_r^2)}{2\pi}\right)^2\left[\mathbf{P}^{(1)}_{ij}(x) + \beta_0 l\mathbf{P}^{(0)}_{ij}\right]\\
&+ \left(\frac{\alpha_s(\mu_r^2)}{2\pi}\right)^3\left[\mathbf{P}^{(2)}_{ij} + \left(\beta_1\mathbf{P}^{(0)}_{ij} + 2\beta_0\mathbf{P}^{(1)}_{ij}\right)l + \beta_0^2\mathbf{P}^{(0)}_{ij}\right] + \mathcal{O}(\alpha_s^4)\,.
\end{aligned} \tag{2.97}$$

In the above, the $\mathbf{P}$'s on the right hand side are evaluated at $\mu_f = \mu_r$ and

$$l = \log\frac{\mu_r^2}{\mu_f^2}\,. \tag{2.98}$$

Taking the expansion of α_s into account, it should be noted that Eq. (2.97) can be rewritten as

$$\mathbf{P}_{ij}(\alpha_s(\mu_r^2),\mu_f^2,\mu_r^2)=\frac{\alpha_s(\mu_f^2)}{2\pi}\mathbf{P}_{ij}^{(0)}(x)+\left(\frac{\alpha_s(\mu_f^2)}{2\pi}\right)^2\mathbf{P}_{ij}^{(1)}(x)+\left(\frac{\alpha_s(\mu_f^2)}{2\pi}\right)^3\mathbf{P}_{ij}^{(2)}(x)+\mathcal{O}(\alpha_s^4)\,. \tag{2.99}$$

In Eq. (2.99), explicit scale dependence on μ_r cancels the implicit dependence on μ_r through dependence on α_s and the scale dependence in the splitting function P reduces to a dependence on μ_f only. As a result, the scale evolution of $f(\mu_r^2,\mu_f^2)$ is the same as for $f(\mu_f^2,\mu_f^2)$ and one has $f\equiv f(\mu_f^2)$. Solutions to Eq. (2.96) give the scale evolution of the PDFs and automatically resum logarithms of the form $\alpha_s\log(Q^2/\mu_f^2)$ at leading order in α_s. Physically, these logarithms appear when a particle of virtuality Q^2 radiates down to virtuality μ_F^2 via multiple strongly ordered emissions [84]. It should be noted that scale choices for μ_f should not vary too much from Q^2 to keep the value of $\alpha_s\log(Q^2/\mu_f^2)$ small such that a truncation of a power expansion in α_s is justified for fixed-order predictions. Splittings occurring inside the proton are non-perturbative in their nature and PDFs cannot be determined by a perturbative ansatz. Quantitatively, PDFs are determined from global fits of the PDFs to a selection of so-called standard candle processes at a particular scale. PDFs are provided by several groups which among others include the ABMP [104], CT14 [105], NNPDF3.1 [106], MMHT [107] and HERAPDF2.0 [108] groups. These sets differ in their fit methodology, data selection and error treatment. Detailed comparisons of fit results are done in the context of the PDF4LHC studies [109]. Once the PDF is determined at a particular perturbative scale however, it can be evolved using the Altarelli-Parisi evolution in Eq. (2.96) to give the PDF at any other perturbative scale. In Fig. 4, a comparison of PDFs at $\mu_f=10$ GeV and $\mu_f=100$ GeV is shown. It can be seen that at larger scales more splittings are resolved and the number of partons at smaller values of x increases. Consequently, the probability of finding partons at larger x decreases as more partons are radiated down to smaller values of x.

Finally, Eq. (2.96) can also be solved to fixed order in α_s such that the aforementioned logarithms are not resummed to all orders. At fixed order, the value of a PDF at a scale μ_1 is then related to the PDF value at some other scale μ_f by

$$\begin{aligned}f_i(\mu_1^2)=f_i(\mu_f^2)&-\frac{\alpha_s(\mu_r)}{2\pi}\mathbf{P}_{ij}^{(0)}\otimes f_j(\mu_f^2)L_F\\&-\left(\frac{\alpha_s(\mu_r^2)}{2\pi}\right)^2\left[\mathbf{P}_{ij}^{(1)}\otimes f_j(\mu_f)L_F-\frac{1}{2}\mathbf{P}_{ij}^{(0)}\otimes\mathbf{P}_{jk}^{(0)}\otimes f_k(\mu_f^2)L_F\right.\\&\left.+\mathbf{P}_{ij}^{(0)}\otimes f_j(\mu_f^2)\beta_0\left(l+\frac{1}{2}L_F\right)\right]+\mathcal{O}(\alpha_s^3)\,,\end{aligned} \tag{2.100}$$

where

$$L_F=\log\frac{\mu_f^2}{\mu_1^2}\,. \tag{2.101}$$

The above will be of importance when the scale dependence of cross sections is discussed in Section 2.10.

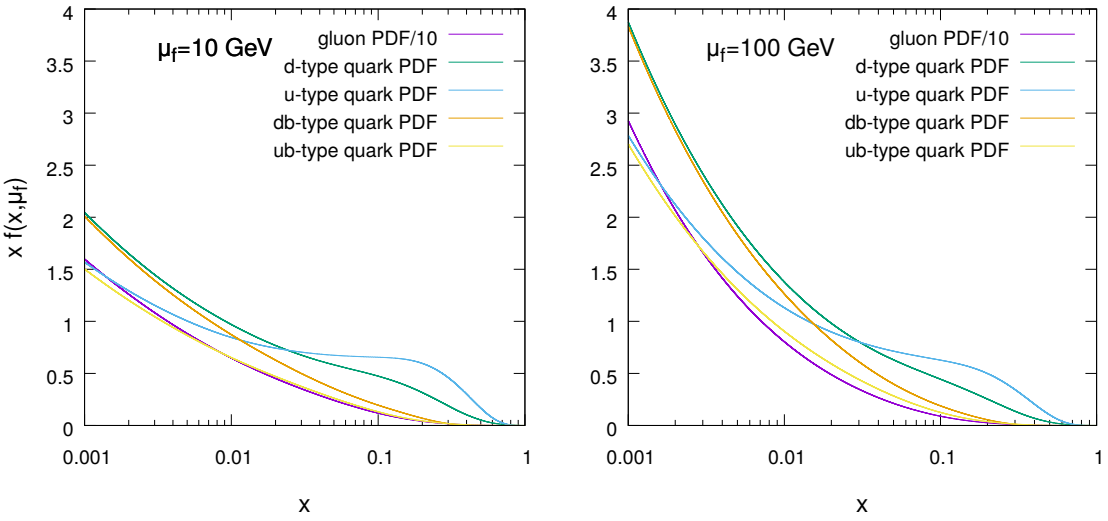

Figure 4. Plot showing the evolution of PDFs with μ_f for $\mu_f = 10$ GeV on the left and $\mu_f = 100$ GeV on the right as determined by NNPDF3.0 with $\alpha_s(M_Z) = 0.118$.

A systematic generalisation of the above analysis was given by Collins and Soper in 1987 [110] and goes under the name of factorisation theorem of QCD. The theorem states that initial-state collinear singularities factorise universally from the hard scattering process and can be systematically absorbed into a redefinition of the PDFs. After renormalistion, the cross section can be written in terms of mass unrenormalised partonic cross sections $\mathrm{d}\hat{\tilde{\sigma}}$ and bare PDFs f_0 as

$$\mathrm{d}\sigma = \sum_{i=q,\bar{q},g} \int_0^1 \frac{\mathrm{d}\xi}{\xi}\, f_{0,i}(\xi)\mathrm{d}\hat{\tilde{\sigma}}_i(\xi p_1, \mu_r^2)\,, \tag{2.102}$$

where the factor $1/\xi$ originates from the relation of the parton to the proton flux and is here explicitly written out. Inserting Eq. (2.88) into Eq. (2.102) to replace the bare PDF with renormalised PDFs gives

$$\mathrm{d}\sigma = \sum_{i=q,\bar{q},g} \int_0^1 \frac{\mathrm{d}\xi}{\xi} \int_\xi^1 \frac{\mathrm{d}z}{z} f_j(\frac{\xi}{z}, \mu_f^2)\mathbf{\Gamma}_{ij}^{-1}(z,\alpha_s)\mathrm{d}\hat{\tilde{\sigma}}_i(\xi p_1, \mu_r^2, \mu_f^2)\,. \tag{2.103}$$

Rescaling $\xi \to z\xi$ results in

$$\mathrm{d}\sigma = \sum_{i=q,\bar{q},g} \int_0^1 \frac{\mathrm{d}\xi}{\xi} \int_0^1 \frac{\mathrm{d}z}{z} f_j(\xi, \mu_f^2)\mathbf{\Gamma}_{ij}^{-1}(z,\alpha_s)\mathrm{d}\hat{\tilde{\sigma}}_i(z\xi p_1, \mu_r^2, \mu_f^2)\,. \tag{2.104}$$

From the above, mass renormalisation counterterms can be defined order by order by expanding both $\mathrm{d}\hat{\tilde{\sigma}}$ and $\Gamma^{-1}(z,\alpha_s)$ in α_s. Defining the mass renormalised partonic cross section $\mathrm{d}\hat{\sigma}$ as

$$\mathrm{d}\hat{\sigma} = \mathrm{d}\hat{\tilde{\sigma}} + \mathrm{d}\hat{\sigma}^{MF}, \tag{2.105}$$

to all orders in pertubation theory, the mass factorisation counterterms are given by

$$\mathrm{d}\hat{\sigma}^{MF}_{i,NLO}(\xi p_{\hat{1}}) = -\int \frac{\mathrm{d}x}{x}\left(\frac{\alpha_s}{2\pi}\right)\bar{C}(\epsilon)\mathbf{\Gamma}^{(1)}_{ji}\mathrm{d}\hat{\sigma}_{j,LO}(z\xi p_{\hat{1}})\,,$$

$$
\begin{aligned}
\mathrm{d}\hat{\sigma}^{MF}_{i,NNLO}(\xi p_{\hat{1}}) = &-\int \frac{\mathrm{d}x}{x}\left(\frac{\alpha_s}{2\pi}\right)^2 \bar{C}(\epsilon)^2 \mathbf{\Gamma}^{(2)}_{ji}\mathrm{d}\hat{\sigma}_{j,LO}(z\xi p_{\hat{1}}) \\
&+\int \frac{\mathrm{d}x}{x}\left(\frac{\alpha_s}{2\pi}\right)^2 \bar{C}(\epsilon)^2 \mathbf{\Gamma}^{(1)}_{jk}\otimes\mathbf{\Gamma}^{(1)}_{ki}\mathrm{d}\hat{\sigma}_{j,LO}(z\xi p_{\hat{1}}) \\
&-\int \frac{\mathrm{d}x}{x}\left(\frac{\alpha_s}{2\pi}\right) \bar{C}(\epsilon) \mathbf{\Gamma}^{(1)}_{ji}\mathrm{d}\hat{\sigma}_{j,NLO}(z\xi p_{\hat{1}})\,.
\end{aligned}
\tag{2.106}
$$

Using these results, Eq. (2.102) can be rewritten as

$$
\mathrm{d}\sigma = \sum_{i=q,\bar{q},g}\int_0^1 \frac{\mathrm{d}\xi}{\xi}\, f_i(\xi,\mu_f^2)\int_0^1 \frac{\mathrm{d}z}{z}\mathrm{d}\hat{\sigma}_i(z, z\xi p_1, \mu_r^2, \mu_f^2)\,, \tag{2.107}
$$

which defines the master formula to be evaluated in theoretical calculations of lepton-hadron cross sections. Finally note that Eq. (2.107) is only valid in the high energy limit as in this case higher twist effects can be neglected [111].

2.10 Scale dependence of cross sections

For lepton-hadron collisions in which the Born process starts at $\mathcal{O}(\alpha_s^n)$, the total cross section can be written in terms of perturbative coefficients $\hat{\sigma}^{(n)}$ at scale $\mu_f = \mu_r = \mu_0$ as

$$
\begin{aligned}
\sigma(\mu_0^2,\mu_0^2,\alpha_s(\mu_0^2)) = &\left(\frac{\alpha(\mu_0)}{2\pi}\right)^n \hat{\sigma}_i^{LO}\otimes f_i(\mu_f^2) \\
&+\left(\frac{\alpha(\mu_0)}{2\pi}\right)^{n+1} \hat{\sigma}_i^{NLO}\otimes f_i(\mu_f^2) \\
&+\left(\frac{\alpha(\mu_0^2)}{2\pi}\right)^{n+2} \hat{\sigma}_i^{NNLO}\otimes f_i(\mu_f^2) + \mathcal{O}(\alpha_s^{n+3})\,.
\end{aligned}
\tag{2.108}
$$

In the above, the $\hat{\sigma}^{(n)}$ are stripped off their α_s-dependence to make the dependence on α_s explicit in their corresponding prefactors. Using the results on the scale dependence to fixed order in α_s for the running of the coupling and for the PDF given in Eq. (2.31) and Eq. (2.100), respectively, the scale dependence of the coefficient in terms of $\log(\mu_r^2)$ and $\log(\mu_f^2)$ can be predicted to NNLO as

$$
\begin{aligned}
&\sigma(\mu_r,\mu_f,\alpha_s(\mu_r),L_r,L_f) = \\
&\left(\frac{\alpha_s(\mu_r)}{2\pi}\right)\hat{\sigma}_i^{LO}\otimes f_i(\mu_f) + \left(\frac{\alpha_s(\mu_r)}{2\pi}\right)^2 \hat{\sigma}_i^{NLO}\otimes f_i(\mu_f) \\
&+L_r\left(\frac{\alpha_s(\mu_r)}{2\pi}\right)^2 \beta_0\,\hat{\sigma}_i^{LO}\otimes f_i(\mu_f) + L_f\left(\frac{\alpha_s(\mu_r)}{2\pi}\right)^2\Big[-\hat{\sigma}_i^{LO}\otimes\left(P^0_{ik}\otimes f_k(\mu_f)\right)\Big] \\
&+\left(\frac{\alpha_s(\mu_r)}{2\pi}\right)^3 \hat{\sigma}_i^{NNLO}\otimes f_i(\mu_f) + L_r\left(\frac{\alpha_s(\mu_r)}{2\pi}\right)^3\left(2\,\beta_0\,\hat{\sigma}_i^{NLO} + \beta_1\,\hat{\sigma}_i^{LO}\right)\otimes f_i(\mu_f) \\
&+L_r^2\left(\frac{\alpha_s(\mu_r)}{2\pi}\right)^3 \beta_0^2\,\hat{\sigma}_i^{LO}\otimes f_i(\mu_f) \\
&+L_f\left(\frac{\alpha_s(\mu_r)}{2\pi}\right)^3\Big[-\hat{\sigma}_i^{NLO}\otimes\left(P^0_{ik}\otimes f_k(\mu_f)\right) - \hat{\sigma}_i^{LO}\otimes\left(P^1_{ik}\otimes f_k(\mu_f)\right)\Big]
\end{aligned}
$$

$$+L_f^2\left(\frac{\alpha_s(\mu_r)}{2\pi}\right)^3\left[\frac{1}{2}\hat{\sigma}_i^{LO}\otimes\left(P_{ik}^0\otimes P_{kl}^0\otimes f_l(\mu_f)\right)+\frac{1}{2}\beta_0\,\hat{\sigma}_i^{LO}\otimes\left(P_{ik}^0\otimes f_k(\mu_f)\right)\right]$$
$$+L_fL_r\left(\frac{\alpha_s(\mu_r)}{2\pi}\right)^3\left[-2\,\beta_0\,\hat{\sigma}_i^{LO}\otimes\left(P_{ik}^0\otimes f_k(\mu_f)\right)\right]+\mathcal{O}(\alpha_s^4) \tag{2.109}$$

with

$$L_r=\log\frac{\mu_r^2}{\mu_0^2},\quad L_f=\log\frac{\mu_f^2}{\mu_0^2}\,. \tag{2.110}$$

Eq. (2.109) can be used as a powerful check to ensure that the scale dependence of calculated cross sections is indeed correct and allows to evolve results obtained at some reference scale to any other scale a posteriori (using the APPLfast-interface).

2.11 Methods for numerical evaluation of cross sections

To calculate observables to a particular fixed order in α_s with particles l and m in the initial states and n particles in the final state, one has to evaluate general expressions of the form

$$\mathrm{d}\hat{\sigma}_{lm}(p_{\hat{1}},p_{\hat{2}};p_3,\cdots,p_{n+2})=\mathcal{N}_{lm}\sum_n\frac{1}{S_n}\mathrm{d}\Phi_n M_{n+2}^{\ell}(p_{\hat{1}},p_{\hat{2}};p_3,\cdots,p_{n+2})J_{n_B}^n(\{p\}_n)\,. \tag{2.111}$$

Here the sum $\sum_n$ is over all matrix elements that have n particles in the final state, with corresponding momentum set $\{p\}_n$ and the symmetry factor S_n depends on the particle content of the matrix element. The phase space measure $\mathrm{d}\Phi_n$ is defined in Eq. (2.81) and ℓ gives the loop order of the correction. Different experimental setups are implemented in the jet function $J_{n_B}^n$ that requires n_B jets, the number of jets defining the Born-level (leading-order) process, to pass the experimental cuts starting from n final state partons in the hard matrix element. The parameter $\mathcal{N}_{lm}$ gives the QCD-independent factors and the dependence on the strong coupling constant α_s for initial states l and m. For each contribution to the fixed-order calculation the value of $\mathcal{N}_{lm}$ is different. For the Born-level process of di-jet and tri-jet production in neutral current DIS and electron-positron annihilation, one has

$$\mathcal{N}_{lm}^B=4(4\pi\alpha)^2V\mathcal{C}_l\mathcal{C}_m\mathcal{S}_{lm}\left(\frac{\alpha_s}{2\pi}\right)\frac{\bar{C}(\epsilon)}{C(\epsilon)}\,, \tag{2.112}$$

where $V=N^2-1$ and α is the fine structure constant. The initial-state colour averaging factor for the incoming particles is given by

$$\mathcal{C}_q=\frac{1}{N}\,,\quad \mathcal{C}_g=\frac{1}{V}\,,\quad \mathcal{C}_e=1\,, \tag{2.113}$$

and the initial-state spin averaging factors are given by

$$\mathcal{S}_{lm}=\frac{1}{s_l s_m}\,, \tag{2.114}$$

where the number of spin states for the various initial-state particles are given by $s_e=s_q=2,\ s_g=2(1-\epsilon)$. Further, the factors

$$C(\epsilon)=\frac{(4\pi)^\epsilon}{8\pi^2}e^{-\epsilon\gamma}\ ,\ \bar{C}(\epsilon)=8\pi^2C(\epsilon) \tag{2.115}$$

which arise from dimensional regularisation, are introduced, where $\bar{C}$ is already defined in Eq. (2.83).

The factor at Born level in Eq. (2.112) is related to the corresponding factor at Born level for single-jet production in DIS by

$$\mathcal{N}_{lm}^{B,1j} = \frac{N}{V}\left(\frac{\alpha_s}{2\pi}\right)^{-1}\left(\frac{\bar{C}(\epsilon)}{C(\epsilon)}\right)^{-1}\mathcal{N}_{lm}^{B}\,. \tag{2.116}$$

Calculations up to NNLO order involve the calculation of a Born-level process (B), a real (R) and a virtual (V) correction that come in at NLO plus virtual-virtual (VV), real-virtual (RV) and double-real (RR) corrections appearing at NNLO. Each of these contributions come with a different overall factor $\mathcal{N}$ which are in general related via

$$\begin{aligned}
\mathcal{N}_{lm}^{V} &= \mathcal{N}_{lm}^{B}\left(\frac{N\alpha_s}{2\pi}\right)\bar{C}(\epsilon)\,,\\
\mathcal{N}_{lm}^{R} &= \mathcal{N}_{lm}^{B}\left(\frac{N\alpha_s}{2\pi}\right)\frac{\bar{C}(\epsilon)}{C(\epsilon)}\,,\\
\mathcal{N}_{lm}^{VV} &= \mathcal{N}_{lm}^{B}\left(\frac{N\alpha_s}{2\pi}\right)^2\bar{C}(\epsilon)^2\,,\\
\mathcal{N}_{lm}^{RV} &= \mathcal{N}_{lm}^{B}\left(\frac{N\alpha_s}{2\pi}\right)^2\frac{\bar{C}(\epsilon)^2}{C(\epsilon)}\,,\\
\mathcal{N}_{lm}^{RR} &= \mathcal{N}_{lm}^{B}\left(\frac{N\alpha_s}{2\pi}\right)^2\frac{\bar{C}(\epsilon)^2}{C(\epsilon)^2}\,.
\end{aligned} \tag{2.117}$$

Analytic evaluation of the phase space integral is in general extremely difficult, if not impossible, for generic experimental setups and measurements. For this reason, expressions in Eq. (2.111) are evaluated numerically. To perform numerical integration of the phase space integral in Eq. (2.111), potential infrared singularities have to be cancelled and moved across different partonic multipliticites. At NLO well-established subtraction methods exist, which include the Frixione-Kunszt-Signer (FKS) [112], phase space slicing [113–116], the Catani-Seymour dipole subtraction [117] and the sector decomposition [118–120] method. In the following, two different approaches that are phase space slicing in the context of q_T- and N-jettiness subtractions and the concept of genuine subtraction methods at NNLO accuracy in QCD will be discussed.

In naive slicing methods, the integral over the real phase space is split up into a resolved and several unresolved regions. Resolved and unresolved regions are classified by identifying and comparing all possible kinematic invariants s_{ij} for every pair of particles i and j against an arbitrary cut parameter s_{cut}. The constraint $s_{ij} > s_{cut}$ for all particle pairs i, j defines the resolved region, unresolved regions can be classified into different singularity regions, i.e. collinear or soft, depending on the size of particular invariants compared to s_{cut}. In the resolved region, the integrand is finite and can be directly evaluated numerically. In a particular unresolved phase space region, the matrix element is approximated by a function that has the same singularity structure as the matrix element in that region. Using factorisation properties of the phase space in unresolved regions, these functions can then

be analytically integrated and added to the virtual correction. To get the correct result, some care has to be taken in choosing the right value of s_{cut}. On the one hand a too small value for s_{cut} ultimately leads to numerical instabilities. On the other hand a too large value for s_{cut} might cause relevant contributions of the matrix element in the unresolved region to be missed. As a result, an ideal value of s_{cut} has to be found that minimises the competing effects to give the best result.

An example of a more sophisticated slicing method is given by the q_T-subtraction method and the following discussion follows the one given in Ref. [121]. To give a sketch of the method, we consider the production of a colourless final state F of invariant mass Q in a proton-proton collision given by

$$p_1 + p_2 \to F(Q) + X\,, \tag{2.118}$$

where p_1, p_2 and X stand for the two incoming and proton remnants, respectively. At leading order, the final state F is constrained to have zero transverse momentum q_T, however, if higher-order radiative corrections are included, F is produced at a $q_T \neq 0$. Using an appropriate subtraction method such as Catani-Seymour dipole subtraction to evaluate F+jet production to NLO accuracy, the cross section at NNLO can be written as

$$\mathrm{d}\sigma^F_{NNLO}\Big|_{q_T\neq 0} = \mathrm{d}\sigma^{F+jet}_{NLO}\,, \tag{2.119}$$

where the constraint $q_T \neq 0$ excludes double-unresolved in real-real and single-unresolved configurations in real-virtual corrections. To subtract the singularities in the limit $q_T \to 0$, a counterterm is introduced that can be written as

$$\mathrm{d}\sigma^{CT} = \mathrm{d}\sigma^F_{LO} \otimes \Sigma^F(q_T/Q)\mathrm{d}^2\mathbf{q}_T\,, \tag{2.120}$$

where it has been exploited that F is produced at $q_T = 0$ at Born kinematics to identify NNLO infrared configurations. The particular expression for $\mathrm{d}\sigma^{CT}$ comes out as a result from the resummation of logarithmically-enhanced contributions to transverse momentum distributions [121]. In particular one has

$$\Sigma^F(q_T/Q) \to_{q_T\to 0} \sum_{n=1}^{\infty}\left(\frac{\alpha_s}{\pi}\right)^n \sum_{k=1}^{2n} \Sigma^{F(n;k)} \frac{Q^2}{q_T^2} \ln^{k-1}\frac{Q^2}{q_T^2}\,, \tag{2.121}$$

with $\Sigma^{F(n;k)}$ being q_T-independent coefficients. The counterterm has to be integrated and added back to the cross section. To this end, the hard collinear function $\mathcal{H}$ is introduced, which also includes the virtual-virtual correction and can be written as

$$\mathcal{H}^F = 1 + \frac{\alpha_s}{\pi}\mathcal{H}^{F(1)} + \left(\frac{\alpha_s}{\pi}\right)^2 \mathcal{H}^{F(2)} + \cdots\,. \tag{2.122}$$

The total NNLO cross section can then finally be written as

$$\mathrm{d}\sigma^F_{NNLO} = \mathcal{H}^F_{NNLO} \otimes \mathrm{d}\sigma^F_{LO} + \left[\mathrm{d}\sigma^{F+jets}_{NLO} - \mathrm{d}\sigma^{CT}_{NLO}\right]\,. \tag{2.123}$$

In practice a cut parameter s_{cut} is introduced to separate the (q_T=0)-region from the resolved region, where the value of s_{cut} has to be chosen sufficiently small such that potential

power corrections, i.e. the non-singular contributions in the unresolved region, can be neglected and this classifies q_T-subtraction as a slicing method. Currently q_T-subtraction is limited to the production of colourless final states, an extension to this method such that singularities appearing in colourful final states can be subtracted, is provided by the N-jettiness subtraction method [122].

Given an M-particle phase space Φ_M, the N-jettiness observable with initial-state particles a and b is defined as [123]

$$\mathcal{T}_N = \sum_i \sum_{k=1}^{M} \min_i \left\{ \frac{2q_i \cdot p_k}{Q_i} \right\} = \sum_{i=a,b,1,\cdots,N} \mathcal{T}_N^i \,, \tag{2.124}$$

where the p's are final-state momenta, the q's massless Born momenta including the initial states and the Qs are normalisation factors that can be defined in several ways. The q's are projected out by clustering final-state momenta according to standard jet algorithms and define the jet-axes. At leading order, $\mathcal{T}_N = 0$ while higher-order radiative corrections lead to $\mathcal{T}_N > 0$. Using soft collinear effective field theory (SCET), the singular structure of the cross section for $\mathcal{T}_N \to 0$ can be predicted via

$$\frac{\mathrm{d}\sigma^{\mathrm{sing}}}{\mathrm{d}\mathcal{T}_N} = \int \left[\prod_i \mathrm{d}\mathcal{T}_N^i\right] \frac{\mathrm{d}\sigma^{\mathrm{sing}}}{\mathrm{d}\mathcal{T}_N^a \mathrm{d}\mathcal{T}_N^b \mathrm{d}\mathcal{T}_N^1 \cdots \mathrm{d}\mathcal{T}_N^N} \delta(\mathcal{T}_N - \sum_i \mathcal{T}_N^i) \,, \tag{2.125}$$

with

$$\begin{aligned} \frac{\mathrm{d}\sigma^{\mathrm{sing}}}{\mathrm{d}\mathcal{T}_N^a \mathrm{d}\mathcal{T}_N^b \mathrm{d}\mathcal{T}_N^1 \cdots \mathrm{d}\mathcal{T}_N^N} &= \int \mathrm{d}t_a B_a(t_a, x_a, \mu) \int \mathrm{d}t_b B_b(t_b, x_b, \mu) \left[\prod_{i=1}^{N} \int \mathrm{d}s_i J_i(s_i, \mu)\right] \\ &\cdot \vec{C}^\dagger(\mu) \hat{S}_\kappa(\mathcal{T}_N^a - \frac{t_a}{Q_a}, \cdots, \mathcal{T}_N^N - \frac{s_N}{Q_N}, \{\frac{q_i}{Q_i}\}, \mu) \vec{C}(\mu) \,, \end{aligned} \tag{2.126}$$

where the $B_{a/b}$'s are the beam functions, the J's the jet functions, the C's the hard Wilson coefficients and S the soft function that is a matrix in the colour space of partonic channel κ and μ is an artificial scale [123–125]. Similarly as in the case of q_T-subtraction the cross section can then be sliced into a non-singular (nons) and a singular (sing) contribution and can be evaluated via

$$\sigma^{\mathrm{NNLO}} = \sigma^{\mathrm{sing}}(\mathcal{T}_{\mathrm{off}}) + \left[\int_{T_\delta} \mathrm{d}\mathcal{T}_N \frac{\mathrm{d}\sigma^{\mathrm{nons}}}{\mathrm{d}\mathcal{T}_N}\right] - \left[\int_{T_\delta}^{\mathcal{T}_{\mathrm{off}}} \mathrm{d}\mathcal{T}_N \frac{\mathrm{d}\sigma^{\mathrm{sing}}}{\mathrm{d}\mathcal{T}_N}\right] + \mathcal{O}(\delta_{IR}) \,, \tag{2.127}$$

where the value of $\mathcal{T}_{\mathrm{off}}$ is arbitrary and cancels between the first and third term. By approximating the radiative contribution below the cutoff T_δ by the singular behaviour of the real radiation only, terms of $\mathcal{O}(\delta_{IR})$ are neglected with $\delta_{IR} = \mathcal{T}_\delta / Q$. So far many processes have been successfully calculated with the above slicing methods at NNLO QCD accuracy in recent years and include $pp \to \gamma\gamma$ [54], $pp \to VH$ [55], $pp \to V\gamma$ [56], $pp \to W + j$ [61], $pp \to Z + j$ [63], $pp \to \gamma + X$ [64],$pp \to ZZ$ [65], $pp \to WW$ [66], $pp \to ZW$ [67] and $ep \to 1j$ [68].

In genuine subtraction methods on the other hand, explicit subtraction terms are constructed that have the same singularity structure as the correction and no other singularities. These subtraction terms are required to be sufficiently simple to allow analytic

integration over the unresolved parton's phase space such that the integrated version of the subtraction term can be added to the virtual corrections. Consequently, the overall effect is a shift of the singularities across different phase space multiplicities to enable explicit infrared singularity cancellation. Schematically, this can be expressed as

$$\begin{aligned}\hat{\sigma}_{ij}^{NLO} = &\int_{\mathrm{d}\Phi_{n+1}} \left[\mathrm{d}\hat{\sigma}_{ij}^{R} - \mathrm{d}\hat{\sigma}_{NLO,ij}^{S}\right] \\ &+ \int_{\mathrm{d}\Phi_{n}} \left[\mathrm{d}\hat{\sigma}_{ij}^{V} - \mathrm{d}\hat{\sigma}_{ij,NLO}^{T}\right] \,, \end{aligned} \tag{2.128}$$

where $\mathrm{d}\hat{\sigma}_{NLO,ij}^{S}$ and $\mathrm{d}\hat{\sigma}_{NLO,ij}^{T}$ are the NLO real and virtual subtraction terms, respectively. Formally one can write the virtual subtraction terms as

$$\mathrm{d}\hat{\sigma}_{NLO,ij}^{T} = \int_{\mathrm{d}\Phi_{one-\mathrm{particle}}} \left[-\mathrm{d}\hat{\sigma}_{NLO,ij}^{S} - \mathrm{d}\hat{\sigma}_{NLO,ij}^{MF}\right] \,, \tag{2.129}$$

where $\mathrm{d}\hat{\sigma}_{NLO,ij}^{MF}$ are the mass factorisation terms that subtract the infrared poles associated with initial-state splittings. Similarly, one can write for the NNLO corrections

$$\begin{aligned}\hat{\sigma}_{ij}^{NNLO} = &\int_{\mathrm{d}\Phi_{n+2}} \left[\mathrm{d}\hat{\sigma}_{ij}^{RR} - \mathrm{d}\hat{\sigma}_{NNLO,ij}^{S}\right] \\ &+ \int_{\mathrm{d}\Phi_{n}} \left[\mathrm{d}\hat{\sigma}_{ij}^{RV} - \mathrm{d}\hat{\sigma}_{ij,NNLO}^{T}\right] \\ &+ \int_{\mathrm{d}\Phi_{n}} \left[\mathrm{d}\hat{\sigma}_{ij}^{VV} - \mathrm{d}\hat{\sigma}_{ij,NNLO}^{U}\right] \,. \end{aligned} \tag{2.130}$$

At NNLO, double-unresolved infrared as well as single radiative infrared limits in one-loop corrections have to be subtracted, in contrast to NLO subtractions. These additional infrared limits make NNLO subtractions a lot more difficult than NLO subtractions. At the moment two such subtraction methods exist at NNLO which are the CoLorFul-NNLO [47, 126] and the antenna subtraction method. For calculations presented in this work, the antenna subtraction was applied and the formalism will be discussed in more detail in the following section. The method of Projection-To-Born was recently proposed and applied successfully to vector boson fusion in the structure function approximation at NNLO [72] and provides yet another subtraction procedure. It is this method we use to calculate single-jet production in DIS in the laboratory frame to N3LO QCD accuracy. The method is described in more detail in Section 12.

3 Antenna subtraction

3.1 Antenna functions

The basic idea of antenna subtraction is the construction of counterterms according to infrared factorisation properties of partial colour-ordered squared amplitudes in unresolved limits, using antenna functions as fundamental building blocks. All antenna functions are constructed from colour-ordered squared matrix elements derived from physical processes and contain two particles that act as hard radiators from which further potentially unresolved particles are radiated. The following three combinations of hard radiators exist:

1. Quark-antiquark: Derived from virtual photon decay into a massless quark-antiquark pair [127].

2. Quark-gluon: Derived from neutralino to gluon-gluino decay [128].

3. Gluon-gluon: Derived from Higgs to gluon-gluon decay [129].

A three-particle antenna function X_3^0 is defined as

$$X_3^0(i,j,k) = \mathcal{S}\frac{M_3^0(p_i,p_k,p_j)}{M_2^0(p_I,p_K)}\,, \tag{3.1}$$

where $\mathcal{S}$ accounts for potential corrections due to a difference in symmetry factors of the three-particle to the two-particle squared matrix element and $s_{IK} = s_{ij} + s_{ik} + s_{jk}$. The normalisation to the two-parton squared matrix element M_2^0 ensures that the antenna function only gives the relevant divergent function when particle j becomes unresolved between hard radiators i and k. At NNLO, singularities from double-unresolved configurations in tree level and single-unresolved configurations in one-loop corrections have to be subtracted. Infrared divergent kernels in double-unresolved configurations are reproduced by four-particle antenna functions

$$X_4^0(i,j,k,l) = \mathcal{S}\frac{M_4^0(p_i,p_j,p_k,p_l)}{M_2^0(p_I,p_L)}\,. \tag{3.2}$$

The more complicated divergence structure at NNLO requires the introduction of an additional function, the soft factor, which is given by

$$S_{ijk} = \frac{2s_{ik}}{s_{ij}s_{jk}}\,, \tag{3.3}$$

to subtract all QCD singularities at NNLO in the framework of antenna subtraction. The soft factor is nothing other than the soft eikonal factor that enables the explicit subtraction of soft singularities when the momentum of particle j colour-neighbouring particles i and k vanishes.

At the real-virtual level, single-unresolved divergences in one-loop corrections are reconstructed by one-loop–three-particle antenna functions which are given by

$$X_3^1(p_i,p_j,p_k,\mu_r) = \mathcal{S}\frac{M_3^1(p_i,p_j,p_k,\mu_r)}{M_2^0(p_I,p_J)} - X_3^0(p_i,p_j,p_k)M_2^1(p_I,p_K,\mu_r)M_2^0(I,K)\,, \tag{3.4}$$

where the one-loop antenna function is UV-renormalised at a scale $\mu_r = s_{IK}$. By using the substitution

$$X_3^1(p_i,p_j,p_k) \to X_3^1(p_i,p_j,p_k) - \frac{\beta_0}{\epsilon} X_3^0(p_i,p_j,p_k) \left(\left(\frac{|s_{IK}|}{\mu^2} \right)^{-1} - 1 \right) , \tag{3.5}$$

the renormalisation scale of the one-loop antenna function can be shifted from $\mu_r = s_{IK}$ to any arbitrary scale $\mu_r = \mu$. The (tree)×(loop)-singularity is explicitly subtracted in the one-loop–three-particle antenna such that X_3^1 only gives the one-loop soft eikonal factor or splitting kernels in relevant unresolved configurations. In some cases, none of the particles in the antenna are protected from becoming unresolved and one such example is given by the full F_3^0 antenna in which hard radiators cannot be uniquely identified. In addition to this, it is sometimes necessary to reduce the number of unresolved limits in a particular antenna to be able to construct appropriate subtraction terms. Both problems are solved by splitting problematic antenna functions into sub-antennae using partial fractioning which is nothing else than using the algebraic identity

$$\frac{1}{xy} = \frac{1}{x+y} \left(\frac{1}{x} + \frac{1}{y} \right) , \tag{3.6}$$

where x and y are kinematic invariants in the context of antenna functions. Finally, antenna functions with initial-state hard radiators are obtained by crossing and this is achieved by inverting the sign of each Lorentz-invariant s_{ij} of particles i and j in which either particle i or j is in the initial state. With this convention, the expressions of antennae as a function of Lorentz invariants remain unchanged.

A list of all antenna and their sub-antenna functions that are required to subtract the QCD singularities up to NNLO for the calculations of this thesis are given together with relevant references in Table 1. Antennae in initial-final kinematics can be obtained from their final-final counterparts by crossing relevant particles into the initial state.

3.2 Phase space factorisation

One ingredient to the antenna subtraction formalism are the factorisation properties of colour-ordered corrections, a second ingredient is the factorisation of phase space measures under suitable linear mappings. These mappings result in momenta that fulfill the following characteristics:

1. Be on their mass-shell.
2. Respect the symmetries of the original momentum set.
3. Tend to the appropriate resolved momenta in a particular unresolved limit.
4. Allow the phase space to factorise.

In general, the mappings depend on the number of particles that are mapped out, at NLO this is one and at NNLO up to two particles, as well as on the number of initial-state particles involved in the mappings. In the following, only final-final mappings and initial-final mappings will be discussed as initial-initial mappings are of no relevance to the calculations presented in this thesis.

X_3^0 antennae	Comments
A_3^0	Eq. (5.5) of [92].
$a_{3,g\to q}^0$	Only contains $i_1 \| \| i_2$ collinear limit.
	Flavour changing $g \to q$.
D_3^0	Eq. (6.8) of [92].
	$D_3^0 = d_3^0(i_1, i_2, i_3) + d_3^0(i_1, i_3, i_2)$.
d_3^0	Eq. (6.13) of [92]. Only has i_2 soft limit.
$d_{3,g\to q}^0$	Eq. (4.28) of [130]. Flavour changing $g \to q$.
E_3^0	Eq. (6.14) of [92].
F_3^0	Eq. (7.9) of [92].
	$F_3^0 = f_3^0(i_1, i_2, i_3) + f_3^0(i_2, i_3, i_1) + f_3^0(i_3, i_1, i_2)$.
f_3^0	Eq. (7.13) of [92]. Only has i_2 soft limit.
G_3^0	Eq. (7.14) of [92]. Only has $i_2 \| \| i_3$ collinear limit.
S^{FF}	Eq. (3.30) of [131].
X_3^1 antennae	
A_3^1	Eqs. (5.12) and (5.13) of [92].
$\hat{A}_3^1$	Eqs. (5.16) and (5.17) of [92].
$\tilde{A}_3^1$	Eqs. (5.14) and (5.15) of [92].
D_3^1	Eqs. (6.18) and (6.19) of [92].
	$D_3^1 = d_3^1(i_1, i_2, i_3) + d_3^1(i_1, i_3, i_2)$.
d_3^1	Only has i_2 soft limit.
$\hat{D}_3^1$	Eqs. (6.20) and (6.21) of [92].
	$\hat{D}_3^1 = \hat{d}_3^1(i_1, i_2, i_3) + \hat{d}_3^1(i_1, i_3, i_2)$.
$\hat{d}_3^1$	Only has i_2 soft limit.
	$F_3^1 = f_3^1(i_1, i_2, i_3) + f_3^1(i_2, i_3, i_1) + f_3^1(i_3, i_1, i_2)$.
E_3^1	Eqs. (6.28) and (6.29) of [92].
$\hat{E}_3^1$	Eqs. (6.32) and (6.33) of [92].
$\tilde{E}_3^1$	Eqs. (6.30) and (6.31) of [92].
X_4^0 antennae	
A_4^0	Eqs. (5.27) and (5.29) of [92].
$\tilde{A}_4^0$	Eqs. (5.28) and (5.30) of [92].
$\tilde{A}_4^{0,a}$	Eqs. (3.16) and (3.17) of [131] and Eq. (5.30) of [92].
B_4^0	Eqs. (5.37) and (5.38) of [92].
C_4^0	Eqs. (5.42) and (5.43) of [92].
D_4^0	Eqs. (6.43) and (6.44) of [92].
$D_4^{0,a}$	Eq. (3.23) of [131].
$D_4^{0,c}$	Eq. (3.23) of [131].
E_4^0	Eq. (6.48) of [92].
$E_4^{0,a}$	Eq. (3.18) of [131].
$E_4^{0,b}$	Eq. (3.19) of [131].
$\tilde{E}_4^0$	Eqs. (6.49) and (6.50) of [92].

Table 1. List of relevant X_3^0, X_3^1 and X_4^0 antennae in final-final kinematics.

3.2.1 Final-final kinematics

In a general phase space mapping, momenta of potentially unresolved particles are mapped out. In any antenna function, potential unresolved particles always have hard radiators associated to them. Now the mappings are such that only the momenta of the associated hard radiators are altered in the reduced momentum set in which unresolved momenta are removed. Momenta of all remaining particles are unchanged. We explicitly take the hard radiators to be i and k and the unresolved particle to be j. Then, phase space mappings suitable for single-unresolved radiation in final-final kinematics are given by [132]

$$\begin{aligned} p_I^\mu &= p_{\widetilde{ij}}^\mu = x p_i^\mu + r p_j^\mu + z p_k^\mu, \\ p_K^\mu &= p_{\widetilde{jk}}^\mu = (1-x) p_i^\mu + (1-r) p_j^\mu + (1-z) p_k^\mu \,. \end{aligned} \tag{3.7}$$

It can be seen that $p_I + p_K = p_i + p_j + p_k$ and momentum is conserved independently of the values of x, y and z. In shorthand notation, the mapping may be written as

$$\{i, j, k\} \to \{I, K\} \,, \tag{3.8}$$

and the parameters x, r, z in Eq. (3.7) are given by

$$\begin{aligned} x &= \frac{1}{2(s_{ij} + s_{ik})} \left[(1+\rho) s_{ijk} - 2 r s_{jk} \right] , \\ r &= \frac{s_{jk}}{s_{ij} + s_{jk}} \,, \\ z &= \frac{1}{2(s_{jk} + s_{ik})} \left[(1-\rho) s_{ijk} - 2 r s_{ij} \right] , \\ \rho &= \left[1 + \frac{4 r (1-r) s_{ij} s_{jk}}{s_{ijk} s_{ik}} \right]^{\frac{1}{2}} \,. \end{aligned} \tag{3.9}$$

Using this mapping, momenta p_I and p_K are on their mass-shell, that is $p_I^2 = 0$ and $p_K^2 = 0$. In each possible phase space configuration in which particle i is unresolved, the mapped momenta tend to

$$\begin{array}{lcll} p_j \to 0 & : & p_I \to p_i & p_K \to p_k \\ p_j || p_k & : & p_I \to p_i & p_K \to p_k + p_j \\ p_j || p_i & : & p_I \to p_i + p_j & p_K \to p_k \end{array}$$

such that this mapping fulfills the third mapping characteristic. Finally, using the above mapping, the phase space factorises according to [130]

$$\begin{aligned} \mathrm{d}\Phi_{n+1}(p_{\hat{1}}, p_{\hat{2}}; p_3, \cdots, p_i, p_j, p_k, \cdots, p_{n+3}) = \mathrm{d}\Phi_n(p_{\hat{1}}, p_{\hat{2}}; p_3, \cdots, \tilde{p}_I, \tilde{p}_K, \cdots, p_{n+3}) \\ \cdot \mathrm{d}\Phi_{X_{ijk}}(p_I, p_K; p_i, p_j, p_k) \,, \end{aligned} \tag{3.10}$$

completing the list of required mapping characteristics. By setting $n = 2$, it can be seen that the antenna phase space $\mathrm{d}\Phi_{X_{ijk}}$ can be related to the three-particle phase space via [92]

$$\mathrm{d}\Phi_{X_{ijk}}(p_I, p_K; p_i, p_j, p_k) = P_2^{-1} \mathrm{d}\Phi_3(p_I, p_K; p_i, p_j, p_k) \,, \tag{3.11}$$

where P_2 is the integrated d-dimensional one-to–two-particle phase space [92]

$$P_2 = \int \mathrm{d}\Phi_2 = 2^{-3+2\epsilon}\pi^{-1+\epsilon}\frac{\Gamma(1-\epsilon)}{\Gamma(2-2\epsilon)}\left(s_{ijk}\right)^{-\epsilon}\,. \tag{3.12}$$

Moving to NNLO, the final-final mapping relevant for final state particles j and k becoming unresolved between final state hard radiators i and l is given by [133, 134]

$$\begin{aligned} p_I^\mu &= p^\mu_{\widetilde{ijk}} = x p_i^\mu + r_1 p_j^\mu + r_2 p_k^\mu + z p_l^\mu\,, \\ p_L^\mu &= p^\mu_{\widetilde{ijl}} = (1-x) p_i^\mu + (1-r_1) p_j^\mu + (1-r_2) p_k^\mu + (1-z) p_l^\mu\,, \end{aligned} \tag{3.13}$$

and it can be seen that this mapping conserves momentum. The parameters x, r_1, r_2 and z are given by

$$\begin{aligned} x &= \frac{1}{2(s_{ij}+s_{ik}+s_{il})}\Bigg[(1+\rho)s_{ijkl} - r_1(s_{jk}+2s_{jl}) \\ &\quad -r_2(s_{jk}+2s_{kl}) + (r_1-r_2)\left(\frac{s_{ij}s_{kl}-s_{ik}s_{jl}}{s_{il}}\right)\Bigg]\,, \\ r_1 &= \frac{s_{jk}+s_{jl}}{s_{ij}+s_{jk}+s_{jl}}\,, \\ r_2 &= \frac{s_{kl}}{s_{ik}+s_{jk}+s_{kl}}\,, \\ z &= \frac{1}{2(s_{il}+s_{kl}+s_{jl})}\Bigg[(1-\rho)s_{ijkl} - r_1(s_{jk}+2s_{ij}) \\ &\quad -r_2(s_{jk}+2s_{ik}) - (r_1-r_2)\left(\frac{s_{ij}s_{kl}-s_{ik}s_{jl}}{s_{il}}\right)\Bigg]\,, \end{aligned} \tag{3.14}$$

where the parameter ρ is defined as

$$\begin{aligned} \rho = \Bigg[&1 + \frac{(r_1-r_2)^2}{s_{il}^2 s_{ijkl}^2}\lambda(s_{ij}s_{kl}, s_{il}s_{jk}, s_{ik}s_{jl}) \\ &+\frac{1}{s_{il}s_{ijkl}}\left(2(r_1(1-r_2)+r_2(1-r_1))(s_{ij}s_{kl}+s_{ik}s_{jl}-s_{jk}s_{il})\right. \\ &\left.+4r_1(1-r_1)s_{ij}s_{jl}+4r_2(1-r_2)s_{ik}s_{kl}\right)\Bigg]^{\frac{1}{2}}\,, \end{aligned} \tag{3.15}$$

and the Källen function is defined as

$$\lambda(x,y,z) = x^2+y^2+z^2-2(xy+xz+yz). \tag{3.16}$$

In each single-unresolved limit, the above mapping coincides with an appropriate NLO mapping of the remaining resolved momenta such that single-unresolved limits in four-particle antennae can be subtracted. This feature will be of importance in the discussion of construction principles for antenna subtraction terms in Section 3.4.1. In each double-unresolved limit, the mapped momenta are given by

$p_j, p_k \to 0$	:	$p_I \to p_i$	$p_L \to p_l$
$p_i \| \| p_j \| \| p_k$	:	$p_I \to p_i + p_j + p_k$	$p_L \to p_l$
$p_l \| \| p_k \| \| p_j$	:	$p_I \to p_i$	$p_L \to p_j + p_k + p_l$
$p_j \to 0, p_k \| \| p_l$	:	$p_I \to p_i$	$p_L \to p_k + p_l$
$p_i \| \| p_j, p_k \to 0$	:	$p_I \to p_i + p_j$	$p_L \to p_l$
$p_i \| \| p_j, p_k \| \| p_l$	:	$p_I \to p_i + p_j$	$p_L \to p_k + p_l$

as required by the third mapping characteristic. In the above example however, momenta required for the double-collinear limit $p_i \| \| p_k, p_l \| \| p_j$ are not reproduced by this mapping. This means that for antenna functions such as $\tilde{A}_4^0(i,j,k,l)$, possessing splittings with non-neighbouring particles in the antenna arguments, must be decomposed into sub-antennae by partial fractioning in final-final kinematics. As a result, limits appropriate to different phase space mappings in final-final kinematics can be isolated. Under this NNLO final-final mapping, the phase space factorises according to

$$\begin{aligned} \mathrm{d}\Phi_{n+2}(p_{\hat{1}}, p_{\hat{2}}; p_3, \cdots, p_i, p_j, p_k, p_l, \cdots, p_{n+4}) = \mathrm{d}\Phi_n(p_{\hat{1}}, p_{\hat{2}}; p_3, \cdots, p_I, p_K, \cdots, p_{n+4}) \\ \cdot \mathrm{d}X_{ijkl}(k_I, k_L; p_i, p_j, p_k, p_l)\,, \end{aligned} \tag{3.17}$$

which completes the list of required mapping characteristics. Using $n = 2$, it can be seen that the four-particle antenna phase space is proportional to the four-particle phase space [92]

$$\mathrm{d}X_{ijkl}(p_I, p_L; p_i, p_j, p_k, p_l) = P_2^{-1} \mathrm{d}\Phi_4(p_I, p_L; p_i, p_j, p_k, p_l)\,. \tag{3.18}$$

3.2.2 Initial-final kinematics

The direction of initial-state momenta is fixed to be along the beam axes and cannot be changed by a mapping. For the mappings discussed so far, the direction of all hard radiators involved in the mapping are altered and for this reason, a different mapping has to be used if one of the hard radiators of an antenna function is in the initial state, i.e. in initial-final kinematics. If particle j becomes unresolved between a hard radiator $\hat{1}$ in the initial and a hard radiator i in the final state, an appropriate mapping is given by [130]

$$\begin{aligned} p_{\tilde{\hat{1}}} &= x p_{\hat{1}} \\ p_I &= p_i + p_j - (1-x) p_{\hat{1}}. \end{aligned} \tag{3.19}$$

This mapping conserves momentum, that is $p_i + p_j + p_{\hat{1}} = p_I + p_{\tilde{\hat{1}}}$, and only rescales the magnitude of the initial state's momentum, as required. The parameter x is given by

$$x = \frac{s_{\hat{1}i} + s_{ij} + s_{\hat{1}j}}{s_{\hat{1}i} + s_{\hat{1}j}}\,. \tag{3.20}$$

Then in single-unresolved limits, the mapped momenta tend to

$$
\begin{aligned}
p_j \to 0 \quad &: \quad p_I \to p_i \quad && p_{\hat{\tilde{1}}} \to p_{\hat{1}} \\
p_i || p_j \quad &: \quad p_I \to p_i + p_j \quad && p_{\hat{\tilde{1}}} \to p_{\hat{1}} \\
p_{\hat{1}} || p_j \quad &: \quad p_I \to p_i \quad && p_{\hat{\tilde{1}}} \to p_{\hat{1}} + p_j
\end{aligned}
$$

Under this initial-final mapping, the phase space factorises into a one-particle reduced phase space, dependent on the resolved momenta, and an antenna phase space that is proportional to a two-particle phase space [130]

$$
\begin{aligned}
\mathrm{d}\Phi_{n+2}(p_{\hat{1}}, p_{\hat{2}}; p_3, \cdots, p_i, p_j, \cdots, p_{n+4}) = \mathrm{d}\Phi_{n+1}(p_{\hat{\tilde{1}}}, p_{\hat{2}}; p_3, \cdots, p_I, \cdots, p_{n+4}) \\
\cdot \mathrm{d}\Phi_2(p_{\hat{1}}, q; p_i, p_j) \frac{Q^2}{2\pi} \frac{\mathrm{d}z}{z} \delta(x - z) \,, \quad (3.21)
\end{aligned}
$$

where $q = p_i + p_j - p_{\hat{1}}$, $Q^2 = -q^2$ and parameter x is defined in Eq. (3.20). The initial-final three-particle antenna phase space can then be defined as

$$
\mathrm{d}\Phi_{X_{\hat{1}ij}}(p_{\hat{1}}, q; p_i, p_j) = \mathrm{d}\Phi_2(p_{\hat{1}}, q; p_i, p_j) \frac{Q^2}{2\pi} \,. \quad (3.22)
$$

For double-unresolved limits in which particles j and k become unresolved between initial and final state hard radiators $\hat{1}$ and i, respectively, the initial-final mapping is given by [130]

$$
\begin{aligned}
p_{\hat{\tilde{1}}} &= x p_{\hat{1}} \,, \\
p_I &= p_i + p_j + p_k - (1 - x) p_{\hat{1}} \,, \quad (3.23)
\end{aligned}
$$

where the parameter x is defined as

$$
x = \frac{s_{\hat{1}i} + s_{\hat{1}j} + s_{\hat{1}k} + s_{ij} + s_{ik} + s_{jk}}{s_{\hat{1}i} + s_{\hat{1}j} + s_{\hat{1}k}} \,. \quad (3.24)
$$

In each single-unresolved configuration, the mapping in Eq. (3.23) reproduces the NLO map of Eq. (3.19) acting on the resolved momenta. In each double-unresolved configuration, the resolved momenta tend to

$$
\begin{aligned}
p_j, p_k \to 0 \quad &: \quad p_I \to p_i \quad && p_{\hat{\tilde{1}}} \to p_{\hat{1}} \\
p_i || p_j || p_k \quad &: \quad p_I \to p_i + p_j + p_k \quad && p_{\hat{\tilde{1}}} \to p_{\hat{1}} \\
p_{\hat{1}} || p_k || p_j \quad &: \quad p_I \to p_i \quad && p_{\hat{\tilde{1}}} \to p_{\hat{1}} - p_j - p_k \\
p_j \to 0, p_k || p_{\hat{1}} \quad &: \quad p_I \to p_i \quad && p_{\hat{\tilde{1}}} \to p_{\hat{1}} - p_k \\
p_i || p_j, p_k \to 0 \quad &: \quad p_I \to p_i + p_j \quad && p_{\hat{\tilde{1}}} \to p_{\hat{1}} \\
p_i || p_j, p_k || p_{\hat{1}} \quad &: \quad p_I \to p_i + p_j \quad && p_{\hat{\tilde{1}}} \to p_{\hat{1}} - p_k \\
p_i || p_k, p_j || p_{\hat{1}} \quad &: \quad p_I \to p_i + p_k \quad && p_{\hat{\tilde{1}}} \to p_{\hat{1}} - p_j
\end{aligned}
$$

In addition, the above initial-final mapping even gives the correct resolved momenta in double-collinear limits of non-adjacent particles in the antenna arguments such that four-particle antennae that are problematic in final-final kinematics do not need to be decomposed into their sub-antennae in initial-final kinematics. Finally, the phase space factorises under this mapping according to

$$\begin{aligned}\mathrm{d}\Phi_{n+2}(p_{\hat{1}},p_{\hat{2}};p_3,\cdots,p_i,p_j,p_k,\cdots,p_{n+4}) = \mathrm{d}\Phi_n(p_{\hat{\tilde{1}}},p_{\hat{\tilde{2}}};p_3,\cdots,p_I,\cdots,p_{n+4}) \\ \cdot\,\mathrm{d}\Phi_3(p_{\hat{1}},q;p_i,p_j,p_k)\frac{Q^2}{2\pi}\frac{\mathrm{d}z}{z}\delta(x-z)\,, \quad (3.25)\end{aligned}$$

with x defined in Eq. (3.24), $q = p_i + p_j + p_k - p_{\hat{1}}$ and the initial-final four-particle antenna phase space is given by

$$\mathrm{d}\Phi_{X_{\hat{1}ijk}}(p_{\hat{1}},q;p_i,p_j,p_k) = \mathrm{d}\Phi_2(p_{\hat{1}},q;p_i,p_j,p_k)\frac{Q^2}{2\pi}\,. \quad (3.26)$$

3.3 Construction principle for antenna subtraction terms at NLO

The construction of subtraction terms in the antenna subtraction formalism follows the infrared factorisation properties of colour-ordered matrix elements and will be discussed for a generic $(2 \to n)$-particle scattering process at Born level.

In general, for a squared colour-ordered matrix element with $n+1$ particles in the final state, a single real-radiation subtraction term in final-final kinematics, relevant for NLO subtraction, can be written as

$$\mathrm{d}\hat{\sigma}^{single,S,FF}_{NLO} \sim X^0_3(p_i,p_j,p_k)M^0_{n+2}(p_{\hat{1}},p_{\hat{2}};\cdots,p_I,p_K,\cdots,p_n)J^n_n(\{\tilde{p}\}_n)\,, \quad (3.27)$$

where $\{\tilde{p}\}_n$ represents the n resolved final-state momenta of the mapped momentum set. It should be noted that only three-particle antennae, X^0_3, are required at NLO. In each

Final-Final Integrated Antennae		
Matrix element, M^0_{n+3}	Integrated antenna factor, $\boldsymbol{J}^{(1)}_2$	Reduced matrix element, M^0_{n+2}
$(\cdots;i_q,j_g,k_{\bar{q}};\cdots)$	$\boldsymbol{J}^{(1)}_2(I_q,K_{\bar{q}}) = \mathcal{A}^0_3(s_{IK})$	$(\cdots;I_q,K_{\bar{q}};\cdots)$
$(\cdots;i_q,j_g,k_{\bar{q}};\cdots)$	$\hat{\boldsymbol{J}}^{(1)}_2(I_q,K_{\bar{q}}) = 0$	$(\cdots;I_q,K_{\bar{q}};\cdots)$
$(\cdots;i_q,j_g,k_g,\cdots)$	$\boldsymbol{J}^{(1)}_2(I_q,K_g) = \frac{1}{2}\mathcal{D}^0_3(s_{IK})$	$(\cdots;I_q,K_g,\cdots)$
$(\cdots;i_{q'},j_{\bar{q}};k_q,\cdots)$	$\hat{\boldsymbol{J}}^{(1)}_2(I_q,K_g) = \frac{1}{2}\mathcal{E}^0_3(s_{IK})$	$(\cdots;I_q,K_g,\cdots)$
$(\cdots,i_g,j_g,k_g,\cdots)$	$\boldsymbol{J}^{(1)}_2(I_g,K_g) = \frac{1}{3}\mathcal{F}^0_3(s_{IK})$	$(\cdots,I_g,K_g,\cdots)$
$(\cdots,i_g,j_{\bar{q}};k_q,\cdots)$	$\hat{\boldsymbol{J}}^{(1)}_2(I_g,K_g) = \mathcal{G}^0_3(s_{IK})$	$(\cdots,I_g,K_g,\cdots)$

Table 2. The correspondence between the real radiation matrix elements, M^0_{n+3} and the NLO integrated antenna factors $\boldsymbol{J}^{(1)}_2$ and reduced matrix elements, M^0_{n+2} for various particle assignments and colour structures for the final-final configuration.

Initial-Final Integrated Antennae		
Matrix element, M^0_{n+3}	Integrated antenna factor, $\boldsymbol{J}^{(1)}_2$	Reduced matrix element, M^0_{n+2}
$(\cdots;\hat{1}_q,i_g,j_{\bar{q}};\cdots)$	$\boldsymbol{J}^{(1)}_2(\hat{\hat{1}}_q,J_{\bar{q}})=\mathcal{A}^0_{3,q}(s_{\bar{1}J})-\Gamma^{(1)}_{qq}(x_1)\delta_2$	$(\cdots;\hat{\hat{1}}_q,J_{\bar{q}};\cdots)$
$(\cdots;\hat{1}_q,i_g,j_{\bar{q}};\cdots)$	$\hat{\boldsymbol{J}}^{(1)}_2(\hat{\hat{1}}_q,J_{\bar{q}})=0$	$(\cdots;\hat{\hat{1}}_q,J_{\bar{q}};\cdots)$
$(\cdots;\hat{1}_q,i_g,j_g,\cdots)$	$\boldsymbol{J}^{(1)}_2(\hat{\hat{1}}_q,J_g)=\frac{1}{2}\mathcal{D}^0_{3,q}(s_{\bar{1}J})-\Gamma^{(1)}_{qq}(x_1)\delta_2$	$(\cdots;\hat{\hat{1}}_q,J_g,\cdots)$
$(\cdots;\hat{1}_q,i_{\bar{q}'};j_{q'},\cdots)$	$\hat{\boldsymbol{J}}^{(1)}_2(\hat{\hat{1}}_q,J_g)=\frac{1}{2}\mathcal{E}^0_{3,q,q'\bar{q}'}(s_{\bar{1}J})$	$(\cdots;\hat{\hat{1}}_q,J_g,\cdots)$
$(\cdots;i_q,j_g,\hat{1}_g,\cdots)$	$\boldsymbol{J}^{(1)}_2(J_q,\hat{\hat{1}}_g)=\mathcal{D}^0_{3,g,gq}(s_{\bar{1}J})-\frac{1}{2}\Gamma^{(1)}_{gg}(x_1)\delta_2$	$(\cdots;J_q,\hat{\hat{1}}_g,\cdots)$
$(\cdots;i_q,j_g,\hat{1}_g,\cdots)$	$\hat{\boldsymbol{J}}^{(1)}_2(J_q,\hat{\hat{1}}_g)=-\frac{1}{2}\hat{\Gamma}^{(1)}_{gg}(x_1)\delta_2$	$(\cdots;J_q,\hat{\hat{1}}_g,\cdots)$
$(\cdots,\hat{1}_g,i_g,j_g,\cdots)$	$\boldsymbol{J}^{(1)}_2(\hat{\hat{1}}_g,J_g)=\frac{1}{2}\mathcal{F}^0_{3,g}(s_{\bar{1}J})-\frac{1}{2}\Gamma^{(1)}_{gg}(x_1)\delta_2$	$(\cdots,\hat{\hat{1}}_g,J_g,\cdots)$
$(\cdots,\hat{1}_g,i_{\bar{q}};j_q,\cdots)$	$\hat{\boldsymbol{J}}^{(1)}_2(\hat{\hat{1}}_g,J_g)=\frac{1}{2}\mathcal{G}^0_{3,g}(s_{\bar{1}J})-\frac{1}{2}\hat{\Gamma}^{(1)}_{gg}(x_1)\delta_2$	$(\cdots,\hat{\hat{1}}_g,J_g,\cdots)$
$(\cdots;i_q,\hat{1}_g,j_{\bar{q}};\cdots)$	$\boldsymbol{J}^{(1)}_{2,g\to q}(\hat{\hat{1}}_q,J_{\bar{q}})=-\frac{1}{2}\mathcal{A}^0_{3,g,q\bar{q}}(s_{\bar{1}J})-S_{g\to q}\Gamma^{(1)}_{qg}(x_1)\delta_2$	$(\cdots;\hat{\hat{1}}_q,J_{\bar{q}};\cdots)$
$(\cdots;i_q,\hat{1}_g,j_g,\cdots)$	$\boldsymbol{J}^{(1)}_{2,g\to q}(\hat{\hat{1}}_q,J_g)=-\mathcal{D}^0_{3,g,qg}(s_{\bar{1}J})-S_{g\to q}\Gamma^{(1)}_{qg}(x_1)\delta_2$	$(\cdots;\hat{\hat{1}}_q,J_g,\cdots)$
$(\cdots;i_{q'},\hat{1}_{q'};j_q,\cdots)$	$\boldsymbol{J}^{(1)}_{2,q\to g}(J_q,\hat{\hat{1}}_g)=-\mathcal{E}^0_{3,q',qq'}(s_{\bar{1}J})-S_{q\to g}\Gamma^{(1)}_{gq}(x_1)\delta_2$	$(\cdots;J_q,\hat{\hat{1}}_g,\cdots)$
$(\cdots,i_g;\hat{1}_q,j_q,\cdots)$	$\boldsymbol{J}^{(1)}_{2,q\to g}(J_g,\hat{\hat{1}}_g)=-\mathcal{G}^0_{3,q}(s_{\bar{1}J})-S_{q\to g}\Gamma^{(1)}_{gq}(x_1)\delta_2$	$(\cdots,J_g,\hat{\hat{1}}_g,\cdots)$

Table 3. The correspondence between the real radiation matrix elements, M^0_{n+3} and the NLO integrated antenna factors $\boldsymbol{J}^{(1)}_2$ and reduced matrix elements, M^0_{n+2} for various particle assignments and colour structures for the initial-final configuration. For brevity $\delta(1-x_i)=\delta_i$ for $i=1,2$.

unresolved limit of particle j, colour-neighbouring particles i and k, the antenna function tends to the relevant infrared divergent function and the reduced squared matrix elements inherits the appropriate momenta from the mappings such that the right-hand side of expression (3.27) mimics the factorisation properties of the squared matrix element. In initial-final kinematics expression (3.27) changes to

$$\mathrm{d}\hat{\sigma}^{single,S,IF}_{NLO}\sim X^0_3(p_{\hat{1}},p_j,p_k)M^0_{n+2}(p_{\hat{\hat{1}}},p_{\hat{2}};\cdots,p_K,\cdots,p_n)J^n_n(\{\tilde{p}\}_n)\,, \tag{3.28}$$

and subtracts infrared singularities according to the factorisation properties of the real emissions in initial-final unresolved configurations. A full NLO subtraction term $\mathrm{d}\hat{\sigma}^S_{NLO}$ is then given by a sum over appropriate single NLO subtraction terms such that the full subtraction term only has the same infrared divergences as the squared matrix element and the integral

$$\int_{\mathrm{d}\Phi_{n+1}}\left[\mathrm{d}\hat{\sigma}^R-\mathrm{d}\hat{\sigma}^S_{NLO}\right] \tag{3.29}$$

is rendered infrared finite. At NLO, the full real-radiation subtraction term can then be written as a sum over such terms

$$\mathrm{d}\hat{\sigma}^S_{NLO,lm}=\mathcal{N}^R_{lm}\sum_j\mathrm{d}\Phi_{n+1}(p_{\hat{1}},p_{\hat{2}};\{p\}_{n+1})\frac{1}{S_{n+1}}\cdot X^0_3(\cdot,p_j,\cdot)M^0_{n+2}(\tilde{p}_{\hat{1}},p_{\hat{2}};\{\tilde{p}\}_n)J^n_n(\{\tilde{p}\}_n)\,, \tag{3.30}$$

where the sum $\sum_j$ is over all particles j in M^0_{n+3} that can develop infrared divergences. These divergences are then subtracted by an appropriate antenna function X^0_3. An initial-

state parton's momentum in the resolved momentum set is represented by $\tilde{p}_{\hat{1}}$, whether it is explicitly involved in the mapping or not (can be either $p_{\hat{1}}$ or $p_{\tilde{\hat{1}}}$) and the dots "$\cdot$" in the antenna arguments stand for appropriate hard radiators whether in the initial or final state. The phase space factorisation under final-final and initial-final mappings can be used to schematically write

$$\int_{\mathrm{d}\Phi_{n+1}} \mathrm{d}\hat{\sigma}_{NLO}^{single,S} \sim \int \mathrm{d}\Phi_{X_{\cdot j\cdot}} X_3^0(\cdot, p_j, \cdot) \cdot \int \mathrm{d}\Phi_n M_{n+2}^0(\tilde{p}_{\hat{1}}, p_{\hat{2}}; \{\tilde{p}\}_n) J_n^n(\{\tilde{p}\}_n)\,, \tag{3.31}$$

for a single subtraction term. An integrated antenna function is defined as the integral of an antenna over its antenna phase space and can be written as [92]

$$\mathcal{X}_3^0(s_{ijk}, z_1, z_2) = \frac{1}{C(\epsilon)}\delta(1-z_1)\delta(1-z_2)\int \mathrm{d}\Phi_{X_{ijk}} X_3^0(p_i, p_j, p_k) \tag{3.32}$$

for final-final kinematics. For initial-final kinematics this changes to [130]

$$\mathcal{X}_3^0(s_{ij\hat{1}}, z_1, z_2) = \frac{1}{C(\epsilon)}\delta(1-z_2)\int \mathrm{d}\Phi_2 \frac{Q^2}{2\pi}\delta(z_1 - x) X_3^0(p_i, p_j, p_{\hat{1}})\,, \tag{3.33}$$

where the parameter x is defined in Eq. (3.20). A list of relevant integrated three-particle antenna functions in final-final kinematics can be found in Table 4. The integrated antenna functions are combined with appropriate symmetry factors and in initial-final kinematics with relevant mass factorisation counterterms to form one-loop two-particle integrated antenna factors $\mathbf{J}_2^{(1)}$. In their singularity structure these coincide with the one-loop Catani-operators

$$\mathbf{J}_2^{(1)}(p_i, p_j, z_1, z_2, \epsilon) = 2\mathbf{I}_{ij}^{(1)}(s_{ij}, \epsilon) + \text{finite}\,. \tag{3.34}$$

Using the $\mathbf{J}$s, a single one-loop NLO subtraction term can be written as a string of $\mathbf{J}_2^{(1)}$s times a squared matrix element and a complete list of $\mathbf{J}_2^{(1)}$s is given in Ref. [98]. For completeness, a list of integrated antenna factors relevant for subtraction in final-final and initial-final kinematics is reproduced in Tables 2 and 3. In Table 3 the factor $S_{q\to g}$ is defined via

$$S_{g\to q} = \frac{S_g}{S_q} = 1 - \epsilon\,, \tag{3.35}$$

and corrects for the fact that in D dimensions the degrees of freedom for quarks and gluons are different and the inverse factor is given by

$$S_{q\to g} = \frac{S_q}{S_g} = \frac{1}{1-\epsilon}\,. \tag{3.36}$$

The full $\mathrm{d}\hat{\sigma}_{NLO}^T$ subtraction term is then given by the sum over all integrated subtraction terms coming from $\mathrm{d}\hat{\sigma}_{NLO}^S$

$$\begin{aligned}\hat{\sigma}_{NLO,lm}^T = -\mathcal{N}_{lm}^V \sum_n \int \frac{dz_1}{z_1}\frac{dz_2}{z_2}\frac{1}{S_n}\mathrm{d}\Phi_n(z_1 p_{\hat{1}}, z_2 p_{\hat{2}}; p_3, \cdots, p_{n+2}) \\ \cdot \mathbf{J}_{n+2}^{(1)}(\{p_{\hat{1}}, p_{\hat{2}}, \{p\}_n\}, z_1, z_2) M_{n+2}^0(z_1 p_{\hat{1}}, z_2 p_{\hat{2}}; p_3, \cdots, p_{n+2}) J_n^n(\{p\}_n)\,,\end{aligned} \tag{3.37}$$

where the integral over z_1 or z_2 becomes trivial for every non-partonic initial state. The $(n+2)$-particle integrated antenna factor $\mathbf{J}^{(1)}_{n+2}$ is the sum over all relevant two-particle integrated antenna factors, integrated up from the real subtraction term

$$\mathbf{J}^{(1)}_{n+2}(\{p_{\hat{1}}, p_{\hat{2}}, \{p\}_n\}, z_1, z_2) = \sum_J \mathbf{J}^{(1)}_2 \,, \tag{3.38}$$

such that

$$Poles(M^1_{n+2}) = Poles(\mathrm{d}\hat{\sigma}^T_{NLO}) \,. \tag{3.39}$$

3.4 Construction of antenna subtraction terms at NNLO

The construction principle of antenna subtraction terms at NNLO is rather involved and this section should therefore be regarded as a short summary of what is discussed in greater detail in Ref. [98]. At NNLO, one has to construct three subtraction terms that each subtract infrared divergences at different phase space multiplicities. These terms are the $\mathrm{d}\hat{\sigma}^S, \mathrm{d}\hat{\sigma}^T$ and $\mathrm{d}\hat{\sigma}^U$, relevant for real-real, real-virtual and virtual-virtual subtraction, respectively, and will be discussed in the following in turn.

$\mathcal{X}^0_3$ antennae	Comments
$\mathcal{A}^0_3$	Eq. (5.6) of [92].
$\mathcal{D}^0_3$	Eq. (6.9) of [92].
$\mathcal{E}^0_3$	Eq. (6.14) of [92].
$\mathcal{F}^0_3$	Eq. (7.9) of [92].
$\mathcal{G}^0_3$	Eq. (7.15) of [92].
$\mathcal{S}^{FF}$	Eq. (3.33) of [131].
$\mathcal{X}^1_3$ antennae	
$\mathcal{A}^1_3$	Eq. (5.18) of [92].
$\hat{\mathcal{A}}^1_3$	Eq. (5.20) of [92].
$\tilde{\mathcal{A}}^1_3$	Eq. (5.19) of [92].
$\mathcal{D}^1_3$	Eq. (6.22) of [92].
$\hat{\mathcal{D}}^1_3$	Eq. (6.23) of [92].
$\mathcal{E}^1_3$	Eq. (6.34) of [92].
$\hat{\mathcal{E}}^1_3$	Eq. (6.36) of [92].
$\tilde{\mathcal{E}}^1_3$	Eq. (6.35) of [92].
$\mathcal{X}^0_4$ antennae	
$\mathcal{A}^0_4$	Eq. (5.31) of [92].
$\tilde{\mathcal{A}}^0_4$	Eq. (5.32) of [92].
$\mathcal{B}^0_4$	Eq. (5.39) of [92].
$\mathcal{C}^0_4$	Eq. (5.44) of [92].
$\mathcal{D}^0_4$	Eq. (6.45) of [92].
$\mathcal{E}^0_4$	Eq. (6.51) of [92].
$\tilde{\mathcal{E}}^0_4$	Eq. (6.52) of [92].

Table 4. List of relevant $\mathcal{X}^0_3$, $\mathcal{X}^1_3$ and $\mathcal{X}^0_4$ antenna functions in final-final kinematics.

3.4.1 Real-real subtraction

The real-real subtraction term $\mathrm{d}\hat{\sigma}^S$ for n-jet production at Born level with at most five partons in the matrix element can be divided into the following contributions

1. A NLO subtraction term $\mathrm{d}\hat{\sigma}^{S,a}$ for $(n+1)$-jet production.

2. A subtraction term $\mathrm{d}\hat{\sigma}^{S,b}$, giving relevant singularities when two colour-connected particles are unresolved. This term can be subdivided into terms containing the four-particle X_4^0 antennae making up $\mathrm{d}\hat{\sigma}^{S,b1}$, and terms that subtract the single-unresolved limits of the four-particle antennae summarised as $\mathrm{d}\hat{\sigma}^{S,b2}$.

3. A subtraction term $\mathrm{d}\hat{\sigma}^{S,c}$ to remove all remaining spurious singularities appearing in $\mathrm{d}\hat{\sigma}^{S,a}$ and $\mathrm{d}\hat{\sigma}^{S,b}$, so that the full subtraction term only contains the same singularities as the real-real correction.

Summing up the above subtraction terms the full real-real subtraction term can be written as

$$\mathrm{d}\hat{\sigma}^S = \mathrm{d}\hat{\sigma}^{S,a} + \mathrm{d}\hat{\sigma}^{S,b1} + \mathrm{d}\hat{\sigma}^{S,b2} + \mathrm{d}\hat{\sigma}^{S,c}\,. \tag{3.40}$$

The $\mathrm{d}\sigma^{S,a}$ can be constructed from NLO construction principles for the real subtraction term for $(n+1)$-jet production. The subtraction term can be written as

$$\begin{aligned}\mathrm{d}\hat{\sigma}^S_{NLO,lm} = \mathcal{N}^{RR}_{lm}\sum_j \mathrm{d}\Phi_{n+2}(p_{\hat{1}},p_{\hat{2}};\{p\}_{n+2})\frac{1}{S_{n+2}} \\ \cdot X_3^0(\cdot,p_j,\cdot)M^0_{n+3}(\tilde{p}_{\hat{1}},p_{\hat{2}};\{\tilde{p}\}_{n+1})J^{n+1}_n(\{\tilde{p}\}_{n+1})\,.\end{aligned} \tag{3.41}$$

Genuine double-unresolved limits are subtracted by the $\mathrm{d}\hat{\sigma}^{b1,S}$ terms. These subtraction terms are built from X_4^0 antennae and a single subtraction term in final-final kinematics may be written as

$$\mathrm{d}\hat{\sigma}^{b1,S,FF}_{single} \quad\sim\quad X_4^0(p_i,p_j,p_k,p_l)M^0_{n+2}(p_{\hat{1}},p_{\hat{2}};p_3,\cdots,p_I,p_L,\cdots,p_{n+4})J^n_n(\{\tilde{p}\}_n)\,, \tag{3.42}$$

where the resolved momenta in the reduced matrix elements are obtained from the NNLO $\{p\}_{n+2}\to\{\tilde{p}\}_n$ final-final phase space mappings. In initial-final kinematics, expression (3.42) changes to

$$\mathrm{d}\hat{\sigma}^{b1,S,IF}_{single} \quad\sim\quad X_4^0(p_{\hat{1}},p_i,p_j,p_k)M^0_{n+2}(p_{\hat{\tilde{1}}},p_{\hat{2}};p_3,\cdots,p_K,\cdots,p_{n+4})J^n_n(\{\tilde{p}\}_n)\,, \tag{3.43}$$

where the NNLO inital-final mapping has been applied to obtain the resolved momenta in the reduced matrix element. Then the full subtraction term is a sum over appropriate X_4^0 antenna functions, represented by $\sum_{j,k}$, to subtract all double-unresolved limits of every pair of colour-neighbouring particles j and k and can be written as

$$\begin{aligned}\mathrm{d}\hat{\sigma}^{b1,S}_{lm} = \mathcal{N}^{RR}_{lm}\sum_{j,k} \mathrm{d}\Phi_{n+2}(p_{\hat{1}},p_{\hat{2}};\{p\}_{n+2})\frac{1}{S_{n+2}} \\ \cdot X_4^0(\cdot,p_j,p_k,\cdot)M^0_{n+2}(\tilde{p}_{\hat{1}},p_{\hat{2}};\{\tilde{p}\}_n)J^n_n(\{\tilde{p}\}_n)\,.\end{aligned} \tag{3.44}$$

The X_4^0 antennae themselves develop single-unresolved singularities which do not coincide with any of the singularities of the double-real correction and have to be subtracted. In a single-unresolved limit, e.g. particle j being unresolved in $X_4^0(p_i, p_j, p_k, p_l)$, the four-particle antenna factorises into a divergent splitting function or soft eikonal factor times a three-particle antenna such that the corresponding infrared singularities can be subtracted by terms of the form

$$\begin{aligned} \mathrm{d}\hat{\sigma}^{b2,S,FF}_{single} \sim X_3^0(p_i, p_j, p_k) X_3^0(p_I, p_K, p_l) \\ \cdot M^0_{n+2}(p_{\hat{1}}, p_{\hat{2}}; p_3, \cdots, \tilde{p}_K, p_L, \cdots, p_{n+4}) J^n_n(\{\tilde{\tilde{p}}\}_n)\,, \end{aligned} \tag{3.45}$$

where the resolved momenta of two successive NLO final-final mappings from $\{p\}_{n+2} \to \{\tilde{p}\}_{n+1} \to \{\tilde{\tilde{p}}\}_n$ are used in the reduced matrix element. In initial-final kinematics, e.g. particle i becoming unresolved in $X_4^0(p_{\hat{1}}, p_i, p_j, p_k)$, the subtraction relevant to single-unresolved singularities in the X_4^0 antennae changes to

$$\begin{aligned} \mathrm{d}\hat{\sigma}^{b2,S,IF}_{single} \sim X_3^0(p_{\hat{1}}, p_i, p_j) X_3^0(p_{\hat{\tilde{1}}}, p_J, p_l) \\ \cdot M^0_{n+2}(p_{\hat{\tilde{1}}}, p_{\hat{2}}; p_3, \cdots, p_L, \cdots, p_{n+4}) J^n_n(\{\tilde{\tilde{p}}\}_n)\,, \end{aligned} \tag{3.46}$$

where the resolved momenta in the reduced matrix element are obtained from two successive NLO initial-final mappings. In general, an iteration of a NLO final-final followed by a NLO initial-final mapping or vice versa is also possible and depends on the type of four-particle antenna X_4^0 appearing in $\mathrm{d}\hat{\sigma}^{b1,S}$ that has to be rendered finite in its single-unresolved limits. Summing up all relevant $b2$ subtraction terms, symbolically represented by $\sum_j$, gives

$$\begin{aligned} \mathrm{d}\hat{\sigma}^{b2,S}_{lm} = -\mathcal{N}^{RR}_{lm} \sum_j \mathrm{d}\Phi_{n+2}(\{p\}_{n+2}) \frac{1}{S_{n+2}} \\ \cdot X_3^0(\cdot, p_j, \cdot) X_3^0(\{\tilde{p}_{\hat{1}}, p_{\hat{2}}, \{\tilde{p}\}_{n+1}\}) M^0_{n+2}(\tilde{\tilde{p}}_{\hat{1}}, p_{\hat{2}}; \{\tilde{\tilde{p}}\}_n) J^n_n(\{\tilde{\tilde{p}}\}_n)\,. \end{aligned} \tag{3.47}$$

The above structures, $\mathrm{d}\hat{\sigma}^{S,a}$ and $\mathrm{d}\hat{\sigma}^{S,b}$, may contain even more singular infrared limits that do not coincide with the singularity structure of the real-real correction. On the one hand such limits originate from single-unresolved configurations in the reduced matrix element of the $\mathrm{d}\hat{\sigma}^{S,a}$ term or on the other hand from unresolved limits in the secondary antenna of the $\mathrm{d}\hat{\sigma}^{S,b2}$ terms. Each of these so-called spurious limits has to be properly subtracted by the $\mathrm{d}\hat{\sigma}^{S,c}$ term and the construction of an appropriate $\mathrm{d}\hat{\sigma}^{S,c}$ poses the main challenge in the construction of antenna subtraction terms. In general, the $\mathrm{d}\hat{\sigma}^{S,c}$ term is constructed from combinations of the type $X_3^0 \times X_3^0$ and (soft factors)$\times X_3^0$. The $\mathrm{d}\hat{\sigma}^{S,c}$ is dependent on the partonic content of an amplitude and has to be constructed individually for every process. For processes with the same infrared QCD singularity structure however, the construction follows a unique pattern such that the same subtraction terms can be recycled and only the reduced matrix elements have to be adopted. All construction patterns relevant for NNLO antenna subtraction are known and are described in greater detail in [98, 135, 136].

3.4.2 Real-virtual subtraction

For a Born process with n jets in the final state, the full real-virtual antenna subtraction term can be divided into the following contributions

1. A NLO subtraction term relevant for (n+1)-jet production $\mathrm{d}\hat{\sigma}^{T,a}$.

2. A subtraction term that subtracts genuine infrared divergences of the loop corrections $\mathrm{d}\hat{\sigma}^{T,b}$.

3. All subtraction terms from the real-real subtraction that are not integrated up into $\mathrm{d}\hat{\sigma}^{T,a}$ or $\mathrm{d}\hat{\sigma}^{T,b}$, are included in $\mathrm{d}\hat{\sigma}^{T,c}$. This term also removes any spurious divergences such that all divergences in the full real-virtual subtraction coincide with those of the real-virtual corrections.

Summing up the contributions, the full real-virtual subtraction is given by

$$\mathrm{d}\hat{\sigma}^{T} = \mathrm{d}\hat{\sigma}^{T,a} + \mathrm{d}\hat{\sigma}^{T,b} + \mathrm{d}\hat{\sigma}^{T,c}\,. \tag{3.48}$$

The $\mathrm{d}\hat{\sigma}^{T,a}$ is constructed following the NLO construction principles for virtual subtraction in (n+1)-jet production. Explicitly this subtraction term can be written as

$$\begin{aligned}
\mathrm{d}\hat{\sigma}^{T,a}_{lm} &= -\int_{\mathrm{d}\Phi_{X_3^0}} \mathrm{d}\hat{\sigma}^{S,a} - \mathrm{d}\hat{\sigma}^{MF,NLO}_{n+1}\,,\\
\hat{\sigma}^{T,a}_{lm} &= -\mathcal{N}^{RV}_{lm} \sum_{n+1} \int \frac{\mathrm{d}z_1}{z_1}\frac{\mathrm{d}z_2}{z_2}\mathrm{d}\Phi_{n+1}(z_1 p_{\hat{1}}, z_2 p_{\hat{2}}; p_3, \cdots, p_{n+3})\frac{1}{S_{n+1}}\\
&\quad \cdot\ \mathbf{J}^{(1)}_{n+3}(\{p_{\hat{1}}, p_{\hat{2}}, \{p\}_{n+1}\}, z_1, z_2) M^0_{n+3}(z_1 p_{\hat{1}}, z_2 p_{\hat{2}}; p_3, \cdots, p_{n+3}) J^{n+1}_n(\{p\}_{n+1})\,,
\end{aligned} \tag{3.49}$$

where $\mathbf{J}^{(1)}_{n+3}$ is the string of integrated antenna functions, including mass factorisation terms, integrated up from $\mathrm{d}\hat{\sigma}^{S,a}$. The construction of the $\mathrm{d}\hat{\sigma}^{T,a}$ can be validated by checking that the ϵ-poles between this subtraction term and the real-virtual correction cancel, that is

$$Poles(M^1_{n+3}) = Poles(\mathrm{d}\hat{\sigma}^{T,a})\,. \tag{3.50}$$

According to the infrared factorisation properties of one-loop corrections, the $\mathrm{d}\hat{\sigma}^{T,b}$ term can be subdivided into contributions that subtract the (tree)$\times$(loop) and the (loop)$\times$(tree) divergences, $\mathrm{d}\hat{\sigma}^{T,b1}$ and $\mathrm{d}\hat{\sigma}^{T,b2}$ respectively.

The (tree)$\times$(loop) subtraction term can be written as

$$\begin{aligned}
\hat{\sigma}^{T,b1} &= \mathcal{N}^{RV}_{lm} \sum_{n+1} \int \frac{\mathrm{d}z_1}{z_1}\frac{\mathrm{d}z_2}{z_2}\mathrm{d}\Phi_{n+1}(z_1 p_{\hat{1}}, z_2 p_{\hat{2}}; p_3, \cdots, p_{n+3})\frac{1}{S_{n+1}}\\
&\quad \cdot \sum_j X^0_3(\cdot, j, \cdot)\left\{\delta(1-z_1)\delta(1-z_2) M^1_{n+2}(z_1\tilde{p}_{\hat{1}}, z_2 p_{\hat{2}}; \{\tilde{p}\}_n)\right.\\
&\quad +\ \left.\mathbf{J}^{(1)}_{n+2}(\{\tilde{p}_{\hat{1}}, p_{\hat{2}}, \{\tilde{p}\}_n\}, z_1, z_2) M^0_{n+2}(z_1\tilde{p}_{\hat{1}}, z_2 p_{\hat{2}}; \{\tilde{p}\}_n)\right\} J^n_n(\{\tilde{p}\}_n)\,,
\end{aligned} \tag{3.51}$$

X_3^1	A_3^1	$\tilde{A}_3^1$	$\hat{A}_3^1$	D_3^1	$\hat{D}_3^1$	E_3^1	$\tilde{E}_3^1$	$\hat{E}_3^1$
N_X	2	1	2	3	3	2	1	0
M_X	1	1	0	2	2	2	0	2

Table 5. Number of colour-connected pairs N_X for the one-loop antenna X_3^1, and the associated constant M_X.

where in the last line $\mathbf{J}^{(1)}_{n+2}$ is a string of integrated antenna such that the poles of the one-loop correction $M^{(1)}_{n+2}$ are subtracted and $\mathrm{d}\hat{\sigma}^{T,b1}$ is free from ϵ-poles

$$Poles(\mathrm{d}\hat{\sigma}^{T,b1}) = 0\,. \tag{3.52}$$

As the integrated antennae in $\mathbf{J}^1_{n+2}$ take the mapped momenta in their arguments, they are not related to any X_3^0 antenna appearing in the real-real subtraction and for this reason, either have to cancel across the real-virtual or must be integrated to the double-virtual subtraction term.

The (loop)×(tree) subtraction term can be written as

$$\begin{aligned}\hat{\sigma}^{T,b2}_{lm} &= \mathcal{N}^{RV}_{lm}\sum_{n+1}\int\frac{\mathrm{d}z_1}{z_1}\frac{\mathrm{d}z_2}{z_2}\mathrm{d}\Phi_{n+1}(z_1p_{\hat{1}},z_2p_{\hat{2}};p_3,\cdots,p_{n+3})\frac{1}{S_{n+1}}\\
&\cdot\sum_j\Big\{X_3^1(\cdot,j,\cdot)\delta(1-z_1)\delta(1-z_2)+\mathbf{J}^{(1)}_{X_3^1}(\{p_{\hat{1}},p_{\hat{2}},\{p\}_{n+1}\},z_1,z_2)X_3^0(\cdot,j,\cdot)\\
&-M_XX_3^0(\cdot,j,\cdot)\mathbf{J}_2^{(1)}(\{\tilde{p}_{\hat{1}},p_{\hat{2}},\{\tilde{p}\}_n\},z_1,z_2)\Big\}M^0_{n+2}(z_1\tilde{p}_{\hat{1}},z_2p_{\hat{2}};\{\tilde{p}\}_n)J^n_n(\{\tilde{p}\}_n)\,,\end{aligned} \tag{3.53}$$

where this construction follows the definition of the X_3^1 antenna from Eq. (3.4) with X_3^1 assumed to be renormalised at the same scale as the matrix elements of the virtual correction. The string of integrated antennae $\mathbf{J}^{(1)}_{X_3^1}$ cancels the infrared ϵ-poles of the M_3^1 amplitude×tree interference appearing in Eq. (3.4) and can in general be directly traced back to the $X_3^0\times X_3^0$ subtraction terms appearing in $\mathrm{d}\hat{\sigma}^{S,b2}$. The last line in Eq. (3.53) cancels the ϵ-poles of the last term on the right-hand side of Eq. (3.4) such that

$$Poles(\mathrm{d}\hat{\sigma}^{T,b2}) = 0\,, \tag{3.54}$$

where the values of M_X are X_3^1 antenna type dependent and are tabulated in Table 5 [98]. Again, the integrated antennae appearing in the block $M_XX_3^0\mathbf{J}_2^{(1)}$ take mapped momenta in their arguments such that they either have to cancel explicitly across the real-virtual or must be integrated to the double-virtual subtraction term.

The remaining subtraction term $\mathrm{d}\hat{\sigma}^{T,c}$ ensures that all $X_3^0 \times X_3^0$ and $S_{ijk} \times X_3^0$ terms appearing in the real-real subtraction term are integrated over to the real-virtual subtraction term. The $\mathrm{d}\hat{\sigma}^{T,c}$ term further ensures that no spurious divergences remain and all infrared limits in the real-virtual subtraction term coincide with the divergences of the real-virtual correction. In final-final kinematics, the integrated soft factor, with hard radiators a and b, unresolved particle j and a primary final-final phase space mapping $(i,j,k) \to (I,K)$, is given by [87]

$$\begin{aligned}\mathcal{S}^{FF}_{ac;ik} &= \int \mathrm{d}\Phi_{X_{ijk}} S_{ajc} \\ &= (s_{IK})^{-\epsilon} \frac{\Gamma^2(1-\epsilon)e^{\epsilon\gamma}}{\Gamma(1-3\epsilon)} \left(-\frac{2}{\epsilon}\right) \left[-\frac{1}{\epsilon} + \ln(x_{ac,IK} + \epsilon \mathrm{Li}_2\left(-\frac{1-x_{ac,IK}}{x_{ac,IK}}\right))\right] ,\end{aligned} \tag{3.55}$$

where

$$x_{ac,IK} = \frac{s_{ac}s_{IK}}{(s_{aI}+s_{aK})(s_{cI}+s_{cK})} . \tag{3.56}$$

If any of the radiators a or b is in the initial state, the integrated soft factor is given by a crossing of the above result as long as the primary mapping is a final-final one. No other form of the integrated soft factor is needed for the calculations discussed in this thesis. Finally the result

$$Poles(\mathrm{d}\hat{\sigma}^{T,c}) = 0 \tag{3.57}$$

holds for a properly constructed $\mathrm{d}\hat{\sigma}^{T,c}$. Process dependent construction principles of $\mathrm{d}\hat{\sigma}^{T,c}$ terms are analysed in more detail in Refs. [98, 135, 136] and if once known for a particular process the construction pattern carries through to related processes with the same QCD infrared singularity structure.

3.4.3 Virtual-virtual subtraction

The construction of the virtual-virtual subtraction term amounts to collecting all remaining unmatched subtraction terms from the real-real and real-virtual which have not yet been subtracted back in or were introduced at the real-virtual level for the first time. The double-virtual subtraction can be divided into the following contributions according to the pole structure of two-loop corrections

1. A term $\mathrm{d}\hat{\sigma}^{U,a}$ that cancels the leading poles of the first line in Eq. (2.75) and integrates up the $X_3^0 \times$(one-loop) reduced matrix element from $\mathrm{d}\hat{\sigma}^{T,b1}$.

2. A term $\mathrm{d}\hat{\sigma}^{U,b}$ that cancels the leading poles of the second line in Eq. (2.75) and integrates up the $X_3^0 \times X_3^0$ terms from $\mathrm{d}\hat{\sigma}^{T,b1}$ together with some unmatched terms from $\mathrm{d}\hat{\sigma}^{T,c}$.

3. A term $\mathrm{d}\hat{\sigma}^{U,c}$ that cancels the remaining poles in Eq. (2.75) and integrates up all remaining as yet unmatched subtraction terms from the real-real and real-virtual subtractions.

Summing up the three contributions, the virtual-virtual subtraction term can be written as

$$\mathrm{d}\hat{\sigma}^{U} = \mathrm{d}\hat{\sigma}^{U,a} + \mathrm{d}\hat{\sigma}^{U,b} + \mathrm{d}\hat{\sigma}^{U,c}\,. \tag{3.58}$$

It should be noted that the mass factorisation counterterms can also be split up into contributions relevant for each of the three above parts

$$\begin{aligned}
\mathrm{d}\hat{\sigma}_i^{MF,a} &= -\int \frac{\mathrm{d}z_1}{z_1}\frac{\mathrm{d}z_2}{z_2}\left(\frac{\alpha_s}{2\pi}\right)\bar{C}(\epsilon)\Gamma_{ij}^{(1)}(z_1)\delta(1-z_2)\left(\mathrm{d}\hat{\sigma}_i^{V} - \frac{\beta_0}{\epsilon}\mathrm{d}\hat{\sigma}_i^{LO}\right)\,,\\
\mathrm{d}\hat{\sigma}_i^{MF,b} &= +\int \frac{\mathrm{d}z_1}{z_1}\frac{\mathrm{d}z_2}{z_2}\left(\frac{\alpha_s}{2\pi}\right)\bar{C}(\epsilon)\Gamma_{ij}^{(1)}(z_1)\delta(1-z_2)\mathrm{d}\hat{\sigma}_{i,NLO}^{T}\\
&\quad -\left(\frac{\alpha_s}{2\pi}\right)^2\bar{C}(\epsilon)^2\frac{1}{2}\left[\Gamma_{ij}^{(1)}\otimes\Gamma_{jk}^{(1)}\right](z_1)\delta(1-z_2)\mathrm{d}\hat{\sigma}_k^{LO}\,,\\
\mathrm{d}\hat{\sigma}_i^{MF,c} &= +\int \frac{\mathrm{d}z_1}{z_1}\frac{\mathrm{d}z_2}{z_2}\left(\frac{\alpha_s}{2\pi}\right)^2\bar{C}(\epsilon)^2\Gamma_{ij}^{(2)}(z_1)\delta(1-z_2)\mathrm{d}\hat{\sigma}_k^{LO}\,.
\end{aligned} \tag{3.59}$$

In the following it is assumed that the integrated three-particle–one-loop antenna $\mathcal{X}_3^1$ is renormalised at scale $\mu^2 = s_{IK}$. In particlular, the integrated one-loop antenna is defined as [92]

$$\mathcal{X}_3^1(s_{ijk},z_1,z_2) = \frac{1}{C(\epsilon)}\delta(1-z_1)\delta(1-z_2)\int \mathrm{d}\Phi_{X_{ijk}}X_3^1(p_i,p_j,p_k) \tag{3.60}$$

in final-final and as

$$\mathcal{X}_3^1(s_{ij\hat{1}},z_1,z_2) = \frac{1}{C(\epsilon)}\delta(1-z_2)\delta(z_1-x)\int \mathrm{d}\Phi_2\frac{Q^2}{2\pi}X_3^1(p_i,p_j,p_{\hat{1}}) \tag{3.61}$$

in initial-final kinematics [137], where parameter x is defined in Eq. (3.20). A list of relevant integrated one-loop–three-particle antennae in final-final kinematics can be found in Table 4.

The terms coming from the shift of the renormalisation scale, $s_{IK} \to \mu_r^2$, in $\mathcal{X}_3^1$ are then split up into terms contributing to $\mathrm{d}\hat{\sigma}^{U,a}$ and $\mathrm{d}\hat{\sigma}^{U,c}$. Then the first subtraction term is given by

$$\begin{aligned}
\hat{\sigma}_{lm}^{U,a} &= -\mathcal{N}_{lm}^{VV}\int \frac{\mathrm{d}z_1}{z_1}\frac{\mathrm{d}z_2}{z_2}\mathrm{d}\Phi_n(z_1p_{\hat{1}},z_2p_{\hat{2}};p_3,\cdots,p_{n+2})\frac{1}{S_n}\mathbf{J}_{n+2}^{(1)}(\{p_{\hat{1}},p_{\hat{2}},\{p\}_n\},z_1,z_2)\\
&\cdot\left(M_{n+2}^1(z_1p_{\hat{1}},z_2p_{\hat{2}};p_3,\cdots,p_{n+2}) - \frac{\beta_0}{\epsilon}M_{n+2}^0(z_1p_{\hat{1}},z_2p_{\hat{2}};p_3,\cdots,p_{n+2})\right)J_n^n(\{p\}_n)
\end{aligned} \tag{3.62}$$

and cancels the leading poles, $\mathcal{O}(\epsilon^{-4})$ and $\mathcal{O}(\epsilon^{-3})$, of the first line in Eq. (2.75). Due to differences in the finite parts of the Catani one-loop operator $\mathbf{I}_2^{(1)}$ and the integrated antenna factor $\mathbf{J}_2^{(1)}$, poles of order $\frac{1}{\epsilon^2}$ and $\frac{1}{\epsilon}$ remain. Similar mismatches with opposite signs in $\mathrm{d}\hat{\sigma}^{U,b}$ and $\mathrm{d}\hat{\sigma}^{U,c}$ lead to a full pole cancellation. The second term can be written as

$$\begin{aligned}
\hat{\sigma}_{lm}^{U,b} &= -\mathcal{N}_{lm}^{VV}\int \frac{\mathrm{d}z_1}{z_1}\frac{\mathrm{d}z_2}{z_2}\mathrm{d}\Phi_n(z_1p_{\hat{1}},z_2p_{\hat{2}};p_3,\cdots,p_{n+2})\frac{1}{S_n}\\
&\cdot\frac{1}{2}\left[\mathbf{J}_{n+2}^{(1)}\otimes\mathbf{J}_{n+2}^{(1)}\right](\{p_{\hat{1}},p_{\hat{2}},\{p\}_n\},z_1,z_2)\cdot M_{n+2}^0(z_1p_{\hat{1}},z_2p_{\hat{2}};p_3,\cdots,p_{n+2})J_n^n(\{p\}_n)
\end{aligned} \tag{3.63}$$

and cancels the leading poles of the second line in Eq. (2.75). The last term is given by

$$\hat{\sigma}^{U,c}_{lm} = -\mathcal{N}^{VV}_{lm} \int \frac{\mathrm{d}z_1}{z_1}\frac{\mathrm{d}z_2}{z_2}\mathrm{d}\Phi_n(z_1 p_{\hat{1}}, z_2 p_{\hat{2}}; p_3, \cdots, p_{n+2}) \\ \cdot \mathbf{J}^{(2)}_{n+2}(\{p_{\hat{1}}, p_{\hat{2}}, \{p\}_n\}, z_1, z_2) M^0_{n+2}(z_1 p_{\hat{1}}, z_2 p_{\hat{2}}; p_3, \cdots, p_{n+2}) J^n_n(\{p\}_n)\,, \quad (3.64)$$

where we have introduced the two-loop–$(n+2)$-particle integrated antenna factor $\mathbf{J}^{(2)}_{n+2}$. In final-final kinematics, a single two-loop integrated antenna factor can schematically be written as

$$\mathbf{J}^{(2)}_2(p_I, p_J, z_1, z_2) = \sum_i \Big[c^{FF}_{1,i}\mathcal{X}^0_{4,i}(s_{IJ}) + c^{FF}_{2,i}\mathcal{X}^1_{3,i}(s_{IJ}) \\ + c^{FF}_{3,i}\frac{\beta_0}{\epsilon}\left(\frac{|s_{IJ}|}{\mu_r^2}\right)^{-\epsilon}\mathcal{X}^0_{3,i}(s_{IJ}) + \sum_j c^{FF}_{4,ij}\mathcal{X}^0_{3,i}\otimes\mathcal{X}^0_{3,j}\Big]\,, \quad (3.65)$$

where $\sum_{i/j}$ indicates a sum over appropriate antenna functions and the c's are constants associated with each two-loop integrated antenna factor. The integrated four-particle antenna in final-final kinematics is defined as [92]

$$\mathcal{X}^0_4(s_{ijkl}, z_1, z_2) = \frac{1}{C(\epsilon)^2}\delta(1-z_1)\delta(1-z_2)\int \mathrm{d}\Phi_{X_{ijkl}} X^0_4(p_i, p_j, p_k, p_l)\,. \quad (3.66)$$

In initial-final kinematics this changes to

$$\mathbf{J}^{(2)}_2(p_{\hat{1}}, p_I, z_1, z_2) = \delta(1-z_2)\cdot\sum_i \Big[c^{IF}_{1,i}\mathcal{X}^0_{4,i}(s_{\hat{1}I}, z_1) + c^{IF}_{2,i}\mathcal{X}^1_{3,i}(s_{\hat{1}I}, z_1) \\ + c^{IF}_{3,i}\frac{\beta_0}{\epsilon}\left(\frac{|s_{\hat{1}I}|}{\mu_r^2}\right)^{-\epsilon}\mathcal{X}^0_{3,i}(s_{\hat{1}I}, z_1) + \sum_j c^{IF}_{4,ij}\mathcal{X}^0_{3,i}\otimes\mathcal{X}^0_{3,j}(s_{\hat{1}I}, z_1) - \bar{\Gamma}^{(2)}(z_1)\Big]\,, \quad (3.67)$$

where the integrated four-particle antenna in initial-final kinematics is defined as [137]

$$\mathcal{X}^0_4(s_{ijk\hat{1}}, z_1, z_2) = \frac{1}{C(\epsilon)^2}\delta(x-z_1)\delta(1-z_2)\int \mathrm{d}\Phi_{X_{ijk}} X^0_4(p_i, p_j, p_k, p_{\hat{1}})\,, \quad (3.68)$$

with x given by Eq. (3.24). A list of relevant integrated X^0_4 antenna functions in final-final kinematics can be found in Table 4. As in the case of the one-loop $(n+2)$-particle integrated antenna factor, the full two-loop $(n+2)$-particle integrated antenna factor is a sum over all appropriate two-loop two-particle integrated antenna factors

$$\mathbf{J}^{(2)}_{n+2}(\{p_{\hat{1}}, p_{\hat{2}}, \{p\}_n\}, z_1, z_2) = \sum_J \mathbf{J}^{(2)}_2\,. \quad (3.69)$$

In summary, the virtual-virtual subtraction term can be written as

$$\begin{aligned}\mathrm{d}\hat{\sigma}^U_{lm} &= \mathrm{d}\hat{\sigma}^{U,a}_{lm} + \mathrm{d}\hat{\sigma}^{U,b}_{lm} + \mathrm{d}\hat{\sigma}^{U,c}_{lm} \\ &= -\mathcal{N}^{VV}_{lm}\int \frac{\mathrm{d}z_1}{z_1}\frac{\mathrm{d}z_2}{z_2}\mathrm{d}\Phi_n(z_1 p_{\hat{1}}, z_2 p_{\hat{2}}; p_3, \cdots, p_{n+2})\frac{1}{S_n}\Big\{\end{aligned}$$

$$
\begin{aligned}
&\mathbf{J}^{(1)}_{n+2}(\{p_{\hat{1}},p_{\hat{2}},\{p\}_n\},z_1,z_2)\Bigg(M^1_{n+2}(z_1p_{\hat{1}},z_2p_{\hat{2}};p_3,\cdots,p_{n+2})\\
&-\frac{\beta_0}{\epsilon}M^0_{n+2}(z_1p_{\hat{1}},z_2p_{\hat{2}};p_3,\cdots,p_{n+2})\Bigg)\\
&+\frac{1}{2}\left[\mathbf{J}^{(1)}_{n+2}\otimes\mathbf{J}^{(1)}_{n+2}\right](\{p_{\hat{1}},p_{\hat{2}},\{p\}_n\},z_1,z_2)M^0_{n+2}(z_1p_{\hat{1}},z_2p_{\hat{2}};p_3,\cdots,p_{n+2})\\
&+\mathbf{J}^{(2)}_{n+2}(\{p_{\hat{1}},p_{\hat{2}},\{p\}_n\},z_1,z_2)M^0_{n+2}(z_1p_{\hat{1}},z_2p_{\hat{2}};p_3,\cdots,p_{n+2})\Bigg\}J^n_n(\{p\}_n)\,,
\end{aligned}
\tag{3.70}
$$

and if properly constructed, one should get

$$
Poles(\mathrm{d}\hat{\sigma}^U)=Poles(M^2_{n+2})\,. \tag{3.71}
$$

A schematic overview of the construction of antenna subtraction terms at NNLO is given in Fig. 5. The figure also shows the inheritance of integrated antenna functions from subtractions at higher to individual contributions at lower partonic multiplicities.

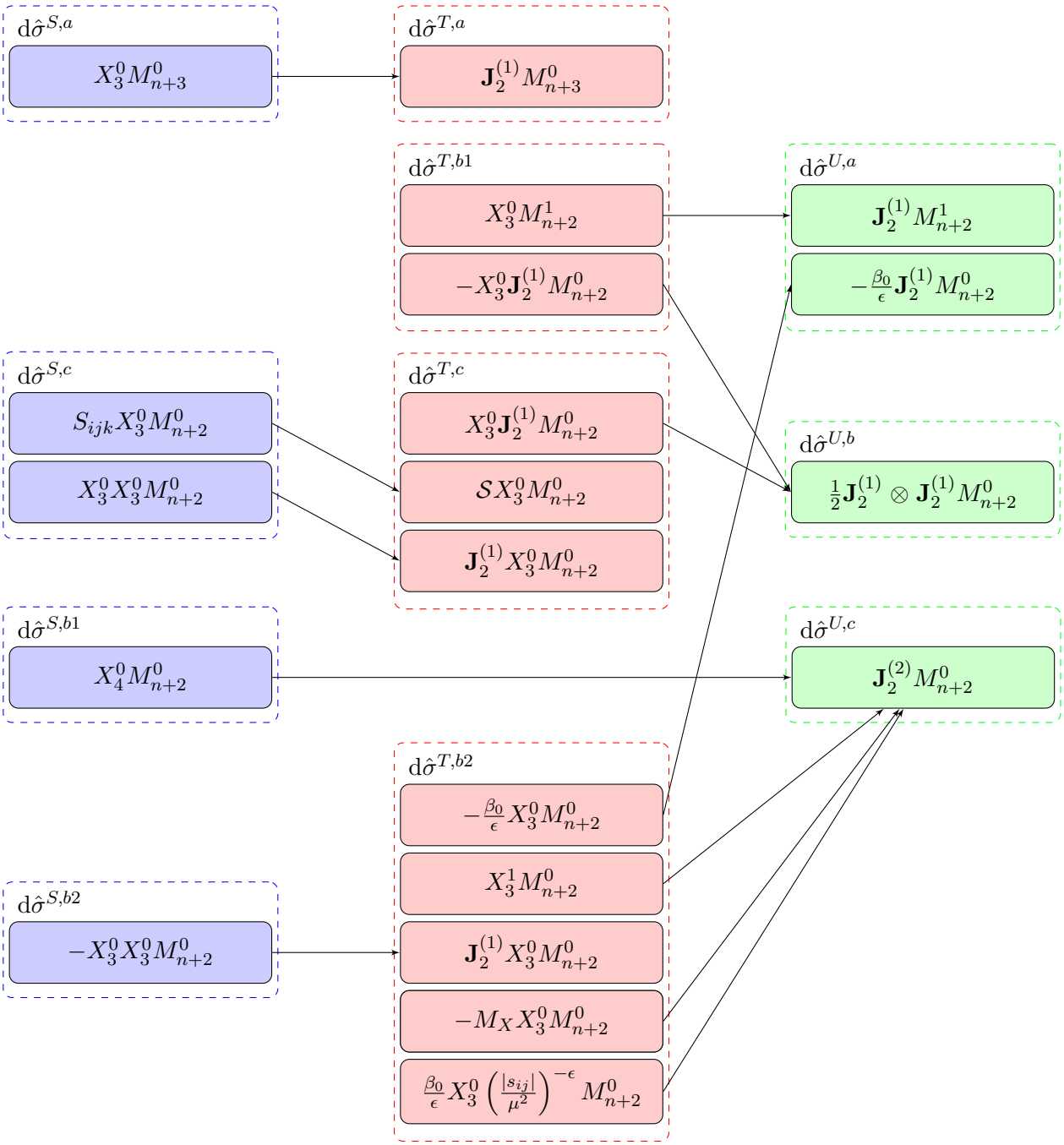

Figure 5. Schematic overview of contributions to NNLO subtraction terms at the real-real (blue), real-virtual (red) and virtual-virtual (green) level with arrows indicating the contributions of integrated subtraction terms to subtraction terms at lower partonic multiplicities.

4 NNLOJET

In this section we first discuss some general aspects of the NNLOJET program and give an overview of the workflow within NNLOJET. Then we will discuss the method of recombination of histogram data from individual production runs which turns out to be crucial for obtaining correct results, in particular for calculations at NNLO accuracy. In the second half of this section, more process specific features of DIS will be discussed, that are on the one hand the generation of phase space points and on the other hand the method of numerical evolution of virtual convolution integrals. The method of evaluation of virtual convolution integrals is important in the CPU performance of the program and is discussed in-depth.

4.1 General overview

All the calculations that are presented in this thesis have been performed within the framework of NNLOJET. The NNLOJET code is a parton-level event generator that provides the framework for the implementation of jet production processes to NNLO accuracy, using the antenna subtraction method. Besides containing the event generator infrastructure (Monte Carlo phase space integration, event handling and analysis routines), it supplies the unintegrated and integrated antenna functions and the phase space mappings relevant to all kinematic situations.

At the heart of the NNLOJET program lies the adaptive vegas algorithm [138] that provides random numbers to generate phase space points. For each subtraction term relevant mapped momenta are evaluated and it is checked that corresponding momentum sets pass a technical y_0 cut. Details of the DIS phase space and the y_0 cut can be found in Section 4.3. Within the event cut routine, partons are clustered into jets and experimental cuts are applied to the generated event. Parton distribution functions and values for α_s are read in from user defined PDF sets using an interface to the LHAPDF program [139]. NNLOJET possesses a highly flexible histogramming routine, that is able to generate user-defined multidimensional histograms that can have variable bin-widths. Post-processing of the output to histograms will be discussed in greater detail in Section 4.2. An overview of the workflow within NNLOJET is given in Table 6. The implementation of processes in the NNLOJET framework is semi-automised in such a way that process libraries are generated by scripts. However, matrix elements for all RR, RV and VV processes, and the construction of the antenna subtraction terms have to be explicitly implemented for each process. The NNLOJET program is controlled through a flexible runcard interface and an example runcard is provided in appendix C.

So far, the following processes have been successfully calculated within the framework of NNLOJET:

- Di-jet production in proton-proton collisions [69],
- $Z + (0/1)$ jet production [62],
- $H + (0/1)$ jet production [60],

and work discussed in this thesis extends the above list by the following processes

- Single-jet production in DIS (up to N3LO),
- Di-jet production in DIS,
- $e^+e^- \to 3$ jet annihilation.

Our NNLOJET implementation of jet production in DIS [71, 152] and in $e^+e^- \to 3j$ annihilation uses the same matrix elements [140–142] as were used in $Z + j$ production [62], however, in different kinematic crossings. While the phase space for $Z + j$ production corresponds to a single crossing region of the electron-positron matrix elements, four different crossing regions are required [15, 143] to describe DIS di-jet production, depending on the relative size of Q^2 compared to the parton-parton invariants.

Recently, the program has been linked to the APPLfast interface which enables the values of α_s and PDFs to be read in and scale variations to be performed a posteriori. This feature is crucial in the fitting of PDFs or the value of α_s which require both theoretical and experimental input. First results from applications of the APPLfast interface will be presented in Section 11.

4.2 Data recombination

To evaluate cross sections with the adaptive vegas algorithm [138], a warm-up run has to be performed first of all. In this warm-up run, a grid is generated that maps random numbers to phase space points, and the mappings are such that in actual production runs more phase space points are generated in regions of phase space where the cross section is large. For individually convergent production runs, the Monte Carlo error goes as $(\sim 1/\sqrt{n})$, where n is the number of points evaluated in that run. In this limit, results from individual runs should be Gaussian distributed such that the best estimate for the error is given by a weighted average according to

$$\sigma = \frac{\sum_{i=1}^{N} \frac{\sigma_i}{\Delta\sigma_i^2}}{\sum_{i=1}^{N} \frac{1}{\Delta\sigma_i^2}}\,, \tag{4.1}$$

where N is the total number of production runs and $\Delta\sigma_i^2$ is the statistical variance on the cross section of the i^{th} production run. It turns out however, that production runs at NNLO are slowly convergent, this in particular for real-real corrections. In this case, individual runs do **not** reach the convergent limit and a direct weighted average of cross sections from individual production runs gives an incorrect result. To solve this issue, the data processing used in NNLOJET merges k individual runs into one single "pseudo"-run by adding results of individual runs linearly, that is

$$\sigma_{\text{pseudo}} = \sum_{i=1}^{k} \frac{\sigma_i}{N_k}\,, \tag{4.2}$$

where N_k is the total number of evaluated events in the sum of k individual runs. For an appropriate value of k, the "pseudo"-runs should be in the convergent limit and the

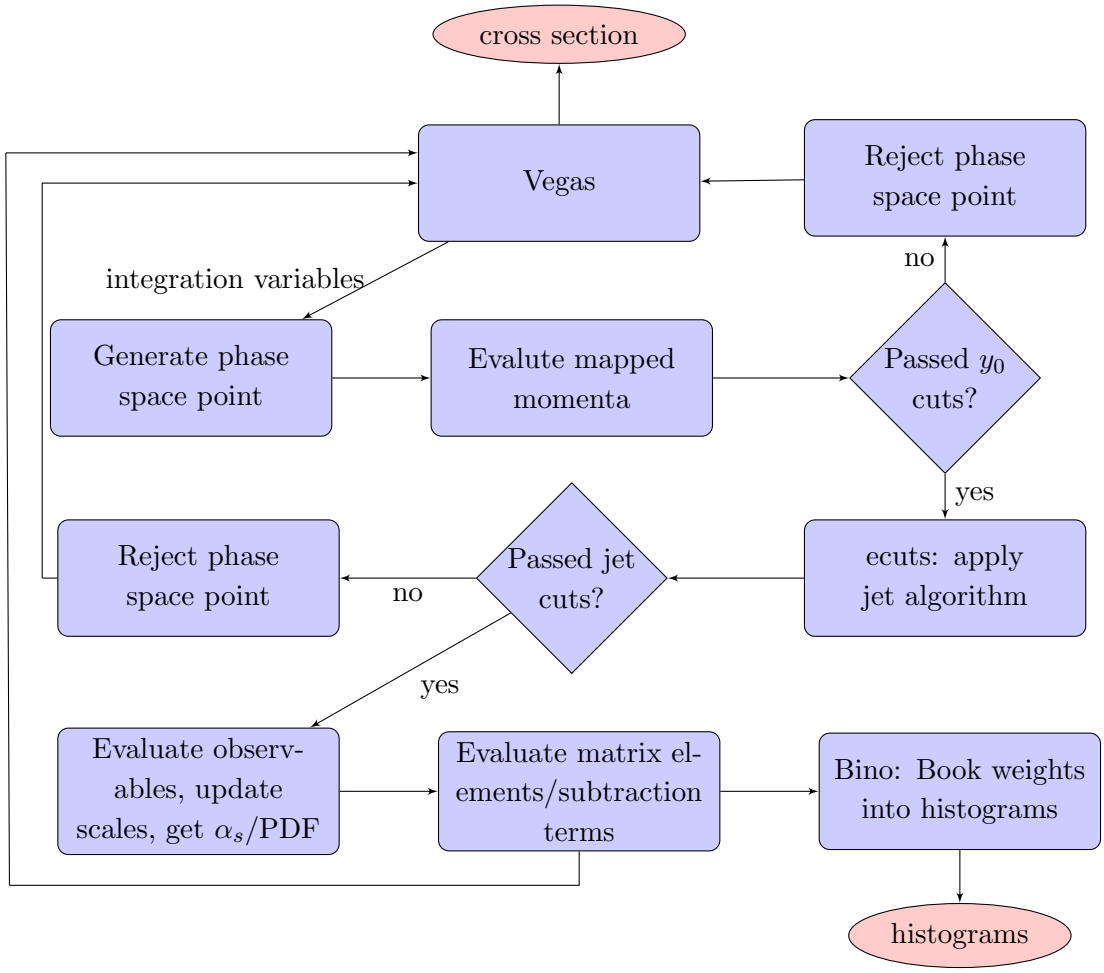

Figure 6. Schematic overview of the NNLOJET program.

weighted average of these "pseudo"-runs evaluates to the correct result. The required value of k is determined by a scan over k and a value is chosen such that weighted averages of the corresponding merged"pseudo"-runs do not change anymore within statistical errors if the value of k is increased. The advantage of using weighted averages is twofold; first of all, weighted averages give the best error estimate and secondly, results for production runs containing outliers are assigned a small weight due to the large variances associated to them such that problematic runs have a diminishing effect on the resultant cross section. More detailed studies on the merging procedure used in NNLOJET can be found in Refs. [136] and [144].

4.3 DIS phase space

The fundamental process in DIS is a $2 \to 2$ lepton-quark scattering

$$p_{\hat{l}} + p_a \to p_l + p_{j_1}(+p_{j_2})(+p_{j_3})(+p_{j_4})\,, \tag{4.3}$$

where p_a is the momentum of the initial-state parton. At leading order, one parton is in the final state and more QCD particles may be radiated at higher orders. In our calculations,

only QCD corrections are considered such that the lepton kinematics are completely fixed by the momentum of the virtual vector boson and the effective scattering is described by a $2 \to 1$ process for single-jet production

$$p_q + p_a \to p_{j_1}(+p_{j_2})(+p_{j_3})(+p_{j_4})\,, \tag{4.4}$$

with

$$p_q = p_l - p_{\hat{l}}\,. \tag{4.5}$$

Knowledge of the vector boson's momentum p_q together with the initial lepton momentum $p_{\hat{l}}$ can be used to reconstruct the final-state lepton kinematics p_l a posteriori. In general, the dimensionality of the phase space integral for DIS processes with n massless particles in the final state is given by

$$N_{dim} = 3n - 5\,. \tag{4.6}$$

Every particle has three degrees of freedom as each is constrained to lie on its mass-shell. Five degrees of freedom have to be subtracted due to total momentum conservation in the event and due to the 2π azimuthal symmetry of the scattering. The full integral in Eq. (2.107) has dimensionality (N_{dim}+1) and (N_{dim}+2) for real and virtual integration, respectively, that is one additional variable for each, the Feynman x and the extra convolution in the virtual integration. Up to initial-state collinear singularities which are subtracted by a minimum transverse momentum cut to define the jets, corrections to DIS with two-particles in the final state are free from infrared singularities and the corresponding phase space depends on one free parameter only.

In Section 2.6 we stated that matrix elements and antenna subtraction terms do not, in general, coincide in unresolved configurations due to angular terms. Corrections to DIS with three-particles in the final state are not free from infrared singularities and angular terms could be removed by generating events in appropriate pairs. In this case however, no angular rotated events are required as all reduced matrix elements only contain quarks and angular terms are absent.

When generating the four-particle final state, phase space points have to be generated in pairs to enable cancellation of angular terms for the first time. The four-particle (three parton) phase space is constructed in a sequential splitting according to

$$p_i + p_{jk} \to p_i + p_j + p_k\,. \tag{4.7}$$

Angular partner events are generated by rotating particles j and k around the initial state's momentum $p_{\hat{1}}$ by an angle of $\pi/2$ in particle j and k's center of mass (CoM) frame. In that frame, angular terms cancel in the collinear limits $(j||\hat{1})$ and $(k||\hat{1})$ between events and their rotated partners. Boosting back into the first frame along the original collinear direction of particles j and k, angular terms related to the $(j||k)$ collinear limit cancel between the partner events in a similar way. If this cancellation holds in a particular frame, it is true in any other frame due to Lorentz invariance of corrections and subtraction terms, making antenna subtraction local. It is clear that in Eq. (4.7), parton i is treated differently compared to partons j and k, and for this reason, so-called phase space wedges are introduced.

The phase space is generated for one particular wedge restricted to kinematic cuts. An appropriate kinematic restriction for a wedge suitable for single-unresolved configurations $(j||k)$, $(j||\hat{1})$ and $(k||\hat{1})$ is given by

$$\begin{aligned}&(s_{min} = s_{jk}) \text{ or}\\ &\Big(s_{min} = s_{\hat{1}j} \text{ and } s_{jk} < s_{ij}\Big) \text{ or } \big(s_{min} = s_{\hat{1}k} \text{ and } s_{jk} < s_{ik}\big)\ ,\end{aligned}$$

where s_{min} is the minimal kinematic invariant of all pairs of partonic momenta in the momentum set. The full phase space is obtained by a sum over three such wedges in which each final-state momentum plays the role of particle i in turn. For double-unresolved configurations going down to a single jet in the final state, no further rotations are required.

The five-particle phase space has two types of unresolved configurations which are the triple-collinear and the double–single-collinear unresolved configurations. Each of these limits requires different rotations to account for angular terms. For this purpose, the five-particle phase space is split into two regions, a and b, treating triple-collinear and double-collinear limits, respectively. In region a, the sequential splitting occurs according to

$$p_i + p_{jkl} \to p_i + p_j + p_{kl} \to p_i + p_j + p_k + p_l\,. \tag{4.8}$$

A particular wedge, suitable for $(j||k||l)$ and $(\hat{1}||k||l)$, is restricted to the following kinematic cuts

$$\begin{aligned}&(s_{min1} = s_{kl} \text{ and } s_{min2} = \min(s_{jk}, s_{jl})) \text{ or}\\ &\big(\{s_{min1}, s_{min2}\} \in \{s_{\hat{1}k}, s_{\hat{1}l}, s_{kl}\} \text{ and } s_{jkl} < s_{ikl}\big)\ ,\end{aligned}$$

where s_{min1} and s_{min2} are the two smallest kinematic invariants in the momentum set. For each event in a particular wedge three additional events are generated:

- One with a $\pi/2$ rotation of p_j and p_{kl} around the axis defined by $p_{\hat{1}}$ in the CoM frame of particles j, k and l. This event accounts for angular terms in the limits $(j||\hat{1})$, $(\hat{1}||k||l)$ and $(j||k||l)$.
- Another event is generated by rotating p_k and p_l around $p_{\hat{1}}$ in particle k and l's CoM frame. This event accounts for angular terms in $(k||l)$, $(k||\hat{1})$ and $(l||\hat{1})$ configurations.
- The last event is generated by consecutively applying both of the above rotations to account for single-unresolved limits of particles k and l in the first, and the $(j||\hat{1})$ single-unresolved limit in the second rotated partner event.

In this way a total of four events are generated for each wedge. The full phase space of region a is spanned by twelve wedges containing all possible combinations for assignments of particles to the roles played by i and j.

Similarly region b is generated according to the sequential splitting

$$p_{ij} + p_{kl} \to p_i + p_j + p_k + p_l\,. \tag{4.9}$$

A single wedge is constrained to

$$\begin{aligned}
&(\{s_{min1}, s_{min2}\} \in \{s_{ij}, s_{kl}\}) \text{ or} \\
&\left(\{s_{min1}, s_{min2}\} \in \{s_{ij}, \min(s_{\hat{1}k}, s_{\hat{1}l})\}\right) \text{ or} \\
&\left(\{s_{min1}, s_{min2}\} \in \{s_{kl}, \min(s_{\hat{1}i}, s_{\hat{1}j})\}\right) .
\end{aligned}$$

In total, three additional rotated partner events are generated by rotating the particle pairs i, j and k, l around $p_{\hat{1}}$ in their respective CoM frames. Summing the six wedges for all possible pairings of (ij) and (kl) gives the full phase space for region b. Taken together, regions a and b give the full five-particle phase space for DIS. For stability reasons, a technical cut

$$|s_{ij}|/s_{\hat{1}\hat{2}} > y_0, \tag{4.10}$$

is applied to every generated phase point and has to be fulfilled by every final-final and initial-final pair of partons i and j. The use of this phase space cut is twofold; very small kinematic invariants are avoided and Lorentz transformations to relevant CoM frames required in the generation of rotated partner events cannot become singular. For calculations presented in this thesis, y_0 is chosen to be equal to or less than $3 \cdot 10^{-7}$. In initial-final mappings, the resultant invariants might be smaller than the original ones such that for momenta that are mapped once, y_0 is taken to be smaller by a factor of 100, and for momenta that are mapped twice, no y_0 cut is applied.

The discussion in this section was constrained to the evaluation of phase space points and the evaluation of convolution integrals of partonic cross sections with PDFs has been ignored. Evaluation of these convolutions can be done in two different ways and this is discussed in the next section.

4.4 Evaluation of +-distributions

The purpose of a Monte Carlo program is to integrate the master formula Eq. (2.107). In the case of DIS, only the convolution for one partonic initial state with the partonic cross section has to be calculated. In general, the cross section can then be expressed as

$$\mathrm{d}\sigma = \int_0^1 \frac{\mathrm{d}\xi}{\xi} f(\xi, \mu_f^2) \int_0^1 \frac{\mathrm{d}x}{x} M(x, \{x\,\xi\,p\}, \mu_r^2)\, J(\{x\,\xi\,p\})\, \mathrm{d}\Phi_n(\{x\,\xi\,p\}) , \tag{4.11}$$

where M is an infrared finite function that includes the matrix elements and subtraction terms for production of n particles in the final state, J is a generic jet function and $\{x\,\xi\,p\}$ represents a general momentum set in which the partonic initial state is rescaled by a factor $x\,\xi$. In the case that M does not include mass factorisation terms, the integration over x is trivial as then the dependence on x factorises according to

$$M(x, \{x\,\xi\,p\}, \mu_r^2, \mu_f^2) = \delta(1-x) M'(\{\xi\,p\}, \mu_r^2, \mu_f^2) . \tag{4.12}$$

If mass factorisation terms are included in M, then M can be decomposed into

$$M(x, \{x\,\xi\,p\}, \mu_r^2, \mu_f^2) = \Big(A(x)\delta(1-x) + B(x) +$$

$$\sum_{m\geq 0} C_m(x) \left(\frac{\ln^m(1-x)}{1-x}\right)_+ \Bigg) M'(\{x\,\xi\,p\},\mu_r^2,\mu_f^2)\,, \quad (4.13)$$

where the coefficients A, B and C have to be distributed into two regions; the δ-contributions are collected in one and the non-delta pieces in the other region. This can be written as

$$\begin{aligned}
\mathrm{d}\sigma = & \int_0^1 \frac{\mathrm{d}\xi}{\xi} f(\xi,\bar{\mu_f}^2) \int_0^1 \mathrm{d}x \Bigg[A(1) \\
& - \frac{1}{(1-x)} \sum_{m\geq 0} C_m(1) \ln^m(1-x) \Bigg] M'(\{\xi\,p\},\bar{\mu_r}^2,\bar{\mu_f}^2)\, J(\{\xi\,p\})\, \mathrm{d}\Phi_n(\{\xi\,p\}) \\
& + \int_0^1 \frac{\mathrm{d}\xi}{\xi} f(\xi,\mu_f^2) \int_0^1 \frac{\mathrm{d}x}{x} \Bigg[B(x) \\
& + \frac{1}{(1-x)} \sum_{m\geq 0} C(x) \ln^m(1-x) \Bigg] M'(\{x\,\xi\,p\},\mu_r^2,\mu_f^2)\, J(\{x\,\xi\,p\})\, \mathrm{d}\Phi_n(\{x\,\xi\,p\})\,,
\end{aligned} \quad (4.14)$$

where $\bar{\mu}^2 \neq \mu^2$ if the factorisation scale is a dynamical scale, i.e. one that depends on the kinematic variables of the phase space point p. The issue in the evaluation of Eq. (4.14) arises because M' has to be evaluated at two different phase space points, one with kinematics $x\xi p$ and the other at ξp. This is in general not optimal for histogram booking and the application of kinematic cuts. In another approach, the substitution $\xi \to zx$ transforms the integral into

$$\int_0^1 \frac{\mathrm{d}\xi}{\xi}\, a(\xi,\mu_f^2) \int_0^1 \frac{\mathrm{d}x}{x} M(x,\{x\,\xi\,p\},\mu_r^2,\mu_f^2) = \int_0^1 \frac{\mathrm{d}z}{z} \int_z^1 a\left(\frac{z}{x},\mu_f^2\right) \frac{\mathrm{d}x}{x} M(x,\{z\,p\},\mu_r^2,\mu_f^2)\,, \quad (4.15)$$

where in Eq. (4.15), M is only evaluated once per phase space point p. The Jacobians for the coefficients in Eq. (4.13) can be derived in the following way: for coefficient A one gets

$$\int_0^1 A(x)\delta(1-x)\,\mathrm{d}x \equiv A(1) \equiv \int_z^1 \mathrm{d}x\, \frac{A(1)}{(1-z)}\,, \quad (4.16)$$

and the Jacobian evaluates to $1/(1-z)$. For coefficient B, the Jacobian is unity. The $+$-distribution for coefficient C can be written as

$$\begin{aligned}
\int_z^1 C_m(x) \left(\frac{\ln^m(1-x)}{1-x}\right)_+ \mathrm{d}x = & \int_z^1 \frac{(C_m(x)-C_m(1))\ln^m(1-x)}{(1-x)}\,\mathrm{d}x \\
& - \int_0^z \frac{C_m(1)\ln^m(1-x)}{(1-x)}\,\mathrm{d}x,
\end{aligned} \quad (4.17)$$

where the integration limits of the second term on the right-hand side of Eq. (4.17) have to be changed to $x \in [z,1]$ and this is achieved by

$$-\int_0^z \frac{C(1)_m \ln^m(1-x)}{(1-x)}\,\mathrm{d}x = \frac{C(1)_m \ln^{m+1}(1-z)}{m+1} = \int_z^1 \mathrm{d}x \frac{\ln^{m+1}(1-z)}{(m+1)(1-z)} C_m(1)\,. \quad (4.18)$$

Then the integral in the master formula given in Eq. (2.107) can be evaluated as

$$\begin{aligned}\mathrm{d}\sigma = \int_0^1 \frac{\mathrm{d}z}{z}\Bigg\{ \int_z^1 a(z,\mu_f^2)\,\mathrm{d}x \left[A'(1) - \sum_{m\geq 0} C_m(1)\frac{\ln^m(1-x)}{(1-x)}\right] \\ + a\left(\frac{z}{x},\mu^2\right)\frac{\mathrm{d}x}{x}\left[B(x) + \sum_{m\geq 0} C_m(x)\frac{\ln^m(1-x)}{(1-x)}\right]\Bigg\} \\ \times M'(\{z\,p\},\mu_r^2,\mu_f^2)\,J(\{z\,p\})dPS(\{z\,p\})\,, \end{aligned} \tag{4.19}$$

where A' is defined as

$$A'(1) = \frac{A(1)}{(1-z)} + \sum_{m\geq 0}\frac{\ln^{m+1}(1-z)}{(m+1)(1-z)}C_m(1)\,. \tag{4.20}$$

The second method is advantegeous over the first as fewer phase space points have to be generated and it is this method that is implemented in NNLOJET to evaluate virtual contributions to cross sections.

5 Kinematics of jet production in deep inelastic scattering

The basic interaction in deep inelastic lepton-proton scattering is mediated by a virtual gauge boson. The kinematics of the fully inclusive process can be inferred from the momenta of the incoming particles and of the outgoing lepton:

$$l(k) + p(P) \to l'(k') + X(p_X),$$

such that a four-momentum $q = k - k'$ is transferred to the proton. Measurements are carried out in terms of the following variables (neglecting the proton mass):

$$s_{lp} = (k + P)^2\,, \quad Q^2 = -q^2\,, \quad x = \frac{Q^2}{2q \cdot P}\,, \quad y = \frac{q \cdot P}{k \cdot P} = \frac{Q^2}{x s_{lp}}\,, \tag{5.1}$$

where x is the Bjorken x variable from Eq. (2.35). The underlying parton-level process is the scattering of a quark from inside the proton with the virtual vector boson. At leading order, this quark carries a momentum fraction x of the proton momentum and scatters by an angle γ_h, defined as

$$\cos\gamma_h = \frac{(1-y)xE_p - yE_l}{(1-y)xE_p + yE_l}\,, \tag{5.2}$$

with E denoting the energy.

More detailed information on the underlying parton-level dynamics can be gained by examining the hadronic final state X. For the work presented in this thesis, we calculated distributions in three different reference frames, which are the laboratory, the photon-proton center of mass and the Breit frame. The Breit frame is defined by requiring proton and gauge boson momenta to take the form

$$P_B = (Q/(2x), 0, 0, Q/(2x))\,, \quad q_B = (0, 0, 0, -Q)\,, \tag{5.3}$$

with $Q = \sqrt{Q^2}$. Momenta in the Breit frame are indicated by a subscript B. The Lorentz transformation from the laboratory frame to the Breit frame can be determined from the

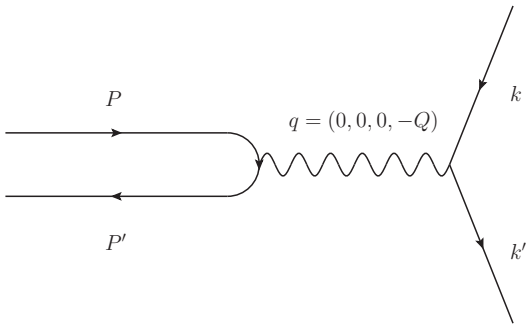

Figure 7. An illustration of the basic hard scattering process in the Breit frame with incoming proton momentum P, incoming lepton momentum k, virtual boson exchange momentum q, outgoing proton momentum P' and outgoing lepton momentum k'.

measured lepton kinematics [1]. In this frame, the leading-order DIS process results in an outgoing quark with vanishing transverse momentum and can be rejected by requiring final states with non-vanishing transverse momentum $p_{T,B}$.

Of particular interest is jet production in the Breit frame, which has a large cross section and allows the measurement of a variety of different distributions that can provide constraints on the parton content of the proton and on the strong coupling constant. Single-jet production in DIS in the laboratory frame at leading order is at $\mathcal{O}(\alpha^2\alpha_s^0)$ and only contains quarks in the initial-state; sensitivity to the strong coupling α_s and initial-state gluons only arises at NLO. In contrast, jet production in the Breit frame is sensitive to α_s and both initial-state quarks and gluons already at LO. Distributions in both frames were measured by experiments H1 and ZEUS at the HERA electron-proton collider.

In run I, HERA operated with beam energies $E_e = 27.5$ GeV and $E_p = 820$ GeV (later also with $E_p = 920$ GeV), resulting in $\sqrt{s_{ep}} = 300$ GeV. Both experiments, H1 and ZEUS, measured inclusive jet production cross sections in the laboratory frame [145, 146] using the JADE algorithm as described in Section 2.4. The experiments in particular studied jet production rates as a function of the y_{cut} parameter. Comparison of these measurements to our predictions to N3LO in the strong coupling constant are presented in Section 12.

In run II, HERA operated with beam energies $E_e = 27.5$ GeV and $E_p = 920$ GeV, resulting in $\sqrt{s_{ep}} = 318$ GeV. The two experiments measured jet production cross sections [3, 5–10, 12, 14] using the k_T algorithm with $R_0 = 1$ as function of the Breit frame jet variables

$$\begin{aligned} M_{jj} = M_{12} &= \sqrt{(p_{j1} + p_{j2})^2}\,, \\ \bar{E}_{T,B} = \langle p_T \rangle_2 &= \frac{1}{2}\left(p_{T,B,j1} + p_{T,B,j2}\right)\,, \\ \xi = \xi_2 &= x\left(1 + \frac{M_{12}^2}{Q^2}\right)\,, \\ \eta^* &= \frac{1}{2}\left|\eta_{B,j1} - \eta_{B,j2}\right|\,, \end{aligned} \tag{5.4}$$

where for leading-order di-jet production, ξ_2 can be identified with the momentum fraction of the incoming parton relative to the proton momentum. Corresponding results obtained with our NNLOJET code are given in Section 9.

Inclusive single-jet measurements in DIS can also be performed in the Breit frame, where even though partonic recoil ensures the production of at least two jets, one of the jets can still fail a particular experimental cut. This class of events has been widely studied by both the H1 [3, 4, 6–9] and ZEUS [11–13] experiments, where inclusive jet-p_T measurements are of particular interest. Corresponding distributions are compared to our NNLOJET predictions using the k_T algorithm with $R_0 = 1$ in Section 8.

In both run periods of the HERA collider, H1 and ZEUS also measured di-jet production in diffractive electron-proton collisions in the photon-proton center of mass frame ($\gamma^* p$-frame) [19–24] and diffractive observables that are measured in this frame are denoted by an asterix. Relevant measurements were taken using the k_T algorithm with $R_0 = 1$ and clustering the jets in the $\gamma^* p$-frame. Experimental measurements are compared to our

NNLOJET predictions in Section 10. In this thesis we restrict the theory-to-data comparison in diffractive DIS to distributions in the DIS-y variable, the transverse momentum of the jets and the proton-photon invariant mass W.

In the following sections, we will give details on the construction of relevant antenna subtraction terms required for the corresponding theoretical predictions before moving on to the phenomenological results for each of the above measurements.

6 NNLO cross section for DIS single-jet production in the laboratory frame

In this section we give the subtraction terms for single-jet production in neutral current DIS in the laboratory frame as well as an outline of procedures to validate the construction of antenna subtraction terms. The calculation of this process with the antenna subtraction formalism was used to validate the method of the Projection-To-Born subtraction at NNLO accuracy for the first time. As a result, the method of Projection-To-Born could be used to calculate single-jet production in the laboratory frame to N3LO accuracy. Phenomenological results of the corresponding calculation are presented in Section 12.

6.1 General notation for matrix elements

In DIS, the initial states l and m appearing in Eq. (2.111) are the electron and a parton, respectively. For single-jet production in the laboratory frame, the leading-order process is quark-initiated. Gluon-initiated processes only enter as real correction at NLO. For this process, the lowest final-state parton multiplicity is one, defining $n_B = 1$, and at NNLO up to two further partons are radiated, giving a maximal value of $n = 3$ in Eq. (2.111). Further, at most two gluons appear in real-real contributions such that the symmetry factor S_n is maximally 2! for such corrections in the quark-initiated case and one otherwise. The jet function J is defined by experimental cuts and depends on the details of the experimental analysis. From the definition in Eq. (2.116) one has

$$\mathcal{N}_{eq}^{B,1j} = (4\pi\alpha)^2 \tag{6.1}$$

at Born level. The $1j$ superscript will be dropped in the following, as only single-jet production in the laboratory frame is discussed in the rest of this section. Starting from this value of $\mathcal{N}_{eq}^{B}$, all other relevant QCD-independent factors can be deduced from the relations given in Eqs. (2.117).

The full set of matrix elements used in our calculations are classified according to their particle content and the adopted conventions are:

- Processes containing one quark-antiquark pair and further n gluons are denoted by

$$B_n^{Z,\ell}.$$

- Processes containing two quark–antiquark pairs of different flavours and n gluons are denoted by

$$C_n^{Z,\ell}.$$

- Processes with two quark-antiquark pairs of the same falvour are denoted by

$$D_n^{Z,\ell},$$

where ℓ donates the loop order of the contribution, which is at most two at NNLO. Note that C-type corrections include the sum of contributions in which the vector boson couples to each of the quark lines, including appropriate interferences. For every matrix element, a Z in the superscript stands for the sum of photon, γ, and Z boson exchanges and their interferences. From this point onwards, we introduce a shorthand notation relevant for all following sections. In matrix elements, momentum arguments are replaced according to $p_i \to i$ for any particle i and the explicit dependence on the lepton momenta in any matrix element is dropped. In the discussion of subtraction terms, only gluon- and quark-initiated subtraction terms are given. Corresponding antiquark-initiated subtraction terms can simply be obtained by line reversals of the arguments in every reduced matrix element at the tree as well as at the loop level.

6.2 Quark-initiated cross section at LO

Adapting the above conventions, the quark-initiated leading-order process evaluates to

$$\mathrm{d}\hat{\sigma}^{LO}_{eq} = \mathcal{N}^{B}_{eq}\mathrm{d}\Phi_2(p_{\hat{1}}, p_{\hat{2}}; p_3, p_4) B_0^{Z,0}(\hat{1}_q, 4_q) J_1^1(\{p\}_1)\,, \tag{6.2}$$

and gluon-initiated processes only enter at NLO.

6.3 Quark-initiated cross sections at NLO

6.3.1 Real contribution

For single radiative corrections at NLO there is only a single contribution from the process $qe \to eqg$ given by

$$\mathrm{d}\hat{\sigma}^{R}_{eq} = \frac{N^2-1}{N^2}\mathcal{N}^{R}_{eq}\mathrm{d}\Phi_2(p_{\hat{1}}, p_{\hat{2}}; p_3, p_4, p_5) B_1^{Z,0}(\hat{1}_q, 4_g, 5_q) J_1^2(\{p\}_2)\,, \tag{6.3}$$

where an expression for squared matrix element is given in Ref. [92], with the quark crossed into the initial state.

6.3.2 Virtual contribution

The virtual correction receives contributions only from the process of $qe \to eq$ at one loop

$$\mathrm{d}\hat{\sigma}^{V}_{eq} = \frac{N^2-1}{N^2}\mathcal{N}^{V}_{eq}\mathrm{d}\Phi_2(p_{\hat{1}}, p_{\hat{2}}; p_3, p_4) B_0^{Z,1}(\hat{1}_q, 4_q) J_1^1(\{p\}_1)\,, \tag{6.4}$$

and the matrix element can be found in Ref. [92], with the quark crossed into the initial state.

6.4 Quark-initiated subtraction terms at NLO

6.4.1 Real subtraction term

The subtraction for the real correction in Eq. (6.3) is given by

$$\mathrm{d}\hat{\sigma}^{S,NLO}_{eq} = \frac{N^2-1}{N^2}\mathcal{N}^{R}_{eq}\mathrm{d}\Phi_2(p_{\hat{1}}, p_{\hat{2}}; p_3, p_4, p_5) B_1^{Z,0,S}(\hat{1}_q, 5_g, 4_q)\,, \tag{6.5}$$

with

$$\begin{aligned} &B_1^{Z,0,S}(\hat{1}, i, k) = \\ &\quad + A_3^0(1, i, k)\, B_0^{Z,0}(\overline{1}, (\widetilde{ik}))\, J_1^1(\{p\}_1)\,. \end{aligned} \tag{6.6}$$

6.4.2 Virtual subtraction term

According to the construction principle for antenna subtraction terms, the virtual subtraction term is given by the integrated real subtraction term combined with mass factorisation terms. Indeed we find that

$$\mathrm{d}\hat{\sigma}_{eq}^{T,NLO} = \frac{N^2-1}{N^2}\mathcal{N}_{eq}^{V}\mathrm{d}\Phi_2(p_{\hat{1}},p_{\hat{2}};p_3,p_4)B_0^{Z,1,T}(\hat{1}_q,4_q)J_1^1(\{p\}_1)\,, \tag{6.7}$$

with

$$\begin{aligned} &B_0^{Z,1,T}(\hat{1},k) = \\ &\quad -J_{2,QQ}^{1,IF}(s_{1k})\,B_0^{Z,0}(1,k,4,2)\,J_1^1(\{p\}_1)\,. \end{aligned} \tag{6.8}$$

6.5 Gluon-initiated cross section at NLO

6.5.1 Real contribution

At NLO, the gluon appears in the initial state in the process $ge \to eq\bar{q}$ for the first time:

$$\mathrm{d}\hat{\sigma}_{eg}^{R} = \frac{N^2-1}{N^2}\mathcal{N}_{eg}^{R}\mathrm{d}\Phi_2(p_{\hat{1}},p_{\hat{2}};p_3,p_4,p_5)B_1^0(4_{\bar{q}},\hat{1}_g,5_q)J_1^2(\{p\}_2)\,. \tag{6.9}$$

A gluon-initiated contribution to the virtual correction does not exist.

6.5.2 Real subtraction term

The infrared divergences of the matrix elements in Eq. (6.9) are subtracted by the following subtraction term:

$$\mathrm{d}\hat{\sigma}_{eg}^{S,NLO} = \frac{N^2-1}{N^2}\mathcal{N}_{eg}^{R}\mathrm{d}\Phi_2(p_{\hat{1}},p_{\hat{2}};p_3,p_4,p_5)B_1^{Z,0,S}(4_{\bar{q}},\hat{1}_g,5_q)\,, \tag{6.10}$$

with

$$\begin{aligned} &B_1^{Z,0,S}(i_{\bar{q}},\hat{1}_g,k_q) = \\ &\quad -a_{3,g\to q}^0(i,1,k)\,B_0^{Z,0}(\overline{1},(\widetilde{ik}))\,J_1^1(\{p\}_1) \\ &\quad -a_{3,g\to q}^0(k,1,i)\,B_0^{Z,0}((\widetilde{ik}),\overline{1})\,J_1^1(\{p\}_1)\,, \end{aligned} \tag{6.11}$$

where a_3^0 is the sub-antenna of A_3^0 that only contains one collinear limit. This antenna is used such that the quark-antiquark assignments of the initial state in the reduced matrix element are correct and the collinear divergence $\hat{1}_g||i_{\bar{q}}$ and $\hat{1}_g||k_q$ can be properly subtracted in Z boson exchange.

6.6 Virtual subtraction term

Even though in this case there is no virtual correction, the finite parts of the real subtraction term have to be integrated. The resultant poles from the infrared divergences cancel with the poles from mass factorisation,

$$\mathrm{d}\hat{\sigma}_{eg}^{T,NLO} = \frac{N^2-1}{N^2}\mathcal{N}_{eg}^{V}\mathrm{d}\Phi_1(p_{\hat{1}},p_{\hat{2}};p_3)B_{0,g\to q}^{Z,1,T}(\hat{1}_q,4_q)\,, \tag{6.12}$$

with

$$B^{Z,1,T}_{0,g\to q}(\hat{1},k) = \\ -2J^{1,IF}_{2,QQ,g\to q}(s_{1k})\,\bar{B}^{Z,0}_{0}(1,k)\,J^{1}_{1}(\{p\}_1)\,, \tag{6.13}$$

where

$$\bar{B}^{Z,0}_{0}(i,j) = \frac{1}{2}\left[B^{Z,0}_{0}(i,j) + B^{Z,0}_{0}(j,i)\right] \tag{6.14}$$

indicates a symmetrisation over the quark-antiquark pair. This notation carries through to all B-type matrix elements containing any number of gluons.

6.7 Quark-initiated cross section at NNLO

6.7.1 Real-real contributions

The real-real contribution to the quark-initiated cross section to single-jet production in DIS can be written as

$$\begin{aligned}\mathrm{d}\hat{\sigma}^{RR}_{eq} = \frac{N^2-1}{N^2}\mathcal{N}^{RR}_{eq}\mathrm{d}\Phi_3(p_{\hat{1}},p_{\hat{2}};p_3,p_4,p_5,p_6)\Bigg\{ \\ \frac{1}{2}\sum_{P(4,5)}\left[B^{Z,0}_{2}(\hat{1}_q,4_g,5_g,6_q)\right] - \frac{1}{2N^2}\tilde{B}^{Z,0}_{2}(\hat{1}_q,4_g,5_g,6_q) \\ - \frac{1}{2N^2}D^{Z,0}_{0}(\hat{1}_q,4_q,5_{\bar{q}},6_q) + \frac{1}{N}\sum_{Q}\bar{C}^{Z,0}_{0}(\hat{1}_q,4_Q,5_{\bar{Q}},6_q)\Bigg\}J^{3}_{1}(\{p\}_3)\,,\end{aligned} \tag{6.15}$$

where $P(4,5)$ denotes a summation over the permutations of gluon 4 and 5 and $\sum_Q$ is the summation over the flavours of the secondary quark line. Further,

$$\bar{C}^{Z,0}_{0}(\hat{1}_q,4_Q,5_{\bar{Q}},6_q) = \frac{1}{2}\left[\bar{C}^{Z,0}_{0}(\hat{1}_q,5_Q,4_{\bar{Q}},6_q) + \bar{C}^{Z,0}_{0}(\hat{1}_q,4_Q,5_{\bar{Q}},6_q)\right] \tag{6.16}$$

is the two–quark-pair matrix element that is symmetrised over the flavour of the secondary quark line. This notation carries through to all C-type matrix elements, including C-type elements containing loops and/or additional gluon radiation. The subleading-colour amplitude $\tilde{B}^{Z,0}_{2}$ is free from triple-gluon vertices such that the gluons are only colour-connected to the quarks. The identical quark-pair correction is free from divergences and does not require any infrared subtraction. All squared matrix elements for this real-real correction can be found in Ref. [92].

6.7.2 Real-virtual contributions

The real-virtual corrections can be written as

$$\begin{aligned}\mathrm{d}\hat{\sigma}^{RV}_{eq} = \frac{N^2-1}{N^2}\mathcal{N}^{RV}_{eq}\mathrm{d}\Phi_2(p_{\hat{1}},p_{\hat{2}};p_3,p_4,p_5)\Bigg\{ \\ B^{Z,1}_{1}(\hat{1}_q,4_g,5_q) - \frac{1}{N^2}\tilde{B}^{Z,1}_{1}(\hat{1}_q,4_g,5_q) + \frac{N_F}{N}\hat{B}^{Z,1}_{1}(\hat{1}_q,4_g,5_q)\Bigg\}J^{2}_{1}(\{p\}_2)\,,\end{aligned} \tag{6.17}$$

where the above matrix elements are given up to $\mathcal{O}(\epsilon)$ in Ref. [92].

6.7.3 Virtual-virtual contributions

The double-virtual correction can be written in colour-ordered form as

$$\mathrm{d}\hat{\sigma}^{VV}_{eq} = \frac{N^2-1}{N^2}\mathcal{N}^{VV}_{eq}\mathrm{d}\Phi_2(p_{\hat{1}},p_{\hat{2}};p_3,p_4)\Big\{ \\ B_0^{Z,2}(\hat{1}_q,4_q) - \frac{1}{N^2}\tilde{B}_0^{Z,2}(\hat{1}_q,4_q) + \frac{N_F}{N}\hat{B}_0^{Z,2}(\hat{1}_q,4_q)\Big\}J_1^1(\{p\}_1)\,, \quad (6.18)$$

and the relevant amplitudes can be found in Ref. [147].

6.8 Quark-initiated subtraction at NNLO

6.8.1 Real-real subtraction

The real-real subtraction term to render the correction in Eq. (6.15) finite can be written as

$$\mathrm{d}\hat{\sigma}^{S}_{eq} = \frac{N^2-1}{N^2}\mathcal{N}^{RR}_{eq}\mathrm{d}\Phi_3(p_{\hat{1}},p_{\hat{2}};p_3,p_4,p_5,p_6)\Big\{ \\ \frac{1}{2}\sum_{P(4,5)}\Big[B_2^{Z,0,S}(\hat{1}_q,4_g,5_g,6_q)\Big] - \frac{1}{2N^2}\tilde{B}_2^{Z,0,S}(\hat{1}_q,4_g,5_g,6_q) \\ + \frac{1}{N}\sum_Q C_0^{Z,0,S}(\hat{1}_q,4_Q,5_{\bar{Q}},6_q)\Big\}\,, \quad (6.19)$$

and individual contributions to the subtraction will be discussed in turn below.

The leading-colour B-type subtraction term is given by

$$\begin{aligned}
&B_2^{Z,0,S}(\hat{1},i,j,k) = \\
&\quad + d^0_{3,q}(1,i,j)\, B_1^{\gamma,0}(\overline{1},(\widetilde{ij}),k)\, J_1^2(\{p\}_2) \\
&\quad + d^0_{3}(k,j,i)\, B_1^{\gamma,0}(1,(\widetilde{ij}),(\widetilde{kj}))\, J_1^2(\{p\}_2) \\
&\\
&\quad + A^0_4(1,i,j,k)\, B_0^{Z,0}(\overline{1},(\widetilde{ijk}))\, J_1^1(\{p\}_1) \\
&\quad - d^0_{3,q}(1,i,j)\, A^0_3(\overline{1},(\widetilde{ij}),k)\, B_0^{Z,0}(\overline{\overline{1}},(\widetilde{(\widetilde{ij})k}))\, J_1^1(\{p\}_1) \\
&\quad - d^0_{3}(k,j,i)\, A^0_3(1,(\widetilde{ij}),(\widetilde{kj}))\, B_0^{Z,0}(\overline{1},(\widetilde{(\widetilde{ij})(\widetilde{kj})}))\, J_1^1(\{p\}_1)\,,
\end{aligned} \quad (6.20)$$

where the first two lines subtract the NLO di-jet infrared singularities and remaining terms explicit double-unresolved singularities such that the infrared singularities of the subtraction term coincide with those of the real-real leading-colour B-type correction.

The subleading-colour B-type subtraction is given by

$$\begin{aligned}
&\tilde{B}_2^{Z,0,S}(\hat{1},i,j,k) = \\
&\quad + A^0_{3,q}(1,j,k)\, B_1^{\gamma,0}(\overline{1},i,(\widetilde{jk}))\, J_1^2(\{p\}_2) \\
&\quad + A^0_{3,q}(1,i,k)\, B_1^{\gamma,0}(\overline{1},j,(\widetilde{ik}))\, J_1^2(\{p\}_2)
\end{aligned}$$

$$
\begin{aligned}
&+\tilde{A}_4^0(1,i,j,k)\,B_0^{Z,0}(\bar{1},\widetilde{(ijk)})\,J_1^1(\{p\}_1)\\
&-A_{3,q}^0(1,i,k)\,A_{3,q}^0(\bar{1},j,(\widetilde{ki}))\,B_0^{Z,0}(\bar{\bar{1}},\widetilde{((\widetilde{ki})j)})\,J_1^1(\{p\}_1)\\
&-A_{3,q}^0(1,j,k)\,A_{3,q}^0(\bar{1},i,(\widetilde{kj}))\,B_0^{Z,0}(\bar{\bar{1}},\widetilde{((\widetilde{kj})i)})\,J_1^1(\{p\}_1)\,. \qquad (6.21)
\end{aligned}
$$

The appropriate subtraction for the C-type contribution is given by

$$
\begin{aligned}
&C_0^{Z,0,S}(\hat{1},i,j,k) =\\
&+\frac{1}{2}\,E_3^0(k,i,j)\,B_{1,q}^{Z,0}(1,(\widetilde{ji}),(\widetilde{ki}))\,J_1^2(\{p\}_2)\\
&+\frac{1}{2}\,E_{3,q}^0(1,i,j)\,B_{1,q}^{Z,0}(\bar{1},(\widetilde{ji}),k)\,J_1^2(\{p\}_2)\\
&-E_{3,q'\to g}^0(j,1,k)\,\bar{B}_{1,Q}^{Z,0}(\widetilde{(jk)},\bar{1},i)\,J_1^2(\{p\}_2)\\
&\\
&+B_4^0(1,i,j,k)\,B_0^{Z,0}(\bar{1},\widetilde{(ijk)})\,J_1^1(\{p\}_1)\\
&-\frac{1}{2}\,E_{3,q}^0(1,i,j)\,A_{3,q}^0(\bar{1},(\widetilde{ij}),k)\,B_0^{Z,0}(\bar{\bar{1}},\widetilde{(k(\widetilde{ij}))})\,J_1^1(\{p\}_1)\\
&-\frac{1}{2}\,E_{3,q}^0(k,i,j)\,A_{3,q}^0(1,(\widetilde{ij}),(\widetilde{ki}))\,B_0^{Z,0}(\bar{1},\widetilde{(\widetilde{ki})(\widetilde{ij})})\,J_1^1(\{p\}_1)\\
&\\
&+B_4^0(j,1,k,i)\,\bar{B}_{0,Q}^{Z,0}(\bar{1},\widetilde{(ijk)})\,J_1^1(\{p\}_1)\\
&-E_{3,q'\to g}^0(j,1,k)\,A_{3,g\to q}^0(i,\bar{1},(\widetilde{kj}))\,\bar{B}_{0,Q}^{Z,0}(\bar{\bar{1}},\widetilde{((\widetilde{kj})i)})\,J_1^1(\{p\}_1). \qquad (6.22)
\end{aligned}
$$

As two different quark flavours appear in the C-type matrix element, the flavour information has to be retained and passed on to the reduced matrix element in the subtraction term such that weak charges relevant for the vector boson coupling are correctly assigned. This is achieved by introducing the notation

$$B_{m,q}^n \text{ and } B_{m,Q}^n$$

for matrix elements in which the vector boson couples to the primary and secondary quark line, respectively. This notation is valid for all B-type matrix elements with any number of n loops and m gluons. The symmetrisation over the secondary quark pair for the $C_0^{Z,0}$ correction in Eq. (6.15) is necessary as in triple-collinear limits of the $B_4^0(j,\hat{1},k,i)$ antenna, the partonic initial state cannot be uniquely assigned to be either a quark or an antiquark in the reduced matrix element. By applying the symmetrisation, all double-unresolved limits of the B_4^0 antenna coincide with relevant divergences of the symmetrised $C_0^{Z,0}$ correction in Eq. (6.16).

6.8.2 Real-virtual subtraction

According to Section 3.4.2, the real-virtual subtraction term is constructed from all $X_3^0 \times$ (anything) terms appearing in $\mathrm{d}\hat{\sigma}^S$ that are integrated over their X_3^0 antenna phase space plus subtraction terms that remove genuine divergences of the one-loop corrections and

terms to remove potential spurious divergences. For single-jet production in DIS, the full subtraction term can be written decomposed in colour as

$$\begin{aligned}
\mathrm{d}\hat{\sigma}^{T}_{eq} = \frac{N^2-1}{N^2}\mathcal{N}^{RV}_{eq}\mathrm{d}\Phi_2(p_{\hat{1}},p_{\hat{2}};p_3,p_4,p_5)\Big\{ & B_1^{Z,1,T}(\hat{1}_q,4_g,5_q) \\
-\frac{1}{N^2}\tilde{B}_1^{Z,1,T}(\hat{1}_q,4_g,5_q) + \frac{N_F}{N}\left[\hat{B}_1^{Z,1,T}(\hat{1}_q,4_g,5_q) + \hat{B}^{Z,1,T}_{1,q\to g}(\hat{1}_q,4_g,5_q)\right]\Big\} & J_1^3(\{p\}_3)\,. \quad (6.23)
\end{aligned}$$

The leading-colour B-type subtraction term is given by

$$\begin{aligned}
&B_1^{Z,1,T}(\hat{1},i,k) = \\
&-\Big[+ J^{1,FF}_{2,QG}(s_{ki}) + J^{1,IF}_{2,QG}(s_{1i})\Big]\, B_1^{Z,0}(1,i,k)\, J_1^2(\{p\}_2) \\
&+ A^0_{3,q}(1,i,k)\Big[B_0^{Z,1}(\overline{1},(\widetilde{ik}))\,\delta(1-x_1)\,\delta(1-x_2) \\
&\quad + J^{1,IF}_{2,QQ}(s_{\overline{1}(\widetilde{ik})})\, B_0^{Z,0}(\overline{1},(\widetilde{ik}))\Big]\, J_1^1(\{p\}_1) \\
&+\Big[A^1_{3,q}(1,i,k)\,\delta(1-x_1)\,\delta(1-x_2) \\
&+\Big(+ J^{1,IF}_{2,QG}(s_{1i}) + J^{1,FF}_{2,QG}(s_{ki}) - J^{1,IF}_{2,QQ}(s_{\overline{1}(\widetilde{ik})})\Big) A^0_{3,q}(1,i,k)\Big]\, B_0^{Z,0}(\overline{1},(\widetilde{ik}))\, J_1^1(\{p\}_1)\,,
\end{aligned} \quad (6.24)$$

where the first line cancels explicit poles of the virtual correction and the remaining lines subtract the infrared singularities of the loop correction in single-unresolved phase space configurations. Each of the (tree)×(loop) and (loop)×(tree) subtractions is individually free from poles in agreement with the construction principles of real-virtual antenna subtraction terms.

The subleading-colour B-type subtraction is given by

$$\begin{aligned}
&\tilde{B}_1^{Z,1,T}(\hat{1},i,k) = \\
&-J^{1,IF}_{2,QQ}(s_{1k})\, B_1^{\gamma,0}(1,i,k)\, J_1^2(\{p\}_2) \\
&+ A^0_{3,q}(1,i,k)\Big[B_0^{Z,1}(\overline{1},(\widetilde{ik}))\,\delta(1-x_1)\,\delta(1-x_2) \\
&\quad + J^{1,IF}_{2,QQ}(s_{\overline{1}(\widetilde{ik})})\, B_0^{Z,0}(\overline{1},(\widetilde{ik}))\Big]\, J_1^1(\{p\}_1) \\
&+\Big[\tilde{A}^1_{3,q}(1,i,k)\,\delta(1-x_1)\,\delta(1-x_2) \\
&+\Big(+ J^{1,IF}_{2,QQ}(s_{1k}) - J^{1,IF}_{2,QQ}(s_{\overline{1}(\widetilde{ki})})\Big) A^0_{3,q}(1,i,k)\Big]\, B_0^{Z,0}(\overline{1},(\widetilde{ki}))\, J_1^1(\{p\}_1)\,. \quad (6.25)
\end{aligned}$$

Finally the identity preserving $\hat{B}$-type subtraction term is given by

$$\begin{aligned}
&\hat{B}_1^{Z,1,T}(\hat{1},i,k) = \\
&-\Big[+ \hat{J}^{1,FF}_{2,QG}(s_{ik}) + \hat{J}^{1,IF}_{2,QG}(s_{1i})\Big]\, B_1^{\gamma,0}(1,i,k)\, J_1^2(\{p\}_2)
\end{aligned}$$

$$
\begin{aligned}
&+\Bigg[\hat{A}^1_{3,q}(1,i,k)\,\delta(1-x_1)\,\delta(1-x_2) \\
&+\Bigg(+\hat{J}^{1,FF}_{2,QG}(s_{ki}) + \hat{J}^{1,IF}_{2,QG}(s_{1i}) \Bigg) A^0_{3,q}(1,i,k) \Bigg] B^{Z,0}_0(\bar{1},(\widetilde{ik}))\, J^1_1(\{p\}_1)\,, \qquad (6.26)
\end{aligned}
$$

with identity changing subtraction term

$$
\begin{aligned}
&\hat{B}^{Z,1,T}_{1,q\to g}(\hat{1},i,k) = \\
&\quad -J^{1,IF}_{2,GQ,q'\to g}(s_{j1})\, B^{Z,0}_1(j,1,k)\, J^2_1(\{p\}_2) \\
&\quad -J^{1,IF}_{2,GQ,q'\to g}(s_{j1})\, A^0_{3,g\to q}(j,1,k)\, \bar{B}^{Z,0}_0(\bar{1},(\widetilde{jk}))\, J^1_1(\{p\}_1)\,. \qquad (6.27)
\end{aligned}
$$

6.8.3 Virtual-virtual subtraction

For the construction of the virtual-virtual subtraction term, remaining unmatched terms containing X^0_4 antennae from $\mathrm{d}\hat{\sigma}^S$ and terms that cancel implicit infrared singularities of the real-virtual corrections together with any additional terms in which a primary X^0_3 antenna takes mapped momenta in $\mathrm{d}\hat{\sigma}^T$ are integrated up and combined with mass factorisation counterterms. The virtual-virtual quark-initiated subtraction term can then be written decomposed in colour and split into identity changing and preserving contributions as

$$
\begin{aligned}
\mathrm{d}\hat{\sigma}^U_{eq} = \frac{N^2-1}{N^2}\mathcal{N}^{VV}_{eq}\mathrm{d}\Phi_2(p_{\hat{1}},p_{\hat{2}};p_3,p_4)\Bigg\{ \\
B^{Z,2,U}_0(\hat{1}_q,4_q) - \frac{1}{N^2}\tilde{B}^{Z,2,U}_0(\hat{1}_q,4_q) + \frac{N_F}{N}\left[\hat{B}^{Z,2,U}_0(\hat{1}_q,4_q) + \hat{B}^{Z,2,U}_{0,q\to Q}(\hat{1}_q,4_q)\right]\Bigg\}\,, \qquad (6.28)
\end{aligned}
$$

where the leading-colour subtraction term is given by

$$
\begin{aligned}
&B^{Z,2,U}_0(\hat{1},3) = \\
&+\Bigg[-\mathcal{A}^0_{3,q}(s_{13}) + \Gamma^{(1)}_{qq}(z_1)\Bigg]\left(-\frac{b_0}{\epsilon}B^{Z,0}_0(1,3) + B^{Z,1}_0(1,3)\right) \\
&+\Bigg[-\frac{1}{2}\,\mathcal{A}^0_{3,q}(s_{13})\otimes\mathcal{A}^0_{3,q}(s_{13}) + \Gamma^{(1)}_{qq}(z_1)\otimes\mathcal{A}^0_{3,q}(s_{13}) - \frac{1}{2}\,\Gamma^{(1)}_{qq}(z_1)\otimes\Gamma^{(1)}_{qq}(z_1)\Bigg]B^{Z,0}_0(1,3) \\
&+\Bigg[-\frac{b_0}{\epsilon}\left(\frac{s_{13}}{\mu^2_R}\right)^{-\epsilon}\mathcal{A}^0_{3,q}(s_{13}) + \frac{1}{2}\,\mathcal{A}^0_{3,q}(s_{13})\otimes\mathcal{A}^0_{3,q}(s_{13}) - \mathcal{A}^0_{4,q}(s_{13}) \\
&\quad -\mathcal{A}^1_{3,q}(s_{13}) + \Gamma^{(2)}_{qq}(z_1)\Bigg]B^{Z,0}_0(1,3)\,. \qquad (6.29)
\end{aligned}
$$

In the above, it should be remembered that the $\mathcal{X}^1_3(s_{ij})$ antennae are renormalised at scale s_{ij}. Further, the construction principle of the virtual-virtual subtraction term should be visible. The first line corresponds to $\mathrm{d}\hat{\sigma}^{a,U}$, the second to $\mathrm{d}\hat{\sigma}^{b,U}$ and the third is $\mathrm{d}\hat{\sigma}^{c,U}$.

The subleading-colour subtraction term is given by

$$
\begin{aligned}
&\tilde{B}^{Z,2,U}_0(\hat{1},3) = \\
&+\Bigg[-\mathcal{A}^0_{3,q}(s_{13}) + \Gamma^{(1)}_{qq}(z_1)\Bigg]B^{Z,1}_0(1,3)
\end{aligned}
$$

$$
\begin{aligned}
&+\Bigg[-\frac{1}{2}\,\mathcal{A}^0_{3,q}(s_{13})\otimes\mathcal{A}^0_{3,q}(s_{13}) + \Gamma^{(1)}_{qq}(z_1)\otimes\mathcal{A}^0_{3,q}(s_{13}) - \frac{1}{2}\,\Gamma^{(1)}_{qq}(z_1)\otimes\Gamma^{(1)}_{qq}(z_1)\Bigg] B_0^{Z,0}(1,3)\\
&+\Bigg[+\frac{1}{2}\,\mathcal{A}^0_{3,q}(s_{13})\otimes\mathcal{A}^0_{3,q}(s_{13}) - \frac{1}{2}\,\tilde{\mathcal{A}}^0_{4,q}(s_{13}) - \tilde{\mathcal{A}}^1_{3,q}(s_{13})\\
&\quad - \widetilde{\widetilde{\Gamma}}^{(2)}_{qq}(z_1) - 2\,\mathcal{C}^0_{4,q}(s_{13}) - \mathcal{C}^0_{4,\bar{q},\bar{q}q\bar{q}}(s_{13})\Bigg] B_0^{Z,0}(1,3)\\
&+\Bigg[-\mathcal{C}^0_{4,\bar{q},q\bar{q}\bar{q}}(s_{13}) - \widetilde{\Gamma}^{(2)}_{q\bar{q}q}(z_1)\Bigg] B_0^{Z,0}(1,3)\,. \qquad (6.30)
\end{aligned}
$$

The identity preserving subtraction term proportional to N_F is given by

$$
\begin{aligned}
&\hat{B}_0^{Z,2,U}(\hat{1},3) =\\
&\quad+\Bigg[+\frac{b_F}{\epsilon}\,\mathcal{A}^0_{3,q}(s_{13})\Bigg] B_0^{Z,0}(1,3)\\
&\quad+\Bigg[-\frac{b_F}{\epsilon}\,\Gamma^{(1)}_{qq}(z_1)\Bigg] B_0^{Z,0}(1,3)\\
&\quad+\Bigg[-\frac{b_F}{\epsilon}\left(\frac{s_{13}}{\mu_R^2}\right)^{-\epsilon}\mathcal{A}^0_{3,q}(s_{13}) - \mathcal{B}^0_{4,q}(s_{13}) - \hat{\mathcal{A}}^1_{3,q}(s_{13})\\
&\qquad + \Gamma^{(2)}_{qq,F}(z_1)\Bigg] B_0^{Z,0}(1,3)\,. \qquad (6.31)
\end{aligned}
$$

The identity changing contribution at $\mathcal{O}(N_F)$ combines with appropriate mass factorisation terms to give an infrared finite contribution to the virtual-virtual subtraction and is given by

$$
\begin{aligned}
&\hat{B}^{Z,2,U}_{0,q\to Q}(\hat{1},3) =\\
&\quad+\Bigg[-\mathcal{B}^0_{4,q'}(s_{13}) + \Gamma^{(2)}_{qQ}(z_1) + \Gamma^{(2)}_{q\bar{Q}}(z_1)\\
&\qquad - S_{q\to g}\,\Gamma^{(1)}_{gq}(z_1)\otimes\mathcal{A}^0_{3,g\to q}(s_{13}) - \Gamma^{(1)}_{qg}(z_1)\otimes\Gamma^{(1)}_{gq}(z_1)\Bigg]\bar{B}_0^{Z,0}(1,3)\,, \qquad (6.32)
\end{aligned}
$$

where the factor $S_{q\to g}$ is defined in Eq. (3.36).

6.9 Gluon-initiated cross section at NNLO

6.9.1 Real-real contribution

The gluon-initiated real-real contribution to the cross section only has B-type matrix elements

$$
\begin{aligned}
\mathrm{d}\hat{\sigma}^{RR}_{eg} = \frac{N^2-1}{N^2}\mathcal{N}^{RR}_{eg}\mathrm{d}\Phi_4(p_{\hat{1}},p_{\hat{2}};p_3,p_4,p_5,p_6)\Bigg\{&\\
\sum_{P(\hat{1},5)}\Big[\bar{B}_2^{Z,0}(4_{\bar{q}},\hat{1}_g,5_g,6_q)\Big] - \frac{1}{N^2}\tilde{\bar{B}}_2^{Z,0}(4_{\bar{q}},\hat{1}_g,5_g,6_q)\Bigg\}&J_1^3(\{p\}_3)\,, \qquad (6.33)
\end{aligned}
$$

where each of the B-type matrix elements is in its symmetrised form as described in Eq. (6.14). Symmetrisation of the B-type matrix elements is necessary as A_4^0-type antennae

subtract both the $(q||g||\hat{g})$ as well as the $(\bar{q}||g||\hat{g})$ triple-collinear limits. The reduced matrix element however, has to be assigned a particular initial state which has to be either a quark or an antiquark. Using the symmetrisation both on the subtraction term and on the real-real correction allows both triple-collinear limits of $A_4^0 \times \bar{B}_0^0$-terms to coincide with the infrared limits of the real-real correction.

6.9.2 Real-virtual contribution

The gluon-initiated real-virtual contribution is given by

$$\begin{aligned}\mathrm{d}\hat{\sigma}_{eg}^{RV} = \frac{N^2-1}{N^2}\mathcal{N}_{eg}^{RV}\mathrm{d}\Phi_3(p_{\hat{1}},p_{\hat{2}};p_3,p_4,p_5)\Big\{ \\ \bar{B}_1^{Z,1}(4_{\bar{q}},\hat{1}_g,5_q) - \frac{1}{N^2}\tilde{\bar{B}}_1^{Z,1}(4_{\bar{q}},\hat{1}_g,5_q) + \frac{N_F}{N}\hat{\bar{B}}_1^{Z,1}(4_{\bar{q}},\hat{1}_g,5_q)\Big\}J_1^2(\{p\}_2)\,, \end{aligned} \tag{6.34}$$

where all matrix elements are symmetrised according to Eq. (6.14). The necessity to symmetrise the B-type matrix elements arises due to a missing decomposition of the one-loop A_3^1-type antennae, that play the same role as the A_4^0-type antennae in the discussion of symmetrisation in Section 6.9.1. In this case the problematic limits are identity changing $(\hat{g} \to \hat{q})$ divergences. Finally, it should be noted that there is no explicit gluon-initiated virtual-virtual correction except for mass factorisation terms.

6.10 Gluon-initiated subtraction at NNLO

6.10.1 Real-real subtraction

The real-real subtraction term can be written as

$$\begin{aligned}\mathrm{d}\hat{\sigma}_{eg}^{S} = \frac{N^2-1}{N^2}\mathcal{N}_{eg}^{RR}\mathrm{d}\Phi_4(p_{\hat{1}},p_{\hat{2}};p_3,p_4,p_5,p_6)\Big\{B_2^{Z,0,S}(4_{\bar{q}},\hat{1}_g,5_g,6_q) \\ -\frac{1}{N^2}\tilde{B}_2^{Z,0,S}(4_{\bar{q}},\hat{1}_g,5_g,6_q)\Big\}\,. \end{aligned} \tag{6.35}$$

The leading-colour subtraction term is given by

$$\begin{aligned}
&B_2^{Z,0,S}(i,\hat{1},j,k) = \\
&\quad + d_{3,g}^0(i,j,1)\,\bar{B}_1^{Z,0}((\widetilde{ij}),\overline{1},k)\,J_1^2(\{p\}_2) \\
&\quad + d_{3,g}^0(k,j,1)\,\bar{B}_1^{Z,0}((\widetilde{jk}),\overline{1},i)\,J_1^2(\{p\}_2) \\
&\quad - A_{3,g\to q}^0(i,1,k)\,\bar{B}_1^{Z,0}(\overline{1},j,(\widetilde{ik}))\,J_1^2(\{p\}_2) \\
&\quad - A_4^0(i,j,1,k)\,\bar{B}_0^{Z,0}(\overline{1},(\widetilde{jik}))\,J_1^1(\{p\}_1) \\
&\quad - A_4^0(i,1,j,k)\,\bar{B}_0^{Z,0}(\overline{1},(\widetilde{jik}))\,J_1^1(\{p\}_1) \\
&\quad + d_{3,g}^0(i,j,1)\,A_{3,g\to q}^0((\widetilde{ji}),\overline{1},k)\,\bar{B}_0^{Z,0}((\widetilde{\widetilde{k(ji)}}),\overline{\overline{1}})\,J_1^1(\{p\}_1) \\
&\quad + d_{3,g}^0(k,j,1)\,A_{3,g\to q}^0((\widetilde{kj}),\overline{1},i)\,\bar{B}_0^{Z,0}((\widetilde{\widetilde{i(kj)}}),\overline{\overline{1}})\,J_1^1(\{p\}_1)
\end{aligned}$$

$$+ A^0_{3,g\to q}(i,1,k)\, A^0_{3,q}(\overline{1},j,(\widetilde{ik}))\, \bar{B}^{Z,0}_0(\overline{1},(\widetilde{j(\widetilde{ik})}))\, J^1_1(\{p\}_1)\,, \tag{6.36}$$

where the first three lines are again the NLO di-jet subtraction terms. In the above, all reduced matrix elements are symmetrised such that the triple-collinear limits of the gluon-initiated A^0_4 antenna give the infrared divergences of the real-real matrix element in Eq. (6.33).

The subleading-colour subtraction term is given by

$$\begin{aligned}
&\tilde{B}^{Z,0,S}_2(i,\hat{1},j,k) = \\
&\quad -A^0_{3,g\to q}(i,1,k)\, \bar{B}^{Z,0}_1(\overline{1},j,(\widetilde{ik}))\, J^2_1(\{p\}_2) \\
&\quad +A^0_3(i,j,k)\, sB^{Z,0}_1((\widetilde{ij}),1,(\widetilde{kj}))\, J^2_1(\{p\}_2)
\end{aligned} \tag{6.37}$$

$$\begin{aligned}
&\quad - \tilde{A}^0_4(k,j,1,i)\, \bar{B}^{Z,0}_0(\overline{1},(\widetilde{ijk}))\, J^1_1(\{p\}_1) \\
&\quad + A^0_3(k,j,i)\, A^0_3((\widetilde{kj}),1,(\widetilde{ji}))\, \bar{B}^{Z,0}_0(\overline{1},(\widetilde{(\widetilde{kj})(\widetilde{ji})}))\, J^1_1(\{p\}_1) \\
&\quad + A^0_{3,g\to q}(k,1,i)\, A^0_{3,q}(\overline{1},j,(\widetilde{ik}))\, \bar{B}^{Z,0}_0(\overline{1},(\widetilde{j(\widetilde{ik})}))\, J^1_1(\{p\}_1)\,.
\end{aligned} \tag{6.38}$$

6.10.2 Real-virtual subtraction

The real-virtual subtraction for the gluon-initiated processes can be written as

$$\begin{aligned}
\mathrm{d}\hat{\sigma}^T_{eg} = \frac{N^2-1}{N^2}\mathcal{N}^{RV}_{eg}\mathrm{d}\Phi_3(p_{\hat{1}},p_{\hat{2}};p_3,p_4,p_5)\Big\{ \\
B^{Z,1,T}_1(4_{\bar{q}},\hat{1}_g,5_q) + B^{Z,1,T}_{1,g\to q}(4_{\bar{q}},\hat{1}_g,5_q) - \frac{1}{N^2}\left[\tilde{B}^{Z,1,T}_1(4_{\bar{q}},\hat{1}_g,5_q) + \tilde{B}^{Z,1,T}_{1,g\to q}(4_{\bar{q}},\hat{1}_g,5_q)\right] \\
+ \frac{N_F}{N}\hat{B}^{Z,1,T}_1(4_{\bar{q}},\hat{1}_g,5_q)\Big\},
\end{aligned} \tag{6.39}$$

where the identity changing $g \to q$ processes combine with mass factorisation terms to give an infrared finite contribution to the real-virtual subtraction term. The leading-colour identity preserving subtraction term is given by

$$\begin{aligned}
&B^{Z,1,T}_1(k,\hat{1},j) = \\
&\quad -\Big[+ J^{1,IF}_{2,GQ}(s_{1k}) + J^{1,IF}_{2,GQ}(s_{1j})\Big]\, \bar{B}^{Z,0}_1(k,1,j)\, J^2_1(\{p\}_2) \\
&\quad - A^0_{3,g\to q}(k,1,j)\, \Big[\bar{B}^{Z,1}_0(\overline{1},(\widetilde{kj}))\, \delta(1-x_1)\, \delta(1-x_2) \\
&\qquad + J^{1,IF}_{2,QQ}(s_{\overline{1}(\widetilde{kj})})\, \bar{B}^{Z,0}_0(\overline{1},(\widetilde{kj}))\Big]\, J^1_1(\{p\}_1) \\
&\quad -\Big[A^1_{3,g}(k,1,j)\, \delta(1-x_1)\, \delta(1-x_2) \\
&\quad +\Big(+ J^{1,IF}_{2,GQ}(s_{1k}) + J^{1,IF}_{2,GQ}(s_{1j}) - J^{1,IF}_{2,QQ}(s_{\overline{1}(\widetilde{kj})})\Big)\, A^0_3(k,1,j)\Big]\, \bar{B}^{Z,0}_0(\overline{1},(\widetilde{kj}))\, J^1_1(\{p\}_1)\,,
\end{aligned} \tag{6.40}$$

and

$$
\begin{aligned}
&B^{Z,1,T}_{1,g\to q}(k,\hat{1},j) = \\
&\quad -2J^{1,IF}_{2,QQ,g\to q}(s_{1k})\,\bar{B}^{Z,0}_{1}(1,j,k)\,J^{1}_{1}(\{p\}_2) \\
&\quad +2J^{1,IF}_{2,QQ,g\to q}(s_{1k})\,A^{0}_{3,q}(1,j,k)\,\bar{B}^{Z,0}_{0}(\overline{1},(\widetilde{jk}))\,J^{1}_{1}(\{p\}_1)\,.
\end{aligned}
\tag{6.41}
$$

The subleading-colour contribution is given by

$$
\begin{aligned}
&\tilde{B}^{Z,1,T}_{1}(j,\hat{1},k) = \\
&\quad -J^{1,FF}_{2,QQ}(s_{kj})\,\bar{B}^{Z,0}_{1}(j,1,k)\,J^{1}_{1}(\{p\}_2) \\
&\quad - A^{0}_{3,g\to q}(j,1,k)\,\Bigg[\,\bar{B}^{Z,1}_{0}(\overline{1},(\widetilde{jk}))\,\delta(1-x_1)\,\delta(1-x_2) \\
&\qquad + J^{1,IF}_{2,QQ}(s_{\overline{1}(\widetilde{jk})})\,\bar{B}^{Z,0}_{0}(\overline{1},(\widetilde{jk}))\Bigg]\,J^{1}_{1}(\{p\}_1) \\
&\quad -\Bigg[\,\tilde{A}^{1}_{3,g}(j,1,k)\,\delta(1-x_1)\,\delta(1-x_2) \\
&\quad +\Bigg(\,+J^{1,FF}_{2,QQ}(s_{jk}) - J^{1,IF}_{2,QQ}(s_{\overline{1}(\widetilde{jk})})\Bigg)\,A^{0}_{3,g\to q}(j,1,k)\Bigg]\,\bar{B}^{Z,0}_{0}(\overline{1},(\widetilde{jk}))\,J^{1}_{1}(\{p\}_1)\,,
\end{aligned}
\tag{6.42}
$$

and

$$
\begin{aligned}
&\tilde{B}^{Z,1,T}_{1,g\to q}(j,\hat{1},k) = \\
&\quad -2J^{1,IF}_{2,QQ,g\to q}(s_{1k})\,\bar{B}^{Z,0}_{1}(1,j,k)\,J^{1}_{1}(\{p\}_2) \\
&\quad +2J^{1,IF}_{2,QQ,g\to q}(s_{1k})\,A^{0}_{3,q}(1,j,k)\,\bar{B}^{Z,0}_{0}(\overline{1},(\widetilde{jk}))\,J^{1}_{1}(\{p\}_1)\,.
\end{aligned}
\tag{6.43}
$$

The $\mathcal{O}(N_F)$ subtraction term is given by

$$
\begin{aligned}
&\hat{B}^{Z,1,T}_{1}(j,\hat{1},k) = \\
&\quad -2\hat{J}^{1,IF}_{2,GQ}(s_{i1})\,\hat{B}^{Z,0}_{1}(i,1,j)\,J^{2}_{1}(\{p\}_2) \\
&\quad -\Bigg[\,\hat{A}^{1}_{3,g}(i,1,j)\,\delta(1-x_1)\,\delta(1-x_2) + 2\hat{J}^{1,IF}_{2,GQ}(s_{i1})\,A^{0}_{3,g\to q}(i,1,j)\Bigg]\,\bar{B}^{Z,0}_{0}(\overline{1},(\widetilde{ij}))\,J^{1}_{1}(\{p\}_1)\,,
\end{aligned}
\tag{6.44}
$$

where the first line in this subtraction term is pure mass factorisation.

6.10.3 Virtual-virtual subtraction

Even if there are no gluon-initiated two-loop corrections to single-jet production in DIS, unmatched terms from the real-real and real-virtual subtraction terms have to be integrated up and combined with the mass factorisation terms to give a virtual-virtual subtraction term that is free from infrared poles. The virtual-virtual subtraction term can be written as

$$\mathrm{d}\hat{\sigma}^{U}_{eg} = \frac{N^2-1}{N^2}\mathcal{N}^{VV}_{eg}\mathrm{d}\Phi_2(p_{\hat{1}},p_{\hat{2}};p_3,p_4)\Big\{ \\ B^{Z,2,U}_{0,g\to q}(\hat{1}_q,4_q) - \frac{1}{N^2}\tilde{B}^{Z,2,U}_{0,g\to q}(\hat{1}_q,4_q) + \frac{N_F}{N}\hat{B}^{Z,2,U}_{0,g\to q}(\hat{1}_q,4_q)\Big\}. \quad (6.45)$$

The leading-colour subtraction term is given by

$$\begin{aligned}
&B^{Z,2,U}_{0,g\to q}(\hat{1},3) = \\
&+\Big[+2S_{g\to q}\,\Gamma^{(1)}_{qg}(z_1) + \mathcal{A}^0_{3,g\to q}(s_{13})\Big]\left(-\frac{b_0}{\epsilon}\bar{B}^{Z,0}_0(1,3) + \bar{B}^{Z,1}_0(1,3)\right) \\
&+\Big[+2S_{g\to q}\,\mathcal{A}^0_{3,q}(s_{13})\otimes\Gamma^{(1)}_{qg}(z_1) - 2S_{g\to q}\,\Gamma^{(1)}_{qq}(z_1)\otimes\Gamma^{(1)}_{qg}(z_1) + \mathcal{A}^0_{3,q}(s_{13})\otimes\mathcal{A}^0_{3,g\to q}(s_{13}) \\
&\quad - \Gamma^{(1)}_{qq}(z_1)\otimes\mathcal{A}^0_{3,g\to q}(s_{13})\Big]\bar{B}^{Z,0}_0(1,3) \\
&+\Big[+S_{g\to q}\,\Gamma^{(1)}_{qq}(z_1)\otimes\Gamma^{(1)}_{qg}(z_1) - S_{g\to q}\,\Gamma^{(1)}_{gg}(z_1)\otimes\Gamma^{(1)}_{qg}(z_1) + \frac{b_0}{\epsilon}\left(\frac{s_{13}}{\mu_R^2}\right)^{-\epsilon}\mathcal{A}^0_{3,g\to q}(s_{13}) \\
&\quad - \mathcal{A}^0_{3,q}(s_{13})\otimes\mathcal{A}^0_{3,g\to q}(s_{13}) + \Gamma^{(1)}_{qq}(z_1)\otimes\mathcal{A}^0_{3,g\to q}(s_{13}) + 2S_{g\to q}\,\Gamma^{(2)}_{qg}(z_1) \\
&\quad - \Gamma^{(1)}_{gg}(z_1)\otimes\mathcal{A}^0_{3,g\to q}(s_{13}) + 2\,\mathcal{A}^0_{4,g}(s_{13}) + \mathcal{A}^1_{3,g}(s_{13})\Big]\bar{B}^{Z,0}_0(1,3)\,. \qquad (6.46)
\end{aligned}$$

The subleading-colour subtraction term is given by

$$\begin{aligned}
&\tilde{B}^{Z,2,U}_{0,g\to q}(\hat{1},3) = \\
&+\Big[+2S_{g\to q}\,\Gamma^{(1)}_{qg}(z_1) + \mathcal{A}^0_{3,g\to q}(s_{13})\Big]\bar{B}^{Z,1}_0(1,3) \\
&+\Big[+2S_{g\to q}\,\mathcal{A}^0_{3,q}(s_{13})\otimes\Gamma^{(1)}_{qg}(z_1) - 2S_{g\to q}\,\Gamma^{(1)}_{qq}(z_1)\otimes\Gamma^{(1)}_{qg}(z_1) + \mathcal{A}^0_{3,q}(s_{13})\otimes\mathcal{A}^0_{3,g\to q}(s_{13}) \\
&\quad - \Gamma^{(1)}_{qq}(z_1)\otimes\mathcal{A}^0_{3,g\to q}(s_{13})\Big]\bar{B}^{Z,0}_0(1,3) \\
&+\Big[+\tilde{\mathcal{A}}^0_{4,g}(s_{13}) + \tilde{\mathcal{A}}^1_{3,g}(s_{13}) - 2S_{g\to q}\,\widetilde{\Gamma}^{(2)}_{qg}(z_1) - \mathcal{A}^0_{3,q}(s_{13})\otimes\mathcal{A}^0_{3,g\to q}(s_{13}) \\
&\quad + \Gamma^{(1)}_{qq}(z_1)\otimes\mathcal{A}^0_{3,g\to q}(s_{13}) + S_{g\to q}\,\Gamma^{(1)}_{qq}(z_1)\otimes\Gamma^{(1)}_{qg}(z_1)\Big]\bar{B}^{Z,0}_0(1,3)\,, \qquad (6.47)
\end{aligned}$$

and the $\mathcal{O}(N_F)$ subtraction term is given by

$$\begin{aligned}
&\hat{B}^{Z,2,U}_{0,g\to q}(\hat{1},3) = \\
&+\Big[-\frac{b_F}{\epsilon}\,\mathcal{A}^0_{3,g\to q}(s_{13})\Big]\bar{B}^{Z,0}_0(1,3) \\
&+\Big[-2S_{g\to q}\frac{b_F}{\epsilon}\,\Gamma^{(1)}_{qg}(z_1)\Big]\bar{B}^{Z,0}_0(1,3) \\
&+\Big[+\frac{b_F}{\epsilon}\left(\frac{s_{13}}{\mu_R^2}\right)^{-\epsilon}\mathcal{A}^0_{3,g\to q}(s_{13}) - S_{g\to q}\,\Gamma^{(1)}_{qg}(z_1)\otimes\Gamma^{(1)}_{gg,F}(z_1) + 2S_{g\to q}\,\Gamma^{(2)}_{qg,F}(z_1) \\
&\quad - \mathcal{A}^0_{3,g\to q}(s_{13})\otimes\Gamma^{(1)}_{gg,F}(z_1) + \hat{\mathcal{A}}^1_{3,g}(s_{13})\Big]\bar{B}^{Z,0}_0(1,3)\,. \qquad (6.48)
\end{aligned}$$

6.11 Validation

The implementation of DIS single-jet production in the laboratory frame into NNLOJET was validated in several ways. Using so-called spike plots, the construction of real-real, real-virtual or single-real subtraction terms can be validated. To this end, many points are generated in some specified unresolved phase space configuration, e.g. in a particular single-collinear limit. How deep a phase space point lies in an unresolved limit is controlled by a user-defined parameter x. In collinear limits, x gives the ratio of the collinear particles' kinematic invariant and in soft limits, x gives the ratio of a soft particle's energy to the total center of mass energy. Smaller values of x therefore correspond to more unresolved phase space points. Then, the behaviour of the quantity

$$R = \frac{\hat{\sigma}^{\text{correction}}}{\hat{\sigma}^{\text{subtraction}}} \tag{6.49}$$

is studied as the value of x is lowered. For a correctly constructed subtraction term, the value of R should statistically be closer to one for smaller than for larger values of x (x should not be too small of course to avoid numerical instabilities). For a particular unresolved configuration, the value of R is evaluated for phase space points within sets of fixed x and the resulting distributions should spike up as the value of x is lowered. This procedure is repeated for all possible infrared limits to ensure that also subleading divergences are properly cancelled (a single-collinear limit would be, for example, subleading compared to a double-collinear limit). Examples of spike plots for real-real subtractions are shown in Figs. 8a and 8b and spikes could be observed for all infrared limits appearing in single-jet production in DIS.

Another check is provided by analytic pole cancellation between the poles of virtual subtraction terms and their corresponding correction. All integrated antenna functions and mass factorisation kernels are known and their analytic expressions are implemented into NNLOJET. From these analytical expressions, the pole structure of the double-virtual as well as the real-virtual subtraction terms can be obtained. For all constructed virtual subtraction terms, this analytic pole cancellation was validated. In addition, it was found

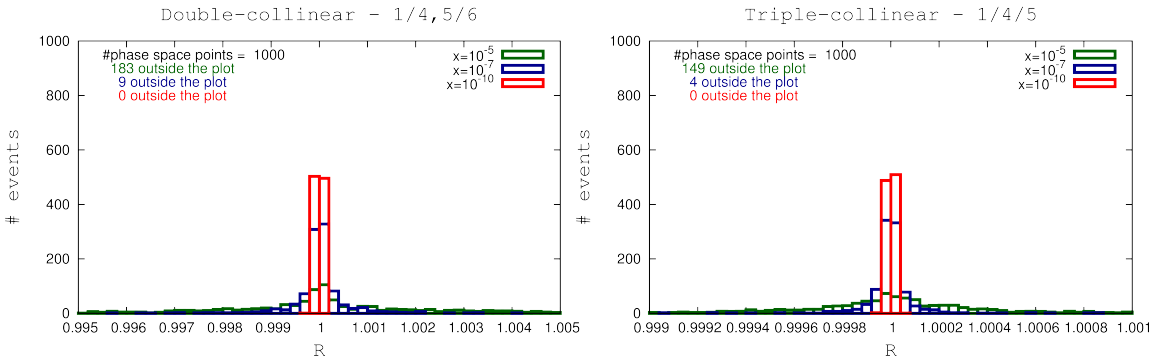

(a) Spike for double-collinear $q||g\ g||g$ limit.

(b) Spike for triple-collinear $q||g||g$ limit.

Figure 8. Example spike plots for the leading-colour B-type real-real subtraction term for single-jet production in DIS.

that the dependence on the renormalisation scale μ_r as predicted by Eq. (2.109) is in agreement with the results obtained from NNLOJET. Finally, it was verified that the total inclusive cross section for DIS for some arbitrary lower cut in Q^2 and x matches the NNLO result predicted by Zijlstra and van Nerveen given in Ref. [103].

7 NNLO cross section for DIS di-jet production in the Breit frame

In this Section we give the subtraction terms relevant for inclusive single- and di-jet production in the Breit frame, which are also relevant for di-jet production in diffractive scattering. Phenomenological results obtained with the presented subtraction terms are given in Sections 8, 9 and 10, some of which are already published in Refs. [71, 152]. Subtraction terms presented in the following sections are also used in the calcualtion of DIS single-jet production in the laboratory frame at N3LO accuracy and this is described in Section 12.

7.1 General notation for matrix elements

The convention for notation for DIS di-jet matrix element follows the conventions adopted in Section 6.1. In the case of di-jet production in DIS, the initial states l and m in Eq. (2.111) are the electron and a parton, respectively. The Born level is defined by $n_B = 2$ for genuine di-jet production and $n_B = 1$ for single-jet production in the Breit frame. The maximal number of partons at NNLO is four, that is $n = 4$. Real-real corrections contain a maximum of three gluons, giving a maximal value for S_n of 3!. Symmetry factors for each correction together with a detailed discussion will be given in the following. At LO, both quark- and gluon-initiated processes contribute and the corresponding QCD-independent factors are defined in Eq. (2.112). From this definition the factors for higher-order corrections can be deduced from Eqs. (2.117).

7.2 Quark-initiated cross section at LO

Di-jet production at leading order receives contributions from quark- and gluon-initiated processes and equals the real-radiation correction to single-jet production in Eq. (6.3.1). Unresolved limits are rendered finite by the jet function such that the leading-order quark-initiated contribution can be written as

$$\mathrm{d}\hat{\sigma}^{LO}_{eq} = \mathcal{N}^{B}_{eq}\mathrm{d}\Phi_3(p_{\hat{1}}, p_{\hat{2}}; p_3, p_4, p_5) B_1^{Z,0}(\hat{1}_q, 4_g, 5_q) J_2^2(\{p\}_2)\,, \tag{7.1}$$

and the expression does not require any infrared subtraction.

7.3 Gluon initiated cross section at LO

Similarly, the leading-order contribution from the gluon-initiated process can be written as

$$\mathrm{d}\hat{\sigma}^{LO}_{eq} = \mathcal{N}^{B}_{eg}\mathrm{d}\Phi_3(p_{\hat{1}}, p_{\hat{2}}; p_3, p_4, p_5) B_1^{Z,0}(4_{\bar{q}}, \hat{1}_q, 5_q) J_2^2(\{p\}_2)\,. \tag{7.2}$$

7.4 Quark-initiated cross section at NLO

7.4.1 Real contribution

In DIS, quark-initiated real corrections to di-jet production are identical to those appearing in the real-real corrections to single-jet production and are given by Eq. (6.15). It is necessary however, to substitute the jet function according to

$$J_1^3(\{p\}_3) \to J_2^3(\{p\}_3)\,, \tag{7.3}$$

such that only NLO infrared singularities appear in the phase space integral.

7.4.2 Virtual contribution

Applying the rule

$$J_1^2(\{p\}_2) \to J_2^2(\{p\}_2) \tag{7.4}$$

to substitute the jet function in the quark-initiated real-virtual corrections given in Eq. (6.17), results in the corresponding quark-initiated virtual corrections to di-jet production, where the substitution in Eq. (7.4) ensures that no implicit infrared divergences have to be subtracted.

7.5 Quark-initiated subtraction at NLO

7.5.1 Real subtraction

The quark-initiated real subtraction terms are the same as the $\mathrm{d}\hat{\sigma}^{S,a}$ terms used in the quark-initiated real-real subtraction in Section 6.8.1. Hence, relevant subtraction terms are given by the first two lines of Eq. (6.20) and of Eq. (6.21) for leading- and subleading-colour B-type contributions, respectively, and the C-type subtraction term is given by the first three lines of Eq. (6.22). To recycle these terms one must however substitute all jet functions according to Eq. (7.3) and to Eq. (7.4).

7.5.2 Virtual subtraction

Similarly, the quark-initiated virtual contribution to the subtraction can be recycled from the real-virtual subtraction term given in Eq. (6.39). The leading-colour B-type, subleading-colour B-type and $\hat{B}$-type subtractions are given by the first line of Eqs. (6.24), (6.25) and (6.26), respectively, when all jet functions are replaced according to Eq. (7.4).

7.6 Gluon-initiated cross section at NLO

7.6.1 Real contribution

Once the jet function is substituted according to Eq. (7.3), the gluon-initiated radiative corrections to di-jet production are identical to the gluon initiated real-real corrections for DIS single-jet production in the laboratory frame in Eq. (6.33).

7.6.2 Virtual contribution

Applying the substitution in Eq. (7.4) to the jet function, the gluon-initiated virtual corrections are given by the modified version of Eq. (6.34).

7.7 Gluon-initiated subtraction at NLO

7.7.1 Real subtraction

The subtraction term for the gluon-initiated real correction is given in Eq. (6.35), that is the subtraction for gluon-initiated real-real contributions to single-jet production in DIS. Replacing all jet functions according to Eq. (7.3) and Eq. (7.4), the leading-colour B-type subtraction term is given by the first two lines of Eq. (6.36) and the subleading-colour B-type subtraction by the first two lines of Eq. (6.38).

7.7.2 Virtual subtraction

The leading-colour gluon-initiated subtraction term is given by the first line of Eq. (6.40) and Eq. (6.41), in identity preserving and changing contributions, respectively. For the subleading-colour subtraction this is the first line of Eq. (6.42) for the identity preserving and Eq. (6.43) for the identity changing contributions. The piece proportional to N_F is given by the first line of Eq. (6.44), where for all recycled terms it is assumed that the jet functions are replaced according to Eq. (7.4).

7.8 Quark-initiated cross section at NNLO

7.8.1 Real-real contribution

The tree-level five-parton contributions are given by the colour decomposition of the two-quark–three-gluon B-type and four-quark–one-gluon matrix elements, that are further decomposed into C-type and D-type elements for quark lines of different and identical flavours, respectively. Expressions for relevant corrections can be found in Ref. [140], with the quark crossed into the initial state. The quark-initiated real-real contribution can then be written as

$$\begin{aligned}
\mathrm{d}\hat{\sigma}^{RR}_{eq} = \mathcal{N}^{RR}_{eq}\mathrm{d}\Phi_5(p_{\hat{1}}, p_{\hat{2}}; p_3, p_4, p_5, p_6, p_7)\Bigg\{ & \\
\frac{1}{3!}\Bigg[\sum_{P(4,5,6)}\Bigg[B_3^{Z,0}(\hat{1}_q, 4_g, 5_g, 6_g, 7_q) - \frac{1}{N^2}\tilde{B}_3^{Z,0}(\hat{1}_q, 4_g, 5_g, 6_g, 7_q)\Bigg] & \\
+\frac{N^2+1}{N^4}\tilde{\tilde{B}}_3^{Z,0}(\hat{1}_q, 4_g, 5_g, 6_g, 7_q)\Bigg] & \\
+\frac{1}{N}\sum_{Q}\Bigg[\bar{C}_1^{Z,0}(\hat{1}_q, 4_g, 5_Q, 6_{\bar{Q}}, 7_q) - \frac{1}{N^2}\tilde{\bar{C}}_1^{Z,0}(\hat{1}_q, 4_g, 5_Q, 6_{\bar{Q}}, 7_q)\Bigg] & \\
-\frac{1}{2!N^2}\Bigg[D_1^{Z,0}(\hat{1}_q, 4_g, 5_q, 6_{\bar{q}}, 7_q) - \frac{1}{N^2}\tilde{D}_1^{Z,0}(\hat{1}_q, 4_g, 5_q, 6_{\bar{q}}, 7_q)\Bigg]\Bigg\} & J_2^4(\{p\}_4)\,, \qquad (7.5)
\end{aligned}$$

where $P(4,5,6)$ gives all permutations of gluons $4, 5$ and 6 and $\bar{C}$ represent C-type matrix elements that are symmetrised over their secondary quark pair's momenta according to Eq. (6.16).

7.8.2 Real-virtual contribution

The colour decomposed real-virtual contributions to the quark channel are given by two-quark–two-gluon– and four-quark–one-loop matrix elements, where the four-quark matrix elements include identical, D-type, and non-identical, C-type, flavoured quarks pairs. The real-virtual correction can be written as

$$\begin{aligned}
\mathrm{d}\hat{\sigma}^{RV}_{eq} = \mathcal{N}^{RV}_{eq}\mathrm{d}\Phi_4(p_{\hat{1}}, p_{\hat{2}}; p_3, p_4, p_5)\Bigg\{ & \\
+\frac{1}{2!}\Bigg[\sum_{P(4,5)} B_2^{Z,1}(\hat{1}_q, 4_g, 5_g, 6_q) - \frac{1}{N^2}\tilde{B}_2^{Z,1}(\hat{1}_q, 4_g, 5_g, 6_q) + \frac{1}{N^4}\tilde{\tilde{B}}_2^{Z,1}(\hat{1}_q, 4_g, 5_g, 6_q)\Bigg] &
\end{aligned}$$

$$
\begin{aligned}
&+\frac{N_F}{2!N}\left[\sum_{P(4,5)}\hat{B}_2^{Z,1}(\hat{1}_q,4_g,5_g,6_q)-\frac{1}{N^2}\hat{\tilde{B}}_2^{Z,1}(\hat{1}_q,4_g,5_g,6_q)\right]\\
&+\frac{1}{N}\sum_{Q}\left[\bar{C}_0^{Z,1}(\hat{1}_q,4_Q,5_{\bar{Q}},6_q)-\frac{1}{N^2}\tilde{C}_0^{Z,1}(\hat{1}_q,4_Q,5_{\bar{Q}},6_q)+\frac{N_F}{N}\hat{C}_0^{Z,1}(\hat{1}_q,4_Q,5_{\bar{Q}},6_q)\right]\\
&+\frac{1}{N^2}\left[D_0^{Z,1}(\hat{1}_q,4_q,5_{\bar{q}},6_q)+\frac{1}{N^2}\tilde{D}_0^{Z,1}(\hat{1}_q,4_q,5_{\bar{q}},6_q)+\frac{N_F}{N}\hat{D}_0^{Z,1}(\hat{1}_q,4_q,5_{\bar{q}},6_q)\right]\Bigg\}J_2^3(\{p\}_3)\,,
\end{aligned}
\tag{7.6}
$$

where all of the above matrix elements can be found in Ref. [141], with the quark crossed into the initial state. In the above, a new colour level at $\mathcal{O}(N_F^2)$ appears for the first time that is absent in the colour decomposition of the real-real correction. For this reason, the $\hat{C}$-correction is free from explicit infrared ϵ-poles. Further, it should be noted that contributions in which the vector boson couples to an internal quark loop are ignored throughout, as such contributions were found to be negligible.

7.8.3 Virtual-virtual contribution

The virtual-virtual contributions to the quark channel are given by the colour decomposition of two-loop two-quark-one-gluon matrix elements and can be written as

$$
\begin{aligned}
\mathrm{d}\hat{\sigma}_{eq}^{VV} = \mathcal{N}_{eq}^{VV}\mathrm{d}\Phi_3(p_{\hat{1}},p_{\hat{2}};p_3,p_4,p_5)\Bigg\{&B_1^{Z,2}(\hat{1}_q,4_g,5_q)\\
&-\frac{1}{N^2}\tilde{B}_1^{Z,2}(\hat{1}_q,4_g,5_q)+\frac{1}{N^4}\tilde{\tilde{B}}_1^{Z,2}(\hat{1}_q,4_g,5_q)\\
&+\frac{N_F}{N}\hat{B}_1^{Z,2}(\hat{1}_q,4_g,5_q)+\frac{N_F}{N^3}\hat{\tilde{B}}_1^{Z,2}(\hat{1}_q,4_g,5_q)+\frac{N_F^2}{N^2}\hat{\hat{B}}_1^{Z,2}(\hat{1}_q,4_g,5_q)\Bigg\}J_1^1(\{p\}_1)\,,
\end{aligned}
\tag{7.7}
$$

where explicit expressions for the matrix elements are taken from [142], with the quark crossed into the initial state.

7.9 Quark-initiated subtraction terms at NNLO

7.9.1 Real-real subtraction

Introducing subtraction terms for contributions at each colour level, the real-real subtraction term for di-jet production in DIS can be written as

$$
\begin{aligned}
\mathrm{d}\hat{\sigma}_{eq}^{RR} = \mathcal{N}_{eq}^{RR}\mathrm{d}\Phi_5(p_{\hat{1}},p_{\hat{2}};p_3,p_4,p_5,p_6,p_7)\Bigg\{&\\
\frac{1}{3!}\Bigg[&\sum_{P_C(4,5,6)}B_3^{Z,0,S}(\hat{1}_q,4_g,5_g,6_g,7_q)-\frac{1}{N^2}\sum_{P(4,5,6)}\tilde{B}_3^{Z,0,S}(\hat{1}_q,4_g,5_g,6_g,7_q)\\
&+\frac{N^2+1}{N^4}\tilde{\tilde{B}}_3^{Z,0,S}(\hat{1}_q,4_g,5_g,6_g,7_q)\Bigg]\\
+\frac{1}{N}\sum_{Q}&\left[\bar{C}_1^{Z,0,S}(\hat{1}_q,4_g,5_q,6_{\bar{q}},7_q)-\frac{1}{N^2}\tilde{\bar{C}}_1^{Z,0,S}(\hat{1}_q,4_g,5_q,6_{\bar{q}},7_q)\right]
\end{aligned}
$$

$$- \frac{1}{2!N^2}\left[D_1^{Z,0,S}(\hat{1}_q,4_g,5_q,6_{\bar{q}},7_q) - \frac{1}{N^2}\tilde{D}_1^{Z,0,S}(\hat{1}_q,4_g,5_q,6_{\bar{q}},7_q)\right]\Bigg\}, \quad (7.8)$$

where $P_C(4,5,6)$ denotes the restricted sum over cyclic permutations of gluons $4,5$ and 6 and here the $\bar{C}$ notation from Eq. (6.16) is also applied to the subtraction terms.

The leading-colour B-type subtraction term is constructed according to the construction principles documented in Ref. [98] and given in Eq. (A.1) of the appendix. Due to the length of almost all NNLO subtraction terms in DIS di-jet production, all terms described in the following are included in the appendix to increase the readability of this thesis. The subleading-colour B-type subtraction term, for which the corresponding matrix element is free from genuine gluon triple-collinear infrared divergences, is given in Eq. (A.2) and the subsubleading-colour B-type subtraction, for which the corresponding matrix element is even free from any gluon-gluon single-collinear infrared limits, is given in Eq. (A.3).

The leading-colour C-type matrix element includes quark-antiquark double-soft and single-collinear limits that are absent in B-type elements. This matrix element is rendered finite by the symmetrised version of the subtraction term given in Eq. (A.4). The subtraction term for the subleading-colour C-type matrix element is given in Eq. (A.5). In both C-type subtraction terms symmetrisation is necessary by analogous reasoning as discussed in Section 6.8.1. Finally, the leading- and subleading-colour subtraction terms for the one-gluon two-identical–quark-pair D-type matrix elements are given in Eq. (A.6) and Eq. (A.7), respectively.

All antiquark-initiated real-real subtraction terms can be obtained by line reversals of the momentum arguments in each reduced matrix element appearing in the above real-real subtraction terms.

7.9.2 Real-virtual subtraction

Decomposing the real-virtual subtraction term into individual contributions that each subtract divergences at a particular colour level, the full real-virtual subtraction term reads

$$\begin{aligned}
\mathrm{d}\hat{\sigma}_{eq}^{T} = \mathcal{N}_{eq}^{RV}\mathrm{d}\Phi_4(p_{\hat{1}},p_{\hat{2}};p_3,p_4,p_5)\Bigg\{ & \\
+\frac{1}{2!}\left[B_2^{Z,1,T}(\hat{1}_q,4_g,5_g,6_q) - \frac{1}{N^2}\tilde{B}_2^{Z,1,T}(\hat{1}_q,4_g,5_g,6_q) + \frac{1}{N^4}\tilde{\tilde{B}}_2^{Z,1,S}(\hat{1}_q,4_g,5_g,6_q)\right] & \\
+\frac{N_F}{2!N}\left[\sum_{P(4,5)}\left(\hat{B}_2^{Z,1,T}(\hat{1}_q,4_g,5_g,6_q) + \frac{1}{2}\hat{B}_{2,q\to g}^{Z,1,T}(\hat{1}_q,4_g,5_g,6_q)\right.\right. & \\
\left.\left.-\frac{1}{2N^2}\left[\hat{\tilde{B}}_2^{Z,1,T}(\hat{1}_q,4_g,5_g,6_q) + \frac{1}{2}\hat{\tilde{B}}_{2,q\to g}^{Z,1,T}(\hat{1}_q,4_g,5_g,6_q)\right]\right)\right] & \\
+\frac{1}{N}\sum_Q\left[\bar{C}_0^{Z,1,T}(\hat{1}_q,4_Q,5_{\bar{Q}},6_q) - \frac{1}{N^2}\tilde{C}_0^{Z,1,T}(\hat{1}_q,4_Q,5_{\bar{Q}},6_q) + \frac{N_F}{N}\hat{C}_0^{Z,1,T}(\hat{1}_q,4_Q,5_{\bar{Q}},6_q)\right] & \\
+\frac{1}{N^2}\left[D_0^{Z,1,T}(\hat{1}_q,4_q,5_{\bar{q}},6_q) + \frac{1}{N^2}\tilde{D}_0^{Z,1,T}(\hat{1}_q,4_q,5_{\bar{q}},6_q)\right]\Bigg\}. & \quad (7.9)
\end{aligned}$$

The quark-initiated leading-colour real-virtual B-type subtraction term is constructed such that all individual subtraction terms, except any terms of the form $X_4^0 \times B_1^{Z,0}$, that ap-

pear in the real-real subtraction of the leading-colour B-type correction, are integrated up. Combining these terms with further appropriate structures, the infrared divergences of the leading-colour real-virtual B-type subtraction term coincide with those of the corresponding correction. An explicit expression for this subtraction term is given in Eq. (A.8). In Eq. (A.8), it should be noted that individual blocks of the form

$$\begin{aligned}
&+\frac{1}{2}\Big[+J_2^1(\{p_{\hat{1}},\{p\}_3\})-J_2^1(\{\tilde{p}_{\hat{1}},\{\tilde{p}\}_2\})+\cdots\\
&+\Big(-\mathcal{S}^{FF}(\{p_{\hat{1}},\{p\}_3\})+\mathcal{S}^{FF}(\{\tilde{p}_{\hat{1}},\{\tilde{p}\}_2\})\Big)+\cdots\Big]\\
&\times X_3^0(\{p_{\hat{1}},\{p\}_3\})\,B_1^{Z,0}(\{\tilde{p}_{\hat{1}},\{\tilde{p}\}_2\})\,J_2^2(\{\tilde{p}\}_2)\,,
\end{aligned} \tag{7.10}$$

that appear as parts of $\mathrm{d}\hat{\sigma}^{T,c}$, are free from explicit poles in ϵ, in agreement with the construction principle described in Ref. [98].

The subleading- and subsubleading-colour real-virtual B-type subtraction terms integrate up all of the relevant antennae appearing in the subleading and subsubleading-colour real-real B-type subtraction terms, respectively. Including further relevant structures, the leading and subleading-colour B-type subtraction terms can be written as in Eq. (A.9) and Eq. (A.10).

Antenna functions appearing in the C-type real-real subtraction term are integrated up to either the $\hat{B}$-type or the C-type real-virtual subtraction terms, depending on the nature of the primary antenna appearing in the real-real subtraction. Primary antennae that subtract infrared divergences of the type $q\bar{q}\to g$, that are the E_3^0 antennae, are integrated up to the $\hat{B}$-type, whereas primary antennae that subtract $gq\to q$-type divergences, that are the A_3^0 antennae, are integrated to the C-type real-virtual subtraction term. Consequently, identity changing subtraction terms appear in the $\hat{B}$-type subtraction which are of the type $\hat{q}\to\hat{g}$. The identity preserving leading-colour $\hat{B}$-type subtraction is given in Eq. (A.11) and the subleading-colour subtraction by Eq. (A.12). Their corresponding identity changing subtraction terms are given in Eq. (A.13) and Eq. (A.14), respectively. In its unsymmetrised form, the leading-colour C-type subtraction term is given in Eq. (A.15). No symmetrisation is necessary for the subleading-colour C-type subtraction term and this term is given in Eq. (A.16). For the real-virtual $\mathcal{O}(N_F^2)$ colour level contribution, that is the $\hat{C}$-type matrix element, the relevant subtraction term is given in Eq. (A.17). Finally, the D-type real-virtual subtraction terms, which inherit their integrated antennae from the real-real D-type subtraction, are given in leading colour by Eq. (A.18) and in subleading colour by Eq. (A.19).

All antiquark-initiated real-virtual subtraction terms can be obtained via line reversals of the momentum arguments in each reduced matrix element appearing in the above quark-initiated real-virtual subtraction terms.

7.9.3 Virtual-virtual subtraction

The full quark-initiated virtual-virtual subtraction term can be written, decomposed in colour, as

$$
\begin{aligned}
\mathrm{d}\hat{\sigma}^{U}_{eq} = \mathcal{N}^{VV}_{eq}\,\mathrm{d}\Phi_3(p_{\hat{1}}, p_{\hat{2}}; p_3, p_4, p_5)\Bigg\{ & \\
& + B_1^{Z,2,U}(\hat{1}_q, 4_g, 5_q) - \frac{1}{N^2}\tilde{B}_1^{Z,2,U}(\hat{1}_q, 4_g, 5_q) + \frac{1}{N^4}\tilde{\tilde{B}}_1^{Z,2,U}(\hat{1}_q, 4_g, 5_q) \\
& + \frac{N_F}{N}\left[\hat{B}_1^{Z,2,U}(\hat{1}_q, 4_g, 5_q) + \hat{B}_{1,q\to g}^{Z,2,U}(\hat{1}_q, 4_g, 5_q) + \hat{B}_{1,q\to Q}^{Z,2,U}(\hat{1}_q, 4_g, 5_q)\right] \\
& + \frac{N_F}{N^3}\left[\hat{\tilde{B}}_1^{Z,2,U}(\hat{1}_q, 4_g, 5_q) + \hat{\tilde{B}}_{1,q\to Q}^{Z,2,U}(\hat{1}_q, 4_g, 5_q) + \hat{\tilde{B}}_{1,q\to g}^{Z,2,U}(\hat{1}_q, 4_g, 5_q)\right] \\
& + \frac{N_F^2}{N^2}\left[\hat{\hat{B}}_1^{Z,2,U}(\hat{1}_q, 4_g, 5_q) + \hat{\hat{B}}_{1,q\to g}^{Z,2,U}(\hat{1}_q, 4_g, 5_q)\right]\Bigg\}, \qquad (7.11)
\end{aligned}
$$

where the subtraction terms are obtained by integrating up all as yet unmatched antennae appearing in the real-real and real-virtual subtractions and by combining them with relevant mass factorisation counterterms.

The leading, subleading and subsubleading-colour B-type subtraction terms are given in Eq. (A.20), Eq. (A.21) and Eq. (A.22), respectively. It should be noted that the subleading-colour B-type subtraction term also includes the integrated terms from the leading-colour D-type real-real subtraction that contains identity changing limits of the form $q \to \bar{q}$. Similarly, the subsubleading-colour B-type subtraction includes integrated terms from the subleading-colour D-type real-real subtraction term that in turn contains the same identity changing limits as the corresponding leading-colour term.

The leading-colour $\hat{B}$-type correction is proportional to N_F such that the integrated antennae relevant for the corresponding subtraction term are integrated up from the leading-colour C-type real-real as well as the leading-colour C-type and $\hat{B}$-type real-virtual subtraction terms. This subtraction term is then decomposed into identity changing and identity preserving contributions, where the latter is given in Eq. (A.23). The identity changing subtraction term is further decomposed according to the identity changing limits $\hat{q} \to \hat{g}$ and $\hat{q} \to \hat{Q}$. Subtractions relevant for the $\hat{q} \to \hat{g}$ and $\hat{q} \to \hat{Q}$ limits are given in Eq. (A.24) and Eq. (A.25), respectively.

Similarly, the subleading-colour $\hat{B}$-type subtraction term contains the as yet unmatched integrated antennae from the subleading-colour C-type real-real and subleading-colour C-type as well as from the subleading-colour $\hat{B}$-type real-virtual subtraction terms. The subleading-colour $\hat{B}$-type subtraction term is decomposed in a similar way as is done for the corresponding leading-colour subtraction. The corresponding identity preserving subtraction is given in Eq. (A.26). Subtractions involving the initial-state splittings $\hat{q} \to \hat{Q}$ and $\hat{q} \to \hat{g}$ are given in Eq. (A.27) and Eq. (A.28), respectively.

Finally, the $\hat{\hat{B}}$-type subtraction term, which is constructed from integrated antennae appearing in the $\hat{C}$-type real-virtual subtraction term, is given in Eq. (A.29) in its identity preserving limits. The identity changing contribution is given in Eq. (A.30).

All relevant antiquark-initiated virtual-virtual subtraction terms are obtained via line reversals of the momentum arguments in each reduced matrix element appearing in the quark-initiated virtual-virtual subtraction terms.

7.10 Gluon-initiated cross section at NNLO

7.10.1 Real-real contribution

Real-real corrections to the gluon-initiated di-jet cross section in DIS can be written, decomposed in colour, as

$$\begin{aligned}
\mathrm{d}\hat{\sigma}^{RR}_{eg} = \mathcal{N}^{RR}_{eg}\mathrm{d}\Phi_5(p_{\hat{1}}, p_{\hat{2}}; p_3, p_4, p_5, p_6, p_7)\Bigg\{ \\
\frac{1}{3!}\Bigg[\sum_{P(\hat{1},5,6)}\Bigg[\bar{B}^{Z,0}_3(4_{\bar{q}}, \hat{1}_g, 5_g, 6_g, 7_q) - \frac{1}{N^2}\tilde{\bar{B}}^{Z,0}_3(4_{\bar{q}}, \hat{1}_g, 5_g, 6_g, 7_q) \\
+\frac{N^2+1}{N^4}\tilde{\tilde{\bar{B}}}^{Z,0}_3(4_{\bar{q}}, \hat{1}_g, 5_g, 6_g, 7_q)\Bigg] \\
+\frac{1}{2!N}\sum_{q,Q}\Bigg[C^{Z,0}_1(4_{\bar{q}}, \hat{1}_g, 5_Q, 6_{\bar{Q}}, 7_q) - \frac{1}{N^2}\tilde{C}^{Z,0}_1(4_{\bar{q}}, \hat{1}_g, 5_Q, 6_{\bar{Q}}, 7_q)\Bigg] \\
-\frac{1}{2!2!N^2}\sum_{q}\Bigg[D^{Z,0}_1(4_{\bar{q}}, \hat{1}_g, 5_q, 6_{\bar{q}}, 7_q) - \frac{1}{N^2}\tilde{D}^{Z,0}_1(4_{\bar{q}}, \hat{1}_g, 5_q, 6_{\bar{q}}, 7_q)\Bigg]\Bigg\}J^4_2(\{p\}_4)\,, \quad (7.12)
\end{aligned}$$

where the bar over the B-type matrix elements denotes a symmetrised matrix element as defined in Eq. (6.14). A symmetrisation of B-type matrix elements for gluon-initiated contributions is necessary for the same reasons as described in Section 6.9.1. All of the above matrix elements are obtained from the matrix elements in Ref. [140] with the gluon crossed into the initial state.

7.10.2 Real-virtual contribution

The real-virtual gluon-initiated contribution to the cross section can be written decomposed in colour as

$$\begin{aligned}
\mathrm{d}\hat{\sigma}^{RV}_{eg} = \mathcal{N}^{RV}_{eg}\mathrm{d}\Phi_4(p_{\hat{1}}, p_{\hat{2}}; p_3, p_4, p_5)\Bigg\{ \\
+\Bigg[\sum_{P(\hat{1},5)}\bar{B}^{Z,1}_2(4_{\bar{q}}, \hat{1}_g, 5_g, 6_q) - \frac{1}{N^2}\tilde{\bar{B}}^{Z,1}_2(4_{\bar{q}}, \hat{1}_g, 5_g, 6_q) + \frac{1}{N^4}\tilde{\tilde{\bar{B}}}^{Z,1}_2(4_{\bar{q}}, \hat{1}_g, 5_g, 6_q)\Bigg] \\
+\frac{N_F}{N}\Bigg[\sum_{P(\hat{1},5)}\hat{\bar{B}}^{Z,1}_2(4_{\bar{q}}, \hat{1}_g, 5_g, 6_q) - \frac{1}{N^2}\hat{\tilde{\bar{B}}}^{Z,1}_2(4_{\bar{q}}, \hat{1}_g, 5_g, 6_q)\Bigg]\Bigg\}J^3_2(\{p\}_3)\,, \quad (7.13)
\end{aligned}$$

where the B-type contributions are calculated in terms of their corresponding symmetrised matrix elements. Symmetrisation is necessary for the same reasons as discussed in Section 6.9.1. The above matrix elements are taken form [141] with the gluon crossed into the initial state. Note that all C- and D-type contributions are absent in the gluon-initiated real-virtual corrections.

7.10.3 Virtual-virtual contribution

Finally, the virtual-virtual correction can be written as

$$\begin{aligned}
\mathrm{d}\hat{\sigma}^{VV}_{eg} = \mathcal{N}^{VV}_{eg}\mathrm{d}\Phi_3(p_{\hat{1}},p_{\hat{2}};p_3,p_4,p_5)\Big\{ \\
+ B_1^{Z,2}(4_{\bar{q}},\hat{1}_g,5_q) - \frac{1}{N^2}\tilde{B}_1^{Z,2}(4_{\bar{q}},\hat{1}_g,5_q) + \frac{1}{N^4}\tilde{B}_1^{Z,2}(4_{\bar{q}},\hat{1}_g,5_q) \\
+ \frac{N_F}{N}\hat{B}_1^{Z,2}(4_{\bar{q}},\hat{1}_g,5_q) + \frac{N_F}{N^3}\hat{\tilde{B}}_1^{Z,2}(4_{\bar{q}},\hat{1}_g,5_q) + \frac{N_F^2}{N^2}\hat{\tilde{B}}_1^{Z,2}(4_{\bar{q}},\hat{1}_g,5_q)\Big\}J_1^1(\{p\}_1)\,, \quad (7.14)
\end{aligned}$$

where the matrix elements are taken from [142] with the gluon crossed into the initial state.

7.11 Gluon-initiated subtraction at NNLO

7.11.1 Real-real subtraction

In terms of colour decomposed contributions, the full real-real subtraction term can be written as

$$\begin{aligned}
\mathrm{d}\hat{\sigma}^{S}_{eg} = \mathcal{N}^{RR}_{eg}\mathrm{d}\Phi_5(p_{\hat{1}},p_{\hat{2}};p_3,p_4,p_5,p_6,p_7)\Big\{ \\
\frac{1}{3!}\Bigg[\sum_{P(\hat{1},5,6)}\Bigg[\bar{B}_3^{Z,0,S}(4_{\bar{q}},\hat{1}_g,5_g,6_g,7_q) - \frac{1}{N^2}\tilde{\bar{B}}_3^{Z,0,S}(4_{\bar{q}},\hat{1}_g,5_g,6_g,7_q)\Bigg] \\
+\frac{N^2+1}{N^4}\tilde{\bar{B}}_3^{Z,0}(4_{\bar{q}},\hat{1}_g,5_g,6_g,7_q)\Bigg] \\
+ \frac{1}{2!N}\sum_{q,Q}\Bigg[\bar{C}_1^{Z,0,S}(4_{\bar{q}},\hat{1}_g,5_Q,6_{\bar{Q}},7_q) - \frac{1}{N^2}\tilde{\bar{C}}_1^{Z,0,S}(4_{\bar{q}},\hat{1}_g,5_Q,6_{\bar{Q}},7_q)\Bigg] \\
- \frac{1}{2!2!N^2}\sum_{q}\Bigg[D_1^{Z,0,S}(4_{\bar{q}},\hat{1}_g,5_q,6_{\bar{q}},7_q) - \frac{1}{N^2}\tilde{D}_1^{Z,0,S}(4_{\bar{q}},\hat{1}_g,5_q,6_{\bar{q}},7_q)\Bigg]\Big\}\,. \quad (7.15)
\end{aligned}$$

Leading, subleading and subsubleading B-type subtraction terms are given in Eq. (B.1), Eq. (B.2) and Eq. (B.3), respectively. In particular, the construction principle for the leading-colour subtraction was unknown at the start of the project and is successfully completed in this work. The leading-colour C-type subtraction terms are given in Eq. (B.4) and the subleading C-type subtraction term in Eq. (B.5). The subtraction terms for matrix elements with two identical quark pairs, which are the D-type matrix elements, are given for the leading and subleading-colour contribution in Eq. (B.6) and Eq. (B.7), respectively.

7.11.2 Real-virtual subtraction

The real-virtual subtraction term for gluon-initiated di-jet production in DIS is given by

$$\begin{aligned}
\mathrm{d}\hat{\sigma}^{T}_{eg} = \mathcal{N}^{RV}_{eg}\mathrm{d}\Phi_4(p_{\hat{1}},p_{\hat{2}};p_3,p_4,p_5)\Big\{ \\
+\Big[B_2^{Z,1,T}(4_{\bar{q}},\hat{1}_g,5_g,6_q) + B_{2,q\to g}^{Z,1,T}(4_{\bar{q}},\hat{1}_g,5_g,6_q)\Big]
\end{aligned}$$

$$
\begin{aligned}
&- \frac{1}{N^2}\left[\tilde{B}_2^{Z,1,T}(4_{\bar{q}},\hat{1}_g,5_g,6_q) + \tilde{B}_{2,q\to g}^{Z,1,T}(4_{\bar{q}},\hat{1}_g,5_g,6_q)\right] \\
&+ \frac{1}{N^4}\left[\tilde{\tilde{B}}_2^{Z,1,T}(4_{\bar{q}},\hat{1}_g,5_g,6_q) + \tilde{\tilde{B}}_{2,g\to q}^{Z,1,T}(4_{\bar{q}},\hat{1}_g,5_g,6_q)\right] \\
&+ \frac{N_F}{N}\left[\left[\hat{B}_2^{Z,1,T}(4_{\bar{q}},\hat{1}_g,5_g,6_q) + \hat{B}_{2,g\to q}^{Z,1,T}(4_{\bar{q}},\hat{1}_g,5_g,6_q)\right]\right. \\
&\qquad \left.\left. - \frac{N_F}{N^2}\left[\hat{\hat{B}}_2^{Z,1,T}(4_{\bar{q}},\hat{1}_g,5_g,6_q) + \hat{\hat{B}}_{2,g\to q}^{Z,1,T}(4_{\bar{q}},\hat{1}_g,5_g,6_q)\right]\right]\right\}. \qquad (7.16)
\end{aligned}
$$

The leading-colour real-virtual B-type subtraction integrates up all relevant antenna subtraction terms from the leading-colour real-real B-type subtraction and combines them with further appropriate structures to give the same infrared divergences as the real-virtual matrix element. The same logic holds for the construction of the subleading and subsubleading-colour subtractions. The B-type subtraction terms are further decomposed according to identity preserving and identity changing contributions, where the identity preserving terms cancel the explicit pole structure of the real-virtual B-type matrix elements. Identity changing subtraction terms combine integrated antennae with mass factorisation counterterms to form contributions that are free from explicit ϵ-poles. For the leading-colour B-type subtraction term, the identity preserving subtraction is given in Eq. (B.8) and the identity changing term in Eq. (B.9). As gluon-initiated real-virtual D-type corrections are absent, relevant $X_3^0\times$(anything) terms appearing in the leading-colour real-real D-type subtraction in Eq. (B.6) are integrated up into the identity changing subtraction term of the subleading-colour B-type subtraction as both contributions appear at the same colour level. Analogously, the corresponding antennae that appear in the real-real subleading D-type subtraction, Eq. (B.7), are integrated up into the identity changing subsubleading-colour B-type subtraction term. Identity changing and preserving contributions for the subleading-colour B-type subtraction are given in Eqs. (B.10) and (B.11). In identity preserving and identity changing limits, the subsubleading-colour B-type subtraction term is given in Eq. (B.12) and Eq. (B.13), respectively.

The real-virtual $\hat{B}$-type subtraction is constructed from all relevant antennae integrated up from the real-real C-type subtraction term together with terms that cancel the implicit infrared divergences of the real-virtual correction. For the leading-colour $\hat{B}$-type subtraction, the identity preserving contribution is given in Eq. (B.14) and the identity changing one in Eq. (B.15). The subleading-colour $\hat{B}$-type subtraction is given in Eq. (B.16) and Eq. (B.17) in identity preserving and identity changing limits, respectively.

7.11.3 Virtual-virtual subtraction

The virtual-virtual subtraction term, decomposed in colour, can be written as

$$
\begin{aligned}
\mathrm{d}\hat{\sigma}_{eg}^{U} &= \mathcal{N}_{eg}^{VV}\,\mathrm{d}\Phi_3(p_{\hat{1}},p_{\hat{2}};p_3,p_4,p_5)\Big\{ \\
&+ \left[B_1^{Z,2,U}(4_{\bar{q}},\hat{1}_g,5_q) + B_{1,g\to q}^{Z,2,U}(4_{\bar{q}},\hat{1}_g,5_q)\right] - \frac{1}{N^2}\left[\tilde{B}_1^{Z,2,U}(4_{\bar{q}},\hat{1}_g,5_q) + \tilde{B}_{1,g\to q}^{Z,2,U}(4_{\bar{q}},\hat{1}_g,5_q)\right] \\
&+ \frac{1}{N^4}\left[\tilde{B}_1^{Z,2,U}(4_{\bar{q}},\hat{1}_g,5_q) + \tilde{B}_{1,g\to q}^{Z,2,U}(4_{\bar{q}},\hat{1}_g,5_q)\right] + \frac{N_F}{N}\left[\hat{B}_1^{Z,2,U}(4_{\bar{q}},\hat{1}_g,5_q) + \hat{B}_{1,g\to q}^{Z,2,U}(4_{\bar{q}},\hat{1}_g,5_q)\right]
\end{aligned}
$$

$$+\frac{N_F}{N^3}\left[\hat{\tilde{B}}_1^{Z,2,U}(4_{\bar{q}},\hat{1}_g,5_q)+\hat{\tilde{B}}_{1,g\to q}^{Z,2,U}(4_{\bar{q}},\hat{1}_g,5_q)\right]+\frac{N_F^2}{N^2}\hat{\tilde{B}}_1^{Z,2,U}(4_{\bar{q}},\hat{1}_g,5_q)\Bigg\}. \quad (7.17)$$

Integrating up all as yet unmatched antenna subtraction terms from the real-real and real-virtual subtractions and combining them with relevant mass factorisation counterterms gives the virtual-virtual subtraction terms. For the leading-colour B-type subtraction term, the identity preserving subtraction term is given in Eq. (B.18) which cancels the explicit ϵ-poles of the corresponding two-loop correction. The leading-colour B-type identity changing subtraction term is free from explicit ϵ-poles and is given in Eq. (B.19). The identity preserving subleading and subsubleading subtraction terms are given in Eq. (B.20) and Eq. (B.22). Similarly to the construction of the gluon-initiated real-virtual subtraction terms, the X_4^0 terms from the real-real D-type subtraction are integrated up, but this time however, added to the identity preserving subtraction of the appropriate subleading and subsubleading-colour B-type subtraction term. Identity changing subleading and subsubleading-colour B-type contributions to the subtractions are given in Eq. (B.21) and Eq. (B.23).

All as yet unmatched subtraction terms from the leading-colour C-type, leading-colour $\hat{B}$-type and subleading-colour $\hat{B}$-type are integrated up and combined with their relevant mass factorisation counterterms to give the virtual-virtual $\hat{B}$-type subtraction terms at leading and subleading colour. The virtual-virtual $\hat{B}$-subtraction term is given for the leading-colour subtraction in Eq. (B.24) in identity preserving and in Eq. (B.27) in identity changing limits. The subleading-colour $\hat{B}$-type virtual-virtual subtraction is given in Eq. (B.26) in identity preserving and in Eq. (B.27) in identity changing limits.

For the gluon-initiated contribution to the cross section, the colour factor of the $\hat{\tilde{B}}$-type matrix element only appears at the virtual-virtual level such that this virtual-virtual subtraction term is solely made up of explicit mass factorisation counterterms and given in Eq. (B.28).

7.12 Validation

To validate our implementation of the tree-level and one-loop matrix elements, we compared our NLO predictions for di-jet and tri-jet production against SHERPA [148] (in DIS kinematics [149]), which uses OpenLoops [150] to automatically generate the one-loop contributions at NLO.

Individual subtraction terms were then validated in a similar way as it was done for the subtraction terms for DIS single-jet production in the laboratory frame, described in Section 6.11. Spike plots, testing the subtraction between the corrections and subtraction terms for implicit infrared divergences, were generated and checked for all possible unresolved phase space configurations for real-real, real-virtual and single-real subtraction terms. It was analytically validated that the pole structure of integrated subtraction terms coincides with that of the one- and two-loop corrections. Further, it was checked that the scale dependence, as predicted by Eq. (2.109), is satisfied by our NNLOJET calculation and that the total cross section is independent of the technical y_0 phase space generation cut for sufficiently small values of y_0.

8 Numerical results for inclusive jet production in the Breit frame

In this section, we apply the kinematic criteria (see Table 6) used in the final H1 measurements [8, 9] to discuss several generic features of the NNLO corrections to inclusive jet production in the Breit frame, followed by an in-depth comparison of the newly derived predictions to the H1 data.

8.1 Structure of the inclusive jet production cross section at NNLO

Inclusive jet production in the Breit frame receives leading-order contributions both from quark-initiated and gluon-initiated processes. The relative magnitude of these depends on the final-state kinematics. Fig. 9 shows the relative contributions from quark and gluon initial states to inclusive jet production, evaluated at NLO and NNLO for a representative range in Q^2, using the cuts from the H1 low-Q^2 analysis (see below). We observe that at low transverse momentum, $p_T \leq 10$ GeV, inclusive jet production is mainly gluon-initiated (to almost 80%). With increasing p_T, the quark-initiated contribution becomes more and more important, reaching 50% at around $p_T \approx 30$ GeV, and further increasing towards higher p_T. NNLO corrections affect the relative importance of the different initial states only in a moderate manner, and only at high-p_T. Compared to NLO, the gluon-initiated fraction decreases more slowly for larger values of p_T. The overall behaviour of the parton fractions and their modification between NLO and NNLO remains largely unchanged at higher Q^2.

The inclusive jet production cross section receives contributions from different jet multiplicities. At NNLO, final states with up to four identified jets contribute. The jets are ordered in transverse momentum. Fig. 10 displays the contribution of the first, second, third and fourth jet to the inclusive jet distribution at NNLO for a given bin in Q^2. It

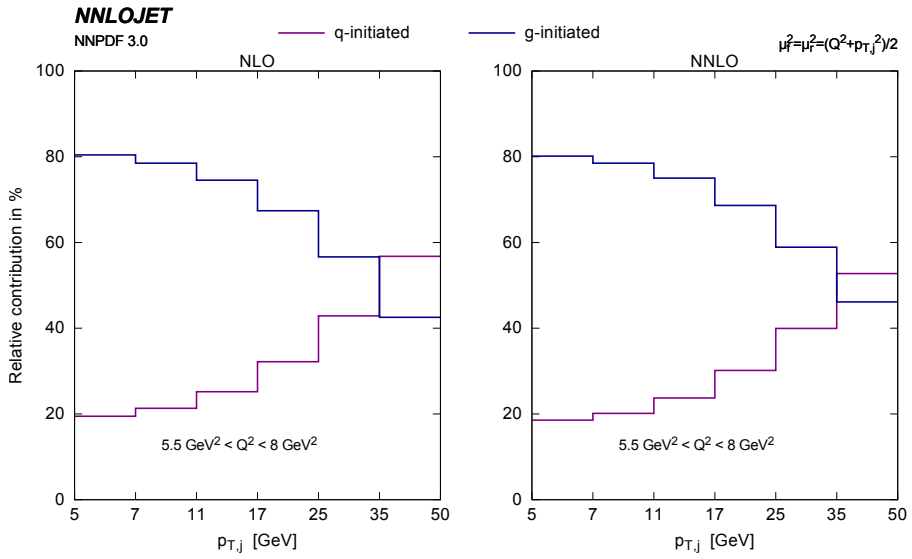

Figure 9. Quark and gluon-initiated contributions to the inclusive jet transverse momentum distribution at NLO and NNLO.

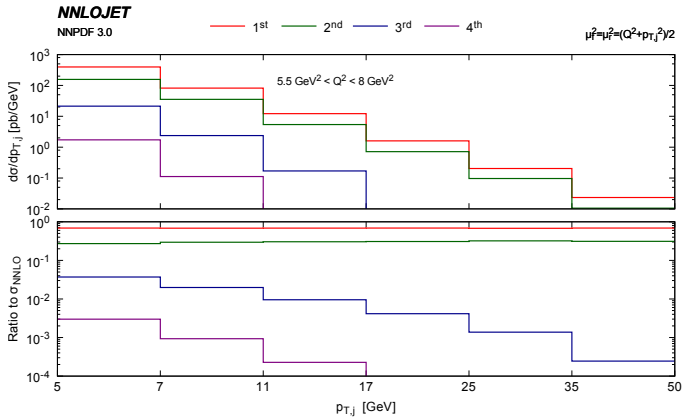

Figure 10. Contributions to inclusive jet production from first, second, third and fourth jet.

H1 (high-Q^2)	H1 (low-Q^2)	ZEUS
$150 < Q^2/\text{GeV}^2 < 15000$	$5.5 < Q^2/\text{GeV}^2 < 80$	$125 < Q^2/\text{GeV}^2$
$0.2 < y < 0.7$	$0.2 < y < 0.6$	$-0.65 < \cos\gamma_h < 0.65$
5 GeV$< p_T^B <$50 GeV	4.5 GeV$< p_T^B <$50 GeV	8 GeV$< p_T^B$
$-1.0 < \eta^L < 2.5$	$-1.0 < \eta^L < 2.5$	$-1.0 < \eta^B < 2$

Table 6. Kinematic cuts used to define the inclusive jet phase space in the measurements of H1 at high-Q^2 [8] and low-Q^2 [9], and ZEUS [12] .

can be seen that the leading jet and subleading jet contribute about 85% and 12% to the distribution over the full p_T range. This behaviour can be understood from the fact that the jet production is measured in the Breit frame, where the leading-order process will always yield a p_T-symmetric two-jet final state. The jets are not necessarily both found inside the rapidity cut, such that in some fraction of the events, only the leading jet is observed. Furthermore, real radiation from higher-order corrections can lower the transverse momentum of the second jet compared to the first one, such that the same event will enter the p_T distribution at a larger value with the first jet than with the second jet. Due to the sharp decrease of the distribution with increasing p_T, the relative importance of the second jet is lower than that of the first jet. The contributions from the third and fourth jet are at the level of a few per-cent and a few per-mille respectively at low p_T. Their importance decreases at higher p_T, which is due to the limited final-state phase space that is available for multi-jet production at large transverse momenta.

8.2 Comparison to HERA data

Inclusive jet production in the Breit frame (using the inclusive k_T algorithm with a massless E_T recombination scheme) was measured double differentially in Q^2 and p_T^B by the H1 experiment, which distinguishes a low-Q^2 [9] and a high-Q^2 sample [8] and by the ZEUS

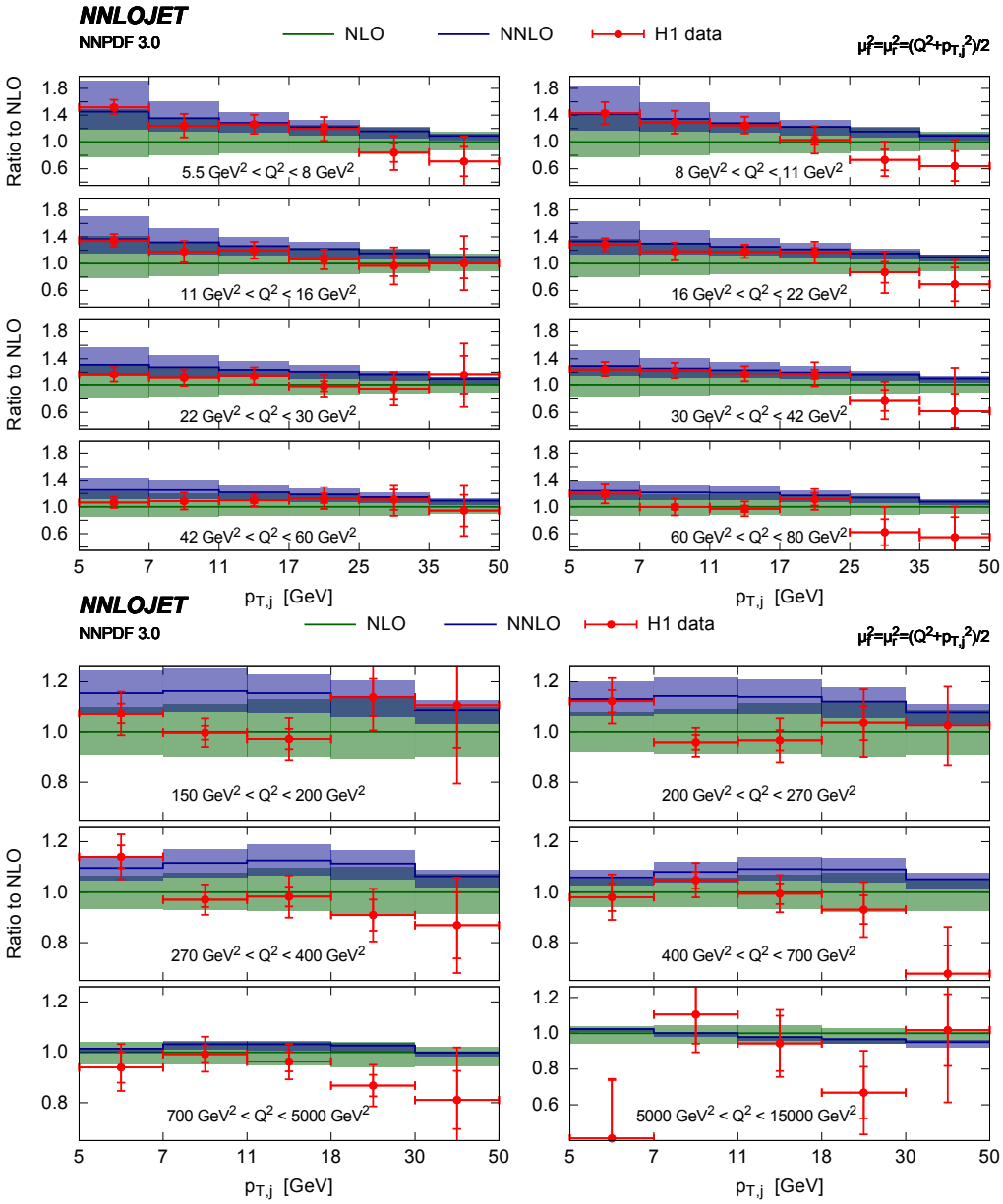

Figure 11. Inclusive jet production cross section as a function of the transverse jet momentum $p_{T,B}$ in bins of Q^2, compared to H1 data.

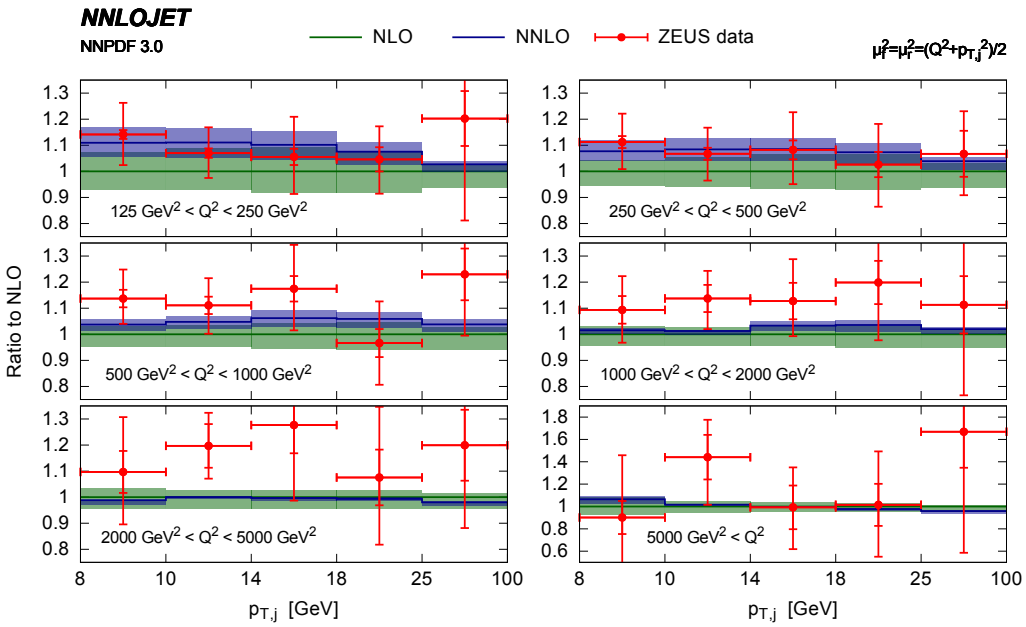

Figure 12. Inclusive jet production cross section as a function of the transverse jet momentum $p_{T,B}$ in bins of Q^2, compared to ZEUS data.

experiment [13]. The event selection criteria for all three studies are summarised in Table 6. We compute theoretical predictions at LO, NLO and NNLO, always using the same set of parton distribution functions (NNPDF3.0 NNLO) with $\alpha_s(M_Z) = 0.118$. Our predictions use a dynamical central scale choice $\mu_r^2 = \mu_f^2 = (Q^2 + p_{T,B}^2)/2$, and the theory uncertainty is determined from a seven-point scale variation with rescaling factors $[1/2, 2]$. The theoretical predictions are multiplicatively corrected for hadronisation effects, using the correction tables from the experimental papers [8, 9].

Fig. 11 compares our NNLO predictions to the H1 data. We observe that the NNLO corrections are very substantial at low Q^2 and low p_T^B, with an enhancement up to 60% with respect to NLO. These large corrections are within the NLO uncertainty band (close to the upper edge), and result in a residual theory uncertainty of 20% even at NNLO. Especially at low Q^2, the shape and normalisation of the theory prediction changes significantly going from NLO to NNLO, and results in a considerably improved theoretical description of the data, as already statistically quantified in the experimental H1 study [9]. A very similar pattern is also observed for the ZEUS measurement shown in Fig. 12. With increasing Q^2, the size of the NNLO corrections decreases, accompanied with very small residual theoretical uncertainties (decreasing from 10% at $Q^2 = 150$ GeV^2 to 2% at 5000 GeV^2). In this region, the combination of precision data with the newly derived NNLO corrections has clearly the potential to provide important new constraints for precision QCD studies.

9 Numerical results for di-jet production in the Breit frame

In the Breit frame, di-jet production and single-jet inclusive production in DIS are mediated by the same Born level processes and are closely related. In contrast to single-jet inclusive production, where only the rapidity and transverse momentum of the jet can be studied, di-jet final states allow for more kinematic observables to be reconstructed (see Section 5 above). Typically, di-jet cross sections are measured inclusively based on the two leading jets in an event, i.e. including events with more than two reconstructed jets.

In this section, we adapt the event selection (see Table 7 below) used in the final H1 measurements [8, 9] to discuss several generic features of the NNLO corrections to inclusive jet production, followed by an in-depth comparison of our NNLO predictions to the ZEUS [14] and H1 [8, 9] data.

9.1 Scale setting in the di-jet production cross section at NNLO

The dependence of the NNLO cross section on the renormalisation and factorisation scales has been derived in Section 2.10, where it can be seen that each order in the perturbative series compensates the dominant scale-dependent terms from the previous order. Consequently, the residual scale dependence of a fixed-order prediction is commonly used to estimate the error on the prediction resulting from missing higher-order corrections. The scale dependence of the theoretical prediction is quantified by choosing central values for μ_f and μ_r, and then evaluating the cross section for variations around these central scales, typically by a factor two.

These central scale values should reflect the dynamics of the process. In processes involving only a single mass scale (such as inclusive DIS, depending only on the photon virtuality Q^2), the central scale choice is unambiguous (at most up to a constant factor). For processes involving multiple physical scales, several choices are possible (and a priori equally well motivated). The only guiding principle for choosing the central scales in this

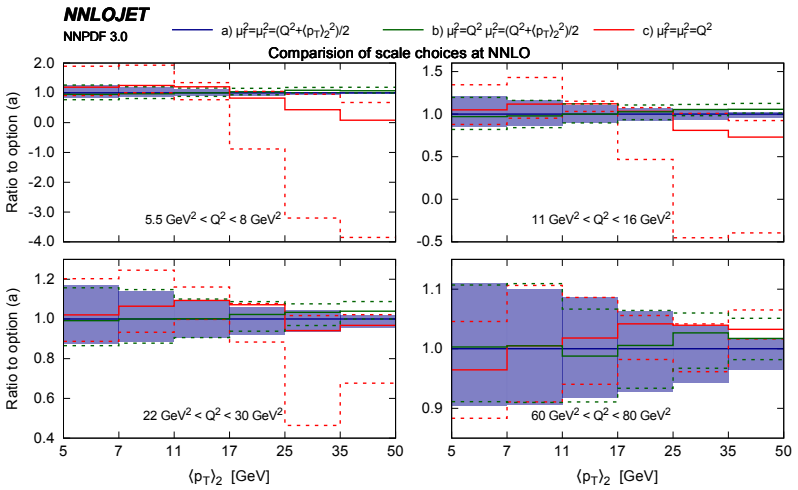

Figure 13. Di-jet production cross sections for different scale settings.

case is the occurrence of large logarithmic terms in each order in perturbation theory, which spoil the convergence of the perturbative expansion and indicate an inappropriate choice of the central scale.

Di-jet production in DIS depends on two scales: the photon virtuality Q^2 and the average transverse momentum of the two jets $\langle p_T^B \rangle_2$. Using the kinematic cuts of some of the bins in the H1 low-Q^2 di-jet measurement (which are discussed in detail in the following subsection) as an example, we study different choices for the central scales in Fig. 13. We compare the following three options:

$$\begin{aligned} &\text{(a)} \quad \mu_f^2 = \mu_r^2 = \left(Q^2 + \langle p_T^B \rangle_2^2\right)/2, \\ &\text{(b)} \quad \mu_f^2 = Q^2, \quad \mu_r^2 = \left(Q^2 + \langle p_T^B \rangle_2^2\right)/2, \\ &\text{(c)} \quad \mu_f^2 = \mu_r^2 = Q^2. \end{aligned}$$

All three options were considered previously in comparisons of NLO predictions to the H1 and ZEUS jet data [3–14]. Option (a) represents the average of both hard scales in the jet production process, and is used as default throughout this paper; option (b) is used frequently in the experimental studies, with the argument that the partonic structure of the proton (μ_f) is resolved by the virtual photon, while it is hard QCD emission (μ_r) that yields the two-jet final state; finally option (c) is entirely based on the photon virtuality to describe the hardness of the interaction.

We observe that the scale choices (a) and (b) yield similar predictions, except in the region of large transverse momentum. Especially at large Q^2, the choice (b) results in slightly higher cross section predictions, accompanied by larger scale uncertainties. In contrast, scale choice (c) results in unphysical predictions (negative cross sections) if applied at low Q^2 and large transverse momentum. These results confirm earlier observations made at NLO [15–18]. By examining the analytical form of some of the NLO contributions [16, 17] for scale choice (c), the emergence of large logarithmic corrections in the jet transverse momenta could be established. These corrections are largely compensated in the hard coefficient functions for scale choices (a) and (b), which are clearly preferable in terms of reliability and perturbative stability. It should be pointed out that the large logarithmic terms alone (which can be inferred from threshold resummation [151]) do not properly account for the bulk of the NNLO corrections, as observed in Ref. [9].

9.2 Comparison to HERA data

Inclusive di-jet production was measured by both HERA experiments: H1 [8, 9] provides double-differential results in Q^2 and $\langle p_T^B \rangle_2$ or Q^2 and ξ_2, using the k_T and anti-k_T jet algorithms in the Breit frame. ZEUS [14] uses only the k_T jet algorithm and provides single-differential results in $\bar{E}_T^B = \langle p_T^B \rangle_2$, Q^2, M_{jj}, η^*, $\xi = \xi_2$ as well as double-differential results in Q^2 and ξ or $\bar{E}_T^B$. The kinematic cuts in the measurements are summarised in Table 7. We compute theoretical predictions at LO, NLO and NNLO, always using the same set of parton distribution functions (NNPDF3.0 NNLO) with $\alpha_s(M_Z) = 0.118$. Our predictions use the central scales $\mu_r^2 = \mu_f^2 = (Q^2 + \langle p_T \rangle_2^2)/2$ and the theory uncertainty is determined from a seven-point scale variation with rescaling factors $[1/2, 2]$.

H1 (high-Q^2)	H1 (low-Q^2)	ZEUS
$150 < Q^2/\text{GeV}^2 < 15000$	$5.5 < Q^2/\text{GeV}^2 < 80$	$125 < Q^2/\text{GeV}^2 < 20000$
$0.2 < y < 0.7$	$0.2 < y < 0.6$	$0.2 < y < 0.6$
5 GeV$< p_T^B <$50 GeV	4 GeV$< p_T^B$	$E_T^B > 8$ GeV
$-1.0 < \eta^L < 2.5$	$-1.0 < \eta^L < 2.5$	$-1.0 < \eta^L < 2.5$
$M_{12} > 16$ GeV		$M_{12} > 20$ GeV

Table 7. Kinematic cuts used to define the inclusive di-jet phase space in the measurements of H1 (high-Q^2 [8] and low-Q^2 [9]) and ZEUS [14].

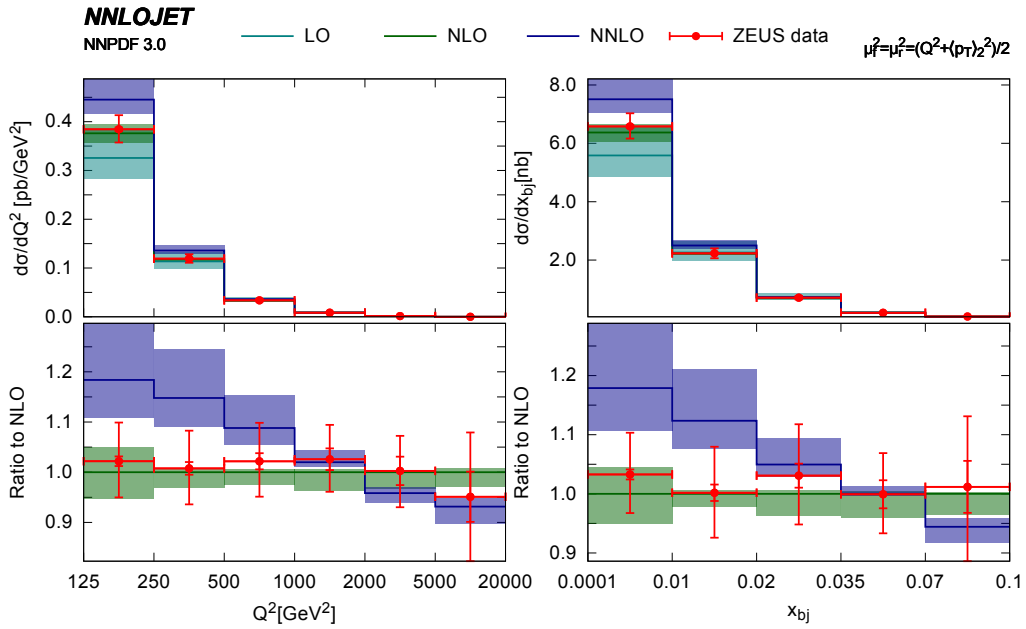

Figure 14. Inclusive di-jet production cross section as a function of the electron variables Q^2 (left) and x (right), compared to ZEUS data.

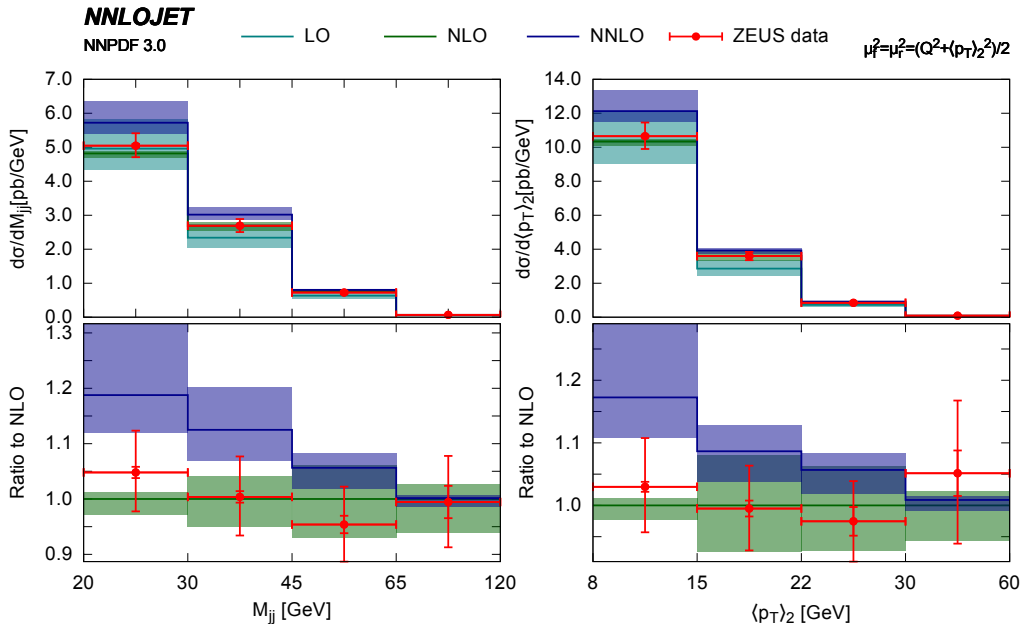

Figure 15. Inclusive di-jet production cross section as a function of $\langle p_T^B \rangle_2$ (left) and M_{jj} (right), compared to ZEUS data.

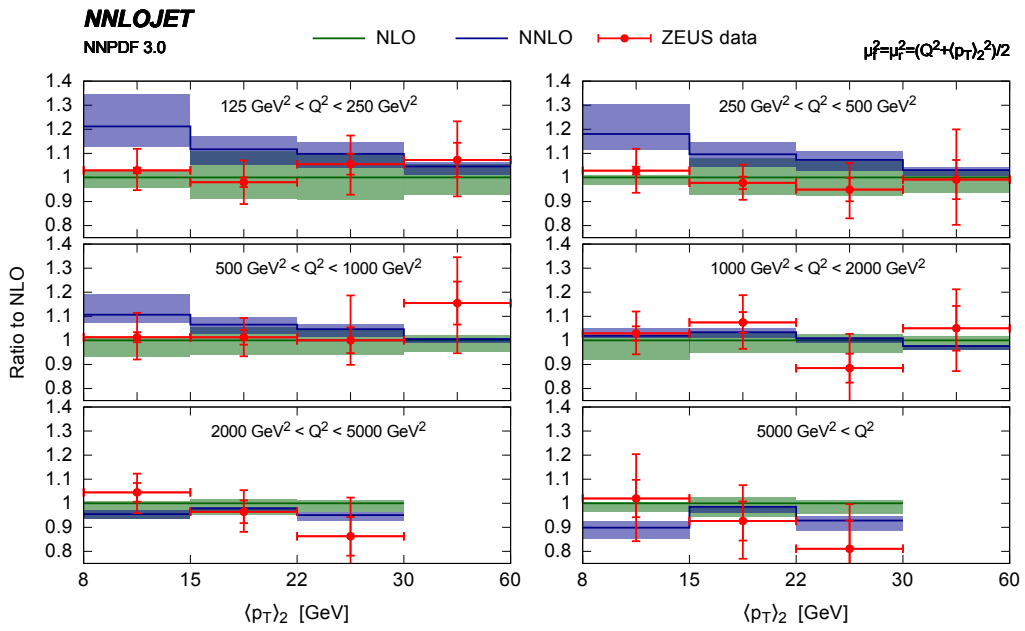

Figure 16. Inclusive di-jet production cross section as a function of $\langle p_T^B \rangle_2$ in bins of Q^2, compared to ZEUS data.

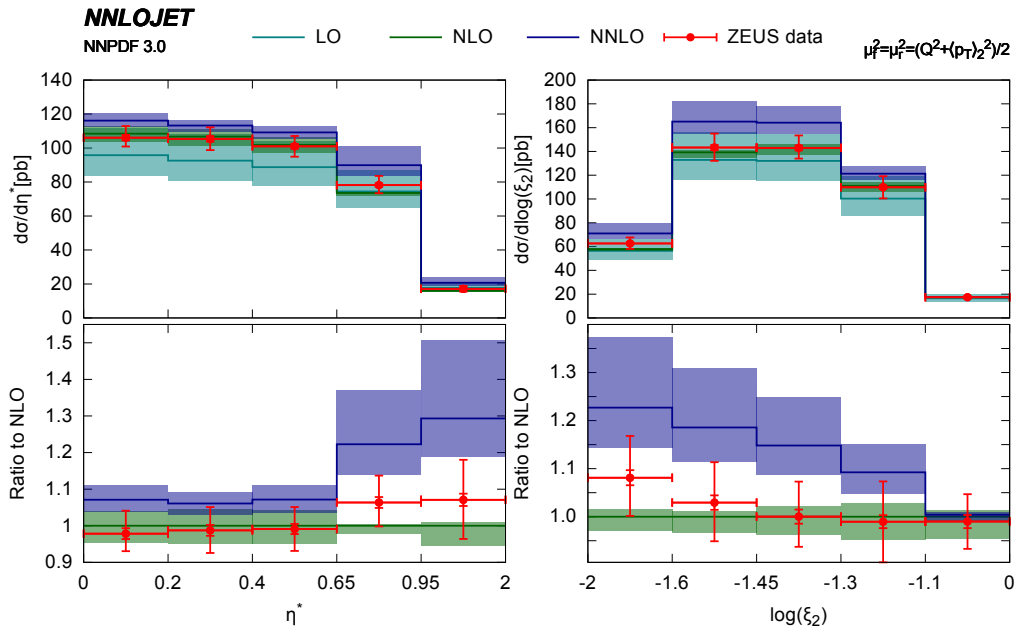

Figure 17. Inclusive di-jet production cross section as a function of η^* (left) and $\log(\xi_2)$ (right), compared to ZEUS data.

The theoretical predictions are multiplicatively corrected for hadronisation effects, using the correction tables from the respective experimental papers [8, 9, 14].

Fig. 14 displays the inclusive di-jet cross section for the ZEUS kinematics as a function of the electron variables Q^2 (left) and of x (right). We observe the NNLO corrections to be sizeable especially at low values of Q^2 or x, where they enhance the NLO prediction by about 15%. In this region, the scale dependence of the NNLO prediction is as large as at NLO, or even larger. We also note that the shape of the data is better described by the NLO prediction than at NNLO. A similar pattern is observed in the distributions in $\langle p_T^B \rangle_2$ and M_{jj} shown in Fig. 15, with sizeable NNLO corrections in the lower range of the distributions. In both these distributions this range clearly correlates with the approach to the infrared limit, as can be seen even more clearly in the double-differential distribution in $\langle p_T^B \rangle_2$ and Q^2, Fig. 16. In this limit, the QCD coupling constant increases and logarithmically enhanced contributions could cause the convergence of the perturbative fixed-order expansion to deteriorate. This issue is further aggravated by the interplay of the M_{jj} cut (see Table 7) with the transverse momentum requirements on the final-state jets. The relatively small scale dependence of the NLO predictions in this range is probably an artefact originating from a cross-over of the upper and lower edges of the scale band, as investigated in detail for hadronic di-jet production in Ref. [69]. The scale variation at NNLO therefore provides the more realistic assessment of the theoretical uncertainty.

The di-jet cross section as function of η^* and of $\log(\xi_2)$ is shown in Fig. 17. While good perturbative convergence is observed in the plateau region $\eta^* < 0.65$, NNLO corrections turn out to be very sizeable at higher rapidities. The perturbative instability in this

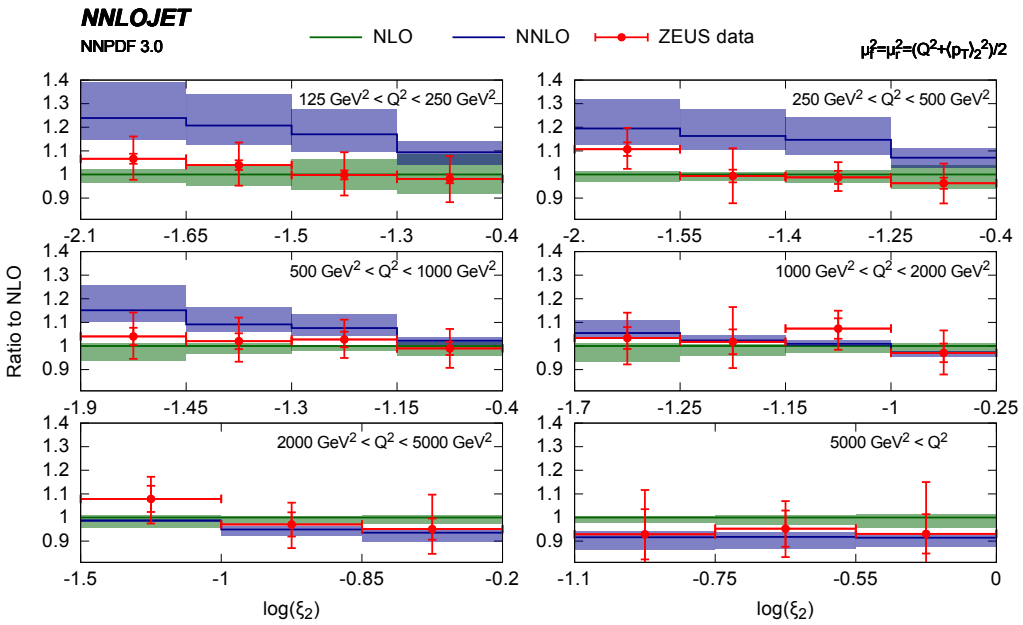

Figure 18. Inclusive di-jet production cross section as a function of $\log(\xi)$ in bins of Q^2, compared to ZEUS data.

region was already pointed out and explained by the ZEUS collaboration [14]. The $\log(\xi_2)$ correlates most directly with the parton distributions, indicating that the ZEUS di-jet data will likely deliver important constraints in the determination of the gluon distribution for momentum fractions in the medium range $0.01 < \xi < 0.1$. The double-differential distribution in $\log(\xi_2)$ and Q^2, Fig. 18, further illustrates this impact, showing a coherent pattern of discrepancy between data and NNLO theory over the full Q^2 range. It will be very interesting to study further the impact of these data in the determination of parton distributions at NNLO.

The H1 dataset is divided into a high-Q^2 and a low-Q^2 sample, see Table 7. For the low-Q^2 sample [9], double-differential distributions were measured in Q^2 and $\langle p_T^B \rangle_2$, which we compare to our NNLO calculation in Fig. 19. Compared to NLO, the NNLO corrections enhance the prediction of the di-jet cross section at lower values of $\langle p_T^B \rangle_2$, leading to a considerable improvement in the description of the H1 data, as already pointed out in Ref. [9]. Moreover, we observe an excellent convergence of the perturbative series and a considerable reduction of the theory uncertainty in going from NLO to NNLO.

For the high-Q^2 sample, slightly different event selection criteria are applied: in particular, a minimum value of M_{jj} is imposed. In a our publication [152], we have already studied the impact of the NNLO corrections in the double-differential distributions in Q^2 and $\langle p_T^B \rangle_2$ for the H1 high-Q^2 sample. Fig. 20 collects these results. It can be seen that the improvement of the theoretical uncertainty from NLO to NNLO is less pronounced than for the low-Q^2 study, and that perturbative instabilities arise at low $\langle p_T^B \rangle_2$. These can be traced back to the M_{jj} cut, which restricts the available LO and NLO phase space for di-jet production at low $\langle p_T^B \rangle_2$. Fig. 21 compares the NNLO predictions for double-differential

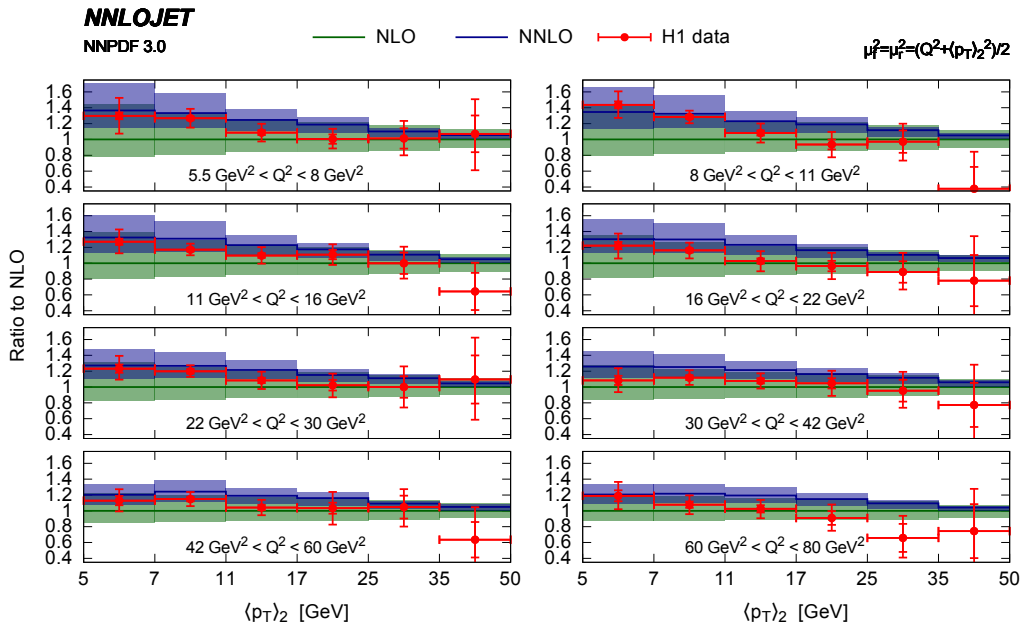

Figure 19. Inclusive di-jet production cross section as a function of $\langle p_T^B \rangle_2$ in bins of Q^2, compared to H1 low-Q^2 data.

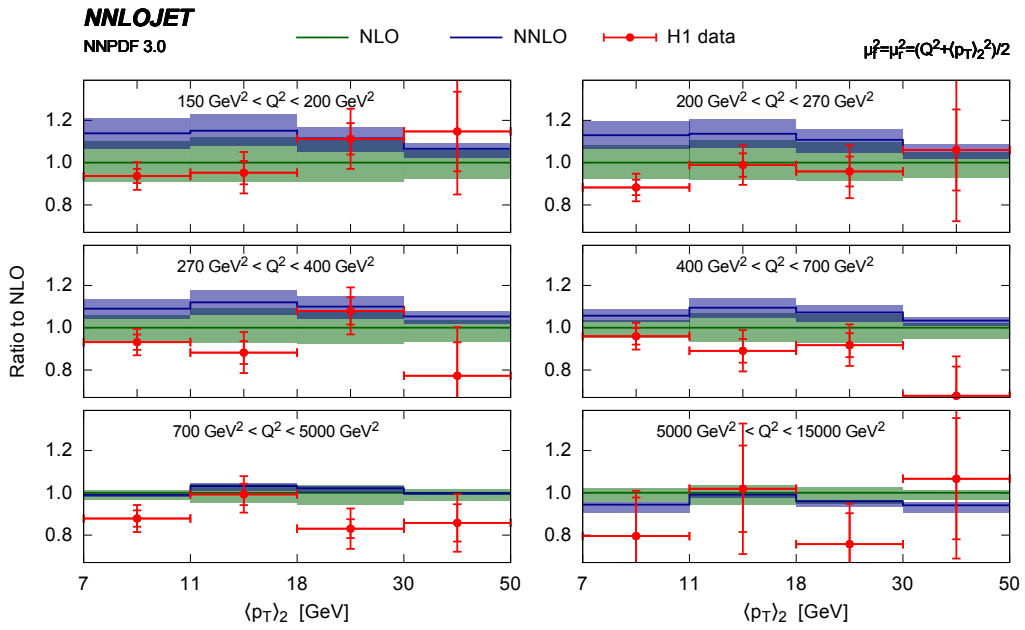

Figure 20. Inclusive di-jet production cross section as a function of $p_{T,2}^B$ in bins of Q^2, compared to H1 high-Q^2 data.

distributions in Q^2 and ξ_2 to the H1 high-Q^2 measurement (these distributions are not available for the H1 low-Q^2 study). We observe that the quantitative behaviour is very similar to the ZEUS distributions, Fig. 18. At LO, ξ_2 is directly related to the momentum fraction carried by the incoming parton, such that Fig. 21 indicates the kinematic range where the H1 data can potentially improve the determination of parton distributions. Recalling the definition of ξ_2 (5.4), we moreover observe that the H1 high-Q^2 data set typically probes lower values of ξ_2 than its low-Q^2 counterpart (which is due to the transverse momentum requirement on the final-state jets, and contrasts with the kinematic correlations in inclusive DIS).

To illustrate the problematic impact of the symmetric cuts on p_T^B, combined with a cut on M_{jj}, we re-evaluated the double-differential distribution in Q^2 and ξ_2 for a different set of jet cuts: $p_{T,j1}^B > 5$ GeV, $p_{T,j2}^B > 4$ GeV. The result is shown in Fig. 22, where we observe a very substantial improvement in the perturbative convergence, compared to the cuts used in the H1 analysis [8].

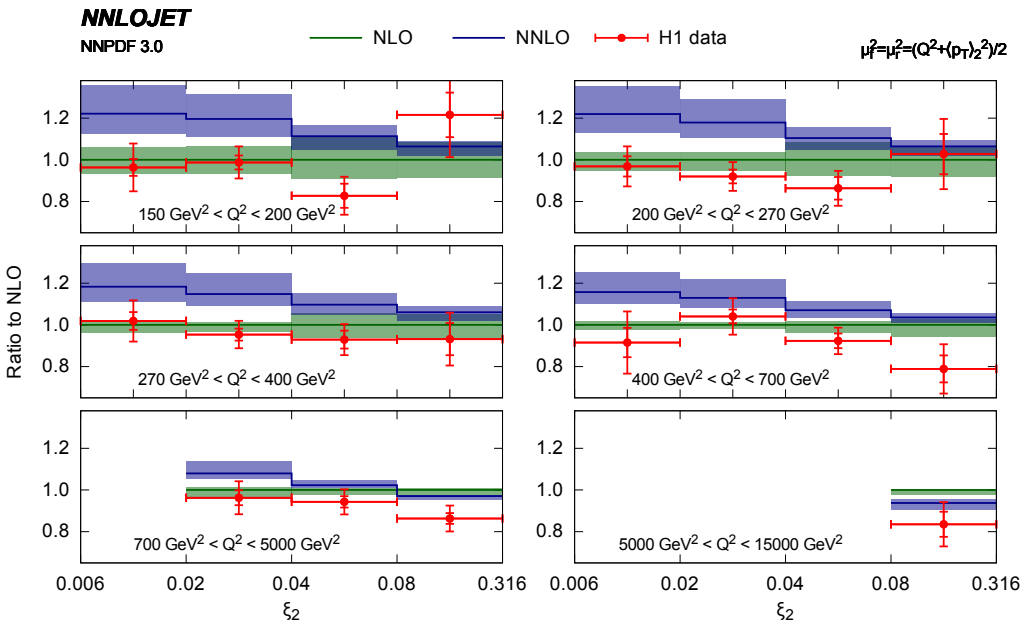

Figure 21. Inclusive di-jet production cross section as a function of ξ_2 in bins of Q^2, compared to H1 high-Q^2 data.

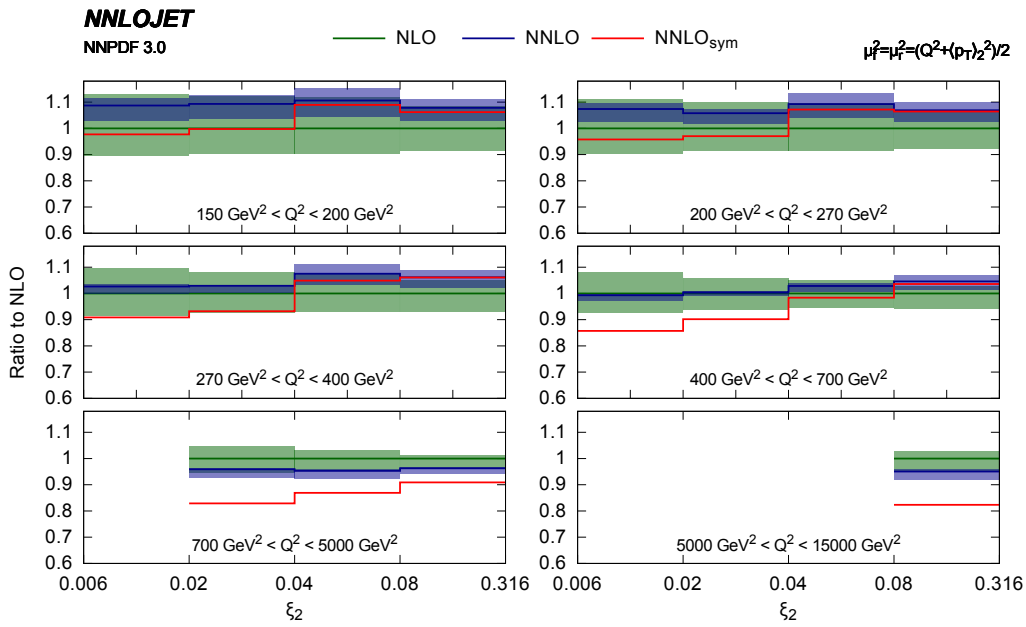

Figure 22. Inclusive di-jet production cross section as a function of ξ_2 in bins of Q^2 with asymmetric cuts on the two jets. The red line indicates the NNLO prediction with symmetric cuts of Fig. 21.

10 Diffractive di-jet production in DIS

In this section we compare our recently obtained theoretical predictions for di-jet production in diffractive electron-proton collision against five different measurements by H1 [19–23] and one by ZEUS [24] that were taken at the HERA collider at DESY. In this thesis, the following phenomenological discussion will be restricted to a smaller subset of the full results which is planned to be published as part of a separate paper in the near future. This work was performed in collaboration with D. Britzger and R. Žlebčik.

10.1 Comparision to HERA data

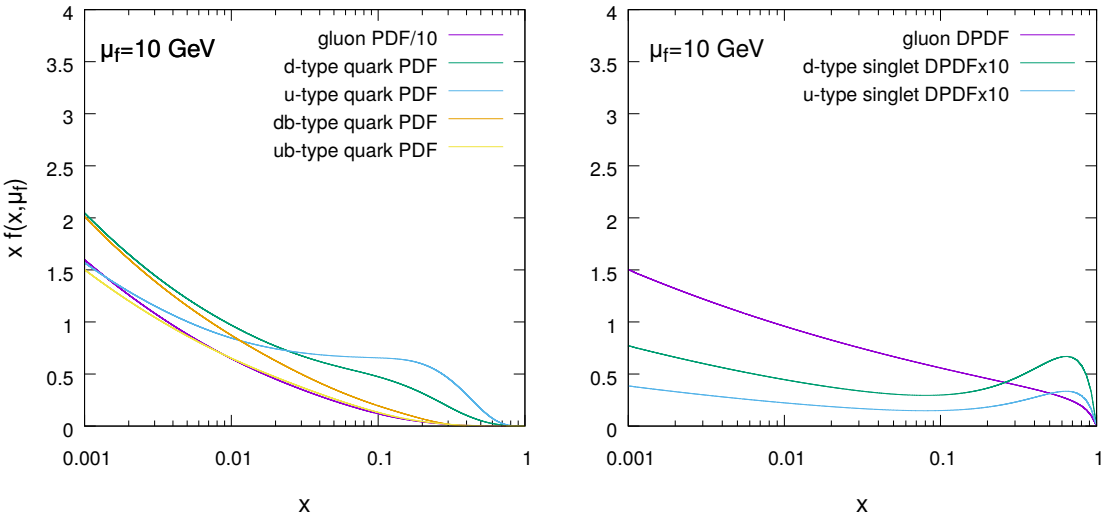

Figure 23. Plot showing a PDF taken from NNPDF3.1 [106] on the left, where the gluon distribution is divided by a factor of ten, compared to a DPDF taken from HERA 2006 Fit B [25] on the right, where the quark singlet distributions are multiplied by a factor of ten, at scale $\mu_f = 10$ GeV with $\alpha_s(M_Z) = 0.118$.

Diffractive scattering describes scattering events in which the proton only interacts via a particle with vacuum quantum number and stays intact after the collison. For diffractive scattering in DIS, the factorisation theorems were proven by Collins *et al.* [153] and allow the total cross section to be written as a partonic cross section convoluted with a diffractive PDF (DPDF). Currently, DPDFs are however only determined to NLO QCD accuracy and diffractive data has not yet been confronted with predictions at NNLO in α_s. A visualisation of a typical DPDF to a usual PDF is shown in Fig. 23, where it should be noted that only gluon and quark singlet distributions are of relevance in DPDFs due to the nature of diffractive scatterings. From the plot one can see that the gluon relative to quark content is larger in DPDFs than in canonical PDFs at typical partonic momentum fractions of $0.001 < x < 1$ in DIS. It can also be seen that each channel in the parton distribution is an order of magnitude smaller in diffractive than in canonical PDFs.

For the first time we could calculate di-jet production in diffractive DIS to NNLO QCD accuracy by using our DIS di-jet calculation to evaluate relevant hard coefficients. We com-

pare our predictions to five diffractive measurements taken by H1 and one by ZEUS which are described in more detail in Section 5. For this purpose, our calculation is performed within the five flavour scheme, using the HERA 2006 FitB DPDF at NLO accuracy [25]. Higher-order effects are estimated by a seven-point scale variation with central scale choice of $\mu_f^2 = \mu_r^2 = (Q^2 + p_{T,1}^{*})^2$ and scale factors of 0.5 and 2. With this choice of scale, appropriate scales are obtained in both kinematic limits $Q^2 \gg p_{T,1}^2$ and $Q^2 \ll p_{T,1}^2$. The setup of our calculation for diffractive scattering was verified against previous calculations performed with the nlojet++ program at NLO [18]. Our predictions are corrected for non-perturbative effects according to correction factors provided by the respective data publications. The publication by ZEUS, however, does not provide relevant correction factors and non-perturbative effects are not accounted for in corresponding predictions.

In Fig. 25 we compare the distribution in y, the energy fraction transferred by the lepton to the proton, from four different H1 measurements [19–22] to our NNLO predictions. In that figure, we also compare the distribution of the invariant mass of the photon-proton system, W^2, measured by H1 in the 820 GeV run [23] and by ZEUS [24] to our predictions. In this figure both theory and data are normalised to the value of the NLO prediction at the central scale choice. In Fig. 24 the transverse momentum distribution of the leading jet is shown for five H1 measurements and the distribution in the sum of all jet-p_T's for the ZEUS measurement.

In general, we observe only a mild reduction in the scale uncertainty going from NLO to NNLO in all distributions. This can be explained by the relatively large values of α_s at typical diffractive scales of $\mu_r^2 \sim \mathcal{O}(10)$ GeV^2 and causes a slow convergence of the perturbative series. A reassuring characteristic of our prediction, however, is that the shape of the data is better described by the NNLO than by the NLO predictions. Unfortunately, we observe that the NNLO predictions overshoot the data by approximately 30%. This seems to not be the case for the ZEUS measurement for which the predictions are, however, not corrected for non-perturbative effects.

Gluon-initiated corrections are usually more sizeable than quark-initiated corrections

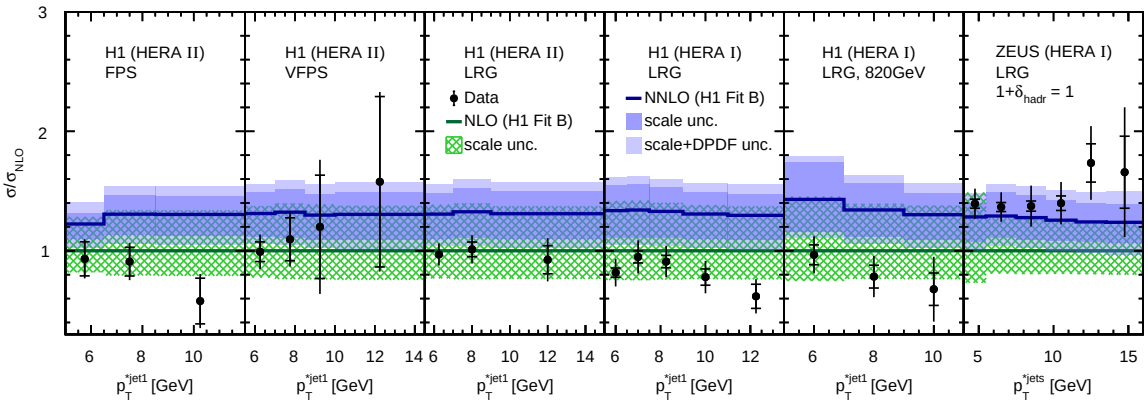

Figure 24. $p_T^{*\,\mathrm{jet1}}$ and $p_T^{*\mathrm{jets}}$, the p_T of the leading jet and inclusive jet p_T in the $\gamma^* p$-frame, distributions in diffractive DIS normalised to NLO results.

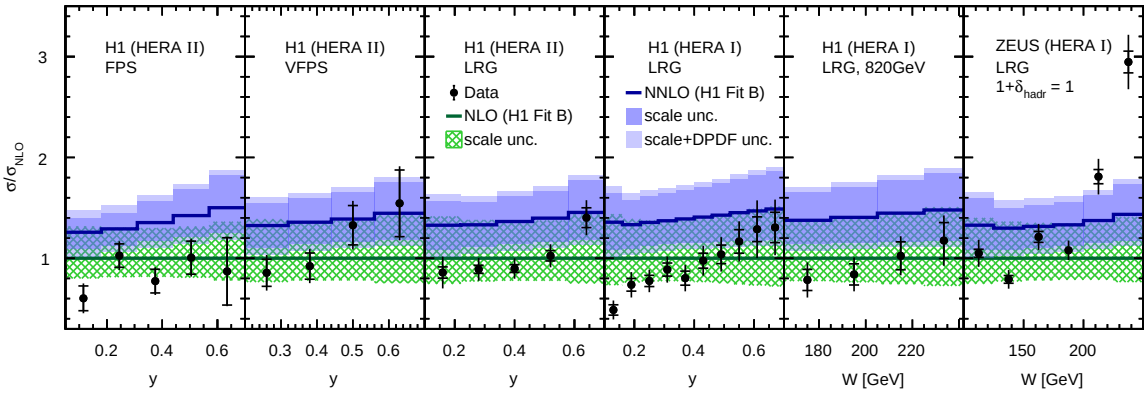

Figure 25. y and W, the proton-photon invariant mass, distributions in diffractive DIS normalised to NLO predictions.

in the hard matrix element. This can be explained by the colour factors associated with initial-state splittings, which are $C_A = 3$ and $C_F = 4/3$ for gluon to gluon-gluon and quark to quark-gluon splittings, respectively. Higher-order effects that have been missed in the NLO calculation might have been absorbed into an increased value of the gluon content in the DPDF such that these contributions are double-counted when including the NNLO correction in combination with NLO DPDFs. The nonetheless large contribution of gluons in DPDFs amplifies this effect leading to an overestimation of the predictions. For this reason, it is crucial that DPDFs are refitted at NNLO accuracy in the near future to obtain consistent results for diffrative scattering in DIS as well as for diffractive proton-proton collisions at the LHC.

11 α_s-fit from HERA data

Precision measurements, consistency tests and searches for physics beyond the SM rely on knowledge of the precise value of the strong coupling constant α_s. The value of α_s at a renormalisation scale corresponding to the mass of the Z boson $\alpha_s(M_Z)$, however, is one of the least known parameters in the Standard Model. Di-jet production in neutral current DIS is sensitive to the value of α_s. For a determination of $\alpha_s(M_Z)$, cross sections are more appropriate than related observables such as event shapes as cross sections are less sensitive to all-order effects. In the past, di-jet data from HERA has been used to extract the value of $\alpha_s(M_Z)$ [6, 8, 11]. The error on all these measurements was dominated by the theory uncertainty inherent to the NLO predictions used in the extraction. This uncertainty was found to be typically a factor of two or more larger than experimental statistical or systematical uncertainties, thereby proving to be the limiting factor to further improving $\alpha_s(M_Z)$ measurements from jet production in DIS. Using the recently implemented bridge code to the APPLfast program in NNLOJET, we can use our fixed-order predictions for inclusive jet and di-jet production in the Breit frame to perform a first fit of $\alpha_s(M_Z)$ from HERA data to NNLO accuracy. In this section a short summary of the method and first results will be given. More detailed results and in-depth discussion will be jointly published with the H1 collaboration in a separate paper in the near future.

11.1 Method and numerical results

For our $\alpha_s(M_Z)$-fit from H1 di-jet data, we use one measurement from the HERA-($\sqrt{s}$ = 300 GeV) run [154], one measurement from the HERA-I run [155] and two measurements

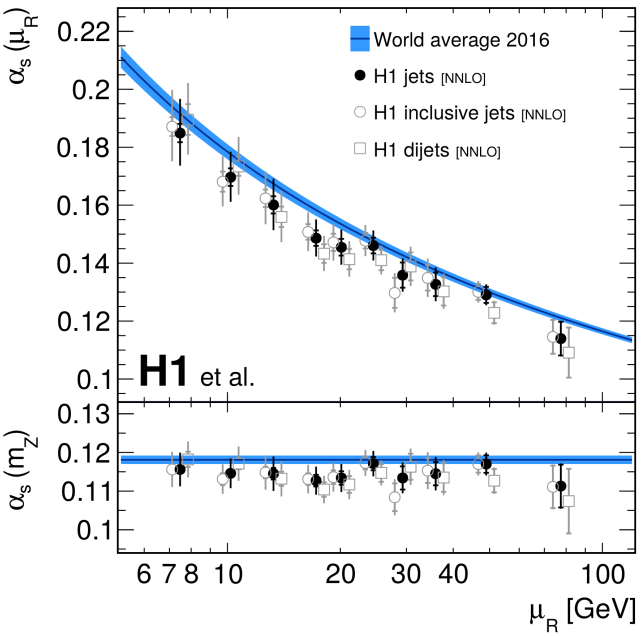

Figure 26. Running of the strong coupling constant α_s as obtained from our fit to H1 data.

from the HERA-II run [8, 9] period. All of the mentioned measurements also recorded inclusive single-jet events in the Breit frame. To fit $\alpha_s(M_Z)$ from inclusive single-jet data, the list of measurements was extended by one more measurement taken in the HERA-I run period [6]. For the combined fit from di-jet and inclusive jet data, summarised as "H1 jets", the di-jet measurements from the HERA-I run are not included as statistical correlations to the respective inclusive jet data is unknown.

The hard coefficients for the theory prediction are calculated using our implementation of DIS di-jet production in NNLOJET with central scale choice of

$$\mu_r^2 = \mu_f^2 = Q^2 + p_T^2\,, \tag{11.1}$$

where for di-jet production $p_T = \langle p_T \rangle_2$ and for single-jet inclusive production in the Breit frame one has $p_T = p_T^{jet}$, which is the individual jet p_T. This choice of scale provides a hard scale in both limits of $Q^2 \to 0$ GeV^2 and $p_T^2 \ll Q^2$. The running of the electromagnetic coupling is evaluated using the EPRC package [156].

In general, both the hard coefficient and the PDF depend on the value of $\alpha_s(M_Z)$. This dependence can be explicitly written as

$$\sigma_i = f_i\left(\alpha_s(M_Z)\right) \otimes \hat{\sigma}_i(\alpha_s(M_Z)) \cdot c_{had,i}\,, \tag{11.2}$$

where i labels the initial state and $c_{had,i}$ are non-perturbative corrections that are given in the respective data publications. Taking the initial values of the PDF to be the same, a shift of the reference value of $\alpha_s(M_Z)$ inside the PDF to $\bar{\alpha}_s(M_Z)$ can be compensated by a shift of the factorisation scale. Explicitly, the PDF at the original value of $\alpha_s(M_Z)$, f, is related to the one with the shifted value $\bar{\alpha}_s(M_Z)$, $\bar{f}$, by

$$\bar{f}(\mu_f) = f(\sqrt{K}\mu_f)\,, \tag{11.3}$$

with

$$\sqrt{K} = \exp\left[\frac{1}{2}\int_{\alpha_s(M_Z)}^{\bar{\alpha}_s(M_Z)} \frac{\mathrm{d}\alpha_s'}{\beta(\alpha_s')}\right]\,. \tag{11.4}$$

The evolution of PDFs from their initial values in NNLO is evaluated with the QCDNUM package using five active flavours. As an input PDF we use the NNPDF3.1 PDF [106] obtained at $\alpha_s(M_Z) = 0.118$ and at a scale of $\mu_0 = 30$ GeV. Theoretical predictions can then be fitted to the experimental measurements using $\alpha_s(M_Z)$ as the only free parameter. For each data point i the corresponding theoretical prediction is calculated at a central scale

$$\tilde{\mu}_i^2 = Q_{avg,i}^2 + p_{T,avg,i}^2\,, \tag{11.5}$$

where Q_{avg}^2 and $p_{T,avg}^2$ are logarithmic averages of the corresponding values at the bin edges [low,up] defined by

$$\log {Q_{avg,i}^2}^2 = \left(\log {Q_{low,i}^2}^2 + \log {Q_{up,i}^2}^2\right)/2, \quad \log {p_{T,avg,i}^2}^2 = \left(\log {p_{T,low,i}^2}^2 + \log {p_{T,up,i}^2}^2\right)/2\,. \tag{11.6}$$

Only data points for which $\tilde{\mu}_i > 2m_b$, where m_b is the mass of the bottom quark, are used to justify the application of NNLO calculations in the five flavour scheme for the fit. By minimising the goodness-of-fit quantity

$$\chi^2 = \sum_{i,j} \log \frac{\xi_i}{\sigma_i} \left(V_{\text{exp}} + V_{\text{had}} + V_{\text{PDF}}\right)^{-1}_{ij} \log \frac{\xi_j}{\sigma_j}\,, \tag{11.7}$$

using the the TMinuit algorithm [157, 158], a best fit value for $\alpha_s(M_Z)$ is found. In Eq. (11.7), the sum is over all data points (ξ_i), and the Vs are the covariance matrices for the experimental (exp), PDF (PDF) and hadronisation correction (had) errors.

The fit is repeated for different choices of $\tilde{\mu}_{cut}$ such that $\tilde{\mu}_{cut} < \tilde{\mu}_i$. For a value of $\mu_{cut} = 28$ GeV we obtain a value of

$$\alpha_s(M_Z) = 0.1152(20)_{\text{exp}}(26)_{\text{th}} \tag{11.8}$$

for a fit to the single inclusive jet data set and a value of

$$\alpha_s(M_Z) = 0.1147(24)_{\text{exp}}(24)_{\text{th}} \tag{11.9}$$

for a fit to the di-jet data set. In the above, the theoretical uncertainty is given by the quadratic sum of PDF, PDFα_s, PDFset, and scale uncertainties. The PDF uncertainties are the usual PDF uncertainties that come with individual PDFs. The PDFset uncertainty is given by half of the maximal difference between results obtained when repeating the fit with ABMP, CT14, HERAPDF2.0 and MMHT PDF sets and the PDFα_s uncertainty is obtained when repeating the fit with a choice of $\alpha_s'(M_Z) = \alpha_s(M_Z) \pm 0.002$ as $\alpha_s(M_Z)$-input to the PDF. For theoretical uncertainties, the scale uncertainty is by far the most dominant. Both fits exhibit good values for $\chi^2/\text{n}_{\text{dof}} \sim 1.0$, where n_{dof} is the degrees of freedom in the fit, showing an overall consistency between theoretical predictions and measurements.

Finally, for the combined "H1 jets" data set, restricted to $\tilde{\mu}_i > 28$ GeV, one gets

$$\alpha_s(M_Z) = 0.1156(19)_{\text{exp}}(6)_{\text{had}}(3)_{\text{PDF}}(1)_{\text{PDF}\alpha_s}(3)_{\text{PDFset}}(25)_{\text{scale}}. \tag{11.10}$$

All obtained results for $\alpha_s(M_Z)$ are consistent with, but somewhat lower than the world average. Repeating the fit for bins in $\tilde{\mu}_r$, the running of the strong coupling constant can be tested. Results for single-jet, di-jet and the combined "H1 jets" is shown in Fig. 26.

12 DIS single-jet production in the laboratory frame at N3LO

In this section we present our recent results for DIS single-jet production in the laboratory frame to N3LO. To obtain the following results, the method of Projection-To-Born was combined with our NNLO di-jet calculation using the antenna subtraction method. A publication on these results is in preparation.

12.1 Method of Projection-to-Born

In case of single-jet production in DIS, the method of Projection-To-Born (P2B) exploits the fact that the Born kinematics of the leading-order process is entirely fixed by the knowledge of Bjorken's x variable and momentum q of the exchanged vector boson. One can therefore define a mapping which, starting from any momentum set of partonic final-state multiplicity n, maps onto to the Born kinematics of partonic final-state multiplicity of one. This mapping $\{p\}_n \to \{p\}_1$ is then given by

$$\begin{aligned} \{p\}_n &\to \{p_{in}; p_{out}\}\,, \\ p_{in} &= xP\,, \\ p_{out} &= xP - q\,, \end{aligned} \tag{12.1}$$

for any $n > 1$ where P is the incoming proton's momentum. In the above it has been used that for jet production at $\mathcal{O}(\alpha_s^0)$ in DIS, Bjorken and Feynman x coincide as can be deduced from Eq. (2.35). Thus once the leptonic kinematics are known, each event can be uniquely mapped onto its Born kinematics by Eq. (12.1), independently of the event's final-state particle multiplicity.

Using the P2B method, knowledge of the inclusive structure function at NNLO differential in Q^2 and x together with a prediction for fully differential NLO di-jet production was used to evaluate the fully differential NNLO single-jet production cross section using the method in Ref. [72]. Analogously, if the perturbative order in α_s is increased, knowledge of the structure function at N3LO can be used together with a prediction of di-jet production at NNLO to evaluate the fully differential single-jet production cross section at N3LO.

The N3LO contributions to single-jet production in DIS are the real-real-real (RRR), real-real-virtual (RRV), real-virtual-virtual (RVV) and virtual-virtual-virtual (VVV) corrections. With a differential subtraction procedure, in our case the antenna subtraction method, di-jet production can be evaluated to NNLO accuracy. If however yet another particle is unresolved and a single-jet is produced, NNLO di-jet subtraction fails to subtract the emerging singularity. In the P2B method, the extra real radiation is subtracted by the manual construction of a counter event that has the same weight as the NNLO di-jet contributions, but is booked differentially into histograms at Born kinematics. In case of phase space configurations resulting in the production of a single jet, Born and single-jet kinematics exactly coincide, leading to a cancellation of the problematic infrared singularities between the corrections and the counter event. When integrated over the entire phase space, the manually constructed counter events are equal to the RRR, RRV and RVV contributions in the calculation of the inclusive single-jet cross section, but come with opposite

sign. If then the inclusive single-jet cross section, projected to Born kinematics, is added as a contribution, the RRR, RRV and RVV contributions cancel and only the missing VVV contribution remains, leading to a result that is fully differential in all jet variables. The subtraction method applied to single-jet production at N3LO can schematically be expressed in the following way:

$$\begin{aligned}\hat{\sigma}^{\mathrm{N3LO}} = &\int_{\mathrm{d}\Phi_4} \left[\mathrm{d}\hat{\sigma}^{RRR} - \mathrm{d}\hat{\sigma}^{S}_{\mathrm{dijet}}\right] - \left[\int_{\mathrm{d}\Phi_4} \mathrm{d}\hat{\sigma}^{RRR} - \mathrm{d}\hat{\sigma}^{S}_{\mathrm{dijet}}\right]_{\mathrm{P2B}} \\ &+ \int_{\mathrm{d}\Phi_3} \left[\mathrm{d}\hat{\sigma}^{RRV} - \mathrm{d}\hat{\sigma}^{T}_{\mathrm{dijet}}\right] - \left[\int_{\mathrm{d}\Phi_3} \mathrm{d}\hat{\sigma}^{RRV} - \mathrm{d}\hat{\sigma}^{T}_{\mathrm{dijet}}\right]_{\mathrm{P2B}} \\ &+ \int_{\mathrm{d}\Phi_2} \left[\mathrm{d}\hat{\sigma}^{RVV} - \mathrm{d}\hat{\sigma}^{U}_{\mathrm{dijet}}\right] - \left[\int_{\mathrm{d}\Phi_2} \mathrm{d}\hat{\sigma}^{RVV} - \mathrm{d}\hat{\sigma}^{U}_{\mathrm{dijet}}\right]_{\mathrm{P2B}} \\ &+ \left[\hat{\sigma}^{N3LO}_{\mathrm{incl}}\right]_{\mathrm{P2B}} , \end{aligned} \tag{12.2}$$

where $\mathrm{d}\hat{\sigma}^{S}_{dijet}$, $\mathrm{d}\hat{\sigma}^{T}_{dijet}$ and $\mathrm{d}\hat{\sigma}^{U}_{dijet}$ are the DIS di-jet subtraction terms discussed in Section 7 and $\left[\hat{\sigma}^{N3LO}_{\mathrm{incl}}\right]_{P2B}$ is the fully inclusive jet N3LO coefficient in DIS projected to Born kinematics. The last terms in each line on the right-hand side represent the counter events that are projected to Born kinematics according to Eq. (12.1). The cancellation of RRR, RRV and RVV contributions between contributions from the counter events and the projected inclusive cross section occurs according to

$$\begin{aligned}\hat{\sigma}^{VVV} = &\left[\hat{\sigma}^{N3LO}_{\mathrm{incl}}\right]_{\mathrm{P2B}} - \left[\int_{\mathrm{d}\Phi_4} \mathrm{d}\hat{\sigma}^{RRR} - \mathrm{d}\hat{\sigma}^{S}_{\mathrm{dijet}}\right]_{\mathrm{P2B}} \\ &- \left[\int_{\mathrm{d}\Phi_3} \mathrm{d}\hat{\sigma}^{RRV} - \mathrm{d}\hat{\sigma}^{T}_{\mathrm{dijet}}\right]_{\mathrm{P2B}} - \left[\int_{\mathrm{d}\Phi_2} \mathrm{d}\hat{\sigma}^{RVV} - \mathrm{d}\hat{\sigma}^{U}_{\mathrm{dijet}}\right]_{\mathrm{P2B}} . \end{aligned} \tag{12.3}$$

The inclusive DIS cross section at N3LO was calculated by Moch, Vermaseren and Vogt and is given in Refs. [73, 74]. Results presented therein are however only available for scale choices of $\mu_f = \mu_r$. Hence, to realise the calculation of fully differential N3LO jet production in DIS, the N3LO scale dependence of the cross section had to be implemented according to Eq.(2.16) of Ref. [159].

We validated our implementation of the P2B method by comparing distributions for single-jet production in DIS at NNLO between results obtained from the antenna and from the P2B method. Results are shown in Fig. 27, where we compare transverse momentum p_T and rapidity η distributions of the leading jet using a seven-point scale variation with central scale choice of $\mu_f^2 = \mu_r^2 = Q^2$, independently varying μ_r and μ_f up and down by factors $[0.5, 2]$ and discarding the two most extreme combinations. In this calculation, the JADE algorithm was used to find jets as described in Section 2.4 and we obtain very good agreement between the two methods. In using the P2B method, it turns out that adaption of the vegas algorithm to the total cross section might be problematic. This is because the counter event has exactly the same weight as the differential di-jet contribution by construction such that if both, the di-jet and the projected to Born phase space, pass the jet cuts, a zero-weight event is returned. Consequently, even if Born and di-jet kinematics

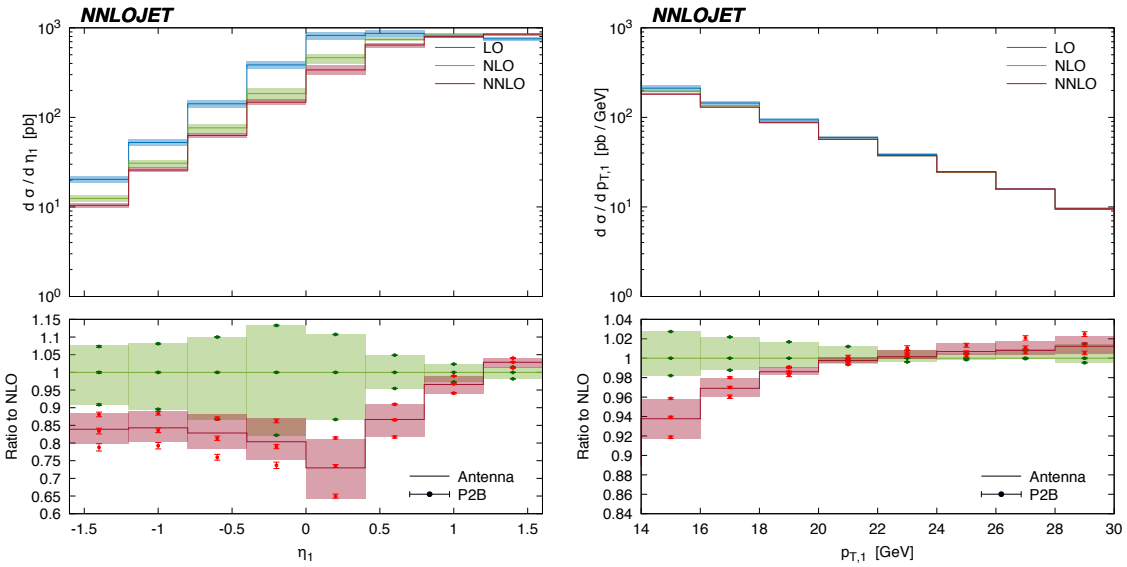

(a) Pseudo-rapidity of the leading jet, η_{j1}. (b) Leading jet's transverse momentum, $p_{T,j1}$.

Figure 27. Comparison of results to NNLO as obtained with the P2B compared to the antenna subtraction method.

are different on a differential level, vegas adaption based on the total cross section fails and causes a problem in particular for very inclusive experimental cuts. A solution can be provided by changing the vegas–return-weight to the total cross section re-weighted by a factor y_{12}^n, where y_{12} is the JADE y_{cut} value for which an event transitions from a two-jet to a one-jet event and $n \geq 1$. For the projected counter events y_{12} is zero and in any unresolved limit of the di-jet phase space going down to a single-jet, y_{12} tends to zero fast enough such that $\sigma \cdot y_{12}^n$ is integrable. As a result, we adopted the vegas algorithm to a re-weighted cross section throughout our calculations when using the P2B method.

12.2 Comparison to HERA data

Single-jet measurements in the laboratory frame were measured by the ZEUS collaboration [145]. In this analysis 820 GeV protons were collided with 27.5 GeV electrons and the JADE clustering algorithm was used in the four-vector recombination scheme to reconstruct jets. The measurements were taken for the following kinematic cuts:

$$\begin{aligned} 160 < Q^2 < 1280\text{GeV}^2\,, \\ 0.01 < x < 0.1\,, \\ 0.04 < y < 0.95\,. \end{aligned}$$

In this particular measurement, the two-jet rate is defined as

$$R_{2+1} = \frac{N_{2+1}}{N_{2+1} + N_{1+1}}\,. \tag{12.4}$$

In the above N_{1+1} and N_{2+1} are the number of recorded (1+1)- and (2+1)-jet events, where the extra +1 denotes the beam jet. The normalisation is chosen such that

$$R_{1+1} \equiv 1 - R_{2+1}\,, \tag{12.5}$$

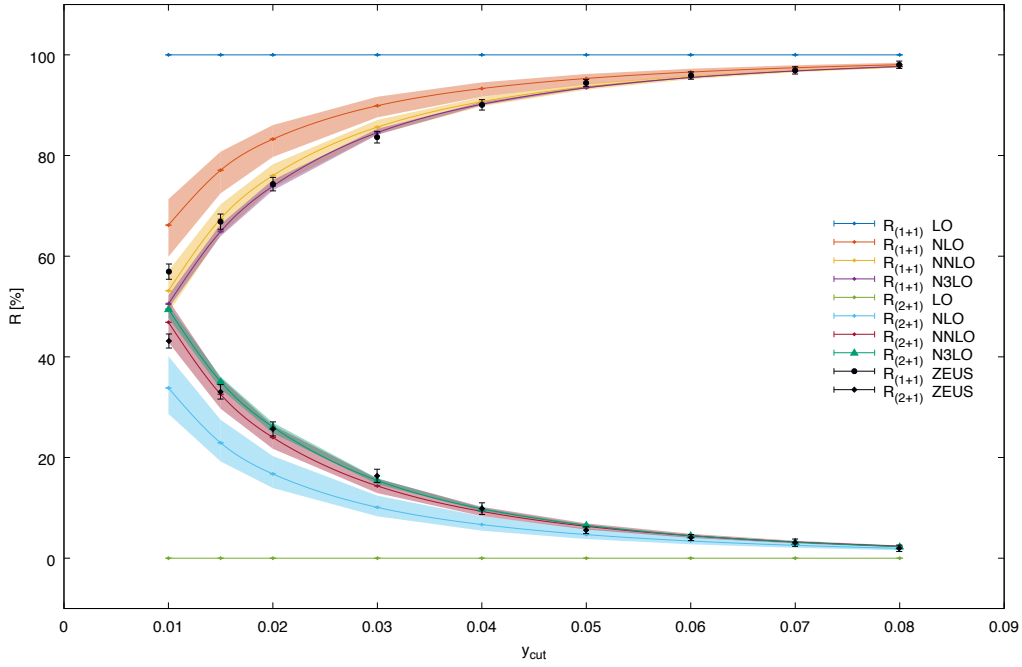

Figure 28. Comparison of ZEUS data [145] to theoretical predictions up to N3LO in QCD for two-jet and single-jet rates, normalised according to Eq. (12.5). Data are corrected to give parton level results.

which is different from the usual convention to normalise to the total hadronic cross section.

Currently PDFs fitted to N3LO accuracy are not available such that presented results are obtained using the NNLO NNPDF3.0 set with $\alpha_s(M_Z) = 0.118$ and a comparison of experimental results to our N3LO prediction as a function of y_{cut} is shown in Fig. 28. In that plot, scale uncertainties of the theoretical prediction were estimated using a seven-point variation with central scale choice of $\mu_r^2 = \mu_f^2 = Q^2$. It can be seen that the N3LO corrections result in a reduction of scale uncertainties. As the value of y_{cut} is lowered, less of the final-state radiation is clustered and more partonic radiation resolved. As a result, the fractions of one- and two-jet events approach each other for lower values of y_{cut}. The low y_{cut}-region is also where the largest scale dependence is observed. At N3LO however, the scale bands start to overlap in the low-y_{cut} region for the first time. We also calculated jet rates not restricted to the unusual normalisation in Eq. (12.5) such that also three- and four-jet rates could be evaluated and results for this are shown in Fig. 29. In Fig. 29, similar features as in the normalised jet rates can be observed, but also that the fractions of one- and two-jet events dominate events with higher jet-multiplicity by at least an order of magnitude.

This calculation provides a first proof of concept for calculations with the P2B method at N3LO and in principle, theoretical predictions for further measurements by H1 and E665 [27, 28, 146] could be reproduced. The P2B method might be used in the near future to evaluate more processes at N3LO accuracy in particular in proton-proton collisions.

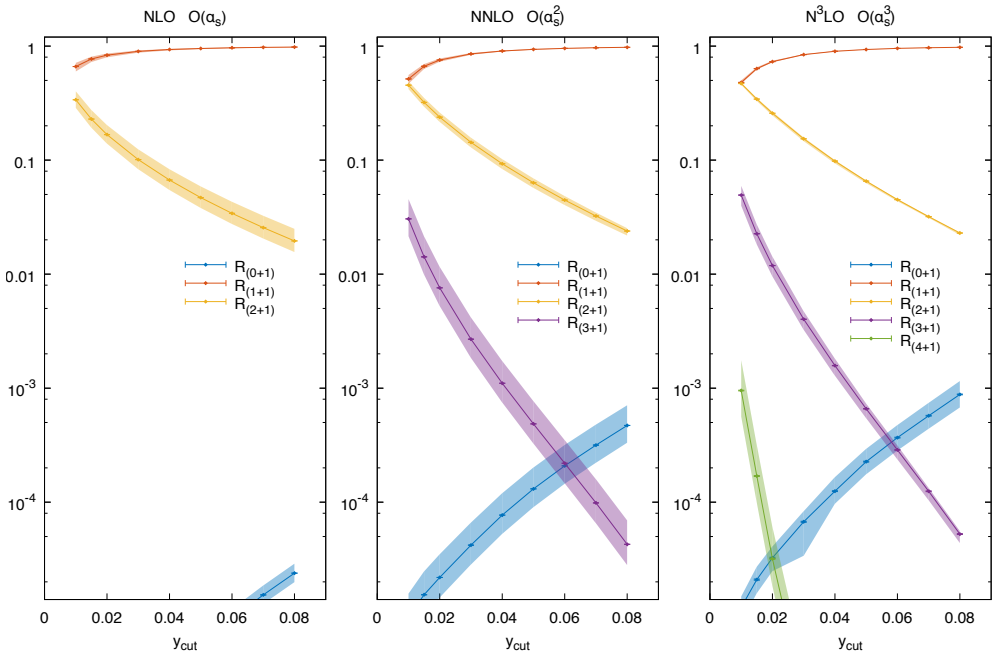

Figure 29. Predictions up to N3LO in QCD for single-, di-, tri- and four-jet rates for ZEUS' experimental cuts [145].

13 Tri-jet production in e^+e^- collisions

In this section we present our recent results on the production of hadronic final states in electron-positron annihilation. This class of processes offers a unique laboratory for testing the theory of the strong interaction, QCD, at high energies. Previously, calculations of $e^+e^- \to 3j$ annihilation were presented in the work of [52, 53, 126], all of which, however, only consider the gauge (Z/γ^*) decay, thereby neglecting the angular correlations with the initial state leptons. A publication on presented results is in preparation.

13.1 Measurements of hadronic final states in e^+e^--annihilation

Experiments at LEP and SLD have collected a wealth of precision data on jet cross sections and event shape distributions [29–33]. The calculation of NNLO corrections to three-jet production and related event shape observables [52, 53] allows us to confront these data with precise predictions, and enabled a variety of precision QCD studies [161].

The LEP and SLC measurements of event shapes and jet cross sections [29–33] were corrected to a full 4π acceptance. They do not depend on the angular correlation between the final-state hadrons and the incoming electron-positron direction. Measurements of fiducial cross sections (restricted to the actual acceptance of the detector) are typically not available. An indication of the quality of the extrapolation to full 4π acceptance can however be gained from studying event orientation variables, which describe the angular correlation between the hadronic final state and the incoming beam direction. Relevant event orientation variables have recently been calculated with our new implementation within NNLOJET.

13.2 Validation

For the calculation of $e^+e^- \to 3j$, the relevant matrix elements correspond to different kinematic crossings of the ones already used in the $Z + j$ [140–142] and DIS jet production processes. The structure of the antenna subtraction terms for these matrix elements is documented in detail in Ref. [162]. We validated the new implementation against EERAD3 [87] for the canonical set of LEP event shapes and jet cross sections. While the EERAD3 implementation [87] was based on the matrix elements for virtual photon decay $\gamma^* \to q\bar{q}g$ (and higher-order corrections to it), NNLOJET now contains the full $e^+e^- \to q\bar{q}g$ matrix elements through to NNLO. It therefore allows to account for the correlation between the final-state parton directions and the incoming electron and positron beams properly.

13.3 Numerical results

Three-particle (or three-jet) production in the e^+e^- centre-of-momentum frame always results in a final state with momenta in a plane, due to momentum conservation. The orientation of this event plane with respect to the initial state is described by three Euler angles: (Θ, Θ_N, χ) [163]. Taking the event plane in (x, z) and using the highest energy final-state object to define the z-axis, the incoming electron direction is defined through the polar angle Θ and the azimuthal angle χ. The third angle Θ_N is then formed from the

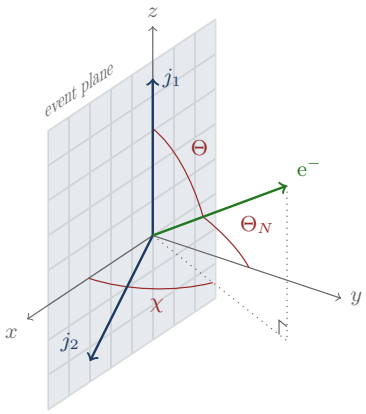

Figure 30. Definition of the three Euler angles defining the event orientation. j_1 denotes the highest energy jet, j_2 the subleading jet.

electron direction and the event plane normal. The choice of coordinate system and the definition of the angles is displayed in Fig. 30.

For three-jet final states, event orientation distributions were measured initially by TASSO [164], and subsequently by DELPHI [165], L3 [166] and SLD [167]. In all measurements, the JADE algorithm was used to identify the final-state jets, and one-dimensional distributions in Θ, Θ_N or χ were measured. These measurements were compared with the leading-order, leading-logarithmic multi-purpose event generator simulations HERWIG [168] and JETSET/PYTHIA [169], which all provided a very good description of the data. This observation motivates the use of these simulation programs to extrapolate the canonical event shape and jet cross sections measurements to full 4π acceptance.

For this procedure to be reliable, it is however vital that the shapes of the leading-order event orientation distributions are not distorted by higher-order QCD corrections. Surprisingly enough, this issue has never been investigated in a systematic manner. By using an approximation to the real radiation contributions, NLO QCD corrections to event orientation were estimated to be small in Ref. [170]. Comparing the JETSET predictions with exact real radiation matrix elements and parton shower approximation, SLD [167] attempted to quantify the potential magnitude of real radiation effects at NLO, which were found to be of moderate impact.

With the NNLOJET implementation of jet production in e^+e^- annihilation, we are able to compute the NLO and NNLO corrections to the event orientation distributions. We consider the kinematic situations that were investigated by L3 [166] and SLD [167], which provide more precise measurements than in the earlier studies. Both experiments perform their measurements on an exclusive three-jet sample. The jets are identified using the JADE algorithm [171], with a range of resolution parameters y_{cut} for L3, and for fixed $y_{\text{cut}} = 0.02$ for SLD. The distributions in (Θ, Θ_N, χ) are normalised to the three-jet cross section, such that they all integrate to unity by construction. Besides cancelling potential sources of systematic uncertainty, this normalisation condition makes the theoretical predictions at leading order independent of α_s. Consequently, the variation of the renormalisation scale

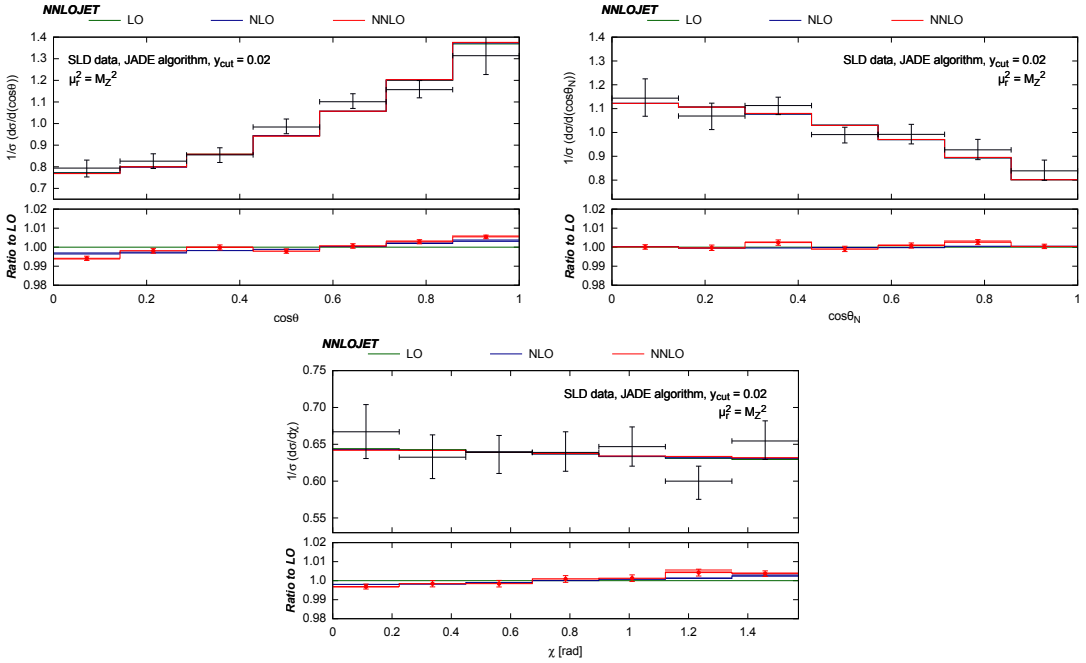

Figure 31. Event orientation distributions for three-jet events (JADE algorithm, $y_{\rm cut} = 0.02$), compared to SLD data [167].

will not necessarily be a good proxy for the potential impact of higher-order corrections, and one should rather look order-by-order into the relative size of the corrections.

The experimental data have all been corrected to 4π acceptance, with SLD [167] also providing the uncorrected data. By comparison, it can be seen that the corrections affect the event orientation distributions only for $\cos(\Theta) \gtrsim 0.7$, $\cos(\Theta_N) \lesssim 0.7$, $\chi \lesssim \pi/4$. These can be identified from Fig. 30 as the regions where the event plane comes close to the beam direction, such that the final-state particles can be partly outside the detector coverage.

Fig. 31 displays the event orientation distributions at LO, NLO and NNLO for exclusive three-jet events and compares them to the SLD data [167]. The error bands on the NLO and NNLO predictions are obtained by varying the renormalisation scale in the strong coupling constant within a factor $[1/2; 2]$ around the central scale $\mu_R = M_Z$. We observe that the perturbative corrections modify the leading-order shape of the distributions only at the level of four per-mille at NLO and at most one per-cent at NNLO. The corrections are most pronounced in $\cos(\Theta)$, where they modify the slope of the distribution, and are even smaller in χ and $\cos(\Theta_N)$.

The L3 experiment measured the event orientation distributions for two ranges in exclusive three-jet events (using the JADE algorithm). Results are given for two jet resolutions: $0.02 \leq y_{\rm cut} \leq 0.05$ (fine jet resolution) and $y_{\rm cut} = 0.25$ (coarse jet resolution). The application of a range in $y_{\rm cut}$ instead of a fixed value is uncommon and requires further explanation: events are classified as three-jet final states if and only if they yield a three-jet final state for all values of $y_{\rm cut}$ in the interval. Since the JADE algorithm yields a monotonic increase in jet multiplicity with decreasing resolution parameter, it is sufficient

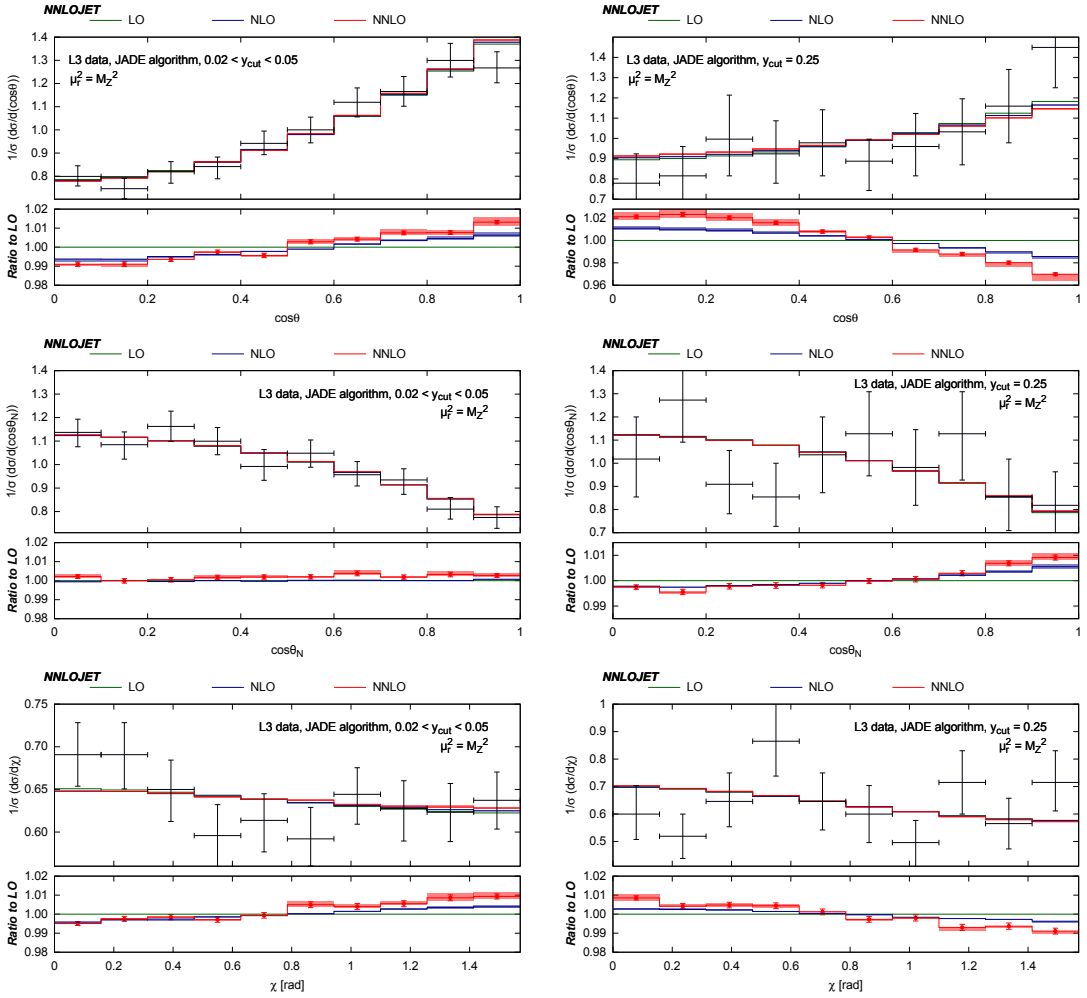

Figure 32. Event orientation distributions for three-jet events (JADE algorithm) compared to L3 data [166]. Left: $0.02 \leq y_{\text{cut}} \leq 0.05$), right: $y_{\text{cut}} = 0.25$.

to find a three-jet final state for both the upper and lower edge of the y_{cut} interval. The event orientation distributions for both values of jet resolution parameters at LO, NLO and NNLO (with error bands defined as above for SLD) are shown in Fig. 32, where they are compared to data from L3 [166]. For the fine jet resolution, we observe a pattern that is very similar to what we saw for SLD, with corrections at the level of at most one per-cent throughout. For the coarse jet resolution, we observe that the corrections to the $\cos(\Theta)$ distribution increase to a maximum of two per-cent at NNLO, and that the slope of the corrections to the $\cos(\Theta)$ and χ distributions is inverted compared to the fine jet resolution.

For all distributions, we observe that the scale variation bands at NLO and NNLO do not overlap and that their size increases from NLO to NNLO. Given that the distributions are normalised such that they become independent of α_s at leading order, scale variation should not be considered a good indicator of residual theoretical uncertainty from missing higher-orders for these particular observables. The small absolute magnitude of the correc-

tions both at NLO and NNLO is however a strong indicator for the perturbative stability of the event orientation distributions.

Compared to previous implementations, we retain the full dependence on the initial-state lepton kinematics, which allows us to compute fiducial cross sections and event orientation distributions. The latter are particularly relevant in view of precision measurements of event shapes and cross sections at LEP and SLD. In these, results were typically extrapolated from the actual measurements done with restricted detector acceptance to full 4π acceptance, using leading-order multi-purpose event simulation programs. By computing the NLO and NNLO corrections to the event orientation distributions, we can now quantify the impact of higher-order QCD effects on these extrapolations. We find that the event orientation distributions are extremely robust under QCD corrections. For fine jet resolution (where the bulk of precision QCD studies is performed), the corrections up to NNLO modify the distributions up to at most one per-cent. By going to more coarse jet resolution, the magnitude of the corrections increases slightly to two per-cent, and the slopes of the corrections in some of the distributions are inverted. Our findings support the validity of the acceptance correction procedure applied in precision QCD studies at LEP and SLD. When aiming for per-mille level precision in QCD measurements at a future Z factory, these corrections will become of relevance, and concentrating on measurements and interpretation of fiducial cross sections should be considered, instead of extrapolating to full acceptance.

14 Conclusions

In this thesis, we described the calculation of higher-order QCD corrections to jet production in DIS. By defining jets in the Breit frame of reference, single-jet events in the laboratory frame can be excluded from experimental analyses. Remaining single-jet and di-jet systems in the Breit frame start both at the same perturbative order and provide sensitivity on the gluon distribution and the strong coupling constant already at leading order.

Our calculation uses the antenna subtraction method to cancel infrared singularities among parton-level sub-processes of different multiplicity. Our calculation is implemented into the NNLOJET parton-level event generator framework, which was also used recently for the NNLO corrections to $pp \to Z + j$ [62], $pp \to H + j$ [60] and $pp \to 2j$ [69].

The HERA experiments H1 and ZEUS have measured inclusive single-jet and di-jet production over a broad kinematic range. We observe that the NNLO corrections to inclusive single-jet production modify the shape of the kinematic distributions, which are now described considerably better than at NLO. The corrections are moderate in size (ten to twenty per-cent) except for very low jet transverse momenta or low photon virtuality Q^2, and their inclusion substantially reduces the scale uncertainty on the predictions, typically well below the experimental statistical and systematical uncertainty.

The NNLO corrections to di-jet production are found to be sizeable, and often well outside the scale uncertainty band of the NLO predictions over a broad kinematic range for most data sets from ZEUS and H1. We could relate [152] this behaviour to the interplay between the cuts on the jet transverse momentum and di-jet invariant mass, which overly restricts the final-state phase space at LO and NLO. Further evidence for this argument is provided by performing dedicated comparisons of the predictions with and without invariant mass cuts, with the latter displaying much-improved perturbative convergence and reduced scale uncertainty. Only one H1 di-jet data set (low-Q^2 [9]) was measured without the invariant mass cut; this data set is well-described by the NNLO theory.

We further applied our calculation of di-jet and inclusive jet production in the Breit frame with the help of the recently developed APPLfast code to extract a value of the strong coupling constant α_s at the renomalisation scale corresponding to the mass of the Z boson to NNLO QCD accuracy. We found the data to be in good agreement with our theoretical predictions. This is expressed in terms of $\chi^2/n_{\text{dof}} \sim 1.0$ for the global fit. Our final result from inclusive and di-jet data in the Breit frame can be summarised as

$$\alpha_s(M_Z) = 0.1156(19)_{\text{exp}}(6)_{\text{had}}(3)_{\text{PDF}}(1)_{\text{PDF}\alpha_s}(3)_{\text{PDFSet}}(25)_{\text{scale}}, \tag{14.1}$$

with similar sized experimental and theoretical errors. Given that previous analyses of inclusive DIS structure function data typically yield values of α_s at the lower boundary of the range indicated by previous determinations [172], we find this trend for DIS data to be confirmed by our result.

The determination of parton distributions at NNLO from a global fit is currently dominated by processes that are only quark-initiated at leading order (inclusive DIS, Drell-Yan processes). Constraints on the gluon distribution come mainly from indirect effects

(scaling violations) or from the inclusion of data from processes (like jet production) where the full NNLO corrections are unknown. In these cases, the NNLO corrections to the hard process cross sections are either approximated using some ad hoc assumptions or discarded altogether. A recent study [173] on the impact of LHC inclusive top quark cross section data on the determination of the gluon distribution illustrated the importance of a consistent treatment of NNLO effects (which are known for top quark production [57, 58]). Our newly derived NNLO corrections to jet production in DIS enable the consistent inclusion of HERA data on this process into global parton distribution fits at NNLO. The magnitude of the corrections, as well as their kinematic dependence, makes it likely that their inclusion will lead to modifications of the gluon distribution, also leading to a substantial reduction of its uncertainty in the crucial region of medium-x.

For di-jet production in diffractive scattering in DIS, we found that NNLO predictions describe the shape of distributions much better than corresponding NLO predictions. NNLO predictions for the hard coefficients, however, overestimate diffractive cross section by approximately 30% when combined with diffractive PDFs that are only determined to NLO accuracy. In this context, it will be very interesting to see whether a fit of diffractive PDFs to NNLO accuracy can resolve this issue. Diffractive PDFs fitted to NNLO QCD accuracy might then be tested in a different collider environment such as in proton-proton collisions at the LHC, to check for consistency in the theoretical description of diffractive scatterings.

For the first time, we found consistency between results evaluated with the Projection-To-Born method and with the antenna subtraction formalism for single-jet production in DIS to NNLO. Combining the two methods we could evaluate fully differential single-jet production in the laboratory frame to N3LO. This calculation may at the moment only be seen as a proof of concept, but might pave the way for more processes to be evaluated to N3LO accuracy in the near future.

We also calculated event orientation in electron-positron annihilation to NNLO accuracy for the first time. The results show that event orientation distributions are very robust with respect to higher-order corrections. Corrections to NNLO amount hereby up to at most one per-cent in differential distributions using fine jet resolution and up to two per-cent using a more coarse jet resolution. Formerly, LEP and SLD only used leading-order Monte Carlo predictions for their acceptance corrections and our findings justify the validity of this procedure in retrospect. Corrections to NNLO QCD accuracy, however, might become relevant for precision measurements aiming at per-mille precision at possible future Z boson factories.

Acknowledgments

First of all I would like to thank Thomas Gehrmann for making this project possible and for his invaluable support in the past years. Further, I would like to thank Xuan Chen, James Currie, Aude Gehrmann-DeRidder, Nigel Glover, Alexander Huss and Tom Morgan for many fruitful discussions. In particular I would like to thank James for sharing his insights and for his patience when introducing the antenna subtraction method to me, Alex for his help during the merge of the DIS calculation into the main branch of the NNLOjet program and for his invaluable support in any computing related issues. I would like to thank Daniel Britzger and Radek Žlebčik for a very pleasant collaboration, Andreas Voigt for his support in our N3LO calculation, Stefan Höche and Marek Schönherr for making a comparison to SHERPA possible and Roland Bernet for managing our computing cluster. I am grateful to Federico Buccioni, Dominik Kara and Daniel Hulme for proof-reading of this thesis. Finally, I would like to thank all current and former members of the physics institute of the University of Zurich for the good time I had here.

A Quark-initiated subtraction terms for DIS di-jet production

The following appendix collects the antenna subtraction terms relevant to the NNLO calculation of quark-initiated di-jet production described in Section 7.9.

A.1 Real-real

$$
\begin{aligned}
&B_3^{Z,0,S}(\hat{1},i,j,k,l) = \\
&\quad + f_3^0(i,j,k)\, B_2^{Z,0}(1,(\widetilde{ij}),(\widetilde{jk}),l)\, J_2^3(\{p\}_3) \\
&\quad + f_3^0(i,j,k)\, B_2^{Z,0}(1,(\widetilde{jk}),(\widetilde{ij}),l)\, J_2^3(\{p\}_3) \\
&\quad + d_3^0(l,k,j)\, B_2^{Z,0}(1,i,(\widetilde{jk}),(\widetilde{lk}))\, J_2^3(\{p\}_3) \\
&\quad + d_3^0(l,i,j)\, B_2^{Z,0}(1,k,(\widetilde{ji}),(\widetilde{li}))\, J_2^3(\{p\}_3) \\
&\quad + d_3^0(1,k,j)\, B_2^{Z,0}(\overline{1},(\widetilde{kj}),i,l)\, J_2^3(\{p\}_3) \\
&\quad + d_3^0(1,i,j)\, B_2^{Z,0}(\overline{1},(\widetilde{ij}),k,l)\, J_2^3(\{p\}_3) \\
&\quad + D_4^{0,a}(l,i,j,k)\, B_1^{Z,0}(1,(\widetilde{ijk}),(\widetilde{lij}))\, J_2^2(\{p\}_2) \\
&\quad - d_3^0(l,i,j)\, d_3^0((\widetilde{li}),(\widetilde{ij}),k)\, B_1^{Z,0}(1,\widetilde{(k(\widetilde{ij}))},\widetilde{(\widetilde{li})(\widetilde{ij})})\, J_2^2(\{p\}_2) \\
&\quad - f_3^0(k,j,i)\, d_3^0(l,(\widetilde{kj}),(\widetilde{ji}))\, B_1^{Z,0}(1,\widetilde{(\widetilde{kj})(\widetilde{ji})},\widetilde{(l(\widetilde{kj}))})\, J_2^2(\{p\}_2) \\
&\quad + D_4^{0,a}(l,k,j,i)\, B_1^{Z,0}(1,(\widetilde{kji}),(\widetilde{lkj}))\, J_2^2(\{p\}_2) \\
&\quad - d_3^0(l,k,j)\, d_3^0((\widetilde{lk}),(\widetilde{kj}),i)\, B_1^{Z,0}(1,\widetilde{(i(\widetilde{kj}))},\widetilde{(\widetilde{lk})(\widetilde{kj})})\, J_2^2(\{p\}_2) \\
&\quad - f_3^0(i,j,k)\, d_3^0(l,(\widetilde{ij}),(\widetilde{jk}))\, B_1^{Z,0}(1,\widetilde{(\widetilde{ij})(\widetilde{jk})},\widetilde{(l(\widetilde{ij}))})\, J_2^2(\{p\}_2) \\
&\quad + D_4^0(1,i,j,k)\, B_1^{Z,0}(\overline{1},(\widetilde{ijk}),l)\, J_2^2(\{p\}_2) \\
&\quad - d_3^0(1,i,j)\, D_3^0(\overline{1},k,(\widetilde{ij}))\, B_1^{Z,0}(\overline{\overline{1}},\widetilde{((\widetilde{ij})k)},l)\, J_2^2(\{p\}_2) \\
&\quad - d_3^0(1,k,j)\, D_3^0(\overline{1},i,(\widetilde{kj}))\, B_1^{Z,0}(\overline{\overline{1}},\widetilde{((\widetilde{kj})i)},l)\, J_2^2(\{p\}_3) \\
&\quad - f_3^0(i,j,k)\, D_3^0(1,(\widetilde{ij}),(\widetilde{kj}))\, B_1^{Z,0}(\overline{1},\widetilde{(\widetilde{ij})(\widetilde{kj})},l)\, J_2^2(\{p\}_2) \\
&\quad + D_4^{0,c}(l,k,i,j)\, B_1^{Z,0}(1,(\widetilde{jik}),(\widetilde{lki}))\, J_2^2(\{p\}_2) \\
&\quad + D_4^{0,c}(l,i,k,j)\, B_1^{Z,0}(1,(\widetilde{jki}),(\widetilde{lik}))\, J_2^2(\{p\}_2) \\
&\quad - d_3^0(l,k,j)\, d_3^0((\widetilde{lk}),i,(\widetilde{kj}))\, B_1^{Z,0}(1,\widetilde{(i(\widetilde{kj}))},\widetilde{(i(\widetilde{lk}))})\, J_2^2(\{p\}_2) \\
&\quad - d_3^0(l,i,j)\, d_3^0((\widetilde{li}),k,(\widetilde{ij}))\, B_1^{Z,0}(1,\widetilde{(k(\widetilde{ij}))},\widetilde{(k(\widetilde{li}))})\, J_2^2(\{p\}_2) \\
&\quad - \tilde{A}_4^0(1,i,k,l)\, B_1^{Z,0}(\overline{1},j,(\widetilde{lki}))\, J_2^2(\{p\}_2)
\end{aligned}
$$

$$
\begin{aligned}
&+ A_3^0(1,i,l)\, A_3^0(\overline{1},k,(\widetilde{li}))\, B_1^{Z,0}(\overline{\overline{1}},j,(\widetilde{\widetilde{k(li)}}))\, J_2^2(\{p\}_2)\\
&+ A_3^0(1,k,l)\, A_3^0(\overline{1},i,(\widetilde{lk}))\, B_1^{Z,0}(\overline{\overline{1}},j,(\widetilde{\widetilde{i(lk)}}))\, J_2^2(\{p\}_2)\\
&+\frac{1}{2}\, d_3^0(1,i,j)\, d_3^0(\overline{1},k,(\widetilde{ij}))\, B_1^{Z,0}(\overline{1},(\widetilde{\widetilde{k(ij)}}),l)\, J_2^2(\{p\}_2)\\
&-\frac{1}{2}\, d_3^0(l,i,j)\, d_3^0(1,k,(\widetilde{ij}))\, B_1^{Z,0}(\overline{1},(\widetilde{\widetilde{k(ij)}}),(\widetilde{li}))\, J_2^2(\{p\}_2)\\
&-\frac{1}{2}\, A_3^0(1,i,l)\, d_3^0(\overline{1},k,j)\, B_1^{Z,0}(\overline{\overline{1}},(\widetilde{kj}),(\widetilde{li}))\, J_2^2(\{p\}_2)\\
&-\frac{1}{2}\left[+ S^{FF}_{1i(\widetilde{ij})} - S^{FF}_{\overline{1}i(\widetilde{\widetilde{k(ij)}})} - S^{FF}_{(\widetilde{li})i(\widetilde{ij})} + S^{FF}_{(\widetilde{li})i(\widetilde{\widetilde{k(ij)}})} - S^{FF}_{1i(\widetilde{li})} + S^{FF}_{\overline{1}i(\widetilde{li})}\right]\\
&\times d_3^0(1,k,(\widetilde{ij}))\, B_1^{Z,0}(\overline{1},(\widetilde{\widetilde{k(ij)}}),(\widetilde{li}))\, J_2^2(\{p\}_2)\\
&+\frac{1}{2}\, d_3^0(1,k,j)\, d_3^0(\overline{1},i,(\widetilde{kj}))\, B_1^{Z,0}(\overline{1},(\widetilde{\widetilde{i(kj)}}),l)\, J_2^2(\{p\}_2)\\
&-\frac{1}{2}\, d_3^0(l,k,j)\, d_3^0(1,i,(\widetilde{kj}))\, B_1^{Z,0}(\overline{1},(\widetilde{\widetilde{i(kj)}}),(\widetilde{lk}))\, J_2^2(\{p\}_2)\\
&-\frac{1}{2}\, A_3^0(1,k,l)\, d_3^0(\overline{1},i,j)\, B_1^{Z,0}(\overline{\overline{1}},(\widetilde{ij}),(\widetilde{lk}))\, J_2^2(\{p\}_2)\\
&-\frac{1}{2}\left[+ S^{FF}_{1k(\widetilde{jk})} - S^{FF}_{\overline{1}k(\widetilde{i(jk)})} - S^{FF}_{(\widetilde{lk})k(\widetilde{jk})} + S^{FF}_{(\widetilde{lk})k(\widetilde{i(jk)})} - S^{FF}_{1k(\widetilde{lk})} + S^{FF}_{\overline{1}k(\widetilde{lk})}\right]\\
&\times d_3^0(1,i,(\widetilde{jk}))\, B_1^{Z,0}(\overline{1},(\widetilde{\widetilde{i(jk)}}),(\widetilde{lk}))\, J_2^2(\{p\}_2)\\
&+\frac{1}{2}\, d_3^0(l,i,j)\, d_3^0((\widetilde{li}),k,(\widetilde{ij}))\, B_1^{Z,0}(1,(\widetilde{\widetilde{k(ij)}}),(\widetilde{(li)}k))\, J_2^2(\{p\}_2)\\
&-\frac{1}{2}\, d_3^0(1,i,j)\, d_3^0(l,k,(\widetilde{ij}))\, B_1^{Z,0}(\overline{1},(\widetilde{\widetilde{k(ij)}}),(\widetilde{lk}))\, J_2^2(\{p\}_2)\\
&-\frac{1}{2}\, A_3^0(1,i,l)\, d_3^0((\widetilde{li}),k,j)\, B_1^{Z,0}(\overline{1},(\widetilde{kj}),(\widetilde{\widetilde{k(li)}}))\, J_2^2(\{p\}_2)\\
&-\frac{1}{2}\left[+ S^{FF}_{(\widetilde{ij})i(\widetilde{li})} - S^{FF}_{(\widetilde{\widetilde{k(ij)}})i(\widetilde{\widetilde{k(li)}})} - S^{FF}_{1i(\widetilde{ij})} + S^{FF}_{1i(\widetilde{\widetilde{k(ij)}})} - S^{FF}_{1i(\widetilde{li})} + S^{FF}_{1i(\widetilde{\widetilde{k(li)}})}\right]\\
&\times d_3^0((\widetilde{li}),k,(\widetilde{ij}))\, B_1^{Z,0}(1,(\widetilde{\widetilde{k(ij)}}),(\widetilde{\widetilde{k(li)}}))\, J_2^2(\{p\}_2)\\
&+\frac{1}{2}\, d_3^0(l,k,j)\, d_3^0((\widetilde{lk}),i,(\widetilde{kj}))\, B_1^{Z,0}(1,(\widetilde{\widetilde{i(kj)}}),(\widetilde{(lk)}i))\, J_2^2(\{p\}_2)\\
&-\frac{1}{2}\, d_3^0(1,k,j)\, d_3^0(l,i,(\widetilde{kj}))\, B_1^{Z,0}(\overline{1},(\widetilde{\widetilde{i(kj)}}),(\widetilde{li}))\, J_2^2(\{p\}_2)\\
&-\frac{1}{2}\, A_3^0(1,k,l)\, d_3^0((\widetilde{lk}),i,j)\, B_1^{Z,0}(\overline{1},(\widetilde{ij}),(\widetilde{\widetilde{i(lk)}}))\, J_2^2(\{p\}_2)\\
&-\frac{1}{2}\left[+ S^{FF}_{(\widetilde{kj})k(\widetilde{lk})} - S^{FF}_{(\widetilde{i(kj)})k(\widetilde{i(lk)})} - S^{FF}_{1k(\widetilde{kj})} + S^{FF}_{1k(\widetilde{i(kj)})} - S^{FF}_{1k(\widetilde{lk})} + S^{FF}_{1k(\widetilde{i(lk)})}\right]\\
&\times d_3^0((\widetilde{lk}),i,(\widetilde{kj}))\, B_1^{Z,0}(1,(\widetilde{\widetilde{i(kj)}}),(\widetilde{\widetilde{i(lk)}}))\, J_2^2(\{p\}_2)\\
&-\frac{1}{2}\, A_3^0(1,i,l)\, A_3^0(\overline{1},k,(\widetilde{li}))\, B_1^{Z,0}(\overline{\overline{1}},j,(\widetilde{\widetilde{k(li)}}))\, J_2^2(\{p\}_2)\\
&+\frac{1}{2}\, d_3^0(1,i,j)\, A_3^0(\overline{1},k,l)\, B_1^{Z,0}(\overline{\overline{1}},(\widetilde{ij}),(\widetilde{lk}))\, J_2^2(\{p\}_2)
\end{aligned}
$$

$$
\begin{aligned}
&+\frac{1}{2}\; d_3^0(l,i,j)\, A_3^0(1,k,(\widetilde{li}))\, B_1^{Z,0}(\overline{1},(\widetilde{ij}),((\widetilde{\widetilde{li}k}))\, J_2^2(\{p\}_2)\\
&-\frac{1}{2}\left[- S^{FF}_{1i(\widetilde{li})} + S^{FF}_{\overline{1}i(\widetilde{k(\widetilde{li})})} + S^{FF}_{(\widetilde{li})i(\widetilde{ij})} - S^{FF}_{(\widetilde{k(\widetilde{li})})i(\widetilde{ij})} + S^{FF}_{1i(\widetilde{ij})} - S^{FF}_{\overline{1}i(\widetilde{ij})}\right]\\
&\times A_3^0(1,k,(\widetilde{li}))\, B_1^{Z,0}(\overline{1},(\widetilde{ij}),(\widetilde{k(\widetilde{li})}))\, J_2^2(\{p\}_2)\\
&-\frac{1}{2}\; A_3^0(1,k,l)\, A_3^0(\overline{1},i,(\widetilde{lk}))\, B_1^{Z,0}(\overline{\overline{1}},j,(\widetilde{i(\widetilde{lk})}))\, J_2^2(\{p\}_2)\\
&+\frac{1}{2}\; d_3^0(1,k,j)\, A_3^0(\overline{1},i,l)\, B_1^{Z,0}(\overline{\overline{1}},(\widetilde{kj}),(\widetilde{li}))\, J_2^2(\{p\}_2)\\
&+\frac{1}{2}\; d_3^0(l,k,j)\, A_3^0(1,i,(\widetilde{lk}))\, B_1^{Z,0}(\overline{1},(\widetilde{kj}),((\widetilde{\widetilde{lk}i}))\, J_2^2(\{p\}_2)\\
&-\frac{1}{2}\left[- S^{FF}_{1k(\widetilde{lk})} + S^{FF}_{\overline{1}k(\widetilde{i(\widetilde{lk})})} + S^{FF}_{(\widetilde{lk})k(\widetilde{kj})} - S^{FF}_{(\widetilde{i(\widetilde{lk})})k(\widetilde{kj})} + S^{FF}_{1k(\widetilde{kj})} - S^{FF}_{\overline{1}k(\widetilde{kj})}\right]\\
&\times A_3^0(1,i,(\widetilde{lk}))\, B_1^{Z,0}(\overline{1},(\widetilde{kj}),(\widetilde{i(\widetilde{lk})}))\, J_2^2(\{p\}_2)\,. \qquad \text{(A.1)}
\end{aligned}
$$

$$
\begin{aligned}
&\tilde{B}_3^{Z,0,S}(\hat{1},i,j,k,l) =\\
&\quad +A_3^0(1,i,l)\, B_2^{Z,0}(\overline{1},j,k,(\widetilde{li}))\, J_2^3(\{p\}_3)\\
&\quad +d_3^0(1,j,k)\, \tilde{B}_2^{Z,0}(\overline{1},i,(\widetilde{jk}),l)\, J_2^3(\{p\}_3)\\
&\quad +d_3^0(l,k,j)\, \tilde{B}_2^{Z,0}(1,i,(\widetilde{jk}),(\widetilde{lk}))\, J_2^3(\{p\}_3)\\
&\\
&\quad + A_4^0(1,j,k,l)\, B_1^{Z,0}(\overline{1},i,(\widetilde{jkl}))\, J_2^2(\{p\}_2)\\
&\quad - d_3^0(1,j,k)\, A_3^0(\overline{1},(\widetilde{jk}),l)\, B_1^{Z,0}(\overline{\overline{1}},i,(\widetilde{l(\widetilde{jk})}))\, J_2^2(\{p\}_2)\\
&\quad - d_3^0(l,k,j)\, A_3^0(1,(\widetilde{jk}),(\widetilde{lk}))\, B_1^{Z,0}(\overline{1},i,(\widetilde{(\widetilde{jk})(\widetilde{lk})}))\, J_2^2(\{p\}_2)\\
&\\
&\quad + \tilde{A}_4^0(1,i,j,l)\, B_1^{Z,0}(\overline{1},k,(\widetilde{ijl}))\, J_2^2(\{p\}_2)\\
&\quad - A_3^0(1,i,l)\, A_3^0(\overline{1},j,(\widetilde{li}))\, B_1^{Z,0}(\overline{\overline{1}},k,(\widetilde{j(\widetilde{li})}))\, J_2^2(\{p\}_3)\\
&\quad - A_3^0(1,j,l)\, A_3^0(\overline{1},i,(\widetilde{lj}))\, B_1^{Z,0}(\overline{\overline{1}},k,(\widetilde{i(\widetilde{lj})}))\, J_2^2(\{p\}_3)\\
&\quad + A_3^0(1,j,l)\, A_3^0(\overline{1},i,(\widetilde{lj}))\, B_1^{Z,0}(\overline{\overline{1}},k,(\widetilde{i(\widetilde{lj})}))\, J_2^2(\{p\}_2)\\
&\quad - d_3^0(1,j,k)\, A_3^0(\overline{1},i,l)\, B_1^{Z,0}(\overline{\overline{1}},(\widetilde{jk}),(\widetilde{li}))\, J_2^2(\{p\}_2)\\
&\quad - d_3^0(l,k,j)\, A_3^0(1,i,(\widetilde{lk}))\, B_1^{Z,0}(\overline{1},(\widetilde{kj}),(\widetilde{i(\widetilde{lk})}))\, J_2^2(\{p\}_2)\\
&\quad -\left[+ S^{FF}_{1j(\widetilde{lj})} - S^{FF}_{\overline{1}j(\widetilde{i(\widetilde{lj})})} - S^{FF}_{1j(\widetilde{kj})} + S^{FF}_{\overline{1}j(\widetilde{kj})} - S^{FF}_{(\widetilde{lj})j(\widetilde{kj})} + S^{FF}_{(\widetilde{i(\widetilde{lj})})j(\widetilde{kj})}\right]\\
&\quad \times A_3^0(1,i,(\widetilde{lj}))\, B_1^{Z,0}(\overline{1},(\widetilde{kj}),(\widetilde{i(\widetilde{lj})}))\, J_2^2(\{p\}_2). \qquad \text{(A.2)}
\end{aligned}
$$

$$
\begin{aligned}
&\tilde{\tilde{B}}_3^{Z,0,S}(\hat{1},i,j,k,l) =\\
&\quad +A_3^0(1,i,l)\, \tilde{B}_2^{Z,0}(\overline{1},j,k,(\widetilde{li}))\, J_2^3(\{p\}_3)\\
&\quad +A_3^0(1,j,l)\, \tilde{B}_2^{Z,0}(\overline{1},i,k,(\widetilde{lj}))\, J_2^3(\{p\}_3)
\end{aligned}
$$

$$
\begin{aligned}
&+A_3^0(1,k,l)\,\tilde{B}_2^{Z,0}(\overline{1},i,j,(\widetilde{lk}))\,J_2^3(\{p\}_3)\\
&\\
&+\tilde{A}_4^0(1,i,j,l)\,B_1^{Z,0}(\overline{1},k,(\widetilde{lij}))\,J_2^2(\{p\}_2)\\
&-A_3^0(1,i,l)\,A_3^0(\overline{1},j,(\widetilde{li}))\,B_1^{Z,0}(\overline{\overline{1}},k,(\widetilde{j(\widetilde{li})}))\,J_2^2(\{p\}_2)\\
&-A_3^0(1,j,l)\,A_3^0(\overline{1},i,(\widetilde{lj}))\,B_1^{Z,0}(\overline{\overline{1}},k,(\widetilde{i(\widetilde{lj})}))\,J_2^2(\{p\}_2)\\
&\\
&+\tilde{A}_4^0(1,i,k,l)\,B_1^{Z,0}(\overline{1},j,(\widetilde{lik}))\,J_2^2(\{p\}_2)\\
&-A_3^0(1,i,l)\,A_3^0(\overline{1},k,(\widetilde{li}))\,B_1^{Z,0}(\overline{\overline{1}},j,(\widetilde{k(\widetilde{li})}))\,J_2^2(\{p\}_2)\\
&-A_3^0(1,k,l)\,A_3^0(\overline{1},i,(\widetilde{lk}))\,B_1^{Z,0}(\overline{\overline{1}},j,(\widetilde{i(\widetilde{lk})}))\,J_2^2(\{p\}_2)\\
&\\
&+\tilde{A}_4^0(1,j,k,l)\,B_1^{Z,0}(\overline{1},i,(\widetilde{ljk}))\,J_2^2(\{p\}_2)\\
&-A_3^0(1,j,l)\,A_3^0(\overline{1},k,(\widetilde{lj}))\,B_1^{Z,0}(\overline{\overline{1}},i,(\widetilde{k(\widetilde{lj})}))\,J_2^2(\{p\}_2)\\
&-A_3^0(1,k,l)\,A_3^0(\overline{1},j,(\widetilde{lk}))\,B_1^{Z,0}(\overline{\overline{1}},i,(\widetilde{j(\widetilde{lk})}))\,J_2^2(\{p\}_2)\,.
\end{aligned}
\tag{A.3}
$$

$$
\begin{aligned}
&C_1^{Z,0,S}(\hat{1},i;j,k;l)=\\
&+A_3^0(1,i,j)\,C_0^{Z,0}(\overline{1};(\widetilde{ji}),k;l)\,J_2^3(\{p\}_3)\\
&+A_3^0(k,i,l)\,C_0^{Z,0}(1;j,(\widetilde{ki});(\widetilde{li}))\,J_2^3(\{p\}_3)\\
&+E_3^0(l,j,k)\,B_{2,q}^{Z,0}(1,(\widetilde{jk}),i,(\widetilde{lj}))\,J_2^3(\{p\}_3)\\
&+E_3^0(l,j,k)\,B_{2,q}^{Z,0}(1,i,(\widetilde{jk}),(\widetilde{lj}))\,J_2^3(\{p\}_3)\\
&\\
&+E_4^{0,a}(l,j,k,i)\,B_{1,q}^{Z,0}(1,(\widetilde{ikj}),(\widetilde{ljk}))\,J_2^2(\{p\}_2)\\
&\\
&+E_4^{0,b}(l,i,k,j)\,B_{1,q}^{Z,0}(1,(\widetilde{jki}),(\widetilde{lik}))\,J_2^2(\{p\}_2)\\
&-E_3^0(l,j,k)\,d_3^0((\widetilde{lj}),i,(\widetilde{jk}))\,B_{1,q}^{Z,0}(1,(\widetilde{(\widetilde{jk})i}),(\widetilde{(\widetilde{lj})i}))\,J_2^2(\{p\}_2)\\
&-E_3^0(l,j,k)\,d_3^0((\widetilde{lj}),(\widetilde{jk}),i)\,B_{1,q}^{Z,0}(1,(\widetilde{i(\widetilde{kj})}),(\widetilde{\widetilde{lj}(\widetilde{jk})}))\,J_2^2(\{p\}_2)\\
&-A_3^0(k,i,l)\,E_3^0((\widetilde{li}),(\widetilde{ki}),j)\,B_{1,q}^{Z,0}(1,(\widetilde{j(\widetilde{ki})}),(\widetilde{\widetilde{ki}(\widetilde{li})}))\,J_2^2(\{p\}_2)\\
&\\
&+E_4^0(1,k,j,i)\,B_{1,q}^{Z,0}(\overline{1},(\widetilde{ijk}),l)\,J_2^2(\{p\}_2)\\
&-E_3^0(l,j,k)\,D_3^0(1,(\widetilde{kj}),i)\,B_{1,q}^{Z,0}(\overline{1},(\widetilde{i(\widetilde{kj})}),(\widetilde{lj}))\,J_2^2(\{p\}_2)\\
&-A_3^0(1,i,j)\,E_3^0(\overline{1},k,(\widetilde{ji}))\,B_{1,q}^{Z,0}(\overline{\overline{1}},(\widetilde{k(\widetilde{ji})}),l)\,J_2^2(\{p\}_2)\\
&-E_{3,q'\to g}^0(k,1,l)\,B_{2,Q}^{Z,0}((\widetilde{kl}),\overline{1},i,j)\,J_2^3(\{p\}_3)\\
&-E_{3,q'\to g}^0(k,1,l)\,B_{2,Q}^{Z,0}((\widetilde{kl}),i,\overline{1},j)\,J_2^3(\{p\}_3)
\end{aligned}
$$

$$
\begin{aligned}
&- E_4^0(k,l,1,i)\, B_{1,Q}^{Z,0}((\widetilde{kli}),\overline{1},j)\, J_2^2(\{p\}_2)\\
&+ E_{3,q'\to g}^0(k,1,l)\, D_3^0((\widetilde{kl}),\overline{1},i)\, B_{1,Q}^{Z,0}(((\widetilde{\widetilde{kl})i}),\overline{\overline{1}},j)\, J_2^2(\{p\}_2)\\
\\
&- E_4^0(k,1,l,i)\, B_{1,Q}^{Z,0}((\widetilde{kli}),\overline{1},j)\, J_2^2(\{p\}_2)\\
&+ E_{3,q'\to g}^0(k,l,1)\, D_3^0((\widetilde{kl}),\overline{1},i)\, B_{1,Q}^{Z,0}(((\widetilde{\widetilde{lk})i}),\overline{\overline{1}},j)\, J_2^2(\{p\}_2)\\
&+ A_3^0(l,i,k)\, E_{3,q'\to g}^0((\widetilde{ki}),1,(\widetilde{li}))\, B_{1,Q}^{Z,0}((\widetilde{\widetilde{ki})(\widetilde{li})},\overline{1},j)\, J_2^2(\{p\}_2)\\
\\
&+ B_4^0(k,1,l,j)\, B_{1,Q}^{Z,0}(i,\overline{1},(\widetilde{jlk}))\, J_2^2(\{p\}_2)\\
&-2\, E_{3,q'\to g}^0(k,1,l)\, a_{3,g\to q}^0((\widetilde{kl}),\overline{1},j)\, B_{1,Q}^{Z,0}(i,\overline{\overline{1}},(\widetilde{j(\widetilde{kl})}))\, J_2^2(\{p\}_2)\\
\\
&+ B_4^0(k,1,l,j)\, \bar{B}_{1,Q}^{Z,0}((\widetilde{jlk}),i,\overline{1})\, J_2^2(\{p\}_2)\\
&- E_{3,q'\to g}^0(k,l,1)\, a_{3,g\to q}^0(j,\overline{1},(\widetilde{kl}))\, B_{1,Q}^{Z,0}((\widetilde{j(\widetilde{kl})}),i,\overline{\overline{1}})\, J_2^2(\{p\}_2)\\
&- E_{3,q'\to g}^0(k,1,l)\, a_{3,g\to q}^0((\widetilde{kl}),\overline{1},j)\, B_{1,Q}^{Z,0}(\overline{\overline{1}},i,\widetilde{\widetilde{j(\widetilde{kl})}}))\, J_2^2(\{p\}_2)\\
&+ A_{3,q}^0(1,i,j)\, E_{3,q'\to g}^0(k,\overline{1},l)\, B_{1,Q}^{Z,0}((\widetilde{kl}),\overline{\overline{1}},(\widetilde{ij}))\, J_2^2(\{p\}_2)\\
&+ A_3^0(k,i,j)\, E_{3,q'\to g}^0((\widetilde{ki}),1,l)\, B_{1,Q}^{Z,0}(((\widetilde{\widetilde{ki})l}),\overline{1},(\widetilde{ji}))\, J_2^2(\{p\}_2)\\
&- E_{3,q'\to g}^0(k,1,l)\, A_3^0((\widetilde{kl}),i,j)\, B_{1,Q}^{Z,0}(((\widetilde{\widetilde{kl})i}),\overline{1},(\widetilde{ij}))\, J_2^2(\{p\}_2)\\
&-\left[+ S_{\overline{1}i(\widetilde{\widetilde{ki})(\widetilde{li})}}^{FF} + S_{(\widetilde{ki})ij}^{FF} - S_{\widetilde{\widetilde{(ki)(li)}}ij}^{FF} - S_{1i(\widetilde{ki})}^{FF} - S_{ji\overline{1}}^{FF} + S_{1ij}^{FF}\right]\\
&\times E_{3,q'\to g}^0((\widetilde{ki}),1,(\widetilde{li}))\, B_{1,Q}^{Z,0}((\widetilde{\widetilde{ki})(\widetilde{li})},\overline{1},j)\, J_2^2(\{p\}_2)\,. \qquad \text{(A.4)}
\end{aligned}
$$

$$
\begin{aligned}
&\tilde{C}_1^{Z,0,S}(\hat{1},i;j,k;l) =\\
&+A_3^0(1,i,l)\, C_0^{Z,0}(\overline{1};j,k;(\widetilde{il}))\, J_2^3(\{p\}_3)\\
&+A_3^0(j,i,k)\, C_0^{Z,0}(1;(\widetilde{ji}),(\widetilde{ki});l)\, J_2^3(\{p\}_3)\\
&-2A_3^0(1,i,k)\, C_0^{Z,0}(\overline{1};j,(\widetilde{ki});l)\, J_2^3(\{p\}_3)\\
&-2A_3^0(j,i,l)\, C_0^{Z,0}(1;(\widetilde{ji}),k;(\widetilde{li}))\, J_2^3(\{p\}_3)\\
&+2A_3^0(1,i,j)\, C_0^{Z,0}(\overline{1};(\widetilde{ji}),k;l)\, J_2^3(\{p\}_3)\\
&+2A_3^0(l,i,k)\, C_0^{Z,0}(1,j,(\widetilde{ki}),(\widetilde{li}))\, J_2^3(\{p\}_3)\\
&+E_3^0(l,j,k)\, \tilde{B}_{2,q}^{Z,0}(1,i,(\widetilde{kj}),(\widetilde{lj}))\, J_2^3(\{p\}_3)\\
\\
&+ B_4^0(1,j,k,l)\, B_{1,q}^{Z,0}(\overline{1},i,(\widetilde{jkl}))\, J_2^2(\{p\}_2)\\
&- E_3^0(l,j,k)\, A_3^0(1,(\widetilde{kj}),(\widetilde{lj}))\, B_{1,q}^{Z,0}(\overline{1},i,\widetilde{\widetilde{(kj)(lj)}}))\, J_2^2(\{p\}_2)\\
\\
&+\frac{1}{2}\, \tilde{E}_4^0(1,j,i,k)\, B_{1,q}^{Z,0}(\overline{1},(\widetilde{ijk}),l)\, J_2^2(\{p\}_2)
\end{aligned}
$$

$$
\begin{aligned}
&-\frac{1}{2}\ A_3^0(j,i,k)\,E_{3,q}^0(1,(\widetilde{ji}),(\widetilde{ki}))\,B_{1,q}^{Z,0}(\overline{1},(\widetilde{(\widetilde{ji})(\widetilde{ki})}),l)\,J_2^2(\{p\}_2)\\
&+\frac{1}{2}\ \tilde{E}_4^0(l,j,i,k)\,B_{1,q}^{Z,0}(1,(\widetilde{kij}),(\widetilde{lji}))\,J_2^2(\{p\}_2)\\
&-\frac{1}{2}\ A_3^0(j,i,k)\,E_3^0(l,(\widetilde{ji}),(\widetilde{ki}))\,B_{1,q}^{Z,0}(1,(\widetilde{(\widetilde{ji})(\widetilde{ki})}),(\widetilde{l(\widetilde{ji})}))\,J_2^2(\{p\}_2)\\
&-E_3^0(l,j,k)\,A_3^0(1,i,(\widetilde{lj}))\,B_{1,q}^{Z,0}(\overline{1},(\widetilde{jk}),(\widetilde{i(\widetilde{lj})}))\,J_2^2(\{p\}_2)\\
&+A_3^0(1,i,k)\,E_3^0(\overline{1},(\widetilde{ik}),j)\,B_{1,q}^{Z,0}(\overline{\overline{1}},(\widetilde{j(\widetilde{ik})}),l)\,J_2^2(\{p\}_2)\\
&+A_3^0(j,i,l)\,E_3^0(1,k,(\widetilde{ji}))\,B_{1,q}^{Z,0}(\overline{1},(\widetilde{k(\widetilde{ji})}),(\widetilde{li}))\,J_2^2(\{p\}_2)\\
&-A_3^0(1,i,j)\,E_3^0(\overline{1},k,(\widetilde{ji}))\,B_{1,q}^{Z,0}(\overline{\overline{1}},(\widetilde{k(\widetilde{ji})}),l)\,J_2^2(\{p\}_2)\\
&-A_3^0(l,i,k)\,E_3^0(1,(\widetilde{ki}),j)\,B_{1,q}^{Z,0}(\overline{1},(\widetilde{(\widetilde{ki})j}),(\widetilde{li}))\,J_2^2(\{p\}_2)\\
&-\Big[+S_{1i(\widetilde{ki})}^{FF}+S_{(\widetilde{ji})il}^{FF}-S_{1i(\widetilde{ji})}^{FF}-S_{li(\widetilde{ik})}^{FF}\Big]\\
&\times E_3^0(1,(\widetilde{ki}),(\widetilde{ji}))\,B_{1,q}^{Z,0}(\overline{1},(\widetilde{(\widetilde{ki})(\widetilde{ji})}),l)\,J_2^2(\{p\}_2)\\
&+A_3^0(1,i,k)\,E_3^0(l,(\widetilde{ik}),j)\,B_{1,q}^{Z,0}(\overline{1},(\widetilde{j(\widetilde{ik})}),(\widetilde{l(\widetilde{ik})}))\,J_2^2(\{p\}_2)\\
&+A_3^0(j,i,l)\,E_3^0((\widetilde{li}),k,(\widetilde{ji}))\,B_{1,q}^{Z,0}(1,(\widetilde{k(\widetilde{ji})}),(\widetilde{(\widetilde{li})k}))\,J_2^2(\{p\}_2)\\
&-A_3^0(1,i,j)\,E_3^0(l,k,(\widetilde{ji}))\,B_{1,q}^{Z,0}(\overline{1},(\widetilde{k(\widetilde{ji})}),(\widetilde{lk}))\,J_2^2(\{p\}_2)\\
&-A_3^0(l,i,k)\,E_3^0((\widetilde{li}),(\widetilde{ki}),j)\,B_{1,q}^{Z,0}(1,(\widetilde{(\widetilde{ki})j}),(\widetilde{(\widetilde{li})(\widetilde{ki})}))\,J_2^2(\{p\}_2)\\
&-\Big[+S_{1i(\widetilde{ki})}^{FF}+S_{(\widetilde{ji})il}^{FF}-S_{1i(\widetilde{ji})}^{FF}-S_{li(\widetilde{ik})}^{FF}\Big]\\
&\times E_3^0(l,(\widetilde{ki}),(\widetilde{ji}))\,B_{1,q}^{Z,0}(1,(\widetilde{(\widetilde{ki})(\widetilde{ji})}),(\widetilde{l(\widetilde{ki})}))\,J_2^2(\{p\}_2)\\
&-\frac{1}{2}\,E_{3,q'\to g}^0(j,1,l)\,\tilde{\bar{B}}_{2,Q}^{Z,0}(k,\overline{1},i,(\widetilde{jl}))\,J_2^3(\{p\}_3)\\
&-\frac{1}{2}\,E_{3,q'\to g}^0(k,1,l)\,\tilde{\bar{B}}_{2,Q}^{Z,0}((\widetilde{kl}),i,\overline{1},j)\,J_2^3(\{p\}_3)\\
&+B_4^0(j,1,l,k)\,\bar{B}_{1,Q}^{Z,0}(\overline{1},i,(\widetilde{jlk}))\,J_2^2(\{p\}_2)\\
&-\frac{1}{2}\ E_{3,q'\to g}^0(j,1,l)\,A_3^0((\widetilde{jl}),\overline{1},k)\,\bar{B}_{1,Q}^{Z,0}(\overline{\overline{1}},i,(\widetilde{(\widetilde{jl})k}))\,J_2^2(\{p\}_2)\\
&-\frac{1}{2}\ E_{3,q'\to g}^0(k,1,l)\,A_3^0((\widetilde{kl}),\overline{1},j)\,\bar{B}_{1,Q}^{Z,0}(\overline{\overline{1}},i,(\widetilde{(\widetilde{kl})j}))\,J_2^2(\{p\}_2)\\
&-\frac{1}{2}\ \tilde{E}_4^0(j,1,i,l)\,B_{1,Q}^{Z,0}(k,\overline{1},(\widetilde{jil}))\,J_2^2(\{p\}_2)\\
&+\frac{1}{2}\ A_3^0(1,i,l)\,E_{3,q'\to g}^0(j,\overline{1},(\widetilde{il}))\,B_{1,Q}^{Z,0}(k,\overline{\overline{1}},(\widetilde{j(\widetilde{il})}))\,J_2^2(\{p\}_2)
\end{aligned}
$$

$$
\begin{aligned}
&-\frac{1}{2}\ \tilde{E}_4^0(k,1,i,l)\, B_{1,Q}^{Z,0}((\widetilde{kil}),\overline{1},j)\, J_2^2(\{p\}_2)\\
&+\frac{1}{2}\ A_3^0(1,i,l)\, E_{3,q'\to g}^0(k,\overline{1},(\widetilde{il}))\, B_{1,Q}^{Z,0}((\widetilde{k(\widetilde{il})}),\overline{\overline{1}},j)\, J_2^2(\{p\}_2)\\
&+\frac{1}{2}\ E_{3,q'\to g}^0(j,1,l)\, A_3^0((\widetilde{jl}),i,k)\, B_{1,Q}^{Z,0}((\widetilde{ki}),\overline{1},(\widetilde{(\widetilde{jl})i}))\, J_2^2(\{p\}_2)\\
&+\frac{1}{2}\ E_{3,q'\to g}^0(k,1,l)\, A_3^0((\widetilde{kl}),i,j)\, B_{1,Q}^{Z,0}((\widetilde{(\widetilde{kl})i}),\overline{1},(\widetilde{ij}))\, J_2^2(\{p\}_2)\\
&-A_3^0(1,i,k)\, E_3^0((\widetilde{ik}),\overline{1},l)\, B_{1,Q}^{Z,0}((\widetilde{l(\widetilde{ik})}),\overline{\overline{1}},j)\, J_2^2(\{p\}_2)\\
&-A_3^0(j,i,l)\, E_3^0(k,1,(\widetilde{li}))\, B_{1,Q}^{Z,0}((\widetilde{k(\widetilde{li})}),\overline{1},(\widetilde{ji}))\, J_2^2(\{p\}_2)\\
&+A_3^0(1,i,j)\, E_3^0(k,\overline{1},l)\, B_{1,Q}^{Z,0}((\widetilde{lk}),\overline{\overline{1}},(\widetilde{ji}))\, J_2^2(\{p\}_2)\\
&+A_3^0(l,i,k)\, E_3^0((\widetilde{ki}),1,(\widetilde{li}))\, B_{1,Q}^{Z,0}((\widetilde{(\widetilde{ki})(\widetilde{li})}),\overline{1},j)\, J_2^2(\{p\}_2)\\
&+\Big[+S_{1i(\widetilde{ik})}^{FF}+S_{ji(\widetilde{li})}^{FF}-S_{1ij}^{FF}-S_{(\widetilde{li})i(\widetilde{ik})}^{FF}\Big]\\
&\times E_3^0((\widetilde{ik}),1,(\widetilde{li}))\, B_{1,Q}^{Z,0}((\widetilde{(\widetilde{ik})(\widetilde{li})}),\overline{1},j)\, J_2^2(\{p\}_2)\\
&-A_3^0(1,i,k)\, E_3^0(j,\overline{1},l)\, B_{1,Q}^{Z,0}((\widetilde{ki}),\overline{\overline{1}},(\widetilde{lj}))\, J_2^2(\{p\}_2)\\
&-A_3^0(j,i,l)\, E_3^0((\widetilde{ji}),1,(\widetilde{li}))\, B_{1,Q}^{Z,0}(k,\overline{1},(\widetilde{(\widetilde{ji})(\widetilde{li})}))\, J_2^2(\{p\}_2)\\
&+A_3^0(1,i,j)\, E_3^0((\widetilde{ji}),\overline{1},l)\, B_{1,Q}^{Z,0}(k,\overline{\overline{1}},(\widetilde{l(\widetilde{ji})}))\, J_2^2(\{p\}_2)\\
&+A_3^0(l,i,k)\, E_3^0(j,1,(\widetilde{li}))\, B_{1,Q}^{Z,0}((\widetilde{ki}),\overline{1},(\widetilde{j(\widetilde{li})}))\, J_2^2(\{p\}_2)\\
&-\Big[+S_{1i(\widetilde{ij})}^{FF}+S_{ki(\widetilde{li})}^{FF}-S_{1ik}^{FF}-S_{(\widetilde{li})i(\widetilde{ij})}^{FF}\Big]\\
&\times E_3^0((\widetilde{ij}),1,(\widetilde{li}))\, B_{1,Q}^{Z,0}(k,\overline{1},(\widetilde{(\widetilde{ij})(\widetilde{li})}))\, J_2^2(\{p\}_2)\,. \qquad \text{(A.5)}
\end{aligned}
$$

$$
\begin{aligned}
&D_1^{Z,0,S}(\hat{1},i,j;k,l)=\\
&\quad +A_3^0(1,i,k)\, D_0^{Z,0}(\overline{1},j;(\widetilde{ik}),l)\, J_2^3(\{p\}_3)\\
&\quad +A_3^0(j,i,l)\, D_0^{Z,0}(1,(\widetilde{ji});k,(\widetilde{li}))\, J_2^3(\{p\}_3)\\
&\\
&\quad +2\, C_4^0(1,k,j,l)\, B_{1,q}^{Z,0}(\overline{1},i,(\widetilde{jkl}))\, J_2^2(\{p\}_2)\\
&\quad +2\, C_4^0(k,1,j,l)\, B_{1,q}^{Z,0}((\widetilde{jkl}),i,\overline{1})\, J_2^2(\{p\}_2)\\
&\quad +2\, C_4^0(l,j,k,1)\, B_{1,q}^{Z,0}(\overline{1},i,(\widetilde{jkl}))\, J_2^2(\{p\}_2)\\
&\quad +2\, C_4^0(j,l,k,1)\, B_{1,q}^{Z,0}(\overline{1},i,(\widetilde{jkl}))\, J_2^2(\{p\}_2)\,. \qquad \text{(A.6)}
\end{aligned}
$$

$$
\begin{aligned}
&\tilde{D}_1^{Z,0,S}(\hat{1},i,j;k,l)=\\
&\quad -A_3^0(1,i,k)\, D_0^{Z,0}(\overline{1},j;(\widetilde{ik}),l)\, J_2^3(\{p\}_3)\\
&\quad +A_3^0(1,i,l)\, D_0^{Z,0}(\overline{1},j;k,(\widetilde{il}))\, J_2^3(\{p\}_3)
\end{aligned}
$$

$$
\begin{aligned}
&+A_3^0(1,i,j)\,D_0^{Z,0}(\overline{1},(\widetilde{ij});k,l)\,J_2^3(\{p\}_3)\\
&+A_3^0(j,i,k)\,D_0^{Z,0}(1,(\widetilde{ji});(\widetilde{ki}),l)\,J_2^3(\{p\}_3)\\
&-A_3^0(j,i,l)\,D_0^{Z,0}(1,(\widetilde{ji});k,(\widetilde{li}))\,J_2^3(\{p\}_3)\\
&+A_3^0(k,i,l)\,D_0^{Z,0}(1,j;(\widetilde{ki}),(\widetilde{li}))\,J_2^3(\{p\}_3)\\
\\
&+2\,C_4^0(1,k,j,l)\,B_{1,q}^{Z,0}(\overline{1},i,(\widetilde{jkl}))\,J_2^2(\{p\}_2)\\
&+2\,C_4^0(k,1,j,l)\,B_{1,q}^{Z,0}((\widetilde{jkl}),i,\overline{1})\,J_2^2(\{p\}_2)\\
&+2\,C_4^0(l,j,k,1)\,B_{1,q}^{Z,0}(\overline{1},i,(\widetilde{jkl}))\,J_2^2(\{p\}_2)\\
&+2\,C_4^0(j,l,k,1)\,B_{1,q}^{Z,0}(\overline{1},i,(\widetilde{jkl}))\,J_2^2(\{p\}_2)\,.
\end{aligned}
\tag{A.7}
$$

A.2 Real-virtual

$$
\begin{aligned}
&B_2^{Z,1,T}(\hat{1},i,j,k)=\\
&-\Big[+J_{2,QG}^{1,IF}(s_{1i})+J_{2,QG}^{1,FF}(s_{kj})+J_{2,GG}^{1,FF}(s_{ij})\Big]\,B_2^{Z,0}(1,i,j,k)\,J_2^3(\{p\}_3)\\
&-\Big[+J_{2,QG}^{1,IF}(s_{1j})+J_{2,QG}^{1,FF}(s_{ki})+J_{2,GG}^{1,FF}(s_{ji})\Big]\,B_2^{Z,0}(1,j,i,k)\,J_2^3(\{p\}_3)\\
&+D_{3,q}^0(1,i,j)\Big[\,B_1^{Z,1}(\overline{1},(\widetilde{ij}),k)\,\delta(1-x_1)\,\delta(1-x_2)\\
&+\Big(+J_{2,QG}^{1,IF}(s_{\overline{1}(\widetilde{ij})})+J_{2,QG}^{1,FF}(s_{k(\widetilde{ij})})\Big)\,B_1^{Z,0}(\overline{1},(\widetilde{ij}),k)\Big]\,J_2^2(\{p\}_2)\\
&+d_3^0(k,j,i)\Big[\,B_1^{Z,1}(1,(\widetilde{ij}),(\widetilde{kj}))\,\delta(1-x_1)\,\delta(1-x_2)\\
&+\Big(+J_{2,QG}^{1,IF}(s_{1(\widetilde{ij})})+J_{2,QG}^{1,FF}(s_{(\widetilde{kj})(\widetilde{ij})})\Big)\,B_1^{Z,0}(1,(\widetilde{ij}),(\widetilde{kj}))\Big]\,J_2^2(\{p\}_2)\\
&+d_3^0(k,i,j)\Big[\,B_1^{Z,1}(1,(\widetilde{ij}),(\widetilde{ki}))\,\delta(1-x_1)\,\delta(1-x_2)\\
&+\Big(+J_{2,QG}^{1,FF}(s_{(\widetilde{ki})(\widetilde{ij})})+J_{2,QG}^{1,IF}(s_{1(\widetilde{ij})})\Big)\,B_1^{Z,0}(1,(\widetilde{ij}),(\widetilde{ki}))\Big]\,J_2^2(\{p\}_2)\\
&+\Big[\,d_3^1(k,i,j)\,\delta(1-x_1)\,\delta(1-x_2)\\
&+\Big(+J_{2,QG}^{1,FF}(s_{kj})+J_{2,GG}^{1,FF}(s_{ij})-2J_{2,QG}^{1,FF}(s_{(\widetilde{ki})(\widetilde{ij})})+J_{2,QG}^{1,FF}(s_{ki})\Big)\,d_3^0(k,i,j)\Big]\\
&\times B_1^{Z,0}(1,(\widetilde{ij}),(\widetilde{ki}))\,J_2^2(\{p\}_2)\\
&+\Big[\,d_3^1(k,j,i)\,\delta(1-x_1)\,\delta(1-x_2)\\
&+\Big(+J_{2,QG}^{1,FF}(s_{kj})+J_{2,GG}^{1,FF}(s_{ij})-2J_{2,QG}^{1,FF}(s_{(\widetilde{kj})(\widetilde{ij})})+J_{2,QG}^{1,FF}(s_{ki})\Big)\,d_3^0(k,j,i)\Big]\\
&\times B_1^{Z,0}(1,(\widetilde{ij}),(\widetilde{kj}))\,J_2^2(\{p\}_2)\\
&+\Big[\,D_{3,q}^1(1,i,j)\,\delta(1-x_1)\,\delta(1-x_2)
\end{aligned}
$$

$$
\begin{aligned}
&+\Bigg(+ J^{1,IF}_{2,QG}(s_{1i}) + J^{1,FF}_{2,GG}(s_{ij}) - 2J^{1,IF}_{2,QG}(s_{\overline{1}(\widetilde{ij})}) + J^{1,IF}_{2,QG}(s_{1j}) \Bigg) D^0_3(1,i,j) \Bigg] \\
&\times B^{Z,0}_1(\overline{1},(\widetilde{ij}),k)\, J^2_2(\{p\}_2) \\
&-\Bigg[\tilde{A}^1_{3,q}(1,i,k)\, \delta(1-x_1)\, \delta(1-x_2) \\
&+\Bigg(+ J^{1,IF}_{2,QQ}(s_{1k}) - J^{1,IF}_{2,QQ}(s_{\overline{1}(\widetilde{ik})}) \Bigg) A^0_3(1,i,k) \Bigg] B^{Z,0}_1(\overline{1},j,(\widetilde{ki}))\, J^2_2(\{p\}_2) \\
&-\Bigg[\tilde{A}^1_{3,q}(1,j,k)\, \delta(1-x_1)\, \delta(1-x_2) \\
&+\Bigg(+ J^{1,IF}_{2,QQ}(s_{1k}) - J^{1,IF}_{2,QQ}(s_{\overline{1}(\widetilde{jk})}) \Bigg) A^0_3(1,j,k) \Bigg] B^{Z,0}_1(\overline{1},i,(\widetilde{kj}))\, J^2_2(\{p\}_2) \\
&+\frac{1}{2}\Bigg[+ J^{1,IF}_{2,QQ}(s_{1k}) - J^{1,IF}_{2,QQ}(s_{\overline{1}k}) - J^{1,IF}_{2,QG}(s_{1j}) \\
&\quad + J^{1,IF}_{2,QG}(s_{\overline{1}(\widetilde{ij})}) + J^{1,FF}_{2,QG}(s_{kj}) - J^{1,FF}_{2,QG}(s_{k(\widetilde{ij})}) \\
&\quad + \Bigg(+ \mathcal{S}^{FF}(s_{1j},s_{kj},x_{1j,kj}) - \mathcal{S}^{FF}(s_{\overline{1}(\widetilde{ij})},s_{kj},x_{\overline{1}(\widetilde{ij}),kj}) - \mathcal{S}^{FF}(s_{kj},s_{kj},1) \\
&\quad + \mathcal{S}^{FF}(s_{k(\widetilde{ij})},s_{kj},x_{k(\widetilde{ij}),kj}) - \mathcal{S}^{FF}(s_{1k},s_{kj},x_{1k,kj}) + \mathcal{S}^{FF}(s_{\overline{1}k},s_{kj},x_{\overline{1}k,kj}) \Bigg) \Bigg] \\
&\times d^0_3(1,i,j)\, B^{Z,0}_1(\overline{1},(\widetilde{ij}),k)\, J^2_2(\{p\}_2) \\
&+\frac{1}{2}\Bigg[+ J^{1,IF}_{2,QQ}(s_{1k}) - J^{1,IF}_{2,QQ}(s_{\overline{1}k}) - J^{1,IF}_{2,QG}(s_{1i}) \\
&\quad + J^{1,IF}_{2,QG}(s_{\overline{1}(\widetilde{ji})}) + J^{1,FF}_{2,QG}(s_{ki}) - J^{1,FF}_{2,QG}(s_{k(\widetilde{ji})}) \\
&\quad + \Bigg(+ \mathcal{S}^{FF}(s_{1i},s_{ki},x_{1i,ki}) - \mathcal{S}^{FF}(s_{\overline{1}(\widetilde{ji})},s_{ki},x_{\overline{1}(\widetilde{ji}),ki}) - \mathcal{S}^{FF}(s_{ki},s_{ki},1) \\
&\quad + \mathcal{S}^{FF}(s_{k(\widetilde{ji})},s_{ki},x_{k(\widetilde{ji}),ki}) - \mathcal{S}^{FF}(s_{1k},s_{ki},x_{1k,ki}) + \mathcal{S}^{FF}(s_{\overline{1}k},s_{ki},x_{\overline{1}k,ki}) \Bigg) \Bigg] \\
&\times d^0_3(1,j,i)\, B^{Z,0}_1(\overline{1},(\widetilde{ij}),k)\, J^2_2(\{p\}_2) \\
&+\frac{1}{2}\Bigg[+ J^{1,IF}_{2,QQ}(s_{1k}) - J^{1,IF}_{2,QQ}(s_{1(\widetilde{ki})}) + J^{1,FF}_{2,QG}(s_{(\widetilde{ki})(\widetilde{ij})}) \\
&\quad + J^{1,IF}_{2,QG}(s_{1j}) - J^{1,IF}_{2,QG}(s_{1(\widetilde{ij})}) - J^{1,FF}_{2,QG}(s_{kj}) \\
&\quad + \Bigg(+ \mathcal{S}^{FF}(s_{kj},s_{kj},1) - \mathcal{S}^{FF}(s_{(\widetilde{ki})(\widetilde{ij})},s_{kj},x_{(\widetilde{ki})(\widetilde{ij}),kj}) - \mathcal{S}^{FF}(s_{1j},s_{kj},x_{1j,kj}) \\
&\quad + \mathcal{S}^{FF}(s_{1(\widetilde{ij})},s_{kj},x_{1(\widetilde{ij}),kj}) - \mathcal{S}^{FF}(s_{1k},s_{kj},x_{1k,kj}) + \mathcal{S}^{FF}(s_{1(\widetilde{ki})},s_{kj},x_{1(\widetilde{ki}),kj}) \Bigg) \Bigg] \\
&\times d^0_3(k,i,j)\, B^{Z,0}_1((\widetilde{ki}),(\widetilde{ij}),1)\, J^2_2(\{p\}_2) \\
&+\frac{1}{2}\Bigg[+ J^{1,IF}_{2,QQ}(s_{1k}) - J^{1,IF}_{2,QQ}(s_{1(\widetilde{kj})}) - J^{1,FF}_{2,QG}(s_{ki}) \\
&\quad + J^{1,FF}_{2,QG}(s_{(\widetilde{kj})(\widetilde{ji})}) + J^{1,IF}_{2,QG}(s_{1i}) - J^{1,IF}_{2,QG}(s_{1(\widetilde{ji})})
\end{aligned}
$$

$$
\begin{aligned}
&+\Big(+\mathcal{S}^{FF}(s_{ki},s_{ki},1)-\mathcal{S}^{FF}(s_{\widetilde{(kj)}(\widetilde{ji})},s_{ki},x_{\widetilde{(kj)}(\widetilde{ji}),ki})-\mathcal{S}^{FF}(s_{1i},s_{ki},x_{1i,ki})\\
&+\mathcal{S}^{FF}(s_{1(\widetilde{ji})},s_{ki},x_{1(\widetilde{ji}),ki})-\mathcal{S}^{FF}(s_{1k},s_{ki},x_{1k,ki})+\mathcal{S}^{FF}(s_{1(\widetilde{kj})},s_{ki},x_{1(\widetilde{kj}),ki})\Big)\Big]\\
&\times d_3^0(k,j,i)\,B_1^{Z,0}(1,(\widetilde{ji}),(\widetilde{kj}))\,J_2^2(\{p\}_2)\\
&+\frac{1}{2}\Big[+J_{2,QQ}^{1,IF}(s_{1k})-J_{2,QQ}^{1,IF}(s_{\overline{1}(\widetilde{ki})})-J_{2,QG}^{1,IF}(s_{1j})\\
&+J_{2,QG}^{1,IF}(s_{\overline{1}j})-J_{2,QG}^{1,FF}(s_{kj})+J_{2,QG}^{1,FF}(s_{(\widetilde{ki})j})\\
&+\Big(-\mathcal{S}^{FF}(s_{1k},s_{kj},x_{1k,kj})+\mathcal{S}^{FF}(s_{\overline{1}(\widetilde{ki})},s_{kj},x_{\overline{1}(\widetilde{ki}),kj})+\mathcal{S}^{FF}(s_{1j},s_{kj},x_{1j,kj})\\
&-\mathcal{S}^{FF}(s_{\overline{1}j},s_{kj},x_{\overline{1}j,kj})\\
&+\mathcal{S}^{FF}(s_{kj},s_{kj},1)-\mathcal{S}^{FF}(s_{(\widetilde{ki})j},s_{kj},x_{(\widetilde{ki})j,kj})\Big)\Big]\\
&\times A_3^0(1,i,k)\,B_1^{Z,0}(\overline{1},j,(\widetilde{ki}))\,J_2^2(\{p\}_2)\\
&+\frac{1}{2}\Big[+J_{2,QQ}^{1,IF}(s_{1k})-J_{2,QQ}^{1,IF}(s_{\overline{1}(\widetilde{kj})})-J_{2,QG}^{1,IF}(s_{1i})\\
&+J_{2,QG}^{1,IF}(s_{\overline{1}i})-J_{2,QG}^{1,FF}(s_{ki})+J_{2,QG}^{1,FF}(s_{(\widetilde{kj})i})\\
&+\Big(-\mathcal{S}^{FF}(s_{1k},s_{ki},x_{1k,ki})+\mathcal{S}^{FF}(s_{\overline{1}(\widetilde{kj})},s_{ki},x_{\overline{1}(\widetilde{kj}),ki})+\mathcal{S}^{FF}(s_{1i},s_{ki},x_{1i,ki})\\
&-\mathcal{S}^{FF}(s_{\overline{1}i},s_{ki},x_{\overline{1}i,ki})+\mathcal{S}^{FF}(s_{ki},s_{ki},1)-\mathcal{S}^{FF}(s_{(\widetilde{kj})i},s_{ki},x_{(\widetilde{kj})i,ki})\Big)\Big]\\
&\times A_3^0(1,j,k)\,B_1^{Z,0}(\overline{1},i,(\widetilde{kj}))\,J_2^2(\{p\}_2)\,. \qquad \text{(A.8)}
\end{aligned}
$$

$$
\begin{aligned}
&\tilde{B}_2^{Z,1,T}(\hat{1},i,j,k)=\\
&-J_{2,QQ}^{1,IF}(s_{1k})\,B_2^{Z,0}(1,i,j,k)\,J_2^3(\{p\}_3)\\
&-J_{2,QQ}^{1,IF}(s_{1k})\,B_2^{Z,0}(1,j,i,k)\,J_2^3(\{p\}_3)\\
&-\Big[+J_{2,QG}^{1,IF}(s_{1j})+J_{2,QG}^{1,FF}(s_{kj})+J_{2,QG}^{1,IF}(s_{1i})+J_{2,QG}^{1,FF}(s_{ki})\Big]\,\tilde{B}_2^{Z,0}(1,i,j,k)\,J_2^3(\{p\}_3)\\
&+J_{2,QQ}^{1,IF}(s_{1k})\,\tilde{B}_2^{Z,0}(1,j,i,k)\,J_2^3(\{p\}_3)\\
&+A_3^0(1,i,k)\Big[B_1^{Z,1}(\overline{1},j,(\widetilde{ki}))\,\delta(1-x_1)\,\delta(1-x_2)\\
&+\Big(+J_{2,QG}^{1,IF}(s_{\overline{1}j})+J_{2,QG}^{1,FF}(s_{(\widetilde{ki})j})\Big)\,B_1^{Z,0}(\overline{1},j,(\widetilde{ki}))\Big]\,J_2^2(\{p\}_2)\\
&+A_3^0(1,j,k)\Big[B_1^{Z,1}(\overline{1},i,(\widetilde{kj}))\,\delta(1-x_1)\,\delta(1-x_2)\\
&+\Big(+J_{2,QG}^{1,IF}(s_{\overline{1}i})+J_{2,QG}^{1,FF}(s_{(\widetilde{kj})i})\Big)\,B_1^{Z,0}(\overline{1},i,(\widetilde{kj}))\Big]\,J_2^2(\{p\}_2)\\
&+d_3^0(k,i,j)\Big[\tilde{B}_1^{Z,1}(1,(\widetilde{ij}),(\widetilde{ki}))\,\delta(1-x_1)\,\delta(1-x_2)
\end{aligned}
$$

$$
\begin{aligned}
&\quad + J^{1,IF}_{2,QQ}(s_{1(\widetilde{ki})})\, B^{Z,0}_1(1,(\widetilde{ij}),(\widetilde{ki}))\Big]\, J^2_2(\{p\}_2)\\
&+ d^0_3(k,j,i)\,\Big[\,\tilde{B}^{Z,1}_1(1,(\widetilde{ji}),(\widetilde{kj}))\,\delta(1-x_1)\,\delta(1-x_2)\\
&\quad + J^{1,IF}_{2,QQ}(s_{1(\widetilde{kj})})\, B^{Z,0}_1(1,(\widetilde{ji}),(\widetilde{kj}))\Big]\, J^2_2(\{p\}_2)\\
&+ D^0_{3,q}(1,i,j)\,\Big[\,\tilde{B}^{Z,1}_1(\overline{1},(\widetilde{ij}),k)\,\delta(1-x_1)\,\delta(1-x_2)\\
&\quad + J^{1,IF}_{2,QQ}(s_{\overline{1}k})\, B^{Z,0}_1(\overline{1},(\widetilde{ij}),k)\Big]\, J^2_2(\{p\}_2)\\
&+\Big[\, A^1_{3,q}(1,i,k)\,\delta(1-x_1)\,\delta(1-x_2)\\
&+\Big(-J^{1,IF}_{2,QQ}(s_{\overline{1}(\widetilde{ki})}) + J^{1,IF}_{2,QG}(s_{1i}) + J^{1,FF}_{2,QG}(s_{ki})\Big)\, A^0_3(1,i,k)\Big]\, B^{Z,0}_1(\overline{1},j,(\widetilde{ki}))\, J^2_2(\{p\}_2)\\
&+\Big[\, A^1_{3,q}(1,j,k)\,\delta(1-x_1)\,\delta(1-x_2)\\
&+\Big(-J^{1,IF}_{2,QQ}(s_{\overline{1}(\widetilde{kj})}) + J^{1,IF}_{2,QG}(s_{1j}) + J^{1,FF}_{2,QG}(s_{kj})\Big)\, A^0_3(1,j,k)\Big]\, B^{Z,0}_1(\overline{1},i,(\widetilde{kj}))\, J^2_2(\{p\}_2)\\
&+\Big[\, \tilde{A}^1_{3,q}(1,i,k)\,\delta(1-x_1)\,\delta(1-x_2)\\
&+\Big(+J^{1,IF}_{2,QQ}(s_{1k}) - J^{1,IF}_{2,QQ}(s_{\overline{1}(\widetilde{ki})})\Big)\, A^0_3(1,i,k)\Big]\, B^{Z,0}_1(\overline{1},j,(\widetilde{ki}))\, J^2_2(\{p\}_2)\\
&+\Big[\, \tilde{A}^1_{3,q}(1,j,k)\,\delta(1-x_1)\,\delta(1-x_2)\\
&+\Big(-J^{1,IF}_{2,QQ}(s_{\overline{1}(\widetilde{kj})}) + J^{1,IF}_{2,QQ}(s_{1k})\Big)\, A^0_3(1,j,k)\Big]\, B^{Z,0}_1(\overline{1},i,(\widetilde{kj}))\, J^2_2(\{p\}_2)\\
&+\Big[\, + J^{1,IF}_{2,QG}(s_{1j}) + J^{1,FF}_{2,QG}(s_{kj}) - J^{1,IF}_{2,QQ}(s_{1k})\\
&\quad - J^{1,IF}_{2,QG}(s_{\overline{1}j}) - J^{1,FF}_{2,QG}(s_{(\widetilde{ki})j}) + J^{1,IF}_{2,QQ}(s_{\overline{1}(\widetilde{ki})})\\
&\quad + \Big(+\mathcal{S}^{FF}(s_{1k},s_{kj},x_{1k,kj}) - \mathcal{S}^{FF}(s_{\overline{1}(\widetilde{ki})},s_{kj},x_{\overline{1}(\widetilde{ki}),kj}) - \mathcal{S}^{FF}(s_{1j},s_{kj},x_{1j,kj})\\
&\quad + \mathcal{S}^{FF}(s_{\overline{1}j},s_{kj},x_{\overline{1}j,kj}) \quad - \mathcal{S}^{FF}(s_{kj},s_{kj},1) + \mathcal{S}^{FF}(s_{(\widetilde{ki})j},s_{kj},x_{(\widetilde{ki})j,kj})\Big)\Big]\\
&\times A^0_3(1,i,k)\, B^{Z,0}_1(\overline{1},j,(\widetilde{ki}))\, J^2_2(\{p\}_2)\\
&+\Big[\, + J^{1,IF}_{2,QG}(s_{1i}) - J^{1,IF}_{2,QG}(s_{\overline{1}i}) + J^{1,FF}_{2,QG}(s_{ki})\\
&\quad - J^{1,FF}_{2,QG}(s_{(\widetilde{kj})i}) - J^{1,IF}_{2,QQ}(s_{1k}) + J^{1,IF}_{2,QQ}(s_{\overline{1}(\widetilde{kj})})\\
&\quad + \Big(+\mathcal{S}^{FF}(s_{1k},s_{ki},x_{1k,ki}) - \mathcal{S}^{FF}(s_{\overline{1}(\widetilde{kj})},s_{ki},x_{\overline{1}(\widetilde{kj}),ki}) - \mathcal{S}^{FF}(s_{1i},s_{ki},x_{1i,ki})\\
&\quad + \mathcal{S}^{FF}(s_{\overline{1}i},s_{ki},x_{\overline{1}i,ki}) \quad - \mathcal{S}^{FF}(s_{ki},s_{ki},1) + \mathcal{S}^{FF}(s_{(\widetilde{kj})i},s_{ki},x_{(\widetilde{kj})i,ki})\Big)\Big]
\end{aligned}
$$

$$\times A_3^0(1,j,k)\, B_1^{Z,0}(\overline{1},i,(\widetilde{kj}))\, J_2^2(\{p\}_2)\,. \tag{A.9}$$

$$\begin{aligned}
&\tilde{\tilde{B}}_2^{Z,1,T}(\hat{1},i,j,k) = \\
&\quad -J_{2,QQ}^{1,IF}(s_{1k})\, \tilde{B}_2^{Z,0}(1,i,j,k)\, J_2^3(\{p\}_3) \\
&\quad + A_3^0(1,i,k) \Bigg[\tilde{B}_1^{Z,1}(\overline{1},j,(\widetilde{ki}))\, \delta(1-x_1)\, \delta(1-x_2) \\
&\qquad + J_{2,QQ}^{1,IF}(s_{\overline{1}(\widetilde{ki})})\, B_1^{Z,0}(\overline{1},j,(\widetilde{ki})) \Bigg] J_2^2(\{p\}_2) \\
&\quad + A_3^0(1,j,k) \Bigg[\tilde{B}_1^{Z,1}(\overline{1},i,(\widetilde{kj}))\, \delta(1-x_1)\, \delta(1-x_2) \\
&\qquad + J_{2,QQ}^{1,IF}(s_{\overline{1}(\widetilde{kj})})\, B_1^{Z,0}(\overline{1},i,(\widetilde{kj})) \Bigg] J_2^2(\{p\}_2) \\
&\quad + \Bigg[\tilde{A}_{3,q}^1(1,i,k)\, \delta(1-x_1)\, \delta(1-x_2) \\
&\quad + \Bigg(+ J_{2,QQ}^{1,IF}(s_{1k}) - J_{2,QQ}^{1,IF}(s_{\overline{1}(\widetilde{ki})}) \Bigg) A_3^0(1,i,k) \Bigg] B_1^{Z,0}(\overline{1},j,(\widetilde{ki}))\, J_2^2(\{p\}_2) \\
&\quad + \Bigg[\tilde{A}_{3,q}^1(1,j,k)\, \delta(1-x_1)\, \delta(1-x_2) \\
&\quad + \Bigg(+ J_{2,QQ}^{1,IF}(s_{1k}) - J_{2,QQ}^{1,IF}(s_{\overline{1}(\widetilde{kj})}) \Bigg) A_3^0(1,j,k) \Bigg] B_1^{Z,0}(\overline{1},i,(\widetilde{kj}))\, J_2^2(\{p\}_2)\,.
\end{aligned} \tag{A.10}$$

$$\begin{aligned}
&\hat{B}_2^{Z,1,T}(\hat{1},i,j,k) = \\
&\quad -\Bigg[+ 2\hat{J}_{2,QG}^{1,FF}(s_{ki}) + 2\hat{J}_{2,QG}^{1,FF}(s_{kj}) \Bigg] B_2^{Z,0}(1,i,j,k)\, J_2^3(\{p\}_3) \\
&\quad + d_3^0(1,i,j) \Bigg[\hat{B}_1^{Z,1}(\overline{1},(\widetilde{ij}),k)\, \delta(1-x_1)\, \delta(1-x_2) \\
&\quad + \Bigg(+ \hat{J}_{2,QG}^{1,IF}(s_{\overline{1}(\widetilde{ij})}) + \hat{J}_{2,QG}^{1,FF}(s_{k(\widetilde{ij})}) \Bigg) B_1^{Z,0}(\overline{1},(\widetilde{ij}),k) \Bigg] J_2^2(\{p\}_2) \\
&\quad + d_3^0(k,j,i) \Bigg[\hat{B}_1^{Z,1}(1,(\widetilde{ij}),(\widetilde{kj}))\, \delta(1-x_1)\, \delta(1-x_2) \\
&\quad + \Bigg(+ \hat{J}_{2,QG}^{1,IF}(s_{1(\widetilde{ij})}) + \hat{J}_{2,QG}^{1,FF}(s_{(\widetilde{kj})(\widetilde{ij})}) \Bigg) B_1^{Z,0}(1,(\widetilde{ij}),(\widetilde{kj})) \Bigg] J_2^2(\{p\}_2) \\
&\quad + \Bigg[\hat{d}_3^1(1,i,j)\, \delta(1-x_1)\, \delta(1-x_2) \\
&\quad + \Bigg(+ 4\hat{J}_{2,QG}^{1,IF}(s_{1i}) - \hat{J}_{2,QG}^{1,IF}(s_{\overline{1}(\widetilde{ij})}) - \hat{J}_{2,QG}^{1,FF}(s_{k(\widetilde{ij})}) \Bigg) d_3^0(1,i,j) \Bigg] B_1^{Z,0}(\overline{1},(\widetilde{ji}),k)\, J_2^2(\{p\}_2) \\
&\quad + \Bigg[\hat{d}_3^1(k,j,i)\, \delta(1-x_1)\, \delta(1-x_2) \\
&\quad + \Bigg(+ 4\hat{J}_{2,QG}^{1,FF}(s_{kj}) - \hat{J}_{2,QG}^{1,FF}(s_{(\widetilde{kj})(\widetilde{ji})}) - \hat{J}_{2,QG}^{1,IF}(s_{1(\widetilde{ij})}) \Bigg) d_3^0(k,j,i) \Bigg] B_1^{Z,0}(1,(\widetilde{ji}),(\widetilde{kj}))\, J_2^2(\{p\}_2) \\
&\quad + \Bigg[+ 2\hat{J}_{2,QG}^{1,FF}(s_{kj}) - 4\hat{J}_{2,QG}^{1,IF}(s_{1i}) + 2\hat{J}_{2,QG}^{1,FF}(s_{ki}) \Bigg] d_3^0(1,i,j)\, B_1^{Z,0}(\overline{1},(\widetilde{ji}),k)\, J_2^2(\{p\}_2)
\end{aligned}$$

$$+\Big[-2\hat{J}^{1,FF}_{2,QG}(s_{kj})+2\hat{J}^{1,FF}_{2,QG}(s_{ki})\Big]d^0_3(k,j,i)\,B^{Z,0}_1(1,(\widetilde{ji}),(\widetilde{kj}))\,J^2_2(\{p\}_2)\,. \tag{A.11}$$

$$\begin{aligned}
&\hat{\tilde{B}}^{Z,1,T}_2(\hat{1},i,j,k)=\\
&\quad -4\hat{J}^{1,FF}_{2,QG}(s_{ki})\,\tilde{B}^{Z,0}_2(1,i,j,k)\,J^3_2(\{p\}_3)\\
&\quad +2\,A^0_3(1,i,k)\Big[\hat{B}^{Z,1}_1(\overline{1},j,(\widetilde{ik}))\,\delta(1-x_1)\,\delta(1-x_2)\\
&\qquad +2\hat{J}^{1,FF}_{2,QG}(s_{(\widetilde{ki})j})\,B^{Z,0}_1(\overline{1},j,(\widetilde{ik}))\Big]\,J^2_2(\{p\}_2)\\
&\quad +2\Big[\hat{A}^1_3(1,i,k)\,\delta(1-x_1)\,\delta(1-x_2)+2\hat{J}^{1,FF}_{2,QG}(s_{ki})\,A^0_3(1,i,k)\Big]\,B^{Z,0}_1(\overline{1},j,(\widetilde{ik}))\,J^2_2(\{p\}_2)\\
&\quad +\Big[+4\hat{J}^{1,FF}_{2,QG}(s_{kj})-4\hat{J}^{1,FF}_{2,QG}(s_{(\widetilde{ki})j})\Big]A^0_3(1,i,k)\,B^{Z,0}_1(\overline{1},j,(\widetilde{ik}))\,J^2_2(\{p\}_2).
\end{aligned}\tag{A.12}$$

$$\begin{aligned}
&\hat{B}^{\gamma,1,T}_{0,q\to g}(\hat{1},i,j,k)=\\
&\quad -2J^{1,IF}_{2,GQ,q'\to g}(s_{1k})\,B^{\gamma,0}_2(k,1,i,j)\,J^3_2(\{p\}_3)\\
&\quad -2J^{1,IF}_{2,GQ,q'\to g}(s_{1k})\,B^{\gamma,0}_2(k,i,1,j)\,J^3_2(\{p\}_3)\\
&\quad +4J^{1,IF}_{2,GQ,q'\to g}(s_{1k})\,D^0_3(k,1,i)\,B^{\gamma,0}_1((\widetilde{ki}),\overline{1},j)\,J^2_2(\{p\}_2)\\
&\quad +\Big[-2J^{1,IF}_{2,GQ,q'\to g}(s_{1k})+2J^{1,IF}_{2,GQ,q'\to g}(s_{(\widetilde{ki})1})\Big]A^0_3(j,i,k)\,B^{\gamma,0}_1((\widetilde{ki}),1,(\widetilde{ji}))\,J^2_2(\{p\}_2)\\
&\quad -4J^{1,IF}_{2,GQ,q'\to g}(s_{1k})\,a^0_{3,g\to q}(k,1,j)\,B^{\gamma,0}_1(i,\overline{1},(\widetilde{kj}))\,J^2_2(\{p\}_2)\\
&\quad +2J^{1,IF}_{2,GQ,q'\to g}(s_{\overline{1}k})\,d^0_{3,g}(j,i,1)\,B^{\gamma,0}_1(k,\overline{1},(\widetilde{ji}))\,J^2_2(\{p\}_2)\\
&\quad -2J^{1,IF}_{2,GQ,q'\to g}(s_{\overline{1}(\widetilde{ki})})\,d^0_{3,g}(k,i,1)\,B^{\gamma,0}_1((\widetilde{ki}),\overline{1},j)\,J^2_2(\{p\}_2)\\
&\quad -2J^{1,IF}_{2,GQ,q'\to g}(s_{1k})\,a^0_{3,g\to q}(k,1,j)\,B^{\gamma,0}_1(\overline{1},i,(\widetilde{jk}))\,J^2_2(\{p\}_2)\\
&\quad -2J^{1,IF}_{2,GQ,q'\to g}(s_{1k})\,a^0_{3,g\to q}(j,1,k)\,B^{\gamma,0}_1((\widetilde{jk}),i,\overline{1})\,J^2_2(\{p\}_2)\,.
\end{aligned}\tag{A.13}$$

$$\begin{aligned}
&\hat{\tilde{B}}^{\gamma,1,T}_{0,q\to g}(\hat{1},i,j,k)=\\
&\quad -\Big[+J^{1,IF}_{2,GQ,q'\to g}(s_{1k})+J^{1,IF}_{2,GQ,q'\to g}(s_{1j})\Big]\,\tilde{B}^{\gamma,0}_2(k,1,i,j)\,J^3_2(\{p\}_3)\\
&\quad +\Big[+J^{1,IF}_{2,GQ,q'\to g}(s_{1k})+J^{1,IF}_{2,GQ,q'\to g}(s_{1j})\Big]A^0_3(k,i,j)\,B^{\gamma,0}_1((\widetilde{ki}),1,(\widetilde{ij}))\,J^2_2(\{p\}_2)\\
&\quad +\Big[-J^{1,IF}_{2,GQ,q'\to g}(s_{1k})-J^{1,IF}_{2,GQ,q'\to g}(s_{1j})\Big]a^0_{3,g\to q}(k,1,j)\,B^{\gamma,0}_1(\overline{1},i,(\widetilde{kj}))\,J^2_2(\{p\}_2)\\
&\quad +\Big[-J^{1,IF}_{2,GQ,q'\to g}(s_{1k})-J^{1,IF}_{2,GQ,q'\to g}(s_{1j})\Big]a^0_{3,g\to q}(j,1,k)\,B^{\gamma,0}_1((\widetilde{kj}),i,\overline{1})\,J^2_2(\{p\}_2)\,.
\end{aligned}\tag{A.14}$$

$$C^{Z,1,T}_0(\hat{1};j,k;i)=$$

$$
\begin{aligned}
&-\Big[+ J^{1,IF}_{2,QQ}(s_{1j}) + J^{1,FF}_{2,QQ}(s_{ik}) \Big]\, C^{Z,0}_0(1;j,k;i)\, J^3_2(\{p\}_3) \\
&+\frac{1}{2}\, E^0_3(i,j,k) \Big[B^{Z,1}_{1,q}(1,(\widetilde{jk}),(\widetilde{ij}))\, \delta(1-x_1)\, \delta(1-x_2) \\
&+ \Big(+ J^{1,FF}_{2,QG}(s_{(\widetilde{ij})(\widetilde{jk})}) + J^{1,IF}_{2,QG}(s_{1(\widetilde{jk})}) \Big)\, B^{Z,0}_{1,q}(1,(\widetilde{jk}),(\widetilde{ij})) \Big]\, J^2_2(\{p\}_2) \\
&+\frac{1}{2}\, E^0_{3,q}(1,j,k) \Big[B^{Z,1}_{1,q}(\overline{1},(\widetilde{jk}),i)\, \delta(1-x_1)\, \delta(1-x_2) \\
&+ \Big(+ J^{1,FF}_{2,QG}(s_{i(\widetilde{jk})}) + J^{1,IF}_{2,QG}(s_{\overline{1}(\widetilde{jk})}) \Big)\, B^{Z,0}_{1,q}(\overline{1},(\widetilde{jk}),i) \Big]\, J^2_2(\{p\}_2) \\
&+\frac{1}{2} \Big[E^1_3(i,j,k)\, \delta(1-x_1)\, \delta(1-x_2) \\
&+ \Big(+ J^{1,FF}_{2,QQ}(s_{ij}) + J^{1,FF}_{2,QQ}(s_{ik}) - 2J^{1,FF}_{2,QG}(s_{(\widetilde{ij})(\widetilde{jk})}) \Big)\, E^0_3(i,j,k) \Big]\, B^{Z,0}_{1,q}(1,(\widetilde{jk}),(\widetilde{ij}))\, J^2_2(\{p\}_2) \\
&+\frac{1}{2} \Big[E^1_3(1,j,k)\, \delta(1-x_1)\, \delta(1-x_2) \\
&+ \Big(+ J^{1,IF}_{2,QQ}(s_{1j}) + J^{1,IF}_{2,QQ}(s_{1k}) - 2J^{1,IF}_{2,QG}(s_{\overline{1}(\widetilde{jk})}) \Big)\, E^0_3(1,j,k) \Big]\, B^{Z,0}_{1,q}(\overline{1},(\widetilde{jk}),i)\, J^2_2(\{p\}_2) \\
&- E^0_{3,q'\to g}(k,1,i) \Big[B^{Z,1}_{1,Q}((\widetilde{ik}),\overline{1},j)\, \delta(1-x_1)\, \delta(1-x_2) \\
&+ \Big(+ J^{1,IF}_{2,GQ}(s_{\overline{1}(\widetilde{ik})}) + J^{1,IF}_{2,GQ}(s_{\overline{1}j}) \\
&\quad - J^{1,IF}_{2,QG,g\to q}(s_{\overline{1}(\widetilde{ik})}) - J^{1,IF}_{2,QG,g\to q}(s_{\overline{1}j}) \Big)\, B^{Z,0}_{1,Q}((\widetilde{ik}),\overline{1},j) \Big]\, J^2_2(\{p\}_2) \\
&-\Big[E^1_{3,q'}(k,1,i)\, \delta(1-x_1)\, \delta(1-x_2) \\
&+ \Big(+ J^{1,IF}_{2,QQ}(s_{1k}) + J^{1,FF}_{2,QQ}(s_{ki}) \\
&\quad - 2J^{1,IF}_{2,GQ}(s_{\overline{1}(\widetilde{ki})}) + 2J^{1,IF}_{2,QG,g\to q}(s_{\overline{1}(\widetilde{ki})}) \Big)\, E^0_{3,q'\to g}(k,1,i) \Big]\, B^{Z,0}_{1,Q}((\widetilde{ki}),\overline{1},j)\, J^2_2(\{p\}_2) \\
&-\Big[+ J^{1,IF}_{2,QQ}(s_{1j}) - J^{1,IF}_{2,QQ}(s_{1k}) + J^{1,FF}_{2,QQ}(s_{kj}) - J^{1,FF}_{2,QQ}(s_{j(\widetilde{ki})}) \\
&\quad + J^{1,IF}_{2,GQ}(s_{\overline{1}(\widetilde{ki})}) - J^{1,IF}_{2,GQ}(s_{\overline{1}j}) - J^{1,IF}_{2,QG,g\to q}(s_{\overline{1}(\widetilde{ki})}) + J^{1,IF}_{2,QG,g\to q}(s_{\overline{1}j}) \\
&\quad + \Big(- \mathcal{S}^{FF}(s_{1j},s_{ki},x_{1j,ki}) + \mathcal{S}^{FF}(s_{1k},s_{ki},x_{1k,ki}) - \mathcal{S}^{FF}(s_{kj},s_{ki},x_{kj,ki}) \\
&\quad + \mathcal{S}^{FF}(s_{j(\widetilde{ki})},s_{ki},x_{j(\widetilde{ki}),ki}) - \mathcal{S}^{FF}(s_{\overline{1}(\widetilde{ki})},s_{ki},x_{\overline{1}(\widetilde{ki}),ki}) + \mathcal{S}^{FF}(s_{\overline{1}j},s_{ki},x_{\overline{1}j,ki}) \Big) \Big] \\
&\times E^0_{3,q'\to g}(k,1,i)\, B^{Z,0}_{1,Q}((\widetilde{ki}),\overline{1},j)\, J^2_2(\{p\}_2)\,. \qquad \text{(A.15)}
\end{aligned}
$$

$$
\begin{aligned}
&\tilde{C}^{Z,1,T}_0(\hat{1};j,k;i) = \\
&\quad + \Big[+ 2J^{1,IF}_{2,QQ}(s_{1k}) - 2J^{1,FF}_{2,QQ}(s_{ki}) - J^{1,IF}_{2,QQ}(s_{1i})
\end{aligned}
$$

$$
\begin{aligned}
&-J^{1,FF}_{2,QQ}(s_{jk}) + 2J^{1,FF}_{2,QQ}(s_{ij}) - 2J^{1,IF}_{2,QQ}(s_{1j})\Big]\, C^{Z,0}_0(1;j,k;i)\, J^3_2(\{p\}_3)\\
&+\frac{1}{2}\left[\,\tilde{E}^1_3(i,j,k)\,\delta(1-x_1)\,\delta(1-x_2) + J^{1,FF}_{2,QQ}(s_{jk})\,E^0_3(i,j,k)\right]\\
&\times B^{Z,0}_{1,q}(1,(\widetilde{jk}),(\widetilde{ij}))\, J^2_2(\{p\}_2)\\
&+\frac{1}{2}\left[\,\tilde{E}^1_{3,q}(1,j,k)\,\delta(1-x_1)\,\delta(1-x_2) + J^{1,FF}_{2,QQ}(s_{jk})\,E^0_{3,q}(1,j,k)\right]\\
&\times B^{Z,0}_{1,q}(\overline{1},(\widetilde{jk}),i)\, J^2_2(\{p\}_2)\\
&+\frac{1}{2}\; E^0_3(i,j,k)\left[\,\tilde{B}^{Z,1}_{1,q}(1,(\widetilde{jk}),(\widetilde{ij}))\,\delta(1-x_1)\,\delta(1-x_2)\right.\\
&\quad\left. + J^{1,IF}_{2,QQ}(s_{1(\widetilde{ij})})\,B^{Z,0}_{1,q}(1,(\widetilde{jk}),(\widetilde{ij}))\right] J^2_2(\{p\}_2)\\
&+\frac{1}{2}\; E^0_{3,q}(1,j,k)\left[\,\tilde{B}^{Z,1}_{1,q}(\overline{1},(\widetilde{jk}),i)\,\delta(1-x_1)\,\delta(1-x_2)\right.\\
&\quad\left. + J^{1,IF}_{2,QQ}(s_{\overline{1}i})\,B^{Z,0}_{1,q}(\overline{1},(\widetilde{jk}),i)\right] J^2_2(\{p\}_2)\\
&-\Big[+ J^{1,IF}_{2,QQ}(s_{1k}) + J^{1,FF}_{2,QQ}(s_{ij}) - J^{1,IF}_{2,QQ}(s_{1j}) - J^{1,FF}_{2,QQ}(s_{ki})\\
&+\Big(- \mathcal{S}^{FF}(s_{1k},s_{kj},x_{1k,kj}) - \mathcal{S}^{FF}(s_{ij},s_{kj},x_{ij,kj}) + \mathcal{S}^{FF}(s_{1j},s_{kj},x_{1j,kj})\\
&+\mathcal{S}^{FF}(s_{ki},s_{kj},x_{ki,kj})\Big)\Big]\, E^0_3(i,j,k)\, B^{Z,0}_{1,q}(1,(\widetilde{jk}),(\widetilde{ij}))\, J^2_2(\{p\}_2)\\
&-\Big[+ J^{1,IF}_{2,QQ}(s_{1k}) + J^{1,FF}_{2,QQ}(s_{ij}) - J^{1,IF}_{2,QQ}(s_{1j}) - J^{1,FF}_{2,QQ}(s_{ki})\\
&+\Big(- \mathcal{S}^{FF}(s_{1k},s_{kj},x_{1k,kj}) - \mathcal{S}^{FF}(s_{ij},s_{kj},x_{ij,kj}) + \mathcal{S}^{FF}(s_{1j},s_{kj},x_{1j,kj})\\
&+\mathcal{S}^{FF}(s_{ki},s_{kj},x_{ki,kj})\Big)\Big]\, E^0_3(1,j,k)\, B^{Z,0}_{1,q}(\overline{1},(\widetilde{jk}),i)\, J^2_2(\{p\}_2)\\
&-\frac{1}{2}\; E^0_{3,q'\to g}(j,1,i)\left[\,\tilde{B}^{Z,1}_{1,Q}(k,\overline{1},(\widetilde{ij}))\,\delta(1-x_1)\,\delta(1-x_2)\right.\\
&\quad\left. + J^{1,FF}_{2,QQ}(s_{k(\widetilde{ij})})\,B^{Z,0}_{1,Q}(k,\overline{1},(\widetilde{ij}))\right] J^2_2(\{p\}_2)\\
&-\frac{1}{2}\; E^0_{3,q'\to g}(k,1,i)\left[\,\tilde{B}^{Z,1}_{1,Q}((\widetilde{ik}),\overline{1},j)\,\delta(1-x_1)\,\delta(1-x_2)\right.\\
&\quad\left. + J^{1,FF}_{2,QQ}(s_{j(\widetilde{ik})})\,B^{Z,0}_{1,Q}((\widetilde{ik}),\overline{1},j)\right] J^2_2(\{p\}_2)\\
&-\frac{1}{2}\left[\,\tilde{E}^1_{3,q'}(j,1,i)\,\delta(1-x_1)\,\delta(1-x_2) + J^{1,IF}_{2,QQ}(s_{1i})\,E^0_{3,q'\to g}(j,1,i)\right]\\
&\times B^{Z,0}_{1,Q}(k,\overline{1},(\widetilde{ij}))\, J^2_2(\{p\}_2)\\
&-\frac{1}{2}\left[\,\tilde{E}^1_{3,q'}(k,1,i)\,\delta(1-x_1)\,\delta(1-x_2) + J^{1,IF}_{2,QQ}(s_{1i})\,E^0_{3,q'\to g}(k,1,i)\right]
\end{aligned}
$$

$$
\begin{aligned}
&\times B^{Z,0}_{1,Q}((\widetilde{ik}),\overline{1},j)\,J^2_2(\{p\}_2)\\
&+\Bigg[+J^{1,IF}_{2,QQ}(s_{1k})+J^{1,FF}_{2,QQ}(s_{ij})-J^{1,IF}_{2,QQ}(s_{1j})-J^{1,FF}_{2,QQ}(s_{ki})\\
&+\Bigg(-\mathcal{S}^{FF}(s_{1k},s_{jk},x_{1k,jk})-\mathcal{S}^{FF}(s_{ij},s_{jk},x_{ij,jk})+\mathcal{S}^{FF}(s_{1j},s_{jk},x_{1j,jk})\\
&+\mathcal{S}^{FF}(s_{ki},s_{jk},x_{ki,jk})\Bigg)\Bigg]\,E^0_3(j,1,i)\,B^{Z,0}_{1,Q}(k,\overline{1},(\widetilde{ij}))\,J^2_2(\{p\}_2)\\
&+\Bigg[+J^{1,IF}_{2,QQ}(s_{1j})+J^{1,FF}_{2,QQ}(s_{ik})-J^{1,IF}_{2,QQ}(s_{1k})-J^{1,FF}_{2,QQ}(s_{ji})\\
&+\Bigg(-\mathcal{S}^{FF}(s_{1j},s_{kj},x_{1j,kj})-\mathcal{S}^{FF}(s_{ik},s_{kj},x_{ik,kj})+\mathcal{S}^{FF}(s_{1k},s_{kj},x_{1k,kj})\\
&+\mathcal{S}^{FF}(s_{ji},s_{kj},x_{ji,kj})\Bigg)\Bigg]\,E^0_3(k,1,i)\,B^{Z,0}_{1,Q}(j,\overline{1},(\widetilde{ik}))\,J^2_2(\{p\}_2)\,.
\end{aligned}
\tag{A.16}
$$

$$
\begin{aligned}
&\hat{C}^{Z,1,T}_0(\hat{1};j,k;i)=\\
&\quad+\frac{1}{2}\,E^0_3(i,j,k)\,\hat{B}^{Z,1}_{1,q}(1,(\widetilde{jk}),(\widetilde{ij}))\,\delta(1-x_1)\,\delta(1-x_2)\\
&\quad+\frac{1}{2}\,E^0_{3,q}(1,j,k)\,\hat{B}^{Z,1}_{1,q}(\overline{1},(\widetilde{jk}),i)\,\delta(1-x_1)\,\delta(1-x_2)\\
&\quad+\frac{1}{2}\,\hat{E}^1_3(i,j,k)\,B^{Z,0}_{1,q}(1,(\widetilde{jk}),(\widetilde{ij}))\,\delta(1-x_1)\,\delta(1-x_2)\\
&\quad+\frac{1}{2}\,\hat{E}^1_{3,q}(1,j,k)\,B^{Z,0}_{1,q}(\overline{1},(\widetilde{jk}),i)\,\delta(1-x_1)\,\delta(1-x_2)\\
&\quad-E^0_{3,q'\to g}(j,1,i)\,\hat{B}^{Z,1}_{1,Q}(k,\overline{1},(\widetilde{ij}))\,\delta(1-x_1)\,\delta(1-x_2)\\
&\quad-\hat{E}^1_{3,q'}(j,1,i)\,B^{Z,0}_{1,Q}(k,\overline{1},(\widetilde{ij}))\,\delta(1-x_1)\,\delta(1-x_2)\,.
\end{aligned}
\tag{A.17}
$$

$$
\begin{aligned}
&D^{Z,1,T}_0(\hat{1},j;k,i)=\\
&\quad+\Bigg[+J^{1,IF}_{2,QQ}(s_{1k})+J^{1,FF}_{2,QQ}(s_{ji})\Bigg]\,D^{Z,0}_0(1,j,k,i)\,J^3_2(\{p\}_3)\,.
\end{aligned}
\tag{A.18}
$$

$$
\begin{aligned}
&\tilde{D}^{Z,1,T}_0(\hat{1},j;k,i)=\\
&\quad+\Bigg[+J^{1,IF}_{2,QQ}(s_{1k})-J^{1,IF}_{2,QQ}(s_{1i})-J^{1,IF}_{2,QQ}(s_{1j})\\
&\quad-J^{1,FF}_{2,QQ}(s_{jk})+J^{1,FF}_{2,QQ}(s_{ji})-J^{1,FF}_{2,QQ}(s_{ki})\Bigg]\,D^{Z,0}_0(1,j,k,i)\,J^3_2(\{p\}_3)\,.
\end{aligned}
\tag{A.19}
$$

A.3 Virtual-virtual

$$
\begin{aligned}
&B^{2,Z,U}_1(\hat{1},3,4)=\\
&\quad+\Bigg[-\frac{1}{2}\,\mathcal{D}^0_{3,q}(s_{13})+\Gamma^{(1)}_{qq}(z_1)-\frac{1}{2}\,\mathcal{D}^0_3(s_{34})\Bigg]\left(-\frac{b_0}{\epsilon}B^{Z,0}_1(1,3,4)+B^{Z,1}_1(1,3,4)\right)\\
&\quad+\Bigg[-\frac{1}{8}\,\mathcal{D}^0_{3,q}(s_{13})\otimes\mathcal{D}^0_{3,q}(s_{13})+\frac{1}{2}\,\Gamma^{(1)}_{qq}(z_1)\otimes\mathcal{D}^0_{3,q}(s_{13})-\frac{1}{4}\,\mathcal{D}^0_{3,q}(s_{13})\otimes\mathcal{D}^0_3(s_{34})
\end{aligned}
$$

$$
\begin{aligned}
&- \frac{1}{2}\,\Gamma^{(1)}_{qq}(z_1)\otimes\Gamma^{(1)}_{qq}(z_1) + \frac{1}{2}\,\Gamma^{(1)}_{qq}(z_1)\otimes\mathcal{D}^0_3(s_{34}) - \frac{1}{8}\,\mathcal{D}^0_3(s_{34})\otimes\mathcal{D}^0_3(s_{34})\Big]B_1^{Z,0}(1,3,4)\\
+\Big[&-\frac{b_0}{2\epsilon}\left(\frac{s_{34}}{\mu_R^2}\right)^{-\epsilon}\mathcal{D}^0_3(s_{34}) + \frac{1}{4}\,\mathcal{D}^0_3(s_{34})\otimes\mathcal{D}^0_3(s_{34}) - \frac{1}{2}\,\mathcal{D}^0_4(s_{34})\\
&- \frac{1}{2}\,\mathcal{D}^1_3(s_{34})\Big]B_1^{Z,0}(1,3,4)\\
+\Big[&-\frac{b_0}{2\epsilon}\left(\frac{s_{13}}{\mu_R^2}\right)^{-\epsilon}\mathcal{D}^0_{3,q}(s_{13}) + \frac{1}{4}\,\mathcal{D}^0_{3,q}(s_{13})\otimes\mathcal{D}^0_{3,q}(s_{13}) - \frac{1}{2}\,\mathcal{D}^0_{4,q}(s_{13})\\
&- \frac{1}{2}\,\mathcal{D}^1_{3,q}(s_{13}) + \Gamma^{(2)}_{qq}(z_1)\Big]B_1^{Z,0}(1,3,4)\\
+\Big[&+\frac{1}{2}\,\tilde{\mathcal{A}}^0_{4,q}(s_{14}) + \tilde{\mathcal{A}}^1_{3,q}(s_{14}) - \frac{1}{2}\,\mathcal{A}^0_{3,q}(s_{14})\otimes\mathcal{A}^0_{3,q}(s_{14})\Big]B_1^{Z,0}(1,3,4)\,.
\end{aligned}
\tag{A.20}
$$

$$
\begin{aligned}
&\tilde{B}_1^{2,Z,U}(\hat{1},3,4) =\\
&+\Big[-\frac{1}{2}\,\mathcal{D}^0_{3,q}(s_{13}) + \Gamma^{(1)}_{qq}(z_1) - \frac{1}{2}\,\mathcal{D}^0_3(s_{34})\Big]\tilde{B}_3^{Z,1}(1,3,4)\\
&+\Big[-\mathcal{A}^0_{3,q}(s_{14}) + \Gamma^{(1)}_{qq}(z_1)\Big]\left(-\frac{b_0}{\epsilon}B_1^{Z,0}(1,3,4) + B_1^{Z,1}(1,3,4)\right)\\
&+\Big[-\frac{1}{2}\,\mathcal{D}^0_{3,q}(s_{13})\otimes\mathcal{A}^0_{3,q}(s_{14}) + \frac{1}{2}\,\Gamma^{(1)}_{qq}(z_1)\otimes\mathcal{D}^0_{3,q}(s_{13}) + \Gamma^{(1)}_{qq}(z_1)\otimes\mathcal{A}^0_{3,q}(s_{14})\\
&\quad- \Gamma^{(1)}_{qq}(z_1)\otimes\Gamma^{(1)}_{qq}(z_1)\Big]B_1^{Z,0}(1,3,4)\\
&+\Big[-\frac{1}{2}\,\mathcal{D}^0_3(s_{34})\otimes\mathcal{A}^0_{3,q}(s_{14}) + \frac{1}{2}\,\Gamma^{(1)}_{qq}(z_1)\otimes\mathcal{D}^0_3(s_{34})\Big]B_1^{Z,0}(1,3,4)\\
&+\Big[-\frac{b_0}{\epsilon}\left(\frac{s_{14}}{\mu_R^2}\right)^{-\epsilon}\mathcal{A}^0_{3,q}(s_{14}) + \mathcal{A}^0_{3,q}(s_{14})\otimes\mathcal{A}^0_{3,q}(s_{14}) - \mathcal{A}^0_{4,q}(s_{14})\\
&\quad- \mathcal{A}^1_{3,q}(s_{14}) + \Gamma^{(2)}_{qq}(z_1)\Big]B_1^{Z,0}(1,3,4)\\
&+\Big[-\frac{1}{2}\,\tilde{\mathcal{A}}^0_{4,q}(s_{14}) - \tilde{\mathcal{A}}^1_{3,q}(s_{14}) - \mathcal{C}^0_{4,\bar{q},\bar{q}q\bar{q}}(s_{14})\\
&\quad- 2\,\mathcal{C}^0_{4,q}(s_{14}) - \tilde{\tilde{\Gamma}}^{(2)}_{qq}(z_1)\Big]B_1^{Z,0}(1,3,4)\\
&+\Big[-\mathcal{C}^0_{4,\bar{q},q\bar{q}\bar{q}}(s_{14}) - \Gamma^{(2)}_{q\bar{q}}t(z_1)\Big]B_1^{Z,0}(4,3,1)\,.
\end{aligned}
\tag{A.21}
$$

$$
\begin{aligned}
&\tilde{\tilde{B}}_1^{2,Z,U}(\hat{1},3,4) =\\
&+\Big[-\mathcal{A}^0_{3,q}(s_{14}) + \Gamma^{(1)}_{qq}(z_1)\Big]\tilde{B}_3^{Z,1}(1,3,4)\\
&+\Big[+\Gamma^{(1)}_{qq}(z_1)\otimes\mathcal{A}^0_{3,q}(s_{14}) - \frac{1}{2}\,\Gamma^{(1)}_{qq}(z_1)\otimes\Gamma^{(1)}_{qq}(z_1) - \frac{1}{2}\,\tilde{\mathcal{A}}^0_{4,q}(s_{14})\\
&\quad- \tilde{\mathcal{A}}^1_{3,q}(s_{14}) - \mathcal{C}^0_{4,\bar{q},\bar{q}q\bar{q}}(s_{14}) - 2\,\mathcal{C}^0_{4,q}(s_{14})
\end{aligned}
$$

$$
\begin{aligned}
&\quad - \widetilde{\widetilde{\Gamma}}^{(2)}_{qq}(z_1)\Big] B_1^{Z,0}(1,3,4) \\
&+\Big[- \mathcal{C}^0_{4,\bar{q},q\bar{q}\bar{q}}(s_{14}) - \Gamma^{(2)}_{q\bar{q}} t(z_1)\Big] B_1^{Z,0}(4,3,1)\,. \qquad \text{(A.22)}
\end{aligned}
$$

$$
\begin{aligned}
&\hat{B}_1^{2,Z,U}(\hat{1},3,4) = \\
&+\Big[-\frac{1}{2}\,\mathcal{D}^0_3(s_{34}) - \frac{1}{2}\,\mathcal{D}^0_{3,q}(s_{13}) + \Gamma^{(1)}_{qq}(z_1)\Big] \left(-\frac{b_F}{\epsilon} B_1^{Z,0}(1,3,4) + \hat{B}_1^{Z,1}(1,3,4)\right) \\
&+\Big[+\frac{1}{2}\,\mathcal{E}^0_{3,q}(s_{13}) + \frac{1}{2}\,\mathcal{E}^0_3(s_{34})\Big] \left(+\frac{b_0}{\epsilon} B_1^{Z,0}(1,3,4) - B_1^{Z,1}(1,3,4)\right) \\
&+\Big[-\frac{1}{4}\,\mathcal{D}^0_3(s_{34}) \otimes \mathcal{E}^0_{3,q}(s_{13}) - \frac{1}{4}\,\mathcal{D}^0_{3,q}(s_{13}) \otimes \mathcal{E}^0_{3,q}(s_{13}) + \frac{1}{2}\,\Gamma^{(1)}_{qq}(z_1) \otimes \mathcal{E}^0_{3,q}(s_{13}) \\
&\quad - \frac{1}{4}\,\mathcal{D}^0_3(s_{34}) \otimes \mathcal{E}^0_3(s_{34}) - \frac{1}{4}\,\mathcal{D}^0_{3,q}(s_{13}) \otimes \mathcal{E}^0_3(s_{34}) + \frac{1}{2}\,\Gamma^{(1)}_{qq}(z_1) \otimes \mathcal{E}^0_3(s_{34})\Big] B_1^{Z,0}(1,3,4) \\
&+\Big[-\frac{b_F}{2\epsilon}\left(\frac{s_{34}}{\mu_R^2}\right)^{-\epsilon} \mathcal{D}^0_3(s_{34}) - \frac{b_0}{2\epsilon}\left(\frac{s_{34}}{\mu_R^2}\right)^{-\epsilon} \mathcal{E}^0_3(s_{34}) + \frac{1}{2}\,\mathcal{D}^0_3(s_{34}) \otimes \mathcal{E}^0_3(s_{34}) \\
&\quad - \mathcal{E}^0_4(s_{34}) - \frac{1}{2}\,\mathcal{E}^1_3(s_{34}) - \frac{1}{2}\,\hat{\mathcal{D}}^1_3(s_{34})\Big] B_1^{Z,0}(1,3,4) \\
&+\Big[-\frac{b_0}{2\epsilon}\left(\frac{s_{13}}{\mu_R^2}\right)^{-\epsilon} \mathcal{E}^0_{3,q}(s_{13}) - \frac{b_F}{2\epsilon}\left(\frac{s_{13}}{\mu_R^2}\right)^{-\epsilon} \mathcal{D}^0_{3,q}(s_{13}) + \frac{1}{2}\,\mathcal{D}^0_{3,q}(s_{13}) \otimes \mathcal{E}^0_{3,q}(s_{13}) \\
&\quad - \mathcal{E}^0_{4,q}(s_{13}) - \frac{1}{2}\,\mathcal{E}^1_{3,q}(s_{13}) - \frac{1}{2}\,\hat{\mathcal{D}}^1_{3,q}(s_{13}) \\
&\quad + \Gamma^{(2)}_{qq,F}(z_1)\Big] B_1^{Z,0}(1,3,4)\,. \qquad \text{(A.23)}
\end{aligned}
$$

$$
\begin{aligned}
&\hat{B}_{1,q\to g}^{2,Z,U}(\hat{1},3,4) = \\
&+\Big[+\,\mathcal{E}^0_{3,q'\to g}(s_{13}) + S_{q\to g}\,\Gamma^{(1)}_{gq}(z_1)\Big] \left(-\frac{b_0}{\epsilon} B_1^{Z,0}(3,1,4) + B_1^{Z,1}(3,1,4)\right) \\
&+\Big[+\,\mathcal{D}^0_{3,g\to g}(s_{13}) \otimes \mathcal{E}^0_{3,q'\to g}(s_{13}) + \mathcal{D}^0_{3,g\to g}(s_{14}) \otimes \mathcal{E}^0_{3,q'\to g}(s_{13}) - \Gamma^{(1)}_{gg}(z_1) \otimes \mathcal{E}^0_{3,q'\to g}(s_{13}) \\
&\quad + S_{q\to g}\,\mathcal{D}^0_{3,g\to g}(s_{13}) \otimes \Gamma^{(1)}_{gq}(z_1) + S_{q\to g}\,\mathcal{D}^0_{3,g\to g}(s_{14}) \otimes \Gamma^{(1)}_{gq}(z_1) - S_{q\to g}\,\Gamma^{(1)}_{gg}(z_1) \otimes \Gamma^{(1)}_{gq}(z_1)\Big] B_1^{Z,0}(3,1,4) \\
&+\Big[+\frac{1}{2} S_{q\to g}\,\Gamma^{(1)}_{gg}(z_1) \otimes \Gamma^{(1)}_{gq}(z_1) - S_{q\to g}\,\mathcal{A}^0_{3,g\to q}(s_{14}) \otimes \Gamma^{(1)}_{gq}(z_1) + 2 S_{q\to g}\,\mathcal{D}^0_{3,g\to q}(s_{13}) \otimes \Gamma^{(1)}_{gq}(z_1) \\
&\quad - \frac{1}{2} S_{q\to g}\,\Gamma^{(1)}_{gq}(z_1) \otimes \Gamma^{(1)}_{qq}(z_1) + \frac{b_0}{\epsilon}\,\mathcal{E}^0_{3,q'\to g}(s_{13}) \left(\frac{s_{13}}{\mu_R^2}\right)^{-\epsilon} - 2\,\mathcal{D}^0_{3,g\to g}(s_{13}) \otimes \mathcal{E}^0_{3,q'\to g}(s_{13}) \\
&\quad + \Gamma^{(1)}_{gg}(z_1) \otimes \mathcal{E}^0_{3,q'\to g}(s_{13}) - \Gamma^{(1)}_{qq}(z_1) \otimes \mathcal{E}^0_{3,q'\to g}(s_{13}) + S_{q\to g}\,\Gamma^{(2)}_{gq}(z_1) \\
&\quad + \mathcal{E}^0_{4,q'}(s_{13}) + \mathcal{E}^0_{4,\bar{q}'}(s_{13}) + \mathcal{E}^1_{3,q'}(s_{13}) \\
&\quad - \mathcal{B}^0_{4,q'}(s_{14})\Big] B_1^{Z,0}(3,1,4)\,. \qquad \text{(A.24)}
\end{aligned}
$$

$$
\begin{aligned}
&\hat{B}^{2,Z,U}_{1,q\to Q}(\hat{1},3,4) = \\
&\quad + \Big[-\ \mathcal{B}^0_{4,q'}(s_{14}) - S_{q\to g}\,\mathcal{A}^0_{3,g\to q}(s_{14}) \otimes \Gamma^{(1)}_{gq}(z_1) - \ \Gamma^{(1)}_{gq}(z_1) \otimes \Gamma^{(1)}_{qg}(z_1) \\
&\qquad + \ \Gamma^{(2)}_{q\bar{Q}}(z_1) + \ \Gamma^{(2)}_{q\bar{Q}}(z_1) \Big] \bar{B}^{Z,0}_1(1,3,4)\,. \qquad \text{(A.25)}
\end{aligned}
$$

$$
\begin{aligned}
&\hat{\tilde{B}}^{2,Z,U}_1(\hat{1},3,4) = \\
&\quad + \Big[+\ \mathcal{A}^0_{3,q}(s_{14}) - \ \Gamma^{(1)}_{qq}(z_1) \Big] \left(-\frac{b_F}{\epsilon} B^{Z,0}_1(1,3,4) + \hat{B}^{Z,1}_1(1,3,4) \right) \\
&\quad + \Big[+\frac{1}{2}\ \mathcal{E}^0_{3,q}(s_{13}) + \frac{1}{2}\ \mathcal{E}^0_3(s_{34}) \Big] \tilde{B}^{Z,1}_3(1,3,4) \\
&\quad + \Big[+\frac{1}{2}\ \mathcal{E}^0_3(s_{34}) \otimes \mathcal{A}^0_{3,q}(s_{14}) + \frac{1}{2}\ \mathcal{E}^0_{3,q}(s_{13}) \otimes \mathcal{A}^0_{3,q}(s_{14}) - \frac{1}{2}\ \Gamma^{(1)}_{qq}(z_1) \otimes \mathcal{E}^0_3(s_{34}) \\
&\qquad - \frac{1}{2}\ \Gamma^{(1)}_{qq}(z_1) \otimes \mathcal{E}^0_{3,q}(s_{13}) \Big] B^{Z,0}_1(1,3,4) \\
&\quad + \Big[+\frac{1}{2}\ \tilde{\mathcal{E}}^0_{4,q}(s_{13}) + \frac{1}{2}\ \tilde{\mathcal{E}}^1_{3,q}(s_{13}) - \ \Gamma^{(2)}_{qq,F}(z_1) \Big] B^{Z,0}_1(1,3,4) \\
&\quad + \Big[+\frac{1}{2}\ \tilde{\mathcal{E}}^0_4(s_{34}) + \frac{1}{2}\ \tilde{\mathcal{E}}^1_3(s_{34}) \Big] B^{Z,0}_1(1,3,4) \\
&\quad + \Big[+\frac{b_F}{\epsilon} \left(\frac{s_{14}}{\mu_R^2} \right)^{-\epsilon} \mathcal{A}^0_{3,q}(s_{14}) + \ \mathcal{B}^0_{4,q}(s_{14}) + \ \hat{\mathcal{A}}^1_{3,q}(s_{14}) \Big] B^{Z,0}_1(1,3,4)\,. \qquad \text{(A.26)}
\end{aligned}
$$

$$
\begin{aligned}
&\hat{\tilde{B}}^{2,Z,U}_{1,q\to Q}(\hat{1},3,4) = \\
&\quad + \Big[+\ \mathcal{B}^0_{4,q'}(s_{14}) - \ \Gamma^{(2)}_{qQ}(z_1) - \ \Gamma^{(2)}_{q\bar{Q}}(z_1) \\
&\qquad + \ \Gamma^{(1)}_{gq}(z_1) \otimes \Gamma^{(1)}_{qg}(z_1) + S_{q\to g}\,\mathcal{A}^0_{3,g\to q}(s_{14}) \otimes \Gamma^{(1)}_{gq}(z_1) \Big] \bar{B}^{Z,0}_1(1,3,4)\,. \qquad \text{(A.27)}
\end{aligned}
$$

$$
\begin{aligned}
&\hat{\tilde{B}}^{2,Z,U}_{1,q\to g}(\hat{1},3,4) = \\
&\quad + \Big[-S_{q\to g}\,\Gamma^{(1)}_{gq}(z_1) - \frac{1}{2}\ \mathcal{E}^0_{3,q'\to g}(s_{13}) - \frac{1}{2}\ \mathcal{E}^0_{3,q'\to g}(s_{14}) \Big] \tilde{B}^{Z,1}_3(3,1,4) \\
&\quad + \Big[-S_{q\to g}\,\Gamma^{(1)}_{gq}(z_1) \otimes \mathcal{A}^0_3(s_{34}) - \frac{1}{2}\ \mathcal{E}^0_{3,q'\to g}(s_{13}) \otimes \mathcal{A}^0_3(s_{34}) - \frac{1}{2}\ \mathcal{E}^0_{3,q'\to g}(s_{14}) \otimes \mathcal{A}^0_3(s_{34}) \Big] B^{Z,0}_1(3,1,4) \\
&\quad + \Big[+1/4 S_{q\to g}\,\Gamma^{(1)}_{qq}(z_1) \otimes \Gamma^{(1)}_{gq}(z_1) + \frac{1}{2}\ \Gamma^{(1)}_{qq}(z_1) \otimes \mathcal{E}^0_{3,q'\to g}(s_{13}) + \frac{1}{2} S_{q\to g}\,\widetilde{\Gamma}^{(2)}_{gq}(z_1) \\
&\qquad - \frac{1}{4}\ \tilde{\mathcal{E}}^0_{4,\bar{q}'}(s_{13}) - \frac{1}{4}\ \tilde{\mathcal{E}}^0_{4,q'}(s_{13}) - \frac{1}{2}\ \tilde{\mathcal{E}}^1_{3,q'}(s_{13}) \Big] B^{Z,0}_1(3,1,4) \\
&\quad + \Big[+1/4 S_{q\to g}\,\Gamma^{(1)}_{qq}(z_1) \otimes \Gamma^{(1)}_{gq}(z_1) + \frac{1}{2}\ \Gamma^{(1)}_{qq}(z_1) \otimes \mathcal{E}^0_{3,q'\to g}(s_{14}) + \frac{1}{2} S_{q\to g}\,\widetilde{\Gamma}^{(2)}_{gq}(z_1) \\
&\qquad - \frac{1}{4}\ \tilde{\mathcal{E}}^0_{4,\bar{q}'}(s_{14}) - \frac{1}{4}\ \tilde{\mathcal{E}}^0_{4,q'}(s_{14}) - \frac{1}{2}\ \tilde{\mathcal{E}}^1_{3,q'}(s_{14}) \Big] B^{Z,0}_1(3,1,4)\,. \qquad \text{(A.28)}
\end{aligned}
$$

$$
\begin{aligned}
&\hat{\hat{B}}_1^{2,Z,U}(\hat{1},3,4) = \\
&\quad + \left[-\frac{1}{2}\,\mathcal{E}_3^0(s_{34}) - \frac{1}{2}\,\mathcal{E}_{3,q}^0(s_{13}) \right] \left(-\frac{b_F}{\epsilon} B_1^{Z,0}(1,3,4) + \hat{B}_1^{Z,1}(1,3,4) \right) \\
&\quad + \left[-\frac{b_F}{2\epsilon}\,\mathcal{E}_3^0(s_{34}) \left(\frac{s_{34}}{\mu_R^2}\right)^{-\epsilon} - \frac{b_F}{2\epsilon}\,\mathcal{E}_{3,q}^0(s_{13}) \left(\frac{s_{13}}{\mu_R^2}\right)^{-\epsilon} - \frac{1}{2}\,\hat{\mathcal{E}}_3^1(s_{34}) \right. \\
&\qquad \left. - \frac{1}{2}\,\hat{\mathcal{E}}_{3,q}^1(s_{13}) \right] B_1^{Z,0}(1,3,4)\,.
\end{aligned}
\tag{A.29}
$$

$$
\begin{aligned}
&\hat{\hat{B}}_{1,q\to g}^{2,Z,U}(\hat{1},3,4) = \\
&\quad + \left[+\,\mathcal{E}_{3,q'\to g}^0(s_{13}) + S_{q\to g}\,\Gamma_{gq}^{(1)}(z_1) \right] \left(-\frac{b_F}{\epsilon} B_1^{Z,0}(3,1,4) + \hat{B}_1^{Z,1}(3,1,4) \right) \\
&\quad + \left[+\,\frac{b_F}{\epsilon} \left(\frac{s_{13}}{\mu_R^2}\right)^{-\epsilon} \mathcal{E}_{3,q'\to g}^0(s_{13}) - \frac{1}{2} S_{q\to g}\,\Gamma_{gg,F}^{(1)}(z_1) \otimes \Gamma_{gq}^{(1)}(z_1) + S_{q\to g}\,\Gamma_{gq,F}^{(2)}(z_1) \right. \\
&\qquad \left. +\,\hat{\mathcal{E}}_{3,q'}^1(s_{13}) \right] B_1^{Z,0}(3,1,4)\,.
\end{aligned}
\tag{A.30}
$$

B Gluon-initiated subtraction terms for DIS di-jet production

The following appendix collects the antenna subtraction terms relevant to the NNLO calculation of gluon-initiated di-jet production described in Section 7.9.

B.1 Real-real

$$
\begin{aligned}
&B_3^{Z,0,S}(k,\hat{1},i,j,l) = \\
&\quad + f_{3,g}^0(1,j,i)\,\bar{B}_2^{Z,0}(k,(\widetilde{ji}),\overline{1},l)\,J_2^3(\{p\}_3) \\
&\quad + f_{3,g}^0(1,i,j)\,\bar{B}_2^{Z,0}(k,(\widetilde{ji}),\overline{1},l)\,J_2^3(\{p\}_3) \\
&\quad + f_{3,g}^0(1,j,i)\,\bar{B}_2^{Z,0}(k,\overline{1},(\widetilde{ji}),l)\,J_2^3(\{p\}_3) \\
&\quad + f_{3,g}^0(1,i,j)\,\bar{B}_2^{Z,0}(k,\overline{1},(\widetilde{ji}),l)\,J_2^3(\{p\}_3) \\
&\quad + d_3^0(l,j,i)\,\bar{B}_2^{Z,0}(k,1,(\widetilde{ji}),(\widetilde{lj}))\,J_2^3(\{p\}_3) \\
&\quad + d_3^0(k,j,i)\,\bar{B}_2^{Z,0}((\widetilde{kj}),(\widetilde{ji}),1,l)\,J_2^3(\{p\}_3) \\
&\quad + d_3^0(l,i,j)\,\bar{B}_2^{Z,0}(k,1,(\widetilde{ij}),(\widetilde{li}))\,J_2^3(\{p\}_3) \\
&\quad + d_3^0(k,i,j)\,\bar{B}_2^{Z,0}((\widetilde{ki}),(\widetilde{ij}),1,l)\,J_2^3(\{p\}_3) \\
&\quad + d_{3,g}^0(k,i,1)\,\bar{B}_2^{Z,0}((\widetilde{ki}),\overline{1},j,l)\,J_2^3(\{p\}_3) \\
&\quad + d_{3,g}^0(k,j,1)\,\bar{B}_2^{Z,0}((\widetilde{kj}),\overline{1},i,l)\,J_2^3(\{p\}_3) \\
&\quad + d_{3,g}^0(l,i,1)\,\bar{B}_2^{Z,0}(k,j,\overline{1},(\widetilde{li}))\,J_2^3(\{p\}_3) \\
&\quad + d_{3,g}^0(l,j,1)\,\bar{B}_2^{Z,0}(k,i,\overline{1},(\widetilde{lj}))\,J_2^3(\{p\}_3) \\
&\quad \\
&\quad + D_4^0(k,i,j,1)\,\bar{B}_1^{Z,0}((\widetilde{kij}),\overline{1},l)\,J_2^2(\{p\}_2) \\
&\quad - d_3^0(k,i,j)\,D_3^0((\widetilde{ki}),(\widetilde{ij}),1)\,\bar{B}_1^{Z,0}(\widetilde{(\widetilde{ki})(\widetilde{ij})},\overline{1},l)\,J_2^2(\{p\}_2)
\end{aligned}
$$

$$- f^0_{3,g}(1,j,i)\, D^0_3(k,(\widetilde{ij}),\overline{1})\, \bar{B}^{Z,0}_1((\widetilde{k(\widetilde{ij})}),\overline{\overline{1}},l)\, J^2_2(\{p\}_2)$$

$$+ D^0_4(k,1,i,j)\, \bar{B}^{Z,0}_1((\widetilde{kij}),\overline{1},l)\, J^2_2(\{p\}_2)$$
$$- d^0_3(k,j,i)\, D^0_3((\widetilde{kj}),(\widetilde{ji}),1)\, \bar{B}^{Z,0}_1((\widetilde{(\widetilde{kj})(\widetilde{ji})}),\overline{1},l)\, J^2_2(\{p\}_2)$$
$$- f^0_{3,g}(1,i,j)\, D^0_3(k,(\widetilde{ij}),\overline{1})\, \bar{B}^{Z,0}_1((\widetilde{k(\widetilde{ij})}),\overline{\overline{1}},l)\, J^2_2(\{p\}_2)$$

$$+ D^0_4(l,i,j,1)\, \bar{B}^{Z,0}_1(k,\overline{1},(\widetilde{lij}))\, J^2_2(\{p\}_2)$$
$$- d^0_3(l,i,j)\, D^0_3((\widetilde{li}),(\widetilde{ij}),1)\, \bar{B}^{Z,0}_1(k,\overline{1},(\widetilde{(\widetilde{li})(\widetilde{ij})}))\, J^2_2(\{p\}_2)$$
$$- f^0_{3,g}(1,j,i)\, D^0_3(l,(\widetilde{ij}),\overline{1})\, \bar{B}^{Z,0}_1(k,\overline{\overline{1}},(\widetilde{l(\widetilde{ij})}))\, J^2_2(\{p\}_2)$$

$$+ D^0_4(l,1,i,j)\, \bar{B}^{Z,0}_1(k,\overline{1},(\widetilde{lij}))\, J^2_2(\{p\}_2)$$
$$- d^0_3(l,j,i)\, D^0_3((\widetilde{lj}),(\widetilde{ji}),1)\, \bar{B}^{Z,0}_1(k,\overline{1},(\widetilde{(\widetilde{lj})(\widetilde{ji})}))\, J^2_2(\{p\}_2)$$
$$- f^0_{3,g}(1,i,j)\, D^0_3(l,(\widetilde{ij}),\overline{1})\, \bar{B}^{Z,0}_1(k,\overline{\overline{1}},(\widetilde{l(\widetilde{ij})}))\, J^2_2(\{p\}_2)$$
$$-2\, A^0_3(k,1,l)\, D^0_3(\overline{1},i,j)\, \bar{B}^{Z,0}_1((\widetilde{kl}),\overline{\overline{1}},(\widetilde{ij}))\, J^2_2(\{p\}_2)$$

$$+ D^0_4(k,i,1,j)\, \bar{B}^{Z,0}_1((\widetilde{kij}),\overline{1},l)\, J^2_2(\{p\}_2)$$
$$- d^0_{3,g}(k,i,1)\, D^0_3((\widetilde{ki}),\overline{1},j)\, \bar{B}^{Z,0}_1((\widetilde{j(\widetilde{ki})}),\overline{\overline{1}},l)\, J^2_2(\{p\}_2)$$
$$- d^0_{3,g}(k,j,1)\, D^0_3((\widetilde{kj}),\overline{1},i)\, \bar{B}^{Z,0}_1((\widetilde{i(\widetilde{kj})}),\overline{\overline{1}},l)\, J^2_2(\{p\}_2)$$

$$+ D^0_4(l,i,1,j)\, \bar{B}^{Z,0}_1(k,\overline{1},(\widetilde{lij}))\, J^2_2(\{p\}_2)$$
$$- d^0_{3,g}(l,i,1)\, D^0_3((\widetilde{li}),\overline{1},j)\, \bar{B}^{Z,0}_1(k,\overline{\overline{1}},(\widetilde{j(\widetilde{li})}))\, J^2_2(\{p\}_2)$$
$$- d^0_{3,g}(l,j,1)\, D^0_3((\widetilde{lj}),\overline{1},i)\, \bar{B}^{Z,0}_1(k,\overline{\overline{1}},(\widetilde{i(\widetilde{lj})}))\, J^2_2(\{p\}_2)$$

$$- A^0_4(k,1,i,l)\, \bar{B}^{Z,0}_1((\widetilde{kil}),\overline{1},j)\, J^2_2(\{p\}_2)$$

$$- A^0_4(k,i,1,l)\, \bar{B}^{Z,0}_1((\widetilde{kil}),\overline{1},j)\, J^2_2(\{p\}_2)$$
$$+ d^0_{3,g}(k,i,1)\, A^0_3((\widetilde{ki}),\overline{1},l)\, \bar{B}^{Z,0}_1((\widetilde{l(\widetilde{ki})}),\overline{\overline{1}},j)\, J^2_2(\{p\}_2)$$
$$+ d^0_{3,g}(l,i,1)\, A^0_3((\widetilde{li}),\overline{1},k)\, \bar{B}^{Z,0}_1((\widetilde{k(\widetilde{li})}),\overline{\overline{1}},j)\, J^2_2(\{p\}_2)$$
$$+ A^0_3(k,1,l)\, A^0_3(\overline{1},i,(\widetilde{kl}))\, \bar{B}^{Z,0}_1((\widetilde{i(\widetilde{kl})}),\overline{\overline{1}},j)\, J^2_2(\{p\}_2)$$

$$- A^0_4(k,1,j,l)\, \bar{B}^{Z,0}_1((\widetilde{kjl}),\overline{1},i)\, J^2_2(\{p\}_2)$$

$$
\begin{aligned}
&- A_4^0(k,j,1,l)\,\bar{B}_1^{Z,0}((\widetilde{kjl}),\overline{1},i)\,J_2^2(\{p\}_2)\\
&+ d_{3,g}^0(k,j,1)\,A_3^0((\widetilde{kj}),\overline{1},l)\,\bar{B}_1^{Z,0}((\widetilde{\widetilde{l(kj)}}),\overline{\overline{1}},i)\,J_2^2(\{p\}_2)\\
&+ d_{3,g}^0(l,j,1)\,A_3^0((\widetilde{lj}),\overline{1},k)\,\bar{B}_1^{Z,0}((\widetilde{\widetilde{k(lj)}}),\overline{\overline{1}},i)\,J_2^2(\{p\}_2)\\
&+ A_3^0(k,1,l)\,A_3^0(\overline{1},j,(\widetilde{kl}))\,\bar{B}_1^{Z,0}((\widetilde{\widetilde{j(kl)}}),\overline{\overline{1}},i)\,J_2^2(\{p\}_2)\\
\\
&- \tilde{A}_4^0(k,j,1,l)\,\bar{B}_1^{Z,0}((\widetilde{kjl}),\overline{1},i)\,J_2^2(\{p\}_2)\\
&+ A_3^0(k,j,l)\,A_3^0((\widetilde{kj}),1,(\widetilde{jl}))\,\bar{B}_1^{Z,0}((\widetilde{(\widetilde{kj})(\widetilde{jl})}),\overline{1},i)\,J_2^2(\{p\}_2)\\
&+ A_3^0(k,1,l)\,A_3^0(\overline{1},j,(\widetilde{kl}))\,\bar{B}_1^{Z,0}((\widetilde{\widetilde{j(kl)}}),\overline{\overline{1}},i)\,J_2^2(\{p\}_2)\\
\\
&- \tilde{A}_4^0(k,i,1,l)\,\bar{B}_1^{Z,0}((\widetilde{kil}),\overline{1},j)\,J_2^2(\{p\}_2)\\
&+ A_3^0(k,i,l)\,A_3^0((\widetilde{ki}),1,(\widetilde{il}))\,\bar{B}_1^{Z,0}((\widetilde{\widetilde{(ki)(il)}}),\overline{1},j)\,J_2^2(\{p\}_2)\\
&+ A_3^0(k,1,l)\,A_3^0(\overline{1},i,(\widetilde{kl}))\,\bar{B}_1^{Z,0}((\widetilde{\widetilde{i(kl)}}),\overline{\overline{1}},j)\,J_2^2(\{p\}_2)\\
\\
&- \tilde{A}_4^{0,a}(k,i,j,l)\,\bar{B}_1^{Z,0}((\widetilde{kij}),1,(\widetilde{lji}))\,J_2^2(\{p\}_2)\\
\\
&- \tilde{A}_4^{0,a}(k,j,i,l)\,\bar{B}_1^{Z,0}((\widetilde{kji}),1,(\widetilde{lij}))\,J_2^2(\{p\}_2)\\
&+ A_3^0(k,i,l)\,A_3^0((\widetilde{ki}),j,(\widetilde{il}))\,\bar{B}_1^{Z,0}((\widetilde{\widetilde{((ki)j)}}),1,(\widetilde{\widetilde{j(il)}}))\,J_2^2(\{p\}_2)\\
&+ A_3^0(k,j,l)\,A_3^0((\widetilde{kj}),i,(\widetilde{jl}))\,\bar{B}_1^{Z,0}((\widetilde{\widetilde{((kj)i)}}),1,(\widetilde{\widetilde{i(jl)}}))\,J_2^2(\{p\}_2)\\
&+ f_{3,g}^0(1,j,i)\,d_{3,g\to q}^0(k,\overline{1},(\widetilde{ij}))\,\bar{B}_1^{Z,0}((\widetilde{\widetilde{k(ij)}}),\overline{\overline{1}},l)\,J_2^2(\{p\}_2)\\
&- d_3^0(k,j,i)\,d_{3,g\to q}^0((\widetilde{kj}),1,(\widetilde{ji}))\,\bar{B}_1^{Z,0}((\widetilde{\widetilde{(kj)}(\widetilde{ji})}),\overline{1},l)\,J_2^2(\{p\}_2)\\
&+ A_3^0(k,j,l)\,d_{3,g\to q}^0((\widetilde{kj}),1,i)\,\bar{B}_1^{Z,0}((\widetilde{\widetilde{i(kj)}}),\overline{1},(\widetilde{lj}))\,J_2^2(\{p\}_2)\\
&- d_{3,g}^0(l,j,1)\,d_{3,g\to q}^0(k,\overline{1},i)\,\bar{B}_1^{Z,0}((\widetilde{ki}),\overline{\overline{1}},(\widetilde{lj}))\,J_2^2(\{p\}_2)\\
&- \Big[+ S^{FF}_{(\widetilde{ij})j1} - S^{FF}_{(\widetilde{kj})j(\widetilde{ji})} + S^{FF}_{(\widetilde{kj})jl} - S^{FF}_{lj1} \Big]\\
&\times d_{3,g\to q}^0((\widetilde{kj}),1,(\widetilde{ij}))\,\bar{B}_1^{Z,0}((\widetilde{\widetilde{(kj)(ij)}}),\overline{1},l)\,J_2^2(\{p\}_2)\\
&+ f_{3,g}^0(1,i,j)\,d_{3,g\to q}^0(k,\overline{1},(\widetilde{ji}))\,\bar{B}_1^{Z,0}((\widetilde{\widetilde{k(ji)}}),\overline{\overline{1}},l)\,J_2^2(\{p\}_2)\\
&- d_3^0(k,i,j)\,d_{3,g\to q}^0((\widetilde{ki}),1,(\widetilde{ij}))\,\bar{B}_1^{Z,0}((\widetilde{\widetilde{(ki)(ij)}}),\overline{1},l)\,J_2^2(\{p\}_2)\\
&+ A_3^0(k,i,l)\,d_{3,g\to q}^0((\widetilde{ki}),1,j)\,\bar{B}_1^{Z,0}((\widetilde{\widetilde{j(ki)}}),\overline{1},(\widetilde{li}))\,J_2^2(\{p\}_2)\\
&- d_{3,g}^0(l,i,1)\,d_{3,g\to q}^0(k,\overline{1},j)\,\bar{B}_1^{Z,0}((\widetilde{kj}),\overline{\overline{1}},(\widetilde{li}))\,J_2^2(\{p\}_2)\\
&- \Big[+ S^{FF}_{(\widetilde{ji})i1} - S^{FF}_{(\widetilde{ki})i(\widetilde{ij})} + S^{FF}_{(\widetilde{ki})il} - S^{FF}_{li1} \Big]
\end{aligned}
$$

$$
\begin{aligned}
&\times d^0_{3,g\to q}((\widetilde{ki}),1,(\widetilde{ji}))\,\bar{B}_1^{Z,0}(\widetilde{(\widetilde{ki})(\widetilde{ji})},\overline{1},l)\,J_2^2(\{p\}_2)\\
&+ f^0_{3,g}(1,j,i)\,d^0_{3,g\to q}(l,\overline{1},(\widetilde{ij}))\,\bar{B}_1^{Z,0}(k,\overline{\overline{1}},(\widetilde{l(\widetilde{ij})}))\,J_2^2(\{p\}_2)\\
&- d^0_3(l,j,i)\,d^0_{3,g\to q}((\widetilde{lj}),1,(\widetilde{ji}))\,\bar{B}_1^{Z,0}(k,\overline{1},\widetilde{(\widetilde{lj})(\widetilde{ji})})\,J_2^2(\{p\}_2)\\
&+ A^0_3(l,j,k)\,d^0_{3,g\to q}((\widetilde{lj}),1,i)\,\bar{B}_1^{Z,0}((\widetilde{kj}),\overline{1},(\widetilde{i(\widetilde{lj})}))\,J_2^2(\{p\}_2)\\
&- d^0_{3,g}(k,j,1)\,d^0_{3,g\to q}(l,\overline{1},i)\,\bar{B}_1^{Z,0}((\widetilde{kj}),\overline{\overline{1}},(\widetilde{li}))\,J_2^2(\{p\}_2)\\
&-\Big[+S^{FF}_{(\widetilde{ij})j1}-S^{FF}_{(\widetilde{lj})j(\widetilde{ji})}+S^{FF}_{(\widetilde{lj})jk}-S^{FF}_{kj1}\Big]\\
&\times d^0_{3,g\to q}((\widetilde{lj}),1,(\widetilde{ij}))\,\bar{B}_1^{Z,0}(k,\overline{1},\widetilde{(\widetilde{lj})(\widetilde{ij})})\,J_2^2(\{p\}_2)\\
&+ f^0_{3,g}(1,i,j)\,d^0_{3,g\to q}(l,\overline{1},(\widetilde{ji}))\,\bar{B}_1^{Z,0}(k,\overline{\overline{1}},(\widetilde{l(\widetilde{ji})}))\,J_2^2(\{p\}_2)\\
&- d^0_3(l,i,j)\,d^0_{3,g\to q}((\widetilde{li}),1,(\widetilde{ij}))\,\bar{B}_1^{Z,0}(k,\overline{1},\widetilde{(\widetilde{li})(\widetilde{ij})})\,J_2^2(\{p\}_2)\\
&+ A^0_3(l,i,k)\,d^0_{3,g\to q}((\widetilde{li}),1,j)\,\bar{B}_1^{Z,0}((\widetilde{ki}),\overline{1},(\widetilde{j(\widetilde{li})}))\,J_2^2(\{p\}_2)\\
&- d^0_{3,g}(k,i,1)\,d^0_{3,g\to q}(l,\overline{1},j)\,\bar{B}_1^{Z,0}((\widetilde{ki}),\overline{\overline{1}},(\widetilde{lj}))\,J_2^2(\{p\}_2)\\
&-\Big[+S^{FF}_{(\widetilde{ji})i1}-S^{FF}_{(\widetilde{li})i(\widetilde{ij})}+S^{FF}_{(\widetilde{li})ik}-S^{FF}_{ki1}\Big]\\
&\times d^0_{3,g\to q}((\widetilde{li}),1,(\widetilde{ji}))\,\bar{B}_1^{Z,0}(k,\overline{1},\widetilde{(\widetilde{li})(\widetilde{ji})})\,J_2^2(\{p\}_2)\\
&+2\,d^0_3(k,i,j)\,A^0_3((\widetilde{ki}),1,l)\,\bar{B}_1^{Z,0}((\widetilde{l(\widetilde{ki})}),\overline{1},(\widetilde{ij}))\,J_2^2(\{p\}_2)\\
&+2\,d^0_3(k,j,i)\,A^0_3((\widetilde{kj}),1,l)\,\bar{B}_1^{Z,0}((\widetilde{l(\widetilde{kj})}),\overline{1},(\widetilde{ji}))\,J_2^2(\{p\}_2)\\
&+2\,d^0_3(l,i,j)\,A^0_3((\widetilde{li}),1,k)\,\bar{B}_1^{Z,0}((\widetilde{k(\widetilde{li})}),\overline{1},(\widetilde{ij}))\,J_2^2(\{p\}_2)\\
&+2\,d^0_3(l,j,i)\,A^0_3((\widetilde{lj}),1,k)\,\bar{B}_1^{Z,0}((\widetilde{k(\widetilde{lj})}),\overline{1},(\widetilde{ji}))\,J_2^2(\{p\}_2)\\
&-2\,A^0_3(k,1,l)\,d^0_3((\widetilde{kl}),i,j)\,\bar{B}_1^{Z,0}(((\widetilde{(\widetilde{kl})i}),\overline{1},(\widetilde{ij}))\,J_2^2(\{p\}_2)\\
&-2\,A^0_3(k,1,l)\,d^0_3((\widetilde{kl}),j,i)\,\bar{B}_1^{Z,0}(((\widetilde{(\widetilde{kl})j}),\overline{1},(\widetilde{ji}))\,J_2^2(\{p\}_2)\\
&-2\,A^0_3(k,i,l)\,A^0_3((\widetilde{ki}),1,(\widetilde{il}))\,\bar{B}_1^{Z,0}(\widetilde{(\widetilde{ki})(\widetilde{il})},\overline{1},j)\,J_2^2(\{p\}_2)\\
&-2\,A^0_3(k,j,l)\,A^0_3((\widetilde{kj}),1,(\widetilde{jl}))\,\bar{B}_1^{Z,0}(\widetilde{(\widetilde{kj})(\widetilde{jl})},\overline{1},i)\,J_2^2(\{p\}_2)\\
&+2\Big[+S^{FF}_{\overline{1}ij}-S^{FF}_{\overline{1}i\widetilde{(\widetilde{ki})(\widetilde{li})}}-S^{FF}_{(\widetilde{ki})ij}-S^{FF}_{(\widetilde{li})ij}+S^{FF}_{\widetilde{(\widetilde{ki})(\widetilde{li})}ij}+S^{FF}_{(\widetilde{ki})i(\widetilde{li})}\Big]\\
&\times A^0_3((\widetilde{ki}),1,(\widetilde{li}))\,\bar{B}_1^{Z,0}(\widetilde{(\widetilde{ki})(\widetilde{li})},\overline{1},j)\,J_2^2(\{p\}_2)\\
&+2\Big[+S^{FF}_{\overline{1}ji}-S^{FF}_{\overline{1}j\widetilde{(\widetilde{kj})(\widetilde{lj})}}-S^{FF}_{(\widetilde{kj})ji}-S^{FF}_{(\widetilde{lj})ji}+S^{FF}_{\widetilde{(\widetilde{kj})(\widetilde{lj})}ji}+S^{FF}_{(\widetilde{kj})j(\widetilde{lj})}\Big]\\
&\times A^0_3((\widetilde{kj}),1,(\widetilde{lj}))\,\bar{B}_1^{Z,0}(\widetilde{(\widetilde{kj})(\widetilde{lj})},\overline{1},i)\,J_2^2(\{p\}_2)\\
&+\frac{1}{2}\,d^0_{3,g}(k,i,1)\,d^0_{3,g}((\widetilde{ki}),j,\overline{1})\,\bar{B}_1^{Z,0}((\widetilde{j(\widetilde{ki})}),\overline{\overline{1}},l)\,J_2^2(\{p\}_2)
\end{aligned}
$$

$$
\begin{aligned}
&-\frac{1}{2}\; d^0_{3,g}(l,i,1)\, d^0_{3,g}(k,j,\overline{1})\, \bar{B}^{Z,0}_1((\widetilde{kj}),\overline{\overline{1}},(\widetilde{li}))\, J^2_2(\{p\}_2)\\
&-\frac{1}{2}\; A^0_3(k,i,l)\, d^0_{3,g}((\widetilde{ki}),j,1)\, \bar{B}^{Z,0}_1(\widetilde{\widetilde{(j(ki))}},\overline{1},(\widetilde{il}))\, J^2_2(\{p\}_2)\\
&-\frac{1}{2}\Big[+ S^{FF}_{(\widetilde{ki})i1} - S^{FF}_{\widetilde{\widetilde{(j(ki))}}i\overline{1}} - S^{FF}_{1i(\widetilde{li})} + S^{FF}_{\overline{1}i(\widetilde{li})} - S^{FF}_{(\widetilde{li})i(\widetilde{ki})} + S^{FF}_{(\widetilde{li})i\widetilde{\widetilde{(j(ki))}}}\Big]\\
&\times d^0_{3,g}((\widetilde{ki}),j,1)\, \bar{B}^{Z,0}_1(\widetilde{\widetilde{(j(ki))}},\overline{1},(\widetilde{li}))\, J^2_2(\{p\}_2)\\
&+\frac{1}{2}\; d^0_{3,g}(k,j,1)\, d^0_{3,g}((\widetilde{kj}),i,\overline{1})\, \bar{B}^{Z,0}_1(\widetilde{\widetilde{(i(kj))}},\overline{\overline{1}},l)\, J^2_2(\{p\}_2)\\
&-\frac{1}{2}\; d^0_{3,g}(l,j,1)\, d^0_{3,g}(k,i,\overline{1})\, \bar{B}^{Z,0}_1((\widetilde{ki}),\overline{\overline{1}},(\widetilde{lj}))\, J^2_2(\{p\}_2)\\
&-\frac{1}{2}\; A^0_3(k,j,l)\, d^0_{3,g}((\widetilde{kj}),i,1)\, \bar{B}^{Z,0}_1(\widetilde{\widetilde{(i(kj))}},\overline{1},(\widetilde{jl}))\, J^2_2(\{p\}_2)\\
&+\frac{1}{2}\Big[- S^{FF}_{(\widetilde{kj})j1} + S^{FF}_{\widetilde{\widetilde{(i(kj))}}j\overline{1}} + S^{FF}_{1j(\widetilde{lj})} - S^{FF}_{\overline{1}j(\widetilde{lj})} + S^{FF}_{(\widetilde{lj})j(\widetilde{kj})} - S^{FF}_{(\widetilde{lj})j\widetilde{\widetilde{(i(kj))}}}\Big]\\
&\times d^0_{3,g}((\widetilde{kj}),i,1)\, \bar{B}^{Z,0}_1(\widetilde{\widetilde{(i(kj))}},\overline{1},(\widetilde{lj}))\, J^2_2(\{p\}_2)\\
&+\frac{1}{2}\; d^0_{3,g}(l,i,1)\, d^0_{3,g}((\widetilde{li}),j,\overline{1})\, \bar{B}^{Z,0}_1(k,\overline{\overline{1}},(\widetilde{j(li)}))\, J^2_2(\{p\}_2)\\
&-\frac{1}{2}\; d^0_{3,g}(k,i,1)\, d^0_{3,g}(l,j,\overline{1})\, \bar{B}^{Z,0}_1((\widetilde{ki}),\overline{\overline{1}},(\widetilde{lj}))\, J^2_2(\{p\}_2)\\
&-\frac{1}{2}\; A^0_3(l,i,k)\, d^0_{3,g}((\widetilde{li}),j,1)\, \bar{B}^{Z,0}_1((\widetilde{ik}),\overline{1},(\widetilde{j(li)}))\, J^2_2(\{p\}_2)\\
&+\frac{1}{2}\Big[- S^{FF}_{(\widetilde{li})i1} + S^{FF}_{\widetilde{\widetilde{(j(li))}}i\overline{1}} + S^{FF}_{(\widetilde{ki})i1} - S^{FF}_{(\widetilde{ki})i\overline{1}} + S^{FF}_{(\widetilde{ki})i(\widetilde{li})} - S^{FF}_{(\widetilde{ki})i\widetilde{\widetilde{(j(li))}}}\Big]\\
&\times d^0_{3,g}((\widetilde{li}),j,1)\, \bar{B}^{Z,0}_1((\widetilde{ki}),\overline{1},(\widetilde{j(li)}))\, J^2_2(\{p\}_2)\\
&+\frac{1}{2}\; d^0_{3,g}(l,j,1)\, d^0_{3,g}((\widetilde{lj}),i,\overline{1})\, \bar{B}^{Z,0}_1(k,\overline{\overline{1}},(\widetilde{i(lj)}))\, J^2_2(\{p\}_2)\\
&-\frac{1}{2}\; d^0_{3,g}(k,j,1)\, d^0_{3,g}(l,i,\overline{1})\, \bar{B}^{Z,0}_1((\widetilde{kj}),\overline{\overline{1}},(\widetilde{li}))\, J^2_2(\{p\}_2)\\
&-\frac{1}{2}\; A^0_3(l,j,k)\, d^0_{3,g}((\widetilde{lj}),i,1)\, \bar{B}^{Z,0}_1((\widetilde{jk}),\overline{1},(\widetilde{i(lj)}))\, J^2_2(\{p\}_2)\\
&+\frac{1}{2}\Big[- S^{FF}_{(\widetilde{lj})j1} + S^{FF}_{\widetilde{\widetilde{(i(lj))}}j\overline{1}} + S^{FF}_{1j(\widetilde{kj})} - S^{FF}_{\overline{1}j(\widetilde{kj})} + S^{FF}_{(\widetilde{kj})j(\widetilde{lj})} - S^{FF}_{(\widetilde{kj})j\widetilde{\widetilde{(i(lj))}}}\Big]\\
&\times d^0_{3,g}((\widetilde{lj}),i,1)\, \bar{B}^{Z,0}_1((\widetilde{kj}),\overline{1},(\widetilde{i(lj)}))\, J^2_2(\{p\}_2)\\
&-\frac{1}{2}\; A^0_3(k,j,l)\, A^0_3((\widetilde{kj}),i,(\widetilde{lj}))\, \bar{B}^{Z,0}_1(\widetilde{\widetilde{(i(kj))}},1,(\widetilde{i(lj)}))\, J^2_2(\{p\}_2)\\
&+\frac{1}{2}\; d^0_{3,g}(k,j,1)\, A^0_3((\widetilde{kj}),i,l)\, \bar{B}^{Z,0}_1(\widetilde{\widetilde{(i(kj))}},\overline{1},(\widetilde{il}))\, J^2_2(\{p\}_2)\\
&+\frac{1}{2}\; d^0_{3,g}(l,j,1)\, A^0_3((\widetilde{lj}),i,k)\, \bar{B}^{Z,0}_1((\widetilde{ik}),\overline{1},\widetilde{\widetilde{(i(lj))}})\, J^2_2(\{p\}_2)\\
&+\frac{1}{2}\Big[+ S^{FF}_{(\widetilde{kj})j(\widetilde{lj})} - S^{FF}_{\widetilde{\widetilde{(i(kj))}}j\widetilde{\widetilde{(i(lj))}}} - S^{FF}_{(\widetilde{kj})j1} + S^{FF}_{\widetilde{\widetilde{(i(kj))}}j1} - S^{FF}_{(\widetilde{lj})j1} + S^{FF}_{\widetilde{\widetilde{(i(lj))}}j1}\Big]\\
&\times A^0_3((\widetilde{kj}),i,(\widetilde{lj}))\, \bar{B}^{Z,0}_1(\widetilde{\widetilde{(i(kj))}},1,(\widetilde{i(lj)}))\, J^2_2(\{p\}_2)
\end{aligned}
$$

$$
\begin{aligned}
&-\frac{1}{2}\; A_3^0(k,i,l)\, A_3^0((\widetilde{ki}),j,(\widetilde{li}))\, \bar{B}_1^{Z,0}((\widetilde{\widetilde{j(\widetilde{ki})}}),1,(\widetilde{\widetilde{j(\widetilde{li})}}))\, J_2^2(\{p\}_2)\\
&+\frac{1}{2}\; d_{3,g}^0(k,i,1)\, A_3^0((\widetilde{ki}),j,l)\, \bar{B}_1^{Z,0}((\widetilde{\widetilde{j(\widetilde{ki})}}),\overline{1},(\widetilde{jl}))\, J_2^2(\{p\}_2)\\
&+\frac{1}{2}\; d_{3,g}^0(l,i,1)\, A_3^0((\widetilde{li}),j,k)\, \bar{B}_1^{Z,0}((\widetilde{jk}),\overline{1},(\widetilde{\widetilde{j(\widetilde{li})}}))\, J_2^2(\{p\}_2)\\
&+\frac{1}{2}\Big[+S^{FF}_{(\widetilde{ki})i(\widetilde{li})}-S^{FF}_{(\widetilde{\widetilde{j(\widetilde{ki})}})i(\widetilde{\widetilde{j(\widetilde{li})}})}-S^{FF}_{(\widetilde{ki})i1}+S^{FF}_{(\widetilde{\widetilde{j(\widetilde{ki})}})i1}-S^{FF}_{(\widetilde{li})i1}+S^{FF}_{(\widetilde{\widetilde{j(\widetilde{li})}})i1}\Big]\\
&\times A_3^0((\widetilde{ki}),j,(\widetilde{li}))\, \bar{B}_1^{Z,0}((\widetilde{\widetilde{j(\widetilde{ki})}}),1,(\widetilde{\widetilde{j(\widetilde{li})}}))\, J_2^2(\{p\}_2)\\
&-A_3^0(k,1,l)\, \bar{B}_2^{Z,0}(\overline{1},j,i,(\widetilde{kl}))\, J_2^3(\{p\}_3)\\
&-A_3^0(k,1,l)\, \bar{B}_2^{Z,0}(\overline{1},i,j,(\widetilde{kl}))\, J_2^3(\{p\}_3)\\
&\\
&-A_4^0(k,1,i,l)\, \bar{B}_1^{Z,0}(\overline{1},j,(\widetilde{kil}))\, J_2^2(\{p\}_2)\\
&\\
&-A_4^0(k,i,1,l)\, \bar{B}_1^{Z,0}(\overline{1},j,(\widetilde{kil}))\, J_2^2(\{p\}_2)\\
&+d_{3,g}^0(k,i,1)\, A_3^0((\widetilde{ki}),\overline{1},l)\, \bar{B}_1^{Z,0}(\overline{\overline{1}},j,(\widetilde{\widetilde{l(\widetilde{ki})}}))\, J_2^2(\{p\}_2)\\
&+d_{3,g}^0(l,i,1)\, A_3^0((\widetilde{li}),\overline{1},k)\, \bar{B}_1^{Z,0}(\overline{\overline{1}},j,(\widetilde{\widetilde{k(\widetilde{li})}}))\, J_2^2(\{p\}_2)\\
&+A_3^0(k,1,l)\, A_3^0(\overline{1},i,(\widetilde{kl}))\, \bar{B}_1^{Z,0}(\overline{\overline{1}},j,(\widetilde{\widetilde{i(\widetilde{kl})}}))\, J_2^2(\{p\}_2)\\
&\\
&-A_4^0(k,1,j,l)\, \bar{B}_1^{Z,0}(\overline{1},i,(\widetilde{kjl}))\, J_2^2(\{p\}_2)\\
&\\
&-A_4^0(k,j,1,l)\, \bar{B}_1^{Z,0}(\overline{1},i,(\widetilde{kjl}))\, J_2^2(\{p\}_2)\\
&+d_{3,g}^0(k,j,1)\, A_3^0((\widetilde{kj}),\overline{1},l)\, \bar{B}_1^{Z,0}(\overline{\overline{1}},i,(\widetilde{\widetilde{l(\widetilde{kj})}}))\, J_2^2(\{p\}_2)\\
&+d_{3,g}^0(l,j,1)\, A_3^0((\widetilde{lj}),\overline{1},k)\, \bar{B}_1^{Z,0}(\overline{\overline{1}},i,(\widetilde{\widetilde{k(\widetilde{lj})}}))\, J_2^2(\{p\}_2)\\
&+A_3^0(k,1,l)\, A_3^0(\overline{1},j,(\widetilde{kl}))\, \bar{B}_1^{Z,0}(\overline{\overline{1}},i,(\widetilde{\widetilde{j(\widetilde{kl})}}))\, J_2^2(\{p\}_2)\\
&+f_{3,g}^0(1,j,i)\, d_{3,g\to q}^0(k,\overline{1},(\widetilde{ij}))\, \bar{B}_1^{Z,0}(\overline{\overline{1}},(\widetilde{k(\widetilde{ij})}),l)\, J_2^2(\{p\}_2)\\
&-d_3^0(k,j,i)\, d_{3,g\to q}^0((\widetilde{kj}),1,(\widetilde{ji}))\, \bar{B}_1^{Z,0}(\overline{1},(\widetilde{\widetilde{kj}(\widetilde{ji})}),l)\, J_2^2(\{p\}_2)\\
&+A_3^0(k,j,l)\, d_{3,g\to q}^0((\widetilde{kj}),1,i)\, \bar{B}_1^{Z,0}(\overline{1},(\widetilde{\widetilde{i(\widetilde{kj})}}),(\widetilde{lj}))\, J_2^2(\{p\}_2)\\
&-d_{3,g}^0(l,j,1)\, d_{3,g\to q}^0(k,\overline{1},i)\, \bar{B}_1^{Z,0}(\overline{\overline{1}},(\widetilde{ki}),(\widetilde{lj}))\, J_2^2(\{p\}_2)\\
&-\Big[+S^{FF}_{(\widetilde{ij})j1}-S^{FF}_{(\widetilde{kj})j(\widetilde{ji})}+S^{FF}_{(\widetilde{kj})jl}-S^{FF}_{lj1}\Big]\\
&\times d_{3,g\to q}^0((\widetilde{kj}),1,(\widetilde{ij}))\, \bar{B}_1^{Z,0}(\overline{1},(\widetilde{\widetilde{kj}(\widetilde{ij})}),l)\, J_2^2(\{p\}_2)\\
&+f_{3,g}^0(1,i,j)\, d_{3,g\to q}^0(k,\overline{1},(\widetilde{ji}))\, \bar{B}_1^{Z,0}(\overline{\overline{1}},(\widetilde{k(\widetilde{ji})}),l)\, J_2^2(\{p\}_2)
\end{aligned}
$$

$$
\begin{aligned}
&- d_3^0(k,i,j)\, d_{3,g\to q}^0((\widetilde{ki}),1,(\widetilde{ij}))\, \bar{B}_1^{Z,0}(\overline{1},(\widetilde{(\widetilde{ki})(\widetilde{ij})}),l)\, J_2^2(\{p\}_2)\\
&+ A_3^0(k,i,l)\, d_{3,g\to q}^0((\widetilde{ki}),1,j)\, \bar{B}_1^{Z,0}(\overline{1},(\widetilde{j(\widetilde{ki})}),(\widetilde{li}))\, J_2^2(\{p\}_2)\\
&- d_{3,g}^0(l,i,1)\, d_{3,g\to q}^0(k,\overline{1},j)\, \bar{B}_1^{Z,0}(\overline{\overline{1}},(\widetilde{kj}),(\widetilde{li}))\, J_2^2(\{p\}_2)\\
&- \Big[+ S^{FF}_{(\widetilde{ji})i1} - S^{FF}_{(\widetilde{ki})i(\widetilde{ij})} + S^{FF}_{(\widetilde{ki})il} - S^{FF}_{li1} \Big]\\
&\times d_{3,g\to q}^0((\widetilde{ki}),1,(\widetilde{ji}))\, \bar{B}_1^{Z,0}(\overline{1},(\widetilde{(\widetilde{ki})(\widetilde{ji})}),l)\, J_2^2(\{p\}_2)\\
&+ f_{3,g}^0(1,j,i)\, d_{3,g\to q}^0(l,\overline{1},(\widetilde{ij}))\, \bar{B}_1^{Z,0}(\overline{\overline{1}},(\widetilde{l(\widetilde{ij})}),k)\, J_2^2(\{p\}_2)\\
&- d_3^0(l,j,i)\, d_{3,g\to q}^0((\widetilde{lj}),1,(\widetilde{ji}))\, \bar{B}_1^{Z,0}(\overline{1},(\widetilde{(\widetilde{lj})(\widetilde{ji})}),k)\, J_2^2(\{p\}_2)\\
&+ A_3^0(l,j,k)\, d_{3,g\to q}^0((\widetilde{lj}),1,i)\, \bar{B}_1^{Z,0}(\overline{1},(\widetilde{i(\widetilde{lj})}),(\widetilde{kj}))\, J_2^2(\{p\}_2)\\
&- d_{3,g}^0(k,j,1)\, d_{3,g\to q}^0(l,\overline{1},i)\, \bar{B}_1^{Z,0}(\overline{\overline{1}},(\widetilde{li}),(\widetilde{kj}))\, J_2^2(\{p\}_2)\\
&- \Big[+ S^{FF}_{(\widetilde{ij})j1} - S^{FF}_{(\widetilde{lj})j(\widetilde{ji})} + S^{FF}_{(\widetilde{lj})jk} - S^{FF}_{kj1} \Big]\\
&\times d_{3,g\to q}^0((\widetilde{lj}),1,(\widetilde{ij}))\, \bar{B}_1^{Z,0}(\overline{1},(\widetilde{(\widetilde{lj})(\widetilde{ij})}),k)\, J_2^2(\{p\}_2)\\
&+ f_{3,g}^0(1,i,j)\, d_{3,g\to q}^0(l,\overline{1},(\widetilde{ji}))\, \bar{B}_1^{Z,0}(\overline{\overline{1}},(\widetilde{l(\widetilde{ji})}),k)\, J_2^2(\{p\}_2)\\
&- d_3^0(l,i,j)\, d_{3,g\to q}^0((\widetilde{li}),1,(\widetilde{ij}))\, \bar{B}_1^{Z,0}(\overline{1},(\widetilde{(\widetilde{li})(\widetilde{ij})}),k)\, J_2^2(\{p\}_2)\\
&+ A_3^0(l,i,k)\, d_{3,g\to q}^0((\widetilde{li}),1,j)\, \bar{B}_1^{Z,0}(\overline{1},(\widetilde{j(\widetilde{li})}),(\widetilde{ki}))\, J_2^2(\{p\}_2)\\
&- d_{3,g}^0(k,i,1)\, d_{3,g\to q}^0(l,\overline{1},j)\, \bar{B}_1^{Z,0}(\overline{\overline{1}},(\widetilde{lj}),(\widetilde{ki}))\, J_2^2(\{p\}_2)\\
&- \Big[+ S^{FF}_{(\widetilde{ji})i1} - S^{FF}_{(\widetilde{li})i(\widetilde{ij})} + S^{FF}_{(\widetilde{li})ik} - S^{FF}_{ki1} \Big]\\
&\times d_{3,g\to q}^0((\widetilde{li}),1,(\widetilde{ji}))\, \bar{B}_1^{Z,0}(\overline{1},(\widetilde{(\widetilde{li})(\widetilde{ji})}),k)\, J_2^2(\{p\}_2)\\
&+ d_3^0(k,i,j)\, A_3^0((\widetilde{ki}),1,l)\, \bar{B}_1^{Z,0}(\overline{1},(\widetilde{ji}),(\widetilde{l(\widetilde{ki})}))\, J_2^2(\{p\}_2)\\
&+ d_3^0(k,j,i)\, A_3^0((\widetilde{kj}),1,l)\, \bar{B}_1^{Z,0}(\overline{1},(\widetilde{ij}),(\widetilde{l(\widetilde{kj})}))\, J_2^2(\{p\}_2)\\
&+ d_3^0(l,i,j)\, A_3^0((\widetilde{li}),1,k)\, \bar{B}_1^{Z,0}(\overline{1},(\widetilde{ji}),(\widetilde{k(\widetilde{li})}))\, J_2^2(\{p\}_2)\\
&+ d_3^0(l,j,i)\, A_3^0((\widetilde{lj}),1,k)\, \bar{B}_1^{Z,0}(\overline{1},(\widetilde{ij}),(\widetilde{k(\widetilde{lj})}))\, J_2^2(\{p\}_2)\\
&- A_3^0(k,j,l)\, A_3^0((\widetilde{kj}),1,(\widetilde{jl}))\, \bar{B}_1^{Z,0}(\overline{1},i,(\widetilde{(\widetilde{kj})(\widetilde{jl})}))\, J_2^2(\{p\}_2)\\
&- A_3^0(k,i,l)\, A_3^0((\widetilde{ki}),1,(\widetilde{il}))\, \bar{B}_1^{Z,0}(\overline{1},j,(\widetilde{(\widetilde{ki})(\widetilde{il})}))\, J_2^2(\{p\}_2)\\
&+ \Big[+ S^{FF}_{\overline{1}ij} - S^{FF}_{\overline{1}i(\widetilde{(\widetilde{ki})(\widetilde{li})})} - S^{FF}_{(\widetilde{ki})ij} - S^{FF}_{(\widetilde{li})ij} + S^{FF}_{(\widetilde{ki})i(\widetilde{li})} + S^{FF}_{ji(\widetilde{(\widetilde{ki})(\widetilde{li})})} \Big]\\
&\times A_3^0((\widetilde{ki}),1,(\widetilde{li}))\, \bar{B}_1^{Z,0}(\overline{1},j,(\widetilde{(\widetilde{ki})(\widetilde{li})}))\, J_2^2(\{p\}_2)\\
&+ \Big[+ S^{FF}_{ij(\widetilde{(\widetilde{kj})(\widetilde{lj})})} + S^{FF}_{\overline{1}ji} - S^{FF}_{\overline{1}j(\widetilde{(\widetilde{kj})(\widetilde{lj})})} - S^{FF}_{(\widetilde{kj})ji} - S^{FF}_{(\widetilde{lj})ji} + S^{FF}_{(\widetilde{kj})j(\widetilde{lj})} \Big]
\end{aligned}
$$

$$\times A_3^0((\widetilde{kj}),1,(\widetilde{lj}))\,\bar{B}_1^{Z,0}(\overline{1},i,(\widetilde{\widetilde{kj})(\widetilde{lj}}))\,J_2^2(\{p\}_2)\,. \tag{B.1}$$

$$\begin{aligned}
&\tilde{B}_3^{Z,0,S}(k,\hat{1},i,j,l) = \\
&\quad +A_3^0(k,i,l)\,\bar{B}_2^{Z,0}((\widetilde{ki}),j,1,(\widetilde{li}))\,J_2^3(\{p\}_3)\\
&\quad +A_3^0(k,i,l)\,\bar{B}_2^{Z,0}((\widetilde{ki}),1,j,(\widetilde{li}))\,J_2^3(\{p\}_3)\\
&\quad +d_{3,g}^0(k,j,1)\,\tilde{\bar{B}}_2^{Z,0}((\widetilde{kj}),i,\overline{1},l)\,J_2^3(\{p\}_3)\\
&\quad +d_{3,g}^0(l,j,1)\,\tilde{\bar{B}}_2^{Z,0}(k,i,\overline{1},(\widetilde{lj}))\,J_2^3(\{p\}_3)\\
&\quad +d_3^0(k,i,j)\,\tilde{\bar{B}}_2^{Z,0}((\widetilde{ki}),1,(\widetilde{ij}),l)\,J_2^3(\{p\}_2)\\
&\quad +d_3^0(l,j,i)\,\tilde{\bar{B}}_2^{Z,0}(k,1,(\widetilde{ij}),(\widetilde{lj}))\,J_2^3(\{p\}_2)\\
&\\
&\quad + A_4^0(k,i,j,l)\,\bar{B}_1^{Z,0}((\widetilde{kij}),1,(\widetilde{lji}))\,J_2^2(\{p\}_2)\\
&\quad - d_3^0(k,i,j)\,A_3^0((\widetilde{ki}),(\widetilde{ji}),l)\,\bar{B}_1^{Z,0}((\widetilde{\widetilde{ki})(\widetilde{ji}}),1,(\widetilde{l(\widetilde{ji})}))\,J_2^2(\{p\}_3)\\
&\quad - d_3^0(l,j,i)\,A_3^0(k,(\widetilde{ji}),(\widetilde{lj}))\,\bar{B}_1^{Z,0}((\widetilde{k(\widetilde{ji})}),1,(\widetilde{\widetilde{ji})(\widetilde{lj}}))\,J_2^2(\{p\}_2)\\
&\\
&\quad + \tilde{A}_4^{0,a}(k,i,j,l)\,\bar{B}_1^{Z,0}((\widetilde{kij}),1,(\widetilde{lji}))\,J_2^2(\{p\}_2)\\
&\\
&\quad + \tilde{A}_4^{0,a}(k,j,i,l)\,\bar{B}_1^{Z,0}((\widetilde{kji}),1,(\widetilde{lij}))\,J_2^2(\{p\}_2)\\
&\quad - A_3^0(k,i,l)\,A_3^0((\widetilde{ki}),j,(\widetilde{li}))\,\bar{B}_1^{Z,0}(((\widetilde{\widetilde{ki})j}),1,(\widetilde{j(\widetilde{li})}))\,J_2^2(\{p\}_2)\\
&\quad - A_3^0(k,j,l)\,A_3^0((\widetilde{kj}),i,(\widetilde{lj}))\,\bar{B}_1^{Z,0}(((\widetilde{\widetilde{kj})i}),1,(\widetilde{i(\widetilde{lj})}))\,J_2^2(\{p\}_2)\\
&\quad + A_3^0(k,j,l)\,A_3^0((\widetilde{kj}),i,(\widetilde{lj}))\,\bar{B}_1^{Z,0}(((\widetilde{\widetilde{kj})i}),1,(\widetilde{i(\widetilde{lj})}))\,J_2^2(\{p\}_2)\\
&\quad - d_{3,g}^0(k,j,1)\,A_3^0((\widetilde{kj}),i,l)\,\bar{B}_1^{Z,0}(((\widetilde{\widetilde{kj})i}),\overline{1},(\widetilde{li}))\,J_2^2(\{p\}_2)\\
&\quad - d_{3,g}^0(l,j,1)\,A_3^0(k,i,(\widetilde{lj}))\,\bar{B}_1^{Z,0}((\widetilde{ki}),\overline{1},((\widetilde{\widetilde{lj})i}))\,J_2^2(\{p\}_2)\\
&\quad - \Big[+ S^{FF}_{(\widetilde{kj})j(\widetilde{lj})} - S^{FF}_{(i(\widetilde{\widetilde{kj}}))j(i(\widetilde{\widetilde{lj}}))} - S^{FF}_{(\widetilde{kj})j1} + S^{FF}_{(i(\widetilde{\widetilde{kj}}))j1} - S^{FF}_{(\widetilde{lj})j1} + S^{FF}_{(i(\widetilde{\widetilde{lj}}))j1} \Big]\\
&\quad \times A_3^0((\widetilde{kj}),i,(\widetilde{lj}))\,\bar{B}_1^{Z,0}((\widetilde{i(\widetilde{kj})}),1,(\widetilde{i(\widetilde{lj})}))\,J_2^2(\{p\}_2)\\
&\quad - A_3^0(k,1,l)\,\tilde{\bar{B}}_2^{Z,0}(\overline{1},i,j,(\widetilde{kl}))\,J_2^3(\{p\}_3)\\
&\quad - A_3^0(k,1,l)\,\bar{B}_2^{Z,0}(\overline{1},i,j,(\widetilde{kl}))\,J_2^3(\{p\}_3)\\
&\\
&\quad - \tilde{A}_4^0(k,1,i,l)\,\bar{B}_1^{Z,0}(\overline{1},j,(\widetilde{kli}))\,J_2^2(\{p\}_2)\\
&\quad + A_3^0(k,1,l)\,A_3^0(\overline{1},i,(\widetilde{kl}))\,\bar{B}_1^{Z,0}(\overline{\overline{1}},j,(\widetilde{i(\widetilde{kl})}))\,J_2^2(\{p\}_2)\\
&\quad + A_3^0(k,i,l)\,A_3^0((\widetilde{ki}),1,(\widetilde{li}))\,\bar{B}_1^{Z,0}(\overline{1},j,(\widetilde{\widetilde{ki})(\widetilde{li}}))\,J_2^2(\{p\}_2)\\
&\\
&\quad - \tilde{A}_4^0(k,1,j,l)\,\bar{B}_1^{Z,0}(\overline{1},i,(\widetilde{klj}))\,J_2^2(\{p\}_2)
\end{aligned}$$

$$
\begin{aligned}
&+ A_3^0(k,1,l)\, A_3^0(\overline{1},j,(\widetilde{kl}))\, \bar{B}_1^{Z,0}(\overline{\overline{1}},i,(\widetilde{\widetilde{j(kl)}}))\, J_2^2(\{p\}_2)\\
&+ A_3^0(k,j,l)\, A_3^0((\widetilde{kj}),1,(\widetilde{lj}))\, \bar{B}_1^{Z,0}(\overline{1},i,(\widetilde{(\widetilde{kj})(\widetilde{lj})}))\, J_2^2(\{p\}_2)\\
&\\
&- A_4^0(k,j,1,l)\, \bar{B}_1^{Z,0}(\overline{1},i,(\widetilde{kjl}))\, J_2^2(\{p\}_2)\\
&+ d_{3,g}^0(k,j,1)\, A_3^0((\widetilde{kj}),\overline{1},l)\, \bar{B}_1^{Z,0}(\overline{\overline{1}},i,(\widetilde{\widetilde{l(kj)}}))\, J_2^2(\{p\}_2)\\
&\\
&- A_4^0(k,1,j,l)\, \bar{B}_1^{Z,0}(\overline{1},i,(\widetilde{kjl}))\, J_2^2(\{p\}_2)\\
&+ d_{3,g}^0(l,j,1)\, A_3^0((\widetilde{lj}),\overline{1},k)\, \bar{B}_1^{Z,0}(\overline{\overline{1}},i,(\widetilde{\widetilde{k(lj)}}))\, J_2^2(\{p\}_2)\\
&+ A_3^0(k,1,l)\, A_3^0(\overline{1},j,(\widetilde{kl}))\, \bar{B}_1^{Z,0}(\overline{\overline{1}},i,(\widetilde{\widetilde{j(kl)}}))\, J_2^2(\{p\}_2)\\
&- A_3^0(k,i,l)\, A_3^0((\widetilde{ki}),1,(\widetilde{li}))\, \bar{B}_1^{Z,0}(\overline{1},j,(\widetilde{(\widetilde{ki})(\widetilde{li})}))\, J_2^2(\{p\}_2)\\
&+ d_3^0(k,i,j)\, A_3^0((\widetilde{ki}),1,l)\, \bar{B}_1^{Z,0}(\overline{1},(\widetilde{ij}),(\widetilde{(\widetilde{ki})l}))\, J_2^2(\{p\}_2)\\
&+ d_3^0(l,i,j)\, A_3^0((\widetilde{li}),1,k)\, \bar{B}_1^{Z,0}(\overline{1},(\widetilde{ij}),(\widetilde{(\widetilde{li})k}))\, J_2^2(\{p\}_2)\\
&+ \Big[+ S^{FF}_{\overline{1}ij} - S^{FF}_{\overline{1}i(\widetilde{(\widetilde{ki})(\widetilde{li})})} - S^{FF}_{(\widetilde{ki})ij} - S^{FF}_{(\widetilde{li})ij} + S^{FF}_{(\widetilde{ki})i(\widetilde{li})} + S^{FF}_{ji(\widetilde{(\widetilde{ki})(\widetilde{li})})} \Big]\\
&\times A_3^0((\widetilde{ki}),1,(\widetilde{li}))\, \bar{B}_1^{Z,0}(\overline{1},j,(\widetilde{(\widetilde{li})(\widetilde{ki})}))\, J_2^2(\{p\}_2)\,. \qquad \text{(B.2)}
\end{aligned}
$$

$$
\begin{aligned}
&\tilde{\bar{B}}_3^{\gamma,0,S}(k,\hat{1},i,j,l) =\\
&\quad + A_3^0(k,i,l)\, \tilde{\bar{B}}_2^{\gamma,0}((\widetilde{ki}),1,j,(\widetilde{li}))\, J_2^3(\{p\}_3)\\
&\quad + A_3^0(k,j,l)\, \tilde{\bar{B}}_2^{\gamma,0}((\widetilde{kj}),1,i,(\widetilde{lj}))\, J_2^3(\{p\}_3)\\
&\\
&\quad + \tilde{A}_4^{0,a}(k,i,j,l)\, \bar{B}_1^{\gamma,0}((\widetilde{kij}),1,(\widetilde{lji}))\, J_2^2(\{p\}_2)\\
&\\
&\quad + \tilde{A}_4^{0,a}(k,j,i,l)\, \bar{B}_1^{\gamma,0}((\widetilde{kji}),1,(\widetilde{lij}))\, J_2^2(\{p\}_2)\\
&\quad - A_3^0(k,i,l)\, A_3^0((\widetilde{ki}),j,(\widetilde{li}))\, \bar{B}_1^{\gamma,0}((\widetilde{\widetilde{j(ki)}}),1,(\widetilde{\widetilde{j(li)}}))\, J_2^2(\{p\}_2)\\
&\quad - A_3^0(k,j,l)\, A_3^0((\widetilde{kj}),i,(\widetilde{lj}))\, \bar{B}_1^{\gamma,0}((\widetilde{\widetilde{i(kj)}}),1,(\widetilde{\widetilde{i(lj)}}))\, J_2^2(\{p\}_2)\\
&\quad - A_3^0(k,1,l)\, \tilde{\bar{B}}_2^{\gamma,0}(\overline{1},i,j,(\widetilde{kl}))\, J_2^3(\{p\}_3)\\
&\\
&\quad - \tilde{A}_4^0(k,1,i,l)\, \bar{B}_1^{\gamma,0}(\overline{1},j,(\widetilde{kil}))\, J_2^2(\{p\}_2)\\
&\quad + A_3^0(k,1,l)\, A_3^0(\overline{1},i,(\widetilde{kl}))\, \bar{B}_1^{\gamma,0}(\overline{\overline{1}},j,(\widetilde{\widetilde{i(kl)}}))\, J_2^2(\{p\}_2)\\
&\quad + A_3^0(k,i,l)\, A_3^0((\widetilde{ki}),1,(\widetilde{li}))\, \bar{B}_1^{\gamma,0}(\overline{1},j,[(\widetilde{ki}),(\widetilde{li})])\, J_2^2(\{p\}_2)\\
&\\
&\quad - \tilde{A}_4^0(k,1,j,l)\, \bar{B}_1^{\gamma,0}(\overline{1},i,(\widetilde{kjl}))\, J_2^2(\{p\}_2)\\
&\quad + A_3^0(k,1,l)\, A_3^0(\overline{1},j,(\widetilde{kl}))\, \bar{B}_1^{\gamma,0}(\overline{\overline{1}},i,(\widetilde{\widetilde{j(kl)}}))\, J_2^2(\{p\}_2)
\end{aligned}
$$

$$+ A_3^0(k,j,l)\, A_3^0((\widetilde{kj}),1,(\widetilde{lj}))\, \bar{B}_1^{\gamma,0}(\overline{1},i,[(\widetilde{kj}),(\widetilde{lj})])\, J_2^2(\{p\}_2)\,. \tag{B.3}$$

$$\begin{aligned}
&C_1^{Z,0,S}(k,\hat{1};i,j;l) = \\
&+E_3^0(l,i,j)\, B_{2,q}^{Z,0}(k,(\widetilde{ji}),1,(\widetilde{li}))\, J_2^3(\{p\}_3) \\
&+E_3^0(k,j,i)\, B_{2,q}^{Z,0}((\widetilde{kj}),1,(\widetilde{ji}),l)\, J_2^3(\{p\}_3) \\
&-a_{3,g\to q}^0(k,1,l)\, C_0^{Z,0}(\overline{1};i,j;(\widetilde{kl}))\, J_2^3(\{p\}_3) \\
&-a_{3,g\to q}^0(l,1,k)\, C_0^{Z,0}((\widetilde{kl});i,j;\overline{1})\, J_2^3(\{p\}_3) \\
&-a_{3,g\to q}^0(i,1,j)\, C_0^{Z,0}(k;\overline{1},(\widetilde{ij});l)\, J_2^3(\{p\}_3) \\
&-a_{3,g\to q}^0(j,1,i)\, C_0^{Z,0}(k;(\widetilde{ij}),\overline{1};l)\, J_2^3(\{p\}_3) \\
&+E_3^0(k,j,i)\, a_{3,g\to q}^0((\widetilde{kj}),1,l)\, B_{1,q}^{Z,0}(\overline{1},(\widetilde{ij}),(\widetilde{(\widetilde{kj})l}))\, J_2^2(\{p\}_2) \\
&+E_3^0(l,i,j)\, a_{3,g\to q}^0((\widetilde{li}),1,k)\, B_{1,q}^{Z,0}(((\widetilde{\widetilde{li})k}),(\widetilde{ij}),\overline{1})\, J_2^2(\{p\}_2) \\
&\\
&+E_4^0(l,i,j,1)\, B_{1,q}^{Z,0}(k,\overline{1},(\widetilde{lij}))\, J_2^2(\{p\}_2) \\
&\\
&+E_4^0(k,j,i,1)\, B_{1,q}^{Z,0}((\widetilde{kji}),\overline{1},l)\, J_2^2(\{p\}_2) \\
&-a_{3,g\to q}^0(l,1,k)\, E_3^0(\overline{1},j,i)\, B_{1,q}^{Z,0}((\widetilde{kl}),\overline{\overline{1}},(\widetilde{ij}))\, J_2^2(\{p\}_2) \\
&-a_{3,g\to q}^0(k,1,l)\, E_3^0(\overline{1},j,i)\, B_{1,q}^{Z,0}((\widetilde{ij}),\overline{\overline{1}},(\widetilde{kl}))\, J_2^2(\{p\}_2) \\
&+E_3^0(k,j,i)\, a_{3,g\to q}^0((\widetilde{kj}),1,l)\, B_{1,q}^{Z,0}((\widetilde{ij}),\overline{1},(\widetilde{(\widetilde{kj})l}))\, J_2^2(\{p\}_2) \\
&+E_3^0(l,i,j)\, a_{3,g\to q}^0((\widetilde{li}),1,k)\, B_{1,q}^{Z,0}(((\widetilde{\widetilde{li})k}),\overline{1},(\widetilde{ij}))\, J_2^2(\{p\}_2) \\
&-a_{3,g\to q}^0(i,1,j)\, E_3^0(k,(\widetilde{ij}),\overline{1})\, B_{1,q}^{Z,0}((\widetilde{k(\widetilde{ij})}),\overline{\overline{1}},l)\, J_2^2(\{p\}_2) \\
&-a_{3,g\to q}^0(j,1,i)\, E_3^0(l,(\widetilde{ij}),\overline{1})\, B_{1,q}^{Z,0}(k,\overline{\overline{1}},(\widetilde{l(\widetilde{ij})}))\, J_2^2(\{p\}_2) \\
&-E_3^0(k,j,i)\, d_{3,g\to q}^0((\widetilde{kj}),1,(\widetilde{ij}))\, B_{1,q}^{Z,0}((\widetilde{(\widetilde{kj})(\widetilde{ij})}),\overline{1},l)\, J_2^2(\{p\}_2) \\
&-E_3^0(l,i,j)\, d_{3,g}^0(k,(\widetilde{ij}),1)\, B_{1,q}^{Z,0}((\widetilde{k(\widetilde{ij})}),\overline{1},(\widetilde{li}))\, J_2^2(\{p\}_2) \\
&-E_3^0(l,i,j)\, d_{3,g\to q}^0((\widetilde{li}),1,(\widetilde{ij}))\, B_{1,q}^{Z,0}(k,\overline{1},(\widetilde{(\widetilde{li})(\widetilde{ij})}))\, J_2^2(\{p\}_2) \\
&-E_3^0(k,j,i)\, d_{3,g}^0(l,(\widetilde{ij}),1)\, B_{1,q}^{Z,0}((\widetilde{kj}),\overline{1},(\widetilde{l(\widetilde{ij})}))\, J_2^2(\{p\}_2) \\
&+E_3^0(j,k,l)\, B_{2,Q}^{Z,0}((\widetilde{jk}),1,(\widetilde{lk}),i)\, J_2^3(\{p\}_3) \\
&+E_3^0(i,l,k)\, B_{2,Q}^{Z,0}(j,(\widetilde{lk}),1,(\widetilde{il}))\, J_2^3(\{p\}_3) \\
&+E_3^0(i,l,k)\, a_{3,g\to q}^0((\widetilde{il}),1,j)\, B_{1,Q}^{Z,0}(((\widetilde{\widetilde{il})j}),(\widetilde{kl}),\overline{1})\, J_2^2(\{p\}_2) \\
&+E_3^0(j,k,l)\, a_{3,g\to q}^0((\widetilde{jk}),1,i)\, B_{1,Q}^{Z,0}(\overline{1},(\widetilde{kl}),(\widetilde{(\widetilde{jk})i}))\, J_2^2(\{p\}_2) \\
&\\
&+E_4^0(i,l,k,1)\, B_{1,Q}^{Z,0}(j,\overline{1},(\widetilde{kli}))\, J_2^2(\{p\}_2)
\end{aligned}$$

$$
\begin{aligned}
&+ E_4^0(j,k,l,1)\, B_{1,Q}^{Z,0}((\widetilde{lkj}),\overline{1},i)\, J_2^2(\{p\}_2)\\
&- a_{3,g\to q}^0(i,1,j)\, E_3^0(\overline{1},k,l)\, B_{1,Q}^{Z,0}((\widetilde{ij}),\overline{\overline{1}},(\widetilde{kl}))\, J_2^2(\{p\}_2)\\
&- a_{3,g\to q}^0(j,1,i)\, E_3^0(\overline{1},k,l)\, B_{1,Q}^{Z,0}((\widetilde{kl}),\overline{\overline{1}},(\widetilde{ij}))\, J_2^2(\{p\}_2)\\
&+ E_3^0(i,l,k)\, a_{3,g\to q}^0((\widetilde{il}),1,j)\, B_{1,Q}^{Z,0}(((\widetilde{\widetilde{il}j}),\overline{1},(\widetilde{kl}))\, J_2^2(\{p\}_2)\\
&+ E_3^0(j,k,l)\, a_{3,g\to q}^0((\widetilde{jk}),1,i)\, B_{1,Q}^{Z,0}((\widetilde{kl}),\overline{1},(\widetilde{(\widetilde{jk})i}))\, J_2^2(\{p\}_2)\\
&- a_{3,g\to q}^0(k,1,l)\, E_3^0(i,(\widetilde{kl}),\overline{1})\, B_{1,Q}^{Z,0}(j,\overline{\overline{1}},(\widetilde{i(\widetilde{kl})}))\, J_2^2(\{p\}_2)\\
&- a_{3,g\to q}^0(l,1,k)\, E_3^0(j,(\widetilde{kl}),\overline{1})\, B_{1,Q}^{Z,0}((\widetilde{j(\widetilde{kl})}),\overline{\overline{1}},i)\, J_2^2(\{p\}_2)\\
&- E_3^0(i,l,k)\, d_{3,g\to q}^0((\widetilde{il}),1,(\widetilde{kl}))\, B_{1,Q}^{Z,0}(j,\overline{1},\widetilde{(\widetilde{il})(\widetilde{kl})})\, J_2^2(\{p\}_2)\\
&- E_3^0(j,k,l)\, d_{3,g}^0(i,(\widetilde{kl}),1)\, B_{1,Q}^{Z,0}((\widetilde{jk}),\overline{1},(\widetilde{i(\widetilde{kl})}))\, J_2^2(\{p\}_2)\\
&- E_3^0(j,k,l)\, d_{3,g\to q}^0((\widetilde{jk}),1,(\widetilde{kl}))\, B_{1,Q}^{Z,0}(\widetilde{(\widetilde{jk})(\widetilde{kl})},\overline{1},i)\, J_2^2(\{p\}_2)\\
&- E_3^0(i,l,k)\, d_{3,g}^0(j,(\widetilde{kl}),1)\, B_{1,Q}^{Z,0}(\widetilde{j(\widetilde{kl})},\overline{1},(\widetilde{il}))\, J_2^2(\{p\}_2)\,. \qquad \text{(B.4)}
\end{aligned}
$$

$$
\begin{aligned}
&\tilde{C}_1^{Z,0,S}(k,\hat{1};i,j;l) =\\
&+\frac{1}{2}\, E_3^0(k,i,j)\, \tilde{B}_{2,q}^{Z,0}((\widetilde{ki}),1,(\widetilde{ij}),l)\, J_2^3(\{p\}_3)\\
&+\frac{1}{2}\, E_3^0(l,i,j)\, \tilde{B}_{2,q}^{Z,0}(k,(\widetilde{ij}),1,(\widetilde{li}))\, J_2^3(\{p\}_3)\\
&-a_{3,g\to q}^0(i,1,j)\, C_0^{Z,0}(k;\overline{1},(\widetilde{ij});l)\, J_2^3(\{p\}_3)\\
&-a_{3,g\to q}^0(k,1,l)\, C_0^{Z,0}(\overline{1};i,j;(\widetilde{kl}))\, J_2^3(\{p\}_3)\\
&-a_{3,g\to q}^0(j,1,i)\, C_0^{Z,0}(k;(\widetilde{ij}),\overline{1};l)\, J_2^3(\{p\}_3)\\
&-a_{3,g\to q}^0(l,1,k)\, C_0^{Z,0}((\widetilde{kl});i,j;\overline{1})\, J_2^3(\{p\}_3)\\
&\\
&+ B_4^0(k,i,j,l)\, B_{1,q}^{Z,0}((\widetilde{kij}),1,(\widetilde{lji}))\, J_2^2(\{p\}_2)\\
&-\frac{1}{2}\, E_3^0(k,i,j)\, A_3^0((\widetilde{ki}),(\widetilde{ij}),l)\, B_{1,q}^{Z,0}((\widetilde{\widetilde{ki}(\widetilde{ij})}),1,(\widetilde{l(\widetilde{ij})}))\, J_2^2(\{p\}_2)\\
&-\frac{1}{2}\, E_3^0(l,i,j)\, A_3^0((\widetilde{li}),(\widetilde{ij}),k)\, B_{1,q}^{Z,0}((\widetilde{k(\widetilde{ij})}),1,(\widetilde{\widetilde{li}(\widetilde{ij})}))\, J_2^2(\{p\}_2)\\
&\\
&+\frac{1}{2}\, \tilde{E}_4^0(k,i,1,j)\, B_{1,q}^{Z,0}((\widetilde{kij}),\overline{1},l)\, J_2^2(\{p\}_2)\\
&-\frac{1}{2}\, A_3^0(i,1,j)\, E_{3,q'\to g}^0(k,\overline{1},(\widetilde{ij}))\, B_{1,q}^{Z,0}((\widetilde{k(\widetilde{ij})}),\overline{\overline{1}},l)\, J_2^2(\{p\}_2)\\
&\\
&+\frac{1}{2}\, \tilde{E}_4^0(l,i,1,j)\, B_{1,q}^{Z,0}(k,\overline{1},(\widetilde{lij}))\, J_2^2(\{p\}_2)\\
&-\frac{1}{2}\, A_3^0(i,1,j)\, E_{3,q'\to g}^0(l,\overline{1},(\widetilde{ij}))\, B_{1,q}^{Z,0}(k,\overline{\overline{1}},(\widetilde{l(\widetilde{ij})}))\, J_2^2(\{p\}_2)
\end{aligned}
$$

$$
\begin{aligned}
&+\frac{1}{2}\, E_3^0(k,i,j)\, a_{3,g\to q}^0((\widetilde{ki}),1,l)\, B_{1,q}^{Z,0}(\overline{1},(\widetilde{ij}),(\widetilde{l(\widetilde{ki})}))\, J_2^2(\{p\}_2)\\
&+\frac{1}{2}\, E_3^0(k,i,j)\, a_{3,g\to q}^0(l,1,(\widetilde{ki}))\, B_{1,q}^{Z,0}((\widetilde{l(\widetilde{ki})}),(\widetilde{ij}),\overline{1})\, J_2^2(\{p\}_2)\\
&+\frac{1}{2}\, E_3^0(l,i,j)\, a_{3,g\to q}^0(k,1,(\widetilde{li}))\, B_{1,q}^{Z,0}(\overline{1},(\widetilde{ij}),(\widetilde{k(\widetilde{li})}))\, J_2^2(\{p\}_2)\\
&+\frac{1}{2}\, E_3^0(l,i,j)\, a_{3,g\to q}^0((\widetilde{li}),1,k)\, B_{1,q}^{Z,0}((\widetilde{k(\widetilde{li})}),(\widetilde{ij}),\overline{1})\, J_2^2(\{p\}_2)\\
&+\frac{1}{2}\, E_3^0(i,k,l)\, \tilde{B}_{2,Q}^{Z,0}(j,(\widetilde{kl}),1,(\widetilde{ik}))\, J_2^3(\{p\}_3)\\
&+\frac{1}{2}\, E_3^0(j,k,l)\, \tilde{B}_{2,Q}^{Z,0}((\widetilde{jk}),1,(\widetilde{kl}),i)\, J_2^3(\{p\}_3)\\
\\
&+B_4^0(i,k,l,j)\, B_{1,Q}^{Z,0}((\widetilde{jlk}),1,(\widetilde{ikl}))\, J_2^2(\{p\}_2)\\
&-\frac{1}{2}\, E_3^0(i,k,l)\, A_3^0((\widetilde{ik}),(\widetilde{kl}),j)\, B_{1,Q}^{Z,0}((\widetilde{j(\widetilde{kl})}),1,(\widetilde{ik})(\widetilde{kl}))\, J_2^2(\{p\}_2)\\
&-\frac{1}{2}\, E_3^0(j,k,l)\, A_3^0((\widetilde{jk}),(\widetilde{kl}),i)\, B_{1,Q}^{Z,0}((\widetilde{jk})(\widetilde{kl}),1,(\widetilde{i(\widetilde{kl})}))\, J_2^2(\{p\}_2)\\
\\
&+\frac{1}{2}\, \tilde{E}_4^0(i,k,1,l)\, B_{1,Q}^{Z,0}(j,\overline{1},(\widetilde{ikl}))\, J_2^2(\{p\}_2)\\
&-\frac{1}{2}\, A_3^0(k,1,l)\, E_{3,q'\to g}^0(i,\overline{1},(\widetilde{kl}))\, B_{1,Q}^{Z,0}(j,\overline{\overline{1}},(\widetilde{i(\widetilde{kl})}))\, J_2^2(\{p\}_2)\\
\\
&+\frac{1}{2}\, \tilde{E}_4^0(j,k,1,l)\, B_{1,Q}^{Z,0}((\widetilde{jkl}),\overline{1},i)\, J_2^2(\{p\}_2)\\
&-\frac{1}{2}\, A_3^0(k,1,l)\, E_{3,q'\to g}^0(j,\overline{1},(\widetilde{kl}))\, B_{1,Q}^{Z,0}((\widetilde{j(\widetilde{kl})}),\overline{\overline{1}},i)\, J_2^2(\{p\}_2)\\
&+\frac{1}{2}\, E_3^0(i,k,l)\, a_{3,g\to q}^0((\widetilde{ik}),1,j)\, B_{1,Q}^{Z,0}((\widetilde{j(\widetilde{ik})}),(\widetilde{kl}),\overline{1})\, J_2^2(\{p\}_2)\\
&+\frac{1}{2}\, E_3^0(i,k,l)\, a_{3,g\to q}^0(j,1,(\widetilde{ik}))\, B_{1,Q}^{Z,0}(\overline{1},(\widetilde{kl}),(\widetilde{j(\widetilde{ik})}))\, J_2^2(\{p\}_2)\\
&+\frac{1}{2}\, E_3^0(j,k,l)\, a_{3,g\to q}^0((\widetilde{jk}),1,i)\, B_{1,Q}^{Z,0}(\overline{1},(\widetilde{kl}),(\widetilde{i(\widetilde{jk})}))\, J_2^2(\{p\}_2)\\
&+\frac{1}{2}\, E_3^0(j,k,l)\, a_{3,g\to q}^0(i,1,(\widetilde{jk}))\, B_{1,Q}^{Z,0}((\widetilde{i(\widetilde{jk})}),(\widetilde{kl}),\overline{1})\, J_2^2(\{p\}_2)\,. \qquad \text{(B.5)}
\end{aligned}
$$

$$
\begin{aligned}
&D_1^{Z,0,S}(k,\hat{1},j;i,l) =\\
&\quad -A_3^0(i,1,k)\, D_0^{Z,0}(\overline{1},j;(\widetilde{ik}),l)\, J_2^3(\{p\}_3)\\
&\quad -A_3^0(j,1,l)\, D_0^{Z,0}(i,\overline{1};k,(\widetilde{jl}))\, J_2^3(\{p\}_3)\\
\\
&\quad +2\, C_4^0(i,k,j,l)\, B_{1,q}^{Z,0}((\widetilde{ikj}),1,(\widetilde{kjl}))\, J_2^2(\{p\}_2)\\
&\quad +2\, C_4^0(k,i,j,l)\, B_{1,q}^{Z,0}((\widetilde{kij}),1,(\widetilde{ijl}))\, J_2^2(\{p\}_2)\\
&\quad +2\, C_4^0(l,j,i,k)\, B_{1,q}^{Z,0}((\widetilde{jik}),1,(\widetilde{lji}))\, J_2^2(\{p\}_2)\\
&\quad +2\, C_4^0(j,l,i,k)\, B_{1,q}^{Z,0}((\widetilde{lik}),1,(\widetilde{jli}))\, J_2^2(\{p\}_2)\,. \qquad \text{(B.6)}
\end{aligned}
$$

$$
\begin{aligned}
&\tilde{D}_1^{Z,0,S}(k,\hat{1},j;i,l) = \\
&\quad -A_3^0(i,1,k)\, D_0^{Z,0}(\overline{1},j;(\widetilde{ik}),l)\, J_2^3(\{p\}_3) \\
&\quad -A_3^0(j,1,l)\, D_0^{Z,0}(i,\overline{1};k,(\widetilde{jl}))\, J_2^3(\{p\}_3) \\
&\\
&\quad +2\, C_4^0(i,k,j,l)\, B_{1,q}^{Z,0}((\widetilde{ikj}),1,(\widetilde{kjl}))\, J_2^2(\{p\}_2) \\
&\quad +2\, C_4^0(k,i,j,l)\, B_{1,q}^{Z,0}((\widetilde{kij}),1,(\widetilde{ijl}))\, J_2^2(\{p\}_2) \\
&\quad +2\, C_4^0(l,j,i,k)\, B_{1,q}^{Z,0}((\widetilde{jik}),1,(\widetilde{lji}))\, J_2^2(\{p\}_2) \\
&\quad +2\, C_4^0(j,l,i,k)\, B_{1,q}^{Z,0}((\widetilde{lik}),1,(\widetilde{jli}))\, J_2^2(\{p\}_2)\,. \qquad \text{(B.7)}
\end{aligned}
$$

B.2 Real-virtual

$$
\begin{aligned}
&B_2^{Z,1,T}(j,\hat{1},i,k) = \\
&\quad -\Big[+ J_{2,GG}^{1,IF}(s_{1i}) + J_{2,QG}^{1,FF}(s_{ki}) + J_{2,GQ}^{1,IF}(s_{1j}) \Big]\, \bar{B}_2^{Z,0}(j,1,i,k)\, J_2^3(\{p\}_3) \\
&\quad -\Big[+ J_{2,GQ}^{1,IF}(s_{1k}) + J_{2,QG}^{1,FF}(s_{ji}) + J_{2,GG}^{1,IF}(s_{1i}) \Big]\, \bar{B}_2^{Z,0}(j,i,1,k)\, J_2^3(\{p\}_3) \\
&\quad + d_{3,g}^0(j,i,1) \Big[\bar{B}_1^{Z,1}((\widetilde{ji}),\overline{1},k)\, \delta(1-x_1)\, \delta(1-x_2) \\
&\quad + \Big(+ J_{2,GQ}^{1,IF}(s_{\overline{1}(\widetilde{ji})}) + J_{2,GQ}^{1,IF}(s_{\overline{1}k}) \Big)\, \bar{B}_1^{Z,0}((\widetilde{ji}),\overline{1},k) \Big]\, J_2^2(\{p\}_2) \\
&\quad + d_{3,g}^0(k,i,1) \Big[\bar{B}_1^{Z,1}(j,\overline{1},(\widetilde{ki}))\, \delta(1-x_1)\, \delta(1-x_2) \\
&\quad + \Big(+ J_{2,GQ}^{1,IF}(s_{\overline{1}(\widetilde{ki})}) + J_{2,GQ}^{1,IF}(s_{\overline{1}j}) \Big)\, \bar{B}_1^{Z,0}(j,\overline{1},(\widetilde{ki})) \Big]\, J_2^2(\{p\}_2) \\
&\quad + \Big[d_{3,g}^1(j,i,1)\, \delta(1-x_1)\, \delta(1-x_2) \\
&\quad + \Big(- 2J_{2,GQ}^{1,IF}(s_{\overline{1}(\widetilde{ji})}) + J_{2,GQ}^{1,IF}(s_{1j}) + J_{2,QG}^{1,FF}(s_{ji}) + J_{2,GG}^{1,IF}(s_{1i}) \Big)\, d_{3,g}^0(j,i,1) \Big] \\
&\quad \times \bar{B}_1^{Z,0}((\widetilde{ji}),\overline{1},k)\, J_2^2(\{p\}_2) \\
&\quad + \Big[d_{3,g\to q}^1(j,1,i)\, \delta(1-x_1)\, \delta(1-x_2) \\
&\quad + \Big(- 2J_{2,GQ}^{1,IF}(s_{\overline{1}(\widetilde{ji})}) + J_{2,GQ}^{1,IF}(s_{1j}) + J_{2,QG}^{1,FF}(s_{ji}) + J_{2,GG}^{1,IF}(s_{1i}) \Big)\, d_{3,g\to q}^0(j,1,i) \Big] \\
&\quad \times \bar{B}_1^{Z,0}((\widetilde{ji}),\overline{1},k)\, J_2^2(\{p\}_2) \\
&\quad + \Big[d_{3,g}^1(k,i,1)\, \delta(1-x_1)\, \delta(1-x_2) \\
&\quad + \Big(+ J_{2,GG}^{1,IF}(s_{1i}) + J_{2,GQ}^{1,IF}(s_{1k}) + J_{2,QG}^{1,FF}(s_{ki}) - 2J_{2,GQ}^{1,IF}(s_{\overline{1}(\widetilde{ki})}) \Big)\, d_{3,g}^0(k,i,1) \Big] \\
&\quad \times \bar{B}_1^{Z,0}(j,\overline{1},(\widetilde{ki}))\, J_2^2(\{p\}_2) \\
&\quad + \Big[d_{3,g\to q}^1(k,1,i)\, \delta(1-x_1)\, \delta(1-x_2)
\end{aligned}
$$

$$
\begin{aligned}
&+\Big(+ J^{1,IF}_{2,GG}(s_{1i}) + J^{1,IF}_{2,GQ}(s_{1k}) + J^{1,FF}_{2,QG}(s_{ki}) - 2J^{1,IF}_{2,GQ}(s_{\overline{1}(\widetilde{ki})}) \Big)\, d^0_{3,g\to q}(k,1,i) \Big] \\
&\times \bar{B}^{Z,0}_1(j,\overline{1},(\widetilde{ki}))\, J^2_2(\{p\}_2) \\
&- \Big[\tilde{A}^1_{3,g}(j,1,k)\, \delta(1-x_1)\, \delta(1-x_2) \\
&+\Big(+ J^{1,FF}_{2,QQ}(s_{jk}) - J^{1,IF}_{2,QQ}(s_{\overline{1}(\widetilde{jk})}) \Big)\, A^0_{3,g\to q}(j,1,k) \Big]\, \bar{B}^{Z,0}_1((\widetilde{jk}),\overline{1},i)\, J^2_2(\{p\}_2) \\
&- \Big[\tilde{A}^1_3(j,i,k)\, \delta(1-x_1)\, \delta(1-x_2) \\
&+\Big(+ J^{1,FF}_{2,QQ}(s_{jk}) - J^{1,FF}_{2,QQ}(s_{(\widetilde{ji})(\widetilde{ki})}) \Big)\, A^0_3(j,i,k) \Big]\, \bar{B}^{Z,0}_1((\widetilde{ji}),1,(\widetilde{ki}))\, J^2_2(\{p\}_2) \\
&- \Big[A^1_{3,g}(j,1,k)\, \delta(1-x_1)\, \delta(1-x_2) \\
&+\Big(- J^{1,IF}_{2,QQ}(s_{\overline{1}(\widetilde{jk})}) + J^{1,IF}_{2,GQ}(s_{1k}) + J^{1,IF}_{2,GQ}(s_{1j}) \Big)\, A^0_{3,g\to q}(j,1,k) \Big] \\
&\times \bar{B}^{Z,0}_1((\widetilde{jk}),\overline{1},i)\, J^2_2(\{p\}_2) \\
&- \Big[+ J^{1,FF}_{2,QQ}(s_{jk}) + J^{1,IF}_{2,GG}(s_{1i}) - J^{1,FF}_{2,QG}(s_{ji}) - J^{1,IF}_{2,GQ}(s_{1k}) \\
&+\Big(- \mathcal{S}^{FF}(s_{1i},s_{ji},x_{1i,ji}) + \mathcal{S}^{FF}(s_{ji},s_{ji},1) - \mathcal{S}^{FF}(s_{jk},s_{ji},x_{jk,ji}) \\
&+\mathcal{S}^{FF}(s_{1k},s_{ji},x_{1k,ji}) \Big) \Big]\, d^0_{3,g\to q}(j,1,i)\, \bar{B}^{Z,0}_1((\widetilde{ji}),\overline{1},k)\, J^2_2(\{p\}_2) \\
&- \Big[+ J^{1,IF}_{2,GG}(s_{1i}) - J^{1,FF}_{2,QG}(s_{ki}) + J^{1,FF}_{2,QQ}(s_{kj}) - J^{1,IF}_{2,GQ}(s_{1j}) \\
&+\Big(- \mathcal{S}^{FF}(s_{1i},s_{ki},x_{1i,ki}) + \mathcal{S}^{FF}(s_{ki},s_{ki},1) - \mathcal{S}^{FF}(s_{kj},s_{ki},x_{kj,ki}) \\
&+\mathcal{S}^{FF}(s_{1j},s_{ki},x_{1j,ki}) \Big) \Big]\, d^0_{3,g\to q}(k,1,i)\, \bar{B}^{Z,0}_1(j,\overline{1},(\widetilde{ki}))\, J^2_2(\{p\}_2) \\
&+2\Big[+ J^{1,FF}_{2,QQ}(s_{jk}) - J^{1,IF}_{2,QQ}(s_{\overline{1}(\widetilde{jk})}) + J^{1,FF}_{2,QG}(s_{(\widetilde{jk})i}) \\
&\quad + J^{1,IF}_{2,QG}(s_{\overline{1}i}) - J^{1,FF}_{2,QG}(s_{ji}) - J^{1,FF}_{2,QG}(s_{ki}) \\
&\quad + \Big(+ \mathcal{S}^{FF}(s_{ji},s_{jk},x_{ji,jk}) + \mathcal{S}^{FF}(s_{ki},s_{jk},x_{ki,jk}) - \mathcal{S}^{FF}(s_{jk},s_{jk},1) \\
&\quad - \mathcal{S}^{FF}(s_{(\widetilde{jk})i},s_{jk},x_{(\widetilde{jk})i,jk}) - \mathcal{S}^{FF}(s_{\overline{1}i},s_{jk},x_{\overline{1}i,jk}) + \mathcal{S}^{FF}(s_{\overline{1}(\widetilde{jk})},s_{jk},x_{\overline{1}(\widetilde{jk}),jk}) \Big) \Big] \\
&\times A^0_{3,g\to q}(j,1,k)\, \bar{B}^{Z,0}_1((\widetilde{jk}),\overline{1},i)\, J^2_2(\{p\}_2) \\
&-\frac{1}{2}\Big[+ J^{1,IF}_{2,GQ}(s_{1j}) - J^{1,IF}_{2,GQ}(s_{\overline{1}(\widetilde{ji})}) - J^{1,IF}_{2,GQ}(s_{1k}) \\
&\quad + J^{1,IF}_{2,GQ}(s_{\overline{1}k}) - J^{1,FF}_{2,QQ}(s_{jk}) + J^{1,FF}_{2,QQ}(s_{(\widetilde{ji})k}) \\
&\quad + \Big(- \mathcal{S}^{FF}(s_{1j},s_{jk},x_{1j,jk}) + \mathcal{S}^{FF}(s_{\overline{1}(\widetilde{ji})},s_{jk},x_{\overline{1}(\widetilde{ji}),jk}) + \mathcal{S}^{FF}(s_{1k},s_{jk},x_{1k,jk})
\end{aligned}
$$

$$
\begin{aligned}
&\quad - \mathcal{S}^{FF}(s_{\overline{1}k}, s_{jk}, x_{\overline{1}k,jk}) + \mathcal{S}^{FF}(s_{jk}, s_{jk}, 1) - \mathcal{S}^{FF}(s_{(\widetilde{ji})k}, s_{jk}, x_{(\widetilde{ji})k,jk}) \Bigg) \Bigg] \\
&\times d^0_{3,g}(j,i,1)\, \bar{B}^{Z,0}_1((\widetilde{ji}), \overline{1}, k)\, J^2_2(\{p\}_2) \\
&- \frac{1}{2} \Bigg[+ J^{1,IF}_{2,GQ}(s_{1k}) - J^{1,IF}_{2,GQ}(s_{\overline{1}(\widetilde{ki})}) - J^{1,IF}_{2,GQ}(s_{1j}) \\
&\quad + J^{1,IF}_{2,GQ}(s_{\overline{1}j}) - J^{1,FF}_{2,QQ}(s_{kj}) + J^{1,FF}_{2,QQ}(s_{(\widetilde{ki})j}) \\
&\quad + \Bigg(- \mathcal{S}^{FF}(s_{1k}, s_{kj}, x_{1k,kj}) + \mathcal{S}^{FF}(s_{\overline{1}(\widetilde{ki})}, s_{kj}, x_{\overline{1}(\widetilde{ki}),kj}) + \mathcal{S}^{FF}(s_{1j}, s_{kj}, x_{1j,kj}) \\
&\quad - \mathcal{S}^{FF}(s_{\overline{1}j}, s_{kj}, x_{\overline{1}j,kj}) + \mathcal{S}^{FF}(s_{kj}, s_{kj}, 1) - \mathcal{S}^{FF}(s_{(\widetilde{ki})j}, s_{kj}, x_{(\widetilde{ki})j,kj}) \Bigg) \Bigg] \\
&\times d^0_{3,g}(k,i,1)\, \bar{B}^{Z,0}_1(j, \overline{1}, (\widetilde{ki}))\, J^2_2(\{p\}_2) \\
&+ \frac{1}{2} \Bigg[+ J^{1,FF}_{2,QQ}(s_{jk}) - J^{1,FF}_{2,QQ}(s_{(\widetilde{ji})(\widetilde{ki})}) - J^{1,IF}_{2,GQ}(s_{1j}) \\
&\quad + J^{1,IF}_{2,GQ}(s_{1(\widetilde{ji})}) - J^{1,IF}_{2,GQ}(s_{1k}) + J^{1,IF}_{2,GQ}(s_{1(\widetilde{ki})}) \\
&\quad + \Bigg(- \mathcal{S}^{FF}(s_{jk}, s_{jk}, 1) + \mathcal{S}^{FF}(s_{(\widetilde{ji})(\widetilde{ki})}, s_{jk}, x_{(\widetilde{ji})(\widetilde{ki}),jk}) + \mathcal{S}^{FF}(s_{1j}, s_{jk}, x_{1j,jk}) \\
&\quad - \mathcal{S}^{FF}(s_{1(\widetilde{ji})}, s_{jk}, x_{1(\widetilde{ji}),jk}) + \mathcal{S}^{FF}(s_{1k}, s_{jk}, x_{1k,jk}) - \mathcal{S}^{FF}(s_{1(\widetilde{ki})}, s_{jk}, x_{1(\widetilde{ki}),jk}) \Bigg) \Bigg] \\
&\times A^0_3(j,i,k)\, \bar{B}^{Z,0}_1((\widetilde{ji}), 1, (\widetilde{ki}))\, J^2_2(\{p\}_2) \\
&+ \Bigg[- 2J^{1,IF}_{2,QQ,g\to q}(s_{1k}) + 2J^{1,IF}_{2,QQ,g\to q}(s_{\overline{1}k}) \Bigg] D^0_3(1,i,j)\, \bar{B}^{Z,0}_1((\widetilde{ij}), \overline{1}, k)\, J^2_2(\{p\}_2) \\
&+ \Bigg[+ 2J^{1,IF}_{2,QQ,g\to q}(s_{1k}) - 2J^{1,IF}_{2,QQ,g\to q}(s_{\overline{1}(\widetilde{ki})}) \Bigg] A^0_3(1,i,k)\, \bar{B}^{Z,0}_1(j, \overline{1}, (\widetilde{ik}))\, J^2_2(\{p\}_2) \\
&+ \Bigg[+ 2J^{1,IF}_{2,QQ,g\to q}(s_{1k}) - 2J^{1,IF}_{2,QQ,g\to q}(s_{\overline{1}(\widetilde{kj})}) \Bigg] A^0_3(1,j,k)\, \bar{B}^{Z,0}_1((\widetilde{jk}), \overline{1}, i)\, J^2_2(\{p\}_2) \\
&+ \Bigg[- 2J^{1,IF}_{2,QQ,g\to q}(s_{1k}) + 2J^{1,IF}_{2,QQ,g\to q}(s_{1(\widetilde{ki})}) \Bigg] d^0_3(k,i,j)\, \bar{B}^{Z,0}_1((\widetilde{ij}), 1, (\widetilde{ki}))\, J^2_2(\{p\}_2) \\
&+ \Bigg[- 2J^{1,IF}_{2,QQ,g\to q}(s_{1k}) + 2J^{1,IF}_{2,QQ,g\to q}(s_{1(\widetilde{kj})}) \Bigg] d^0_3(k,j,i)\, \bar{B}^{Z,0}_1((\widetilde{ji}), 1, (\widetilde{kj}))\, J^2_2(\{p\}_2) \\
&+ \Bigg[- 2J^{1,IF}_{2,QG}(s_{\overline{1}(\widetilde{ki})}) + 2J^{1,IF}_{2,GQ}(s_{\overline{1}(\widetilde{ki})}) \Bigg] d^0_{3,g\to q}(k,1,i)\, \bar{B}^{Z,0}_1(j, \overline{1}, (\widetilde{ki}))\, J^2_2(\{p\}_2) \\
&+ \Bigg[- 2J^{1,IF}_{2,QG}(s_{\overline{1}(\widetilde{ji})}) + 2J^{1,IF}_{2,GQ}(s_{\overline{1}(\widetilde{ji})}) \Bigg] d^0_{3,g\to q}(j,1,i)\, \bar{B}^{Z,0}_1((\widetilde{ji}), \overline{1}, k)\, J^2_2(\{p\}_2) \\
&- A^0_3(j,1,k) \Bigg[\bar{B}^{Z,1}_1(\overline{1}, i, (\widetilde{jk}))\, \delta(1-x_1)\, \delta(1-x_2) \\
&+ \Bigg(+ J^{1,IF}_{2,QG}(s_{\overline{1}i}) + J^{1,FF}_{2,QG}(s_{(\widetilde{jk})i}) \Bigg) \bar{B}^{Z,0}_1(\overline{1}, i, (\widetilde{jk})) \Bigg] J^2_2(\{p\}_2) \\
&- \Bigg[A^1_{3,g}(j,1,k)\, \delta(1-x_1)\, \delta(1-x_2) \\
&+ \Bigg(- J^{1,IF}_{2,QQ}(s_{\overline{1}(\widetilde{jk})}) + J^{1,IF}_{2,GQ}(s_{1k}) + J^{1,IF}_{2,GQ}(s_{1j}) \Bigg) A^0_3(j,1,k) \Bigg] \bar{B}^{Z,0}_1(\overline{1}, i, (\widetilde{kj}))\, J^2_2(\{p\}_2)
\end{aligned}
$$

$$
\begin{aligned}
&-\Big[+ J^{1,FF}_{2,QQ}(s_{jk}) - J^{1,IF}_{2,GQ}(s_{1k}) - J^{1,FF}_{2,QG}(s_{ji}) + J^{1,IF}_{2,GG}(s_{1i}) \\
&+\Big(- \mathcal{S}^{FF}(s_{1i}, s_{ji}, x_{1i,ji}) + \mathcal{S}^{FF}(s_{ji}, s_{ji}, 1) - \mathcal{S}^{FF}(s_{jk}, s_{ji}, x_{jk,ji}) \\
&\quad + \mathcal{S}^{FF}(s_{1k}, s_{ji}, x_{1k,ji}) \Big) \Big] \, d^0_{3,g\to q}(j,1,i)\, \bar{B}^{Z,0}_1(\overline{1}, (\widetilde{ji}), k)\, J^2_2(\{p\}_2) \\
&-\Big[+ J^{1,IF}_{2,GG}(s_{1i}) + J^{1,FF}_{2,QQ}(s_{kj}) - J^{1,IF}_{2,GQ}(s_{1j}) - J^{1,FF}_{2,QG}(s_{ki}) \\
&+\Big(- \mathcal{S}^{FF}(s_{1i}, s_{ki}, x_{1i,ki}) + \mathcal{S}^{FF}(s_{ki}, s_{ki}, 1) - \mathcal{S}^{FF}(s_{kj}, s_{ki}, x_{kj,ki}) \\
&\quad + \mathcal{S}^{FF}(s_{1j}, s_{ki}, x_{1j,ki}) \Big) \Big] \, d^0_{3,g\to q}(k,1,i)\, \bar{B}^{Z,0}_1(\overline{1}, (\widetilde{ki}), j)\, J^2_2(\{p\}_2) \\
&+\Big[+ J^{1,FF}_{2,QQ}(s_{jk}) - J^{1,FF}_{2,QG}(s_{ji}) - J^{1,FF}_{2,QG}(s_{ki}) \\
&\quad - J^{1,IF}_{2,QQ}(s_{\overline{1}(\widetilde{jk})}) + J^{1,FF}_{2,QG}(s_{(\widetilde{jk})i}) + J^{1,IF}_{2,QG}(s_{\overline{1}i}) \\
&\quad + \Big(+ \mathcal{S}^{FF}(s_{ji}, s_{jk}, x_{ji,jk}) + \mathcal{S}^{FF}(s_{ki}, s_{jk}, x_{ki,jk}) - \mathcal{S}^{FF}(s_{jk}, s_{jk}, 1) \\
&\quad - \mathcal{S}^{FF}(s_{(\widetilde{jk})i}, s_{jk}, x_{(\widetilde{jk})i,jk}) - \mathcal{S}^{FF}(s_{\overline{1}i}, s_{jk}, x_{\overline{1}i,jk}) + \mathcal{S}^{FF}(s_{\overline{1}(\widetilde{jk})}, s_{jk}, x_{\overline{1}(\widetilde{jk}),jk}) \Big) \Big] \\
&\times A^0_3(j,1,k)\, \bar{B}^{Z,0}_1(\overline{1}, i, (\widetilde{jk}))\, J^2_2(\{p\}_2)\,. \qquad \text{(B.8)}
\end{aligned}
$$

$$
\begin{aligned}
&B^{Z,1,T}_{2,g\to q}(j,\hat{1},i,k) = \\
&\quad -J^{1,IF}_{2,QQ,g\to q}(s_{1k})\, \bar{B}^{Z,0}_2(1,i,j,k)\, J^3_2(\{p\}_3) \\
&\quad -J^{1,IF}_{2,QQ,g\to q}(s_{1k})\, \bar{B}^{Z,0}_2(1,j,i,k)\, J^3_2(\{p\}_3) \\
&\quad +\Big[+ J^{1,IF}_{2,QQ,g\to q}(s_{1k}) - J^{1,IF}_{2,QQ,g\to q}(s_{\overline{1}(\widetilde{ki})}) \Big] A^0_3(1,i,k)\, \bar{B}^{Z,0}_1(\overline{1}, j, (\widetilde{ik}))\, J^2_2(\{p\}_2) \\
&\quad +\Big[+ J^{1,IF}_{2,QQ,g\to q}(s_{1k}) - J^{1,IF}_{2,QQ,g\to q}(s_{\overline{1}(\widetilde{kj})}) \Big] A^0_3(1,j,k)\, \bar{B}^{Z,0}_1(\overline{1}, i, (\widetilde{jk}))\, J^2_2(\{p\}_2) \\
&\quad +J^{1,IF}_{2,QQ,g\to q}(s_{1(\widetilde{ki})})\, d^0_3(k,i,j)\, \bar{B}^{Z,0}_1(1, (\widetilde{ij}), (\widetilde{ki}))\, J^2_2(\{p\}_2) \\
&\quad +J^{1,IF}_{2,QQ,g\to q}(s_{\overline{1}k})\, d^0_3(1,j,i)\, \bar{B}^{Z,0}_1(\overline{1}, (\widetilde{ij}), k)\, J^2_2(\{p\}_2) \\
&\quad +J^{1,IF}_{2,QQ,g\to q}(s_{1(\widetilde{kj})})\, d^0_3(k,j,i)\, \bar{B}^{Z,0}_1(1, (\widetilde{ji}), (\widetilde{kj}))\, J^2_2(\{p\}_2) \\
&\quad +J^{1,IF}_{2,QQ,g\to q}(s_{\overline{1}k})\, d^0_3(1,i,j)\, \bar{B}^{Z,0}_1(\overline{1}, (\widetilde{ji}), k)\, J^2_2(\{p\}_2)\,. \qquad \text{(B.9)}
\end{aligned}
$$

$$
\begin{aligned}
&\tilde{B}^{Z,1,T}_2(j,\hat{1},i,k) = \\
&\quad -J^{1,FF}_{2,QQ}(s_{jk})\, \bar{B}^{Z,0}_2(j,1,i,k)\, J^3_2(\{p\}_3) \\
&\quad -J^{1,FF}_{2,QQ}(s_{jk})\, \bar{B}^{Z,0}_2(j,i,1,k)\, J^3_2(\{p\}_3) \\
&\quad -\Big[+ J^{1,IF}_{2,GQ}(s_{1k}) + J^{1,IF}_{2,GQ}(s_{1j}) \Big] \tilde{\bar{B}}^{Z,0}_2(j,1,i,k)\, J^3_2(\{p\}_3)
\end{aligned}
$$

$$
\begin{aligned}
&-\Big[+ J^{1,FF}_{2,QG}(s_{ji}) + J^{1,FF}_{2,QG}(s_{ki}) \Big] \, \tilde{\bar{B}}^{Z,0}_2(j,1,i,k) \, J^3_2(\{p\}_3) \\
&+ J^{1,FF}_{2,QQ}(s_{jk}) \, \tilde{\bar{B}}^{Z,0}_2(j,1,i,k) \, J^3_2(\{p\}_3) \\
&+ A^0_3(j,i,k) \Big[\bar{B}^{Z,1}_1((\widetilde{ji}),1,(\widetilde{ki})) \, \delta(1-x_1) \, \delta(1-x_2) \\
&+ \Big(+ J^{1,IF}_{2,GQ}(s_{1(\widetilde{ji})}) + J^{1,IF}_{2,GQ}(s_{1(\widetilde{ki})}) \Big) \, \bar{B}^{Z,0}_1((\widetilde{ji}),1,(\widetilde{ki})) \Big] \, J^2_2(\{p\}_2) \\
&+ d^0_{3,g}(j,i,1) \Big[\tilde{\bar{B}}^{Z,1}_1((\widetilde{ji}),\overline{1},k) \, \delta(1-x_1) \, \delta(1-x_2) \\
&\quad + J^{1,FF}_{2,QQ}(s_{(\widetilde{ji})k}) \, \bar{B}^{Z,0}_1((\widetilde{ji}),\overline{1},k) \Big] \, J^2_2(\{p\}_2) \\
&+ d^0_{3,g}(k,i,1) \Big[\tilde{\bar{B}}^{Z,1}_1(j,\overline{1},(\widetilde{ki})) \, \delta(1-x_1) \, \delta(1-x_2) \\
&\quad + J^{1,FF}_{2,QQ}(s_{(\widetilde{ki})j}) \, \bar{B}^{Z,0}_1(j,\overline{1},(\widetilde{ki})) \Big] \, J^2_2(\{p\}_2) \\
&+ \Big[A^1_3(j,i,k) \, \delta(1-x_1) \, \delta(1-x_2) \\
&+ \Big(+ J^{1,FF}_{2,QG}(s_{ji}) + J^{1,FF}_{2,QG}(s_{ki}) - J^{1,FF}_{2,QQ}(s_{(\widetilde{ki})(\widetilde{ji})}) \Big) \, A^0_3(j,i,k) \Big] \\
&\times \bar{B}^{Z,0}_1((\widetilde{ji}),1,(\widetilde{ki})) \, J^2_2(\{p\}_2) \\
&+ \Big[\tilde{A}^1_3(j,i,k) \, \delta(1-x_1) \, \delta(1-x_2) \\
&+ \Big(+ J^{1,FF}_{2,QQ}(s_{jk}) - J^{1,FF}_{2,QQ}(s_{(\widetilde{ki})(\widetilde{ji})}) \Big) \, A^0_3(j,i,k) \Big] \, \bar{B}^{Z,0}_1((\widetilde{ji}),1,(\widetilde{ki})) \, J^2_2(\{p\}_2) \\
&- \Big[+ J^{1,FF}_{2,QQ}(s_{jk}) - J^{1,FF}_{2,QQ}(s_{(\widetilde{ji})(\widetilde{ki})}) - J^{1,IF}_{2,GQ}(s_{1j}) \\
&\quad + J^{1,IF}_{2,GQ}(s_{1(\widetilde{ji})}) - J^{1,IF}_{2,GQ}(s_{1k}) + J^{1,IF}_{2,GQ}(s_{1(\widetilde{ki})}) \\
&+ \Big(- \mathcal{S}^{FF}(s_{jk},s_{jk},1) + \mathcal{S}^{FF}(s_{(\widetilde{ji})(\widetilde{ki})},s_{jk},x_{(\widetilde{ji})(\widetilde{ki}),jk}) + \mathcal{S}^{FF}(s_{1j},s_{jk},x_{1j,jk}) \\
&\quad - \mathcal{S}^{FF}(s_{1(\widetilde{ij})},s_{jk},x_{1(\widetilde{ij}),jk}) + \mathcal{S}^{FF}(s_{1k},s_{jk},x_{1k,jk}) - \mathcal{S}^{FF}(s_{1(\widetilde{ki})},s_{jk},x_{1(\widetilde{ki}),jk}) \Big) \Big] \\
&\times A^0_3(j,i,k) \, \bar{B}^{Z,0}_1((\widetilde{ji}),1,(\widetilde{ki})) \, J^2_2(\{p\}_2) \\
&- A^0_3(j,1,k) \Big[\bar{B}^{Z,1}_1(\overline{1},i,(\widetilde{jk})) \, \delta(1-x_1) \, \delta(1-x_2) \\
&+ \Big(+ J^{1,IF}_{2,QG}(s_{\overline{1}i}) + J^{1,FF}_{2,QG}(s_{(\widetilde{jk})i}) \Big) \, \bar{B}^{Z,0}_1(\overline{1},i,(\widetilde{jk})) \Big] \, J^2_2(\{p\}_2) \\
&- A^0_3(j,1,k) \Big[\tilde{\bar{B}}^{Z,1}_1(\overline{1},i,(\widetilde{jk})) \, \delta(1-x_1) \, \delta(1-x_2) \\
&\quad + J^{1,IF}_{2,QQ}(s_{\overline{1}(\widetilde{jk})}) \, \bar{B}^{Z,0}_1(\overline{1},i,(\widetilde{jk})) \Big] \, J^2_2(\{p\}_2)
\end{aligned}
$$

$$
\begin{aligned}
&-\Bigg[A^{1}_{3,g}(j,1,k)\,\delta(1-x_1)\,\delta(1-x_2) \\
&+\Bigg(- J^{1,IF}_{2,QQ}(s_{\overline{1}(\widetilde{jk})}) + J^{1,IF}_{2,GQ}(s_{1j}) + J^{1,IF}_{2,GQ}(s_{1k}) \Bigg) A^{0}_{3}(j,1,k) \Bigg] \\
&\times \bar{B}^{Z,0}_{1}(\overline{1},i,(\widetilde{jk}))\, J^{2}_{2}(\{p\}_2) \\
&-\Bigg[\tilde{A}^{1}_{3,g}(j,1,k)\,\delta(1-x_1)\,\delta(1-x_2) \\
&+\Bigg(- J^{1,IF}_{2,QQ}(s_{\overline{1}(\widetilde{jk})}) + J^{1,FF}_{2,QQ}(s_{jk}) \Bigg) A^{0}_{3}(j,1,k) \Bigg]\, \bar{B}^{Z,0}_{1}(\overline{1},i,(\widetilde{jk}))\, J^{2}_{2}(\{p\}_2) \\
&-\Bigg[+ J^{1,IF}_{2,QQ}(s_{(\widetilde{jk})\overline{1}}) + J^{1,FF}_{2,QG}(s_{ji}) + J^{1,FF}_{2,QG}(s_{ki}) \\
&\quad - J^{1,IF}_{2,QG}(s_{\overline{1}i}) - J^{1,FF}_{2,QG}(s_{(\widetilde{jk})i}) - J^{1,FF}_{2,QQ}(s_{jk}) \\
&\quad + \Bigg(- \mathcal{S}^{FF}(s_{(\widetilde{jk})\overline{1}}, s_{jk}, x_{(\widetilde{jk})\overline{1},jk}) - \mathcal{S}^{FF}(s_{ij}, s_{jk}, x_{ij,jk}) - \mathcal{S}^{FF}(s_{ki}, s_{jk}, x_{ki,jk}) \\
&\quad + \mathcal{S}^{FF}(s_{(\widetilde{jk})i}, s_{jk}, x_{(\widetilde{jk})i,jk}) + \mathcal{S}^{FF}(s_{\overline{1}i}, s_{jk}, x_{\overline{1}i,jk}) + \mathcal{S}^{FF}(s_{jk}, s_{jk}, 1) \Bigg) \Bigg] \\
&\times A^{0}_{3}(j,1,k)\, \bar{B}^{Z,0}_{1}(\overline{1},i,(\widetilde{jk}))\, J^{2}_{2}(\{p\}_2)\,. \qquad \text{(B.10)}
\end{aligned}
$$

$$
\begin{aligned}
&\tilde{B}^{Z,1,T}_{2,g\to q}(j,\hat{1},i,k) = \\
&\quad - J^{1,IF}_{2,QQ,g\to q}(s_{1k})\, \bar{B}^{Z,0}_{2}(1,i,j,k)\, J^{3}_{2}(\{p\}_3) \\
&\quad - J^{1,IF}_{2,QQ,g\to q}(s_{1k})\, \bar{B}^{Z,0}_{2}(1,j,i,k)\, J^{3}_{2}(\{p\}_3) \\
&\quad - J^{1,IF}_{2,QQ,g\to q}(s_{1k})\, \tilde{\bar{B}}^{Z,0}_{2}(1,i,j,k)\, J^{3}_{2}(\{p\}_3) \\
&\quad + J^{1,IF}_{2,QQ,g\to q}(s_{k1})\, A^{0}_{3}(1,i,k)\, \bar{B}^{Z,0}_{1}(\overline{1},j,(\widetilde{ik}))\, J^{2}_{2}(\{p\}_2) \\
&\quad + J^{1,IF}_{2,QQ,g\to q}(s_{k1})\, A^{0}_{3}(1,j,k)\, \bar{B}^{Z,0}_{1}(\overline{1},i,(\widetilde{jk}))\, J^{2}_{2}(\{p\}_2) \\
&\quad + \Bigg[+ J^{1,IF}_{2,QQ,g\to q}(s_{1k}) - J^{1,IF}_{2,QQ,g\to q}(s_{\overline{1}(\widetilde{ki})}) \Bigg] A^{0}_{3}(1,i,k)\, \bar{B}^{Z,0}_{1}(\overline{1},j,(\widetilde{ik}))\, J^{2}_{2}(\{p\}_2) \\
&\quad + \Bigg[- J^{1,IF}_{2,QQ,g\to q}(s_{\overline{1}(\widetilde{kj})}) + J^{1,IF}_{2,QQ,g\to q}(s_{1k}) \Bigg] A^{0}_{3}(1,j,k)\, \bar{B}^{Z,0}_{1}(\overline{1},i,(\widetilde{jk}))\, J^{2}_{2}(\{p\}_2) \\
&\quad + J^{1,IF}_{2,QQ,g\to q}(s_{1(\widetilde{ki})})\, d^{0}_{3}(k,i,j)\, \bar{B}^{Z,0}_{1}(1,(\widetilde{ij}),(\widetilde{ki}))\, J^{2}_{2}(\{p\}_2) \\
&\quad + J^{1,IF}_{2,QQ,g\to q}(s_{\overline{1}k})\, d^{0}_{3}(1,j,i)\, \bar{B}^{Z,0}_{1}(\overline{1},(\widetilde{ij}),k)\, J^{2}_{2}(\{p\}_2) \\
&\quad + J^{1,IF}_{2,QQ,g\to q}(s_{1(\widetilde{kj})})\, d^{0}_{3}(k,j,i)\, \bar{B}^{Z,0}_{1}(1,(\widetilde{ji}),(\widetilde{kj}))\, J^{2}_{2}(\{p\}_2) \\
&\quad + J^{1,IF}_{2,QQ,g\to q}(s_{\overline{1}k})\, d^{0}_{3}(1,i,j)\, \bar{B}^{Z,0}_{1}(\overline{1},(\widetilde{ji}),k)\, J^{2}_{2}(\{p\}_2) \\
&\quad - \frac{1}{2} J^{1,IF}_{2,QQ,g\to q}(s_{1k})\, D^{Z,0}_{0}(1,j;k,i)\, J^{3}_{2}(\{p\}_3) \\
&\quad - \frac{1}{2} J^{1,IF}_{2,QQ,g\to q}(s_{1k})\, D^{Z,0}_{0}(i,1;j,k)\, J^{3}_{2}(\{p\}_3)\,. \qquad \text{(B.11)}
\end{aligned}
$$

$$
\tilde{\tilde{B}}^{Z,1,T}_{2}(j,\hat{1},i,k) =
$$

$$
\begin{aligned}
&-J^{1,FF}_{2,QQ}(s_{jk})\,\tilde{\bar{B}}^{Z,0}_{2}(j,1,i,k)\,J^{3}_{2}(\{p\}_3)\\
&+A^{0}_{3}(j,i,k)\,\Bigg[\,\tilde{\bar{B}}^{Z,1}_{1}((\widetilde{ji}),1,(\widetilde{ki}))\,\delta(1-x_1)\,\delta(1-x_2)\\
&\quad+J^{1,FF}_{2,QQ}(s_{(\widetilde{ji})(\widetilde{ki})})\,\bar{B}^{Z,0}_{1}((\widetilde{ji}),1,(\widetilde{ki}))\Bigg]\,J^{2}_{2}(\{p\}_2)\\
&+\Bigg[\,\tilde{A}^{1}_{3}(j,i,k)\,\delta(1-x_1)\,\delta(1-x_2)\\
&+\Bigg(+J^{1,FF}_{2,QQ}(s_{jk})-J^{1,FF}_{2,QQ}(s_{(\widetilde{ji})(\widetilde{ki})})\Bigg)\,A^{0}_{3}(j,i,k)\Bigg]\,\bar{B}^{Z,0}_{1}((\widetilde{ji}),1,(\widetilde{ki}))\,J^{2}_{2}(\{p\}_2)\\
&-A^{0}_{3}(j,1,k)\,\Bigg[\,\tilde{\bar{B}}^{Z,1}_{1}(\overline{1},i,(\widetilde{jk}))\,\delta(1-x_1)\,\delta(1-x_2)\\
&\quad+J^{1,IF}_{2,QQ}(s_{\overline{1}(\widetilde{jk})})\,\bar{B}^{Z,0}_{1}(\overline{1},i,(\widetilde{jk}))\Bigg]\,J^{2}_{2}(\{p\}_2)\\
&-\Bigg[\,\tilde{A}^{1}_{3,g}(j,1,k)\,\delta(1-x_1)\,\delta(1-x_2)\\
&+\Bigg(+J^{1,FF}_{2,QQ}(s_{jk})-J^{1,IF}_{2,QQ}(s_{\overline{1}(\widetilde{jk})})\Bigg)\,A^{0}_{3}(j,1,k)\Bigg]\,\bar{B}^{Z,0}_{1}(\overline{1},i,(\widetilde{jk}))\,J^{2}_{2}(\{p\}_2)\,.
\end{aligned}
\tag{B.12}
$$

$$
\begin{aligned}
&\tilde{\bar{B}}^{Z,1,T}_{2,g\to q}(j,\hat{1},i,k)=\\
&\quad-J^{1,IF}_{2,QQ,g\to q}(s_{1k})\,\tilde{\bar{B}}^{Z,0}_{2}(1,i,j,k)\,J^{3}_{2}(\{p\}_3)\\
&\quad+J^{1,IF}_{2,QQ,g\to q}(s_{1k})\,A^{0}_{3,q}(1,i,k)\,\bar{B}^{Z,0}_{1}(\overline{1},j,(\widetilde{ki}))\,J^{2}_{2}(\{p\}_2)\\
&\quad+J^{1,IF}_{2,QQ,g\to q}(s_{1k})\,A^{0}_{3,q}(1,j,k)\,\bar{B}^{Z,0}_{1}(\overline{1},i,(\widetilde{kj}))\,J^{2}_{2}(\{p\}_2)\\
&\quad-\frac{1}{2}J^{1,IF}_{2,QQ,g\to q}(s_{1k})\,D^{Z,0}_{0}(1,j;k,i)\,J^{3}_{2}(\{p\}_3)\\
&\quad-\frac{1}{2}J^{1,IF}_{2,QQ,g\to q}(s_{1j})\,D^{Z,0}_{0}(i,1;k,j)\,J^{3}_{2}(\{p\}_3)\,.
\end{aligned}
\tag{B.13}
$$

$$
\begin{aligned}
&\hat{B}^{Z,1,T}_{2}(j,\hat{1},i,k)=\\
&\quad-\Bigg[+2\hat{J}^{1,IF}_{2,GQ}(s_{ji})+2\hat{J}^{1,FF}_{2,QG}(s_{ji})\Bigg]\,\bar{B}^{Z,0}_{2}(j,1,i,k)\,J^{3}_{2}(\{p\}_3)\\
&\quad-\Bigg[+2\hat{J}^{1,IF}_{2,GQ}(s_{ji})+2\hat{J}^{1,FF}_{2,QG}(s_{ki})\Bigg]\,\bar{B}^{Z,0}_{2}(j,i,1,k)\,J^{3}_{2}(\{p\}_3)\\
&\quad+D^{0}_{3,g}(j,i,1)\,\Bigg[\,\hat{\bar{B}}^{Z,1}_{1}((\widetilde{ji}),\overline{1},k)\,\delta(1-x_1)\,\delta(1-x_2)\\
&\qquad+2\hat{J}^{1,IF}_{2,GQ}(s_{k\overline{1}})\,\bar{B}^{Z,0}_{1}((\widetilde{ji}),\overline{1},k)\Bigg]\,J^{2}_{2}(\{p\}_2)\\
&\quad+D^{0}_{3,g}(k,i,1)\,\Bigg[\,\hat{\bar{B}}^{Z,1}_{1}(j,\overline{1},(\widetilde{ki}))\,\delta(1-x_1)\,\delta(1-x_2)\\
&\qquad+2\hat{J}^{1,IF}_{2,GQ}(s_{j\overline{1}})\,\bar{B}^{Z,0}_{1}(j,\overline{1},(\widetilde{ki}))\Bigg]\,J^{2}_{2}(\{p\}_2)\\
&\quad-A^{0}_{3}(k,1,j)\,\Bigg[\,\hat{\bar{B}}^{Z,1}_{1}(\overline{1},i,(\widetilde{jk}))\,\delta(1-x_1)\,\delta(1-x_2)
\end{aligned}
$$

$$
\begin{aligned}
&+ 2\hat{J}^{1,IF}_{2,GQ}(s_{\widetilde{(jk)}i})\,\bar{B}^{Z,0}_{1}(\overline{1},i,\widetilde{(jk)})\Big]\,J^2_2(\{p\}_2)\\
&- A^0_3(k,1,j)\,\Big[\,\hat{\bar{B}}^{Z,1}_{1}(\widetilde{(jk)},\overline{1},i)\,\delta(1-x_1)\,\delta(1-x_2)\\
&+ 2\hat{J}^{1,IF}_{2,GQ}(s_{\widetilde{(jk)}\overline{1}})\,\bar{B}^{Z,0}_{1}(\widetilde{(jk)},\overline{1},i)\Big]\,J^2_2(\{p\}_2)\\
&-\Big[\,\hat{A}^1_{3,g}(j,1,k)\,\delta(1-x_1)\,\delta(1-x_2)+2\hat{J}^{1,FF}_{2,QG}(s_{jk})\,A^0_{3,g\to q}(j,1,k)\Big]\\
&\times\bar{B}^{Z,0}_{1}(\overline{1},i,\widetilde{(kj)})\,J^2_2(\{p\}_2)\\
&+\Big[+2\hat{J}^{1,FF}_{2,QG}(s_{jk})-2\hat{J}^{1,FF}_{2,QG}(s_{ki})\Big]a^0_{3,g\to q}(k,1,j)\,\bar{B}^{Z,0}_{1}(\overline{1},i,\widetilde{(kj)})\,J^2_2(\{p\}_2)\\
&+\Big[-2\hat{J}^{1,FF}_{2,QG}(s_{ji})+2\hat{J}^{1,FF}_{2,QG}(s_{jk})\Big]a^0_{3,g\to q}(j,1,k)\,\bar{B}^{Z,0}_{1}(\overline{1},i,\widetilde{(kj)})\,J^2_2(\{p\}_2)\\
&-\Big[\,\hat{A}^1_{3,g}(j,1,k)\,\delta(1-x_1)\,\delta(1-x_2)+2\hat{J}^{1,FF}_{2,QG}(s_{jk})\,A^0_{3,g\to q}(j,1,k)\Big]\\
&\times\bar{B}^{Z,0}_{1}(\widetilde{(kj)},\overline{1},i)\,J^2_2(\{p\}_2)\\
&+\Big[+2\hat{J}^{1,FF}_{2,QG}(s_{jk})-2\hat{J}^{1,FF}_{2,QG}(s_{ki})\Big]a^0_{3,g\to q}(k,1,j)\,\bar{B}^{Z,0}_{1}(\widetilde{(jk)},\overline{1},i)\,J^2_2(\{p\}_2)\\
&+\Big[-2\hat{J}^{1,FF}_{2,QG}(s_{ji})+2\hat{J}^{1,FF}_{2,QG}(s_{jk})\Big]a^0_{3,g\to q}(j,1,k)\,\bar{B}^{Z,0}_{1}(\widetilde{(jk)},\overline{1},i)\,J^2_2(\{p\}_2)\\
&+\Big[\,\hat{D}^1_{3,g}(j,i,1)\,\delta(1-x_1)\,\delta(1-x_2)+2\hat{J}^{1,IF}_{2,QG}(s_{1j})\,D^0_{3,g}(j,i,1)\Big]\\
&\times\bar{B}^{Z,0}_{1}(\widetilde{(ji)},\overline{1},k)\,J^2_2(\{p\}_2)\\
&+\Big[+2\hat{J}^{1,FF}_{2,QG}(s_{ki})-2\hat{J}^{1,IF}_{2,QG}(s_{1j})\Big]d^0_{3,g}(j,i,1)\,\bar{B}^{Z,0}_{1}(\widetilde{(ji)},\overline{1},k)\,J^2_2(\{p\}_2)\\
&+2\hat{J}^{1,FF}_{2,QG}(s_{ki})\,d^0_{3,g\to q}(k,1,i)\,\bar{B}^{Z,0}_{1}(j,\overline{1},\widetilde{(ki)})\,J^2_2(\{p\}_2)\\
&-2\hat{J}^{1,IF}_{2,QG}(s_{1j})\,d^0_{3,g\to q}(j,1,i)\,\bar{B}^{Z,0}_{1}(\widetilde{(ji)},\overline{1},k)\,J^2_2(\{p\}_2)\\
&+\Big[\,\hat{D}^1_{3,g}(k,i,1)\,\delta(1-x_1)\,\delta(1-x_2)+2\hat{J}^{1,IF}_{2,QG}(s_{1k})\,D^0_{3,g}(k,i,1)\Big]\\
&\times\bar{B}^{Z,0}_{1}(j,\overline{1},\widetilde{(ki)})\,J^2_2(\{p\}_2)\\
&+\Big[+2\hat{J}^{1,FF}_{2,QG}(s_{ji})-2\hat{J}^{1,IF}_{2,QG}(s_{1k})\Big]d^0_{3,g}(k,i,1)\,\bar{B}^{Z,0}_{1}(j,\overline{1},\widetilde{(ki)})\,J^2_2(\{p\}_2)\\
&+2\hat{J}^{1,FF}_{2,QG}(s_{ji})\,d^0_{3,g\to q}(j,1,i)\,\bar{B}^{Z,0}_{1}(\widetilde{(ji)},\overline{1},k)\,J^2_2(\{p\}_2)\\
&-2\hat{J}^{1,IF}_{2,QG}(s_{1k})\,d^0_{3,g\to q}(k,1,i)\,\bar{B}^{Z,0}_{1}(j,\overline{1},\widetilde{(ki)})\,J^2_2(\{p\}_2)\,. \qquad \text{(B.14)}
\end{aligned}
$$

$$
\begin{aligned}
&\hat{B}^{Z,1,T}_{2,g\to q}(j,\hat{1},k,i)=\\
&\quad-J^{1,IF}_{2,QQ,g\to q}(s_{1i})\,C^{Z,0}_{0}(1;j,k;i)\,J^3_2(\{p\}_3)\\
&\quad-J^{1,IF}_{2,QQ,g\to q}(s_{1i})\,C^{Z,0}_{0}(i;j,k;1)\,J^3_2(\{p\}_3)\\
&\quad+J^{1,IF}_{2,QQ,g\to q}(s_{1\widetilde{(ij)}})\,E^0_3(i,j,k)\,\bar{B}^{Z,0}_{1,q}(1,\widetilde{(jk)},\widetilde{(ij)})\,J^2_2(\{p\}_2)
\end{aligned}
$$

$$
\begin{aligned}
&+J^{1,IF}_{2,QQ,g\to q}(s_{\bar{1}i})\,E^0_{3,q}(1,j,k)\,\bar{B}^{Z,0}_{1,q}(\bar{1},(\widetilde{jk}),i)\,J^2_2(\{p\}_2)\\
&+\Big[-2J^{1,IF}_{2,QQ,g\to q}(s_{1i})+2J^{1,IF}_{2,QQ,g\to q}(s_{\bar{1}i})\Big]E^0_{3,q}(1,j,k)\,\bar{B}^{Z,0}_{1,q}((\widetilde{jk}),\bar{1},i)\,J^2_2(\{p\}_2)\\
&-J^{1,IF}_{2,QQ,g\to q}(s_{1i})\,E^0_{3,q'\to g}(j,1,i)\,\bar{B}^{Z,0}_{1,Q}(k,\bar{1},(\widetilde{ij}))\,J^2_2(\{p\}_2)\\
&-J^{1,IF}_{2,QQ,g\to q}(s_{1i})\,E^0_{3,q'\to g}(k,1,i)\,\bar{B}^{Z,0}_{1,Q}((\widetilde{ik}),\bar{1},j)\,J^2_2(\{p\}_2)\,.
\end{aligned}
\tag{B.15}
$$

$$
\begin{aligned}
&\hat{\bar{B}}^{Z,1,T}_2(j,\hat{1},i,k)=\\
&-\Big[+\hat{J}^{1,FF}_{2,QG}(s_{ji})+\hat{J}^{1,FF}_{2,QG}(s_{ki})+2\hat{J}^{1,IF}_{2,GQ}(s_{jk})\Big]\,\tilde{\bar{B}}^{Z,0}_2(j,1,i,k)\,J^3_2(\{p\}_3)\\
&-A^0_3(j,1,k)\Big[\,\hat{\bar{B}}^{Z,1}_1(\bar{1},i,(\widetilde{jk}))\,\delta(1-x_1)\,\delta(1-x_2)\\
&\quad+2\hat{J}^{1,FF}_{2,QG}(s_{(\widetilde{jk})i})\,\bar{B}^{Z,0}_1(\bar{1},i,(\widetilde{jk}))\Big]\,J^2_2(\{p\}_2)\\
&+A^0_3(j,i,k)\Big[\,\hat{\bar{B}}^{Z,1}_1((\widetilde{ji}),1,(\widetilde{ik}))\,\delta(1-x_1)\,\delta(1-x_2)\\
&\quad+2\hat{J}^{1,IF}_{2,GQ}(s_{(\widetilde{ji})(\widetilde{ik})})\,\bar{B}^{Z,0}_1((\widetilde{ji}),1,(\widetilde{ik}))\Big]\,J^2_2(\{p\}_2)\\
&+\Big[\hat{A}^1_3(j,i,k)\,\delta(1-x_1)\,\delta(1-x_2)\\
&+\Big(+\hat{J}^{1,FF}_{2,QG}(s_{ji})+\hat{J}^{1,FF}_{2,QG}(s_{ki})\Big)\,A^0_3(j,i,k)\Big]\,\bar{B}^{Z,0}_1((\widetilde{ji}),1,(\widetilde{ik}))\,J^2_2(\{p\}_2)\\
&-\Big[\hat{A}^1_{3,g}(j,1,k)\,\delta(1-x_1)\,\delta(1-x_2)+2\hat{J}^{1,IF}_{2,GQ}(s_{jk})\,A^0_3(j,1,k)\Big]\,\bar{B}^{Z,0}_1(\bar{1},i,(\widetilde{jk}))\,J^2_2(\{p\}_2)\\
&+\Big[-\hat{J}^{1,FF}_{2,QG}(s_{ki})-\hat{J}^{1,FF}_{2,QG}(s_{ji})+2\hat{J}^{1,FF}_{2,QG}(s_{(\widetilde{jk})i})\Big]A^0_3(j,1,k)\,\bar{B}^{Z,0}_1(\bar{1},i,(\widetilde{jk}))\,J^2_2(\{p\}_2)\,.
\end{aligned}
\tag{B.16}
$$

$$
\begin{aligned}
&\hat{\bar{B}}^{Z,1,T}_{2,g\to q}(j,\hat{1},i,k)=\\
&\quad-J^{1,IF}_{2,QQ,g\to q}(s_{1i})\,C^{Z,0}_0(1;j,k;i)\,J^3_2(\{p\}_3)\\
&\quad-J^{1,IF}_{2,QQ,g\to q}(s_{1i})\,C^{Z,0}_0(i;j,k;1)\,J^3_2(\{p\}_3)\\
&\quad+J^{1,IF}_{2,QQ,g\to q}(s_{1(\widetilde{ij})})\,E^0_3(i,j,k)\,\bar{B}^{Z,0}_{1,q}(1,(\widetilde{jk}),(\widetilde{ij}))\,J^2_2(\{p\}_2)\\
&\quad+J^{1,IF}_{2,QQ,g\to q}(s_{\bar{1}i})\,E^0_3(1,j,k)\,\bar{B}^{Z,0}_{1,q}(\bar{1},(\widetilde{jk}),i)\,J^2_2(\{p\}_2)\\
&\quad-J^{1,IF}_{2,QQ,g\to q}(s_{1i})\,E^0_{3,q'\to g}(j,1,i)\,\bar{B}^{Z,0}_{1,Q}(k,\bar{1},(\widetilde{ji}))\,J^2_2(\{p\}_2)\\
&\quad-J^{1,IF}_{2,QQ,g\to q}(s_{1i})\,E^0_{3,q'\to g}(k,1,i)\,\bar{B}^{Z,0}_{1,Q}((\widetilde{ki}),\bar{1},j)\,J^2_2(\{p\}_2)\,.
\end{aligned}
\tag{B.17}
$$

B.3 Virtual-virtual

$$
\begin{aligned}
&B^{Z,2,U}_1(3,\hat{1},4)=\\
&+\Big[-\mathcal{D}^0_{3,g\to g}(s_{13})+\Gamma^{(1)}_{gg}(z_1)-\mathcal{D}^0_{3,g\to g}(s_{14})\Big]\left(-\frac{b_0}{\epsilon}B^{Z,0}_1(3,1,4)+B^{Z,1}_1(3,1,4)\right)
\end{aligned}
$$

$$
\begin{aligned}
&+\Bigg[-\frac{1}{2}\,\mathcal{D}^0_{3,g\to g}(s_{14})\otimes\mathcal{D}^0_{3,g\to g}(s_{14}) - \frac{1}{2}\,\mathcal{D}^0_{3,g\to g}(s_{13})\otimes\mathcal{D}^0_{3,g\to g}(s_{13}) - \mathcal{D}^0_{3,g\to g}(s_{13})\otimes\mathcal{D}^0_{3,g\to g}(s_{14}) \\
&\quad + \Gamma^{(1)}_{gg}(z_1)\otimes\mathcal{D}^0_{3,g\to g}(s_{13}) + \Gamma^{(1)}_{gg}(z_1)\otimes\mathcal{D}^0_{3,g\to g}(s_{14}) - \frac{1}{2}\,\Gamma^{(1)}_{gg}(z_1)\otimes\Gamma^{(1)}_{gg}(z_1)\Bigg] B_1^{Z,0}(3,1,4) \\
&+\Bigg[-\frac{b_0}{\epsilon}\left(\frac{s_{13}}{\mu_R^2}\right)^{-\epsilon}\mathcal{D}^0_{3,g}(s_{13}) + \mathcal{D}^0_{3,g\to g}(s_{13})\otimes\mathcal{D}^0_{3,g\to g}(s_{13}) + \mathcal{D}^0_{3,q}(s_{13})\otimes\mathcal{D}^0_{3,g\to q}(s_{13}) \\
&\quad + \Gamma^{(1)}_{gg}(z_1)\otimes\mathcal{D}^0_{3,g\to q}(s_{13}) - 2\,\Gamma^{(1)}_{qq}(z_1)\otimes\mathcal{D}^0_{3,g\to q}(s_{13}) + \frac{b_0}{\epsilon}\,\mathcal{D}^0_{3,g\to q}(s_{13}) \\
&\quad - \mathcal{D}^0_{4,g}(s_{13}) - \frac{1}{2}\,\mathcal{D}^0_{4,g'}(s_{13}) - \mathcal{D}^1_{3,g}(s_{13}) \\
&\quad + \frac{1}{2}\,\Gamma^{(2)}_{gg}(z_1)\Bigg] B_1^{Z,0}(3,1,4) \\
&+\Bigg[-\frac{b_0}{\epsilon}\left(\frac{s_{14}}{\mu_R^2}\right)^{-\epsilon}\mathcal{D}^0_{3,g}(s_{14}) + \Gamma^{(1)}_{gg}(z_1)\otimes\mathcal{D}^0_{3,g\to q}(s_{14}) - 2\,\Gamma^{(1)}_{qq}(z_1)\otimes\mathcal{D}^0_{3,g\to q}(s_{14}) \\
&\quad + \mathcal{D}^0_{3,g\to g}(s_{14})\otimes\mathcal{D}^0_{3,g\to g}(s_{14}) + \mathcal{D}^0_{3,q}(s_{14})\otimes\mathcal{D}^0_{3,g\to q}(s_{14}) + \frac{b_0}{\epsilon}\,\mathcal{D}^0_{3,g\to q}(s_{14}) \\
&\quad + \frac{1}{2}\,\Gamma^{(2)}_{gg}(z_1) - \mathcal{D}^0_{4,g}(s_{14}) - \frac{1}{2}\,\mathcal{D}^0_{4,g'}(s_{14}) \\
&\quad - \mathcal{D}^1_{3,g}(s_{14})\Bigg] B_1^{Z,0}(3,1,4) \\
&+\Bigg[+\frac{1}{2}\,\tilde{\mathcal{A}}^0_4(s_{34}) + \tilde{\mathcal{A}}^1_3(s_{34}) - \frac{1}{2}\,\mathcal{A}^0_3(s_{34})\otimes\mathcal{A}^0_3(s_{34})\Bigg] B_1^{Z,0}(3,1,4) \\
&+\Bigg[+\frac{b_0}{2\epsilon}\left(\frac{s_{13}}{\mu_R^2}\right)^{-\epsilon}\mathcal{A}^0_{3,g\to q}(s_{13}) - \frac{1}{2}\,\mathcal{A}^0_{3,g\to q}(s_{13})\otimes\Gamma^{(1)}_{gg}(z_1) + \mathcal{A}^0_{3,g\to q}(s_{13})\otimes\Gamma^{(1)}_{qq}(z_1) \\
&\quad - \mathcal{A}^0_{3,g\to q}(s_{13})\otimes\mathcal{A}^0_{3,q}(s_{13}) - \frac{b_0}{2\epsilon}\,\mathcal{A}^0_{3,g\to q}(s_{13}) + \mathcal{A}^0_{4,g}(s_{13}) \\
&\quad + \frac{1}{2}\,\tilde{\mathcal{A}}^0_{4,g}(s_{13}) + \frac{1}{2}\,\tilde{\mathcal{A}}^1_{3,g}(s_{13}) + \frac{1}{2}\,\mathcal{A}^1_{3,g}(s_{13})\Bigg] B_1^{Z,0}(3,1,4) \\
&+\Bigg[+\frac{b_0}{2\epsilon}\left(\frac{s_{14}}{\mu_R^2}\right)^{-\epsilon}\mathcal{A}^0_{3,g\to q}(s_{14}) - \mathcal{A}^0_{3,g\to q}(s_{14})\otimes\mathcal{A}^0_{3,q}(s_{14}) - \frac{1}{2}\,\mathcal{A}^0_{3,g\to q}(s_{14})\otimes\Gamma^{(1)}_{gg}(z_1) \\
&\quad + \mathcal{A}^0_{3,g\to q}(s_{14})\otimes\Gamma^{(1)}_{qq}(z_1) - \frac{b_0}{2\epsilon}\,\mathcal{A}^0_{3,g\to q}(s_{14}) + \mathcal{A}^0_{4,g}(s_{14}) \\
&\quad + \frac{1}{2}\,\tilde{\mathcal{A}}^0_{4,g}(s_{14}) + \frac{1}{2}\,\tilde{\mathcal{A}}^1_{3,g}(s_{14}) + \frac{1}{2}\,\mathcal{A}^1_{3,g}(s_{14})\Bigg] B_1^{Z,0}(3,1,4)\,. \qquad \text{(B.18)}
\end{aligned}
$$

$$
\begin{aligned}
&B^{Z,2,U}_{1,g\to q}(3,\hat{1},4) = \\
&+\Bigg[+\mathcal{A}^0_{3,g\to q}(s_{14}) + 2S_{g\to q}\,\Gamma^{(1)}_{qg}(z_1)\Bigg]\left(-\frac{b_0}{\epsilon}\bar{B}_1^{Z,0}(1,3,4) + \bar{B}_1^{Z,0}(1,3,4)\right) \\
&+\Bigg[+\frac{1}{2}\,\mathcal{A}^0_{3,g\to q}(s_{14})\otimes\mathcal{D}^0_3(s_{34}) + \frac{1}{2}\,\mathcal{A}^0_{3,g\to q}(s_{14})\otimes\mathcal{D}^0_{3,q}(s_{13}) + S_{g\to q}\,\Gamma^{(1)}_{qg}(z_1)\otimes\mathcal{D}^0_{3,q}(s_{13}) \\
&\quad + S_{g\to q}\,\Gamma^{(1)}_{qg}(z_1)\otimes\mathcal{D}^0_3(s_{34}) - \Gamma^{(1)}_{qq}(z_1)\otimes\mathcal{A}^0_{3,g\to q}(s_{14}) - 2S_{g\to q}\,\Gamma^{(1)}_{qg}(z_1)\otimes\Gamma^{(1)}_{qq}(z_1)\Bigg]\bar{B}_1^{Z,0}(1,3,4)
\end{aligned}
$$

$$
\begin{aligned}
&+\Bigg[+ \frac{b_0}{\epsilon}\left(\frac{s_{14}}{\mu_R^2}\right)^{-\epsilon} \mathcal{A}^0_{3,g\to q}(s_{14}) + S_{g\to q}\,\Gamma^{(1)}_{qg}(z_1)\otimes\Gamma^{(1)}_{qq}(z_1) - S_{g\to q}\,\Gamma^{(1)}_{qg}(z_1)\otimes\Gamma^{(1)}_{gg}(z_1) \\
&\quad - \mathcal{A}^0_{3,g\to q}(s_{14})\otimes\mathcal{A}^0_{3,q}(s_{14}) + \Gamma^{(1)}_{qq}(z_1)\otimes\mathcal{A}^0_{3,g\to q}(s_{14}) - \Gamma^{(1)}_{gg}(z_1)\otimes\mathcal{A}^0_{3,g\to q}(s_{14}) \\
&\quad + 2S_{g\to q}\,\Gamma^{(2)}_{qg}(z_1) + 2\,\mathcal{A}^0_{4,g}(s_{14}) + \mathcal{A}^1_{3,g}(s_{14})\Bigg]\bar{B}^{Z,0}_1(1,3,4)\,. \qquad \text{(B.19)}
\end{aligned}
$$

$$
\begin{aligned}
&\tilde{B}^{Z,2,U}_1(3,\hat{1},4) = \\
&+\Bigg[+ \mathcal{A}^0_3(s_{34})\Bigg]\left(+\frac{b_0}{\epsilon}B^{Z,0}_1(3,1,4) - B^{Z,1}_1(3,1,4)\right) \\
&+\Bigg[+ \Gamma^{(1)}_{gg}(z_1) - \mathcal{D}^0_{3,g\to g}(s_{13}) - \mathcal{D}^0_{3,g\to g}(s_{14})\Bigg]\tilde{B}^{Z,1}_3(3,1,4) \\
&+\Bigg[- \mathcal{D}^0_{3,g\to g}(s_{13})\otimes\mathcal{A}^0_3(s_{34}) - \mathcal{D}^0_{3,g\to g}(s_{14})\otimes\mathcal{A}^0_3(s_{34}) + \Gamma^{(1)}_{gg}(z_1)\otimes\mathcal{A}^0_3(s_{34})\Bigg]B^{Z,0}_1(3,1,4) \\
&+\Bigg[- \frac{b_0}{\epsilon}\left(\frac{s_{34}}{\mu_R^2}\right)^{-\epsilon}\mathcal{A}^0_3(s_{34}) + \mathcal{A}^0_3(s_{34})\otimes\mathcal{A}^0_3(s_{34}) - \mathcal{A}^0_4(s_{34}) \\
&\quad - \mathcal{A}^1_3(s_{34})\Bigg]B^{Z,0}_1(3,1,4) \\
&+\Bigg[- \frac{1}{2}\,\tilde{\mathcal{A}}^0_4(s_{34}) - \tilde{\mathcal{A}}^1_3(s_{34}) - 2\,\mathcal{C}^0_4(s_{34})\Bigg]B^{Z,0}_1(3,1,4)\,. \qquad \text{(B.20)}
\end{aligned}
$$

$$
\begin{aligned}
&\tilde{B}^{Z,2,U}_{1,g\to q}(\hat{1},3,4) = \\
&+\Bigg[- \mathcal{A}^0_{3,g\to q}(s_{14}) - 2S_{g\to q}\,\Gamma^{(1)}_{qg}(z_1)\Bigg]\left(+\frac{b_0}{\epsilon}\bar{B}^{Z,0}_1(1,3,4) - \bar{B}^{Z,1}_1(1,3,4)\right) \\
&+\Bigg[+ \frac{1}{2}\,\mathcal{A}^0_{3,g\to q}(s_{14})\otimes\mathcal{D}^0_3(s_{34}) + \frac{1}{2}\,\mathcal{A}^0_{3,g\to q}(s_{14})\otimes\mathcal{D}^0_{3,q}(s_{13}) + S_{g\to q}\,\Gamma^{(1)}_{qg}(z_1)\otimes\mathcal{D}^0_{3,q}(s_{13}) \\
&\quad + S_{g\to q}\,\Gamma^{(1)}_{qg}(z_1)\otimes\mathcal{D}^0_3(s_{34}) - \Gamma^{(1)}_{qq}(z_1)\otimes\mathcal{A}^0_{3,g\to q}(s_{14}) - 2S_{g\to q}\,\Gamma^{(1)}_{qg}(z_1)\otimes\Gamma^{(1)}_{qq}(z_1)\Bigg]\bar{B}^{Z,0}_1(1,3,4) \\
&+\Bigg[+ \frac{b_0}{\epsilon}\left(\frac{s_{14}}{\mu_R^2}\right)^{-\epsilon}\mathcal{A}^0_{3,g\to q}(s_{14}) + S_{g\to q}\,\Gamma^{(1)}_{qg}(z_1)\otimes\Gamma^{(1)}_{qq}(z_1) - S_{g\to q}\,\Gamma^{(1)}_{qg}(z_1)\otimes\Gamma^{(1)}_{gg}(z_1) \\
&\quad + \Gamma^{(1)}_{qq}(z_1)\otimes\mathcal{A}^0_{3,g\to q}(s_{14}) - \mathcal{A}^0_{3,g\to q}(s_{14})\otimes\mathcal{A}^0_{3,q}(s_{14}) - \Gamma^{(1)}_{gg}(z_1)\otimes\mathcal{A}^0_{3,g\to q}(s_{14}) \\
&\quad + 2S_{g\to q}\,\Gamma^{(2)}_{qg}(z_1) + 2\,\mathcal{A}^0_{4,g}(s_{14}) + \mathcal{A}^1_{3,g}(s_{14})\Bigg]\bar{B}^{Z,0}_1(1,3,4) \\
&+\Bigg[+ \mathcal{A}^0_{3,g\to q}(s_{14}) + 2S_{g\to q}\,\Gamma^{(1)}_{qg}(z_1)\Bigg]\bar{B}t1g1A(1,3,4) \\
&+\Bigg[+ \mathcal{A}^0_{3,g\to q}(s_{14})\otimes\mathcal{A}^0_{3,q}(s_{14}) + 2S_{g\to q}\,\Gamma^{(1)}_{qg}(z_1)\otimes\mathcal{A}^0_{3,q}(s_{14}) - \Gamma^{(1)}_{qq}(z_1)\otimes\mathcal{A}^0_{3,g\to q}(s_{14}) \\
&\quad - 2S_{g\to q}\,\Gamma^{(1)}_{qg}(z_1)\otimes\Gamma^{(1)}_{qq}(z_1)\Bigg]\bar{B}^{Z,0}_1(1,3,4) \\
&+\Bigg[+ \tilde{\mathcal{A}}^0_{4,g}(s_{14}) + \tilde{\mathcal{A}}^1_{3,g}(s_{14}) - \mathcal{A}^0_{3,g\to q}(s_{14})\otimes\mathcal{A}^0_{3,q}(s_{14})
\end{aligned}
$$

$$+\,\Gamma^{(1)}_{qq}(z_1)\otimes\mathcal{A}^0_{3,g\to q}(s_{14})+S_{g\to q}\,\Gamma^{(1)}_{qg}(z_1)\otimes\Gamma^{(1)}_{qq}(z_1)-2S_{g\to q}\,\widetilde{\Gamma}^{(2)}_{qg}(z_1)\Big]\bar{B}^{Z,0}_1(1,3,4)\,. \tag{B.21}$$

$$\begin{aligned}\tilde{\tilde{B}}^{Z,2,U}_1(3,\hat{1},4)=&\\ &+\Big[-\,\mathcal{A}^0_3(s_{34})\Big]\tilde{B}^{Z,1}_3(3,1,4)\\ &+\Big[-\frac{1}{2}\,\tilde{\mathcal{A}}^0_4(s_{34})-\,\tilde{\mathcal{A}}^1_3(s_{34})-2\,\mathcal{C}^0_4(s_{34})\Big]B^{Z,0}_1(3,1,4)\,.\end{aligned} \tag{B.22}$$

$$\begin{aligned}\tilde{\tilde{B}}^{Z,2,U}_{1,g\to q}(3,\hat{1},4)=&\\ &+\Big[+\,\mathcal{A}^0_{3,g\to q}(s_{14})+2S_{g\to q}\,\Gamma^{(1)}_{qg}(z_1)\Big]\bar{B}^{Z,1}_1(1,3,4)\\ &+\Big[+\,\mathcal{A}^0_{3,g\to q}(s_{14})\otimes\mathcal{A}^0_{3,q}(s_{14})+2S_{g\to q}\,\Gamma^{(1)}_{qg}(z_1)\otimes\mathcal{A}^0_{3,q}(s_{14})-\,\Gamma^{(1)}_{qq}(z_1)\otimes\mathcal{A}^0_{3,g\to q}(s_{14})\\ &\quad-2S_{g\to q}\,\Gamma^{(1)}_{qg}(z_1)\otimes\Gamma^{(1)}_{qq}(z_1)\Big]\bar{B}^{\gamma,0}_1(1,3,4)\\ &+\Big[+\,\tilde{\mathcal{A}}^0_{4,g}(s_{14})+\,\tilde{\mathcal{A}}^1_{3,g}(s_{14})-\,\mathcal{A}^0_{3,g\to q}(s_{14})\otimes\mathcal{A}^0_{3,q}(s_{14})\\ &\quad+\,\Gamma^{(1)}_{qq}(z_1)\otimes\mathcal{A}^0_{3,g\to q}(s_{14})+S_{g\to q}\,\Gamma^{(1)}_{qg}(z_1)\otimes\Gamma^{(1)}_{qq}(z_1)-2S_{g\to q}\,\widetilde{\Gamma}^{(2)}_{qg}(z_1)\Big]\bar{B}^{\gamma,0}_1(1,3,4)\,.\end{aligned} \tag{B.23}$$

$$\begin{aligned}\hat{B}^{Z,2,U}_1(3,\hat{1},4)=&\\ &+\Big[-\,\mathcal{D}^0_{3,g}(s_{13})-\,\mathcal{D}^0_{3,g}(s_{14})+\frac{1}{2}\,\mathcal{A}^0_{3,g\to q}(s_{13})\\ &\quad+\frac{1}{2}\,\mathcal{A}^0_{3,g\to q}(s_{14})+\,\Gamma^{(1)}_{gg}(z_1)\Big]\left(-\frac{b_F}{\epsilon}B^{Z,0}_1(3,1,4)+\hat{B}^{Z,1}_1(3,1,4)\right)\\ &+\Big[-\,\Gamma^{(1)}_{gg,F}(z_1)\Big]\left(+\frac{b_0}{\epsilon}B^{Z,0}_1(3,1,4)-B^{Z,1}_1(3,1,4)\right)\\ &+\Big[-\frac{b_F}{\epsilon}\,\mathcal{D}^0_{3,g}(s_{13})\left(\frac{s_{13}}{\mu_R^2}\right)^{-\epsilon}+\frac{b_F}{2\epsilon}\,\mathcal{A}^0_{3,g\to q}(s_{13})\left(\frac{s_{13}}{\mu_R^2}\right)^{-\epsilon}-S_{g\to q}\,\Gamma^{(1)}_{qg}(z_1)\otimes\mathcal{E}^0_{3,q'\to g}(s_{13})\\ &\quad+\,\Gamma^{(1)}_{gg,F}(z_1)\otimes\mathcal{D}^0_{3,g}(s_{13})-\frac{1}{2}\,\mathcal{A}^0_{3,g\to q}(s_{13})\otimes\Gamma^{(1)}_{gg,F}(z_1)+\frac{1}{2}\,\mathcal{A}^0_{3,g\to q}(s_{13})\otimes\mathcal{E}^0_{3,q}(s_{14})\\ &\quad-\frac{1}{2}\,\Gamma^{(1)}_{gg}(z_1)\otimes\Gamma^{(1)}_{gg,F}(z_1)-\frac{1}{2}\,\Gamma^{(1)}_{qg}(z_1)\otimes\Gamma^{(1)}_{gq}(z_1)-\,\mathcal{E}^0_{4,g}(s_{13})\\ &\quad-\,\hat{\mathcal{D}}^1_{3,g}(s_{13})+\frac{1}{2}\,\hat{\mathcal{A}}^1_{3,g}(s_{13})+\frac{1}{2}\,\Gamma^{(2)}_{gg,F}(z_1)\Big]B^{Z,0}_1(3,1,4)\\ &+\Big[-S_{g\to q}\,\Gamma^{(1)}_{qg}(z_1)\otimes\mathcal{E}^0_{3,q'\to g}(s_{14})-\frac{b_F}{\epsilon}\left(\frac{s_{14}}{\mu_R^2}\right)^{-\epsilon}\mathcal{D}^0_{3,g}(s_{14})+\frac{b_F}{2\epsilon}\left(\frac{s_{14}}{\mu_R^2}\right)^{-\epsilon}\mathcal{A}^0_{3,g\to q}(s_{14})\\ &\quad-\frac{1}{2}\,\Gamma^{(1)}_{qg}(z_1)\otimes\Gamma^{(1)}_{gq}(z_1)-\frac{1}{2}\,\Gamma^{(1)}_{gg}(z_1)\otimes\Gamma^{(1)}_{gg,F}(z_1)+\,\Gamma^{(1)}_{gg,F}(z_1)\otimes\mathcal{D}^0_{3,g}(s_{14})\end{aligned}$$

$$
\begin{aligned}
&- \frac{1}{2}\,\mathcal{A}^0_{3,g\to q}(s_{14}) \otimes \Gamma^{(1)}_{gg,F}(z_1) + \frac{1}{2}\,\mathcal{A}^0_{3,g\to q}(s_{13}) \otimes \mathcal{E}^0_{3,q}(s_{14}) + \frac{1}{2}\,\Gamma^{(2)}_{gg,F}(z_1) \\
&- \mathcal{E}^0_{4,g}(s_{14}) - \hat{\mathcal{D}}^1_{3,g}(s_{14}) + \frac{1}{2}\,\hat{\mathcal{A}}^1_{3,g}(s_{14})\Big] B_1^{Z,0}(3,1,4)\,. \qquad \text{(B.24)}
\end{aligned}
$$

$$
\begin{aligned}
&\hat{B}^{Z,2,U}_{1,g\to q}(3,\hat{1},4) = \\
&+\Big[+ \mathcal{A}^0_{3,g\to q}(s_{14}) + 2S_{g\to q}\,\Gamma^{(1)}_{qg}(z_1)\Big]\left(-\frac{b_F}{\epsilon}\bar{B}_1^{Z,0}(1,3,4) + \bar{\hat{B}}_1^{Z,1}(1,3,4)\right) \\
&+\Big[+ \frac{1}{2}\,\mathcal{E}^0_3(s_{34}) \otimes \mathcal{A}^0_{3,g\to q}(s_{14}) + \frac{1}{2}\,\mathcal{E}^0_{3,q}(s_{13}) \otimes \mathcal{A}^0_{3,g\to q}(s_{14}) + S_{g\to q}\,\mathcal{E}^0_3(s_{34}) \otimes \Gamma^{(1)}_{qg}(z_1) \\
&\quad + S_{g\to q}\,\mathcal{E}^0_{3,q}(s_{13}) \otimes \Gamma^{(1)}_{qg}(z_1)\Big] \bar{B}_1^{Z,0}(1,3,4) \\
&+\Big[+ \frac{b_F}{\epsilon}\left(\frac{s_{14}}{\mu_R^2}\right)^{-\epsilon} \mathcal{A}^0_{3,g\to q}(s_{14}) - S_{g\to q}\,\Gamma^{(1)}_{gg,F}(z_1) \otimes \Gamma^{(1)}_{qg}(z_1) - \mathcal{A}^0_{3,g\to q}(s_{14}) \otimes \Gamma^{(1)}_{gg,F}(z_1) \\
&\quad + 2S_{g\to q}\,\Gamma^{(2)}_{qg,F}(z_1) + \hat{\mathcal{A}}^1_{3,g}(s_{14})\Big] \bar{B}_1^{Z,0}(1,3,4). \qquad \text{(B.25)}
\end{aligned}
$$

$$
\begin{aligned}
&\hat{\bar{B}}^{Z,2,U}_1(3,\hat{1},4) = \\
&+\Big[- \mathcal{A}^0_3(s_{34})\Big]\left(+\frac{b_F}{\epsilon}B_1^{Z,0}(3,1,4) - \hat{B}_1^{Z,1}(3,1,4)\right) \\
&+\Big[- \Gamma^{(1)}_{gg,F}(z_1)\Big]\tilde{B}_3^{Z,1}(3,1,4) \\
&+\Big[+ \frac{b_F}{\epsilon}\left(\frac{s_{34}}{\mu_R^2}\right)^{-\epsilon} \mathcal{A}^0_3(s_{34}) - \Gamma^{(1)}_{gg,F}(z_1) \otimes \mathcal{A}^0_3(s_{34}) + \mathcal{B}^0_4(s_{34}) \\
&\quad + \hat{\mathcal{A}}^1_3(s_{34}) + \widetilde{\Gamma}^{(2)}_{gg,F}(z_1)\Big] B_1^{Z,0}(3,1,4) \\
&+\Big[+ \frac{1}{2}\,\tilde{\mathcal{E}}^0_{4,g}(s_{13}) + S_{g\to q}\,\Gamma^{(1)}_{qg}(z_1) \otimes \mathcal{E}^0_{3,q'\to g}(s_{13}) + \frac{1}{2}\,\Gamma^{(1)}_{qg}(z_1) \otimes \Gamma^{(1)}_{gq}(z_1)\Big] B_1^{Z,0}(3,1,4) \\
&+\Big[+ \frac{1}{2}\,\tilde{\mathcal{E}}^0_{4,g}(s_{14}) + S_{g\to q}\,\Gamma^{(1)}_{qg}(z_1) \otimes \mathcal{E}^0_{3,q'\to g}(s_{14}) + \frac{1}{2}\,\Gamma^{(1)}_{qg}(z_1) \otimes \Gamma^{(1)}_{gq}(z_1)\Big] B_1^{Z,0}(3,1,4)\,. \\
&\qquad \text{(B.26)}
\end{aligned}
$$

$$
\begin{aligned}
&\hat{\bar{B}}^{Z,2,U}_{1,g\to q}(3,\hat{1},4) = \\
&+\Big[- \mathcal{A}^0_{3,g\to q}(s_{14}) - 2S_{g\to q}\,\Gamma^{(1)}_{qg}(z_1)\Big]\left(-\frac{b_F}{\epsilon}\bar{B}_1^{Z,0}(1,3,4) + \bar{\hat{B}}_1^{Z,1}(1,3,4)\right) \\
&+\Big[- \frac{b_F}{\epsilon}\left(\frac{s_{14}}{\mu_R^2}\right)^{-\epsilon} \mathcal{A}^0_{3,g\to q}(s_{14}) + S_{g\to q}\,\Gamma^{(1)}_{gg,F}(z_1) \otimes \Gamma^{(1)}_{qg}(z_1) - S_{g\to q}\,\mathcal{E}^0_{3,q}(s_{13}) \otimes \Gamma^{(1)}_{qg}(z_1) \\
&\quad - S_{g\to q}\,\mathcal{E}^0_3(s_{34}) \otimes \Gamma^{(1)}_{qg}(z_1) + \mathcal{A}^0_{3,g\to q}(s_{14}) \otimes \Gamma^{(1)}_{gg,F}(z_1) - \frac{1}{2}\,\mathcal{E}^0_{3,q}(s_{13}) \otimes \mathcal{A}^0_{3,g\to q}(s_{14}) \\
&\quad - \frac{1}{2}\,\mathcal{E}^0_3(s_{34}) \otimes \mathcal{A}^0_{3,g\to q}(s_{14}) - 2S_{g\to q}\,\Gamma^{(2)}_{qg,F}(z_1) - \hat{\mathcal{A}}^1_{3,g}(s_{14})\Big] \bar{B}_1^{Z,0}(1,3,4)\,. \qquad \text{(B.27)}
\end{aligned}
$$

$$\hat{\hat{B}}_1^{Z,2,U}(3,\hat{1},4) =$$
$$+\left[+\,\Gamma^{(1)}_{gg,F}(z_1)\right]\left(-\frac{b_F}{\epsilon}B_1^{Z,0}(3,1,4)+\hat{B}_1^{Z,1}(3,1,4)\right)$$
$$+\left[-\frac{1}{2}\,\Gamma^{(1)}_{gg,F}(z_1)\otimes\Gamma^{(1)}_{gg,F}(z_1)+\Gamma^{(2)}_{gg,F^2}(z_1)\right]B_1^{Z,0}(3,1,4)\,. \tag{B.28}$$

C NNLOJET Runcard

A runcard for a typical DIS di-jet production setup:

```
NNLOJET_RUNCARD
EXM                   ! Job name id, must be less than 10 characters
DIS                   ! Process name
10000                 ! Number of events
1                     ! Number of iterations
1                     ! Seed number
.true.                ! Warmup
.false.               ! Production
NNPDF23_nnlo_as_0118  ! PDF set
0                     ! Member of PDF set
kt                    ! Jet algorithm, accepts 'kt', 'cam' or 'antikt'
1d0                   ! Rcut
.false.               ! exclusive
1                     ! Heavy particle decay type
1d-6                  ! Technical cutoff y0
.true.                ! angular averaging of the phase space, default to true
2                     ! Virtual Integration method, use 2 if you're not sure
b                     ! RR a/b region flag. Accepts 'a','b' or 'all'.
0                     ! set to zero for MC, 2 for point test
.false.               ! print max weight flag
.false.               ! momentum mapping and PDF storage flag
.false.               ! colour sampling flag
.false.               ! explicit pole check flag, stops integration when set to true

PHYSICAL_PARAMETERS
8000d0                ! roots <- overwritten in collider block
125d0                 ! Mass of the Higgs Boson
0.004029643852d0      ! Width of the Higgs Boson
91.1876d0             ! Mass of the Z Boson
2.4952d0              ! Width of the Z Boson
80.398d0              ! Mass of the W Boson
2.1054d0              ! Width of the W Boson
173.2d0               ! Mass of the Top Quark
```

```
1.41d0                ! Width of the Top Quark
4.18d0                ! Mass of the Bottom Quark
0d0                   ! Width of the Bottom Quark
1.275d0               ! Mass of the Charm Quark
0d0                   ! Width of the Charm Quark
1.77d0                ! Mass of the Tau lepton
0d0                   ! Width of the Tau lepton

COLLIDER  ep  E1=27.5  E2=920 ! Choose collider type and energies


SETUP
Recom_Scheme Et  ! Recombination scheme
END_SETUP


SELECTORS

!####### SYNTAX ######################
!##
!##   [select|accept|reject] {observable-name} [min={val_min}] [max={val_max}]
!##
!#####################################
!#
!#  * comments begin with the character `!` and will be excluded from the parser
!#    just like this documentation block. This way, one can maintain various setups
!#    in one runcard and comment in/out parts as needed.
!#
!#  * multiple selectors are combined with a logical "and"
!#
!#  * only necessary to specify at least one of the two: min, max
!#
!#  * if both are set, the order of the min/max specification is irrelevant
!#
!#  * each line here generates a new Selector and it is therefore better to reduce
!#    the number of lines if possible. For instance the following cases are
!#    all equivalent and the one-liners should be preferred:
!#
!#    a) select ylp min = -5           ! --> accept [-5, +infty]
!#       select ylp max = +5           ! --> accept [-infty, +5]
!#                                     ! combined:  [-5, +5]
!#
!#    b) reject ylp max = -5           ! --> reject [+5, +infty]
```

```
!#       reject ylp min = +5           ! --> reject [-infty, -5]
!#                                     ! combined:  [-5, +5]
!#
!#    c) select ylp min = -5 max = +5  ! --> accept [-5, +5]
!#
!#    d) select abs_ylp max = +5       ! --> accept |y| < 5 => [-5, +5]
!#
!#    e) reject abs_ylp min = +5       ! --> reject |y| > 5 => [-5, +5]
!#
!#  * the ‘reject‘ option actually has a very nice use-case in the exclusion
!#    of the barrel--endcap region like this
!#
!#    a) select abs_ylp max = +5                    ! global selector
!#       reject abs_ylp min = +1.4442 max = +1.560  ! CMS barrel-endcap region
!#
!#    b) select ylp min = -5      max = -1.560
!#       select ylp min = -1.4442 max = +1.4442
!#       select ylp min = +1.560  max = +5
!#
!#    where the second one is clearly more tedious to specify
!#
!#####################################

select njets min = 2

!----- jet veto
select jets_pt       min = 5
select m12           min=16
        !---- cuts on DIS variables
        select q2            min = 150  max = 15000
        select y             min=0.2 max=0.7

!----- jet cuts in the HERA frame
select hera_jets_eta  min = -1  max = 2.5


END_SELECTORS



HISTOGRAMS

!####### SYNTAX ######################
```

```
!##
!## a) equal-sized bins:
!##   {observable-name}[>{file-name}] nbins={val_nbins} min={val_min} max={val_max}
!##
!## b) non-uniform bins:
!##   {observable-name}[>{file-name}] [bound0,bound1,bound2,...,boundN]
!##
!## *) conditional binning:
!##    dress a histogram with additional selectors by specifying them inside a block:
!##
!##        HISTOGRAM_SELECTORS
!##         {SELECTOR}
!##             .
!##             .
!##             .
!##        END_HISTOGRAM_SELECTORS
!##
!##    where {SELECTOR} follows the same syntax described above. A binning into
!##    this histogram is then only performed when the event passes all selectors
!##    specified in this block.
!##
!#####################################
!#
!#  * comments begin with the character `!` and will be excluded from the parser
!#
!#####################################

! Some general jet histograms
 ptj1     nbins = 60    min = 0d0    max = 600d0
 ptj2     nbins = 60    min = 0d0    max = 600d0
 ptj3     nbins = 60    min = 0d0    max = 600d0
 etaj1    nbins = 50    min =-5d0    max = 5d0
 etaj2    nbins = 50    min =-5d0    max = 5d0
 etaj3    nbins = 50    min =-5d0    max = 5d0

 ! DIS histograms with cuts defined for every histogram
 ptavg_12 > ptavg_12_q2_150_200 [7,11,18,30,50]
   HISTOGRAM_SELECTORS
    select  q2  min = 150  max = 200
   END_HISTOGRAM_SELECTORS

 ptavg_12 > ptavg_12_q2_200_270 [7,11,18,30,50]
   HISTOGRAM_SELECTORS
```

```
    select  q2  min = 200  max = 270
   END_HISTOGRAM_SELECTORS

 ptavg_12 > ptavg_12_q2_270_400 [7,11,18,30,50]
   HISTOGRAM_SELECTORS
    select  q2  min = 270  max = 400
   END_HISTOGRAM_SELECTORS

 ptavg_12 > ptavg_12_q2_400_700 [7,11,18,30,50]
   HISTOGRAM_SELECTORS
    select  q2  min = 400  max = 700
   END_HISTOGRAM_SELECTORS

 ptavg_12 > ptavg_12_q2_700_5000 [7,11,18,30,50]
   HISTOGRAM_SELECTORS
    select  q2  min = 700  max = 5000
   END_HISTOGRAM_SELECTORS

 ptavg_12 > ptavg_12_q2_5000_15000 [7,11,18,30,50]
   HISTOGRAM_SELECTORS
    select  q2  min = 5000  max = 15000
   END_HISTOGRAM_SELECTORS
END_HISTOGRAMS



SCALES

!####### SYNTAX ######################
!##
!## a) fixed scale:
!##   fixed muF={val_muf} muR={val_mur}
!##
!## b) dynamic scale:
!##   {observable-name} facF={val_facf} facR={val_facr}
!##
!#####################################
!#
!#  * for fixed scales:    facscale = {val_muf},         renscale = {val_mur}
!#
!#  * for dynamic scales:  facscale = {val_facf}*{obs},  renscale = {val_facr}*{obs}
!#
!#  * the observable for dynamic scales must be [GeV] (this is not checked)
```

```
!#
!####################################

 ! dscl = (Q^2+<p_T>^2)/2
 muf = dscl  mur = dscl

END_SCALES



!####### SYNTAX ######################
!##
!## REWEIGHT {observable-name}**{val_power}
!##
!#####################################

! can potentially reweight the cross section here
! REWEIGHT ht_part**4



CHANNELS

!####### SYNTAX ######################
!##
!## list of process id's (see selectchannelXYZ.f)
!##
!#####################################
!#
!#  * any number of whitespace-separated process id's in one line allowed
!#
!#  * self-explaning wild-cards:
!#    - ALL
!#    - LO, NLO, NNLO
!#    - V, R
!#    - VV, RV, RR
!#
!####################################

R
END_CHANNELS
```

References

[1] R. Devenish and A. Cooper-Sarkar, *Deep inelastic scattering*, Oxford University Press (Oxford, 2004).

[2] P. Newman, M. Wing, Rev. Mod. Phys. **86** (2014) 1037 [arXiv:1308.3368].

[3] C. Adloff *et al.* [H1 Collaboration], Eur. Phys. J. C **19** (2001) 289 [hep-ex/0010054].

[4] C. Adloff *et al.* [H1 Collaboration], Phys. Lett. B **542** (2002) 193 [hep-ex/0206029].

[5] A. Aktas *et al.* [H1 Collaboration], Eur. Phys. J. C **33** (2004) 477 [hep-ex/0310019].

[6] A. Aktas *et al.* [H1 Collaboration], Phys. Lett. B **653** (2007) 134 [arXiv:0706.3722].

[7] F. D. Aaron *et al.* [H1 Collaboration], Eur. Phys. J. C **65** (2010) 363 [arXiv:0904.3870].

[8] V. Andreev *et al.* [H1 Collaboration], Eur. Phys. J. C **75** (2015) 65 [arXiv:1406.4709].

[9] V. Andreev *et al.* [H1 Collaboration], [arXiv:1611.03421].

[10] J. Breitweg *et al.* [ZEUS Collaboration], Phys. Lett. B **507** (2001) 70 [hep-ex/0102042].

[11] S. Chekanov *et al.* [ZEUS Collaboration], Phys. Lett. B **547** (2002) 164 [hep-ex/0208037]; Eur. Phys. J. C **44** (2005) 183 [hep-ex/0502007].

[12] S. Chekanov *et al.* [ZEUS Collaboration], Nucl. Phys. B **765** (2007) 1 [hep-ex/0608048].

[13] S. Chekanov *et al.* [ZEUS Collaboration], Phys. Lett. B **649** (2007) 12 [hep-ex/0701039]; H. Abramowicz *et al.* [ZEUS Collaboration], Phys. Lett. B **691** (2010) 127 [arXiv:1003.2923].

[14] H. Abramowicz *et al.* [ZEUS Collaboration], Eur. Phys. J. C **70** (2010) 965 [arXiv:1010.6167].

[15] D. Graudenz, Phys. Rev. D **49** (1994) 3291 [hep-ph/9307311]; hep-ph/9710244.

[16] E. Mirkes and D. Zeppenfeld, Phys. Lett. B **380** (1996) 205 [hep-ph/9511448].

[17] M. Klasen, G. Kramer and B. Pötter, Eur. Phys. J. C **1** (1998) 261 [hep-ph/9703302]; B. Pötter, Comput. Phys. Commun. **119** (1999) 45 [hep-ph/9806437].

[18] Z. Nagy and Z. Trocsanyi, Phys. Rev. Lett. **87** (2001) 082001 [hep-ph/0104315].

[19] V. Andreev *et al.* [H1 Collaboration], JHEP **1505** (2015) 056 [arXiv:1502.01683].

[20] V. Andreev *et al.* [H1 Collaboration], JHEP **1503** (2015) 092 [arXiv:1412.0928].

[21] F. D. Aaron *et al.* [H1 Collaboration], Eur. Phys. J. C **72** (2012) 1970 [arXiv:1111.0584].

[22] F. D. Aaron *et al.*, Eur. Phys. J. C **71** (2011) 1578 [arXiv:1010.1476].

[23] A. Aktas *et al.* [H1 Collaboration], JHEP **0710** (2007) 042 [arXiv:0708.3217].

[24] S. Chekanov *et al.* [ZEUS Collaboration], Eur. Phys. J. C **52** (2007) 813 [arXiv:0708.1415].

[25] A. Aktas *et al.* [H1 Collaboration], Eur. Phys. J. C **48** (2006) 715 [hep-ex/0606004].

[26] V. Andreev *et al.* [H1 Collaboration], JHEP **1503** (2015) 092 [arXiv:1412.0928].

[27] M. R. Adams *et al.* [E665 Collaboration], Phys. Rev. Lett. **69** (1992) 1026.

[28] M. R. Adams *et al.* [E665 Collaboration], Phys. Rev. Lett. **72** (1994) 466.

[29] A. Heister *et al.* [ALEPH Collaboration], Eur. Phys. J. C **35** (2004) 457.

[30] G. Abbiendi *et al.* [OPAL Collaboration], Eur. Phys. J. C **40** (2005) 287 [hep-ex/0503051].

[31] P. Achard *et al.* [L3 Collaboration], Phys. Rept. **399** (2004) 71 [hep-ex/0406049].

[32] J. Abdallah *et al.* [DELPHI Collaboration], Eur. Phys. J. C **29** (2003) 285 [hep-ex/0307048].

[33] K. Abe *et al.* [SLD Collaboration], Phys. Rev. D **51** (1995) 962 [hep-ex/9501003].

[34] G. Dissertori, I. Knowles and M. Schmelling, "Quantum Chromodynamics," International Series of Monographs on Physics (112).

[35] R.K. Ellis, D.A. Ross and A.E. Terrano, Nucl. Phys. B **178** (1981) 421.

[36] Z. Kunszt and P. Nason, in *Z Physics at LEP 1*, CERN Yellow Report 89-08, Vol. 1, p. 373; W. T. Giele and E.W.N. Glover, Phys. Rev. D **46** (1992) 1980; S. Catani and M. H. Seymour, Phys. Lett. B **378** (1996) 287 [hep-ph/9602277].

[37] L.J. Dixon and A. Signer, Phys. Rev. Lett. **78** (1997) 811 [hep-ph/9609460]; J. Campbell, M.A. Cullen and E.W.N. Glover, Eur. Phys. J. C **9** (1999) 245 [hep-ph/9809429]; Z. Nagy and Z. Trocsanyi, Phys. Rev. Lett. **79** (1997) 3604 [hep-ph/9707309]; S. Weinzierl and D.A. Kosower, Phys. Rev. D **60** (1999) 054028 [hep-ph/9901277].

[38] S. Laporta, Int. J. Mod. Phys. A **15** (2000) 5087 [hep-ph/0102033].

[39] T. Gehrmann and E. Remiddi, Nucl. Phys. B **580** (2000) 485 [hep-ph/9912329].

[40] J. M. Henn, Phys. Rev. Lett. **110** (2013) 251601 [arXiv:1304.1806].

[41] T. Binoth and G. Heinrich, Nucl. Phys. B **693** (2004) 134 [hep-ph/0402265]; C. Anastasiou, K. Melnikov and F. Petriello, Phys. Rev. D **69** (2004) 076010 [hep-ph/0311311].

[42] S. Catani and M. Grazzini, Phys. Rev. Lett. **98** (2007) 222002 [hep-ph/0703012].

[43] A. Gehrmann-De Ridder, T. Gehrmann and E.W.N. Glover, JHEP **0509** (2005) 056 [hep-ph/0505111]; Phys. Lett. B **612** (2005) 49 [hep-ph/0502110]; Phys. Lett. B **612** (2005) 36 [hep-ph/0501291].

[44] J. Currie, E. W. N. Glover and S. Wells, JHEP **1304** (2013) 066 [arXiv:1301.4693].

[45] M. Czakon, Phys. Lett. B **693** (2010) 259 [arXiv:1005.0274]; R. Boughezal, K. Melnikov and F. Petriello, Phys. Rev. D **85** (2012) 034025 [arXiv:1111.7041].

[46] R. Boughezal, C. Focke, X. Liu and F. Petriello, Phys. Rev. Lett. **115** (2015) 062002 [arXiv:1504.02131]; R. Boughezal, X. Liu and F. Petriello, Phys. Rev. D **91** (2015) 094035; [arXiv:1504.02540]; J. Gaunt, M. Stahlhofen, F. J. Tackmann and J. R. Walsh, JHEP **1509** (2015) 058 [arXiv:1505.04794].

[47] G. Somogyi and Z. Trocsanyi, JHEP **0808** (2008) 042 [arXiv:0807.0509]; V. Del Duca, C. Duhr, A. Kardos, G. Somogyi, Z. Ször, Z. Trocsanyi and Z. Tulipant, Phys. Rev. D **94** (2016) 074019 [arXiv:1606.03453].

[48] S. Catani, L. Cieri, G. Ferrera, D. de Florian and M. Grazzini, Phys. Rev. Lett. **103** (2009) 082001 [arXiv:0903.2120].

[49] K. Melnikov and F. Petriello, Phys. Rev. D **74** (2006) 114017 [hep-ph/0609070].

[50] C. Anastasiou, K. Melnikov and F. Petriello, Nucl. Phys. B **724** (2005) 197 [hep-ph/0501130].

[51] M. Grazzini, JHEP **0802** (2008) 043 [arXiv:0801.3232].

[52] A. Gehrmann-De Ridder, T. Gehrmann, E.W.N. Glover and G. Heinrich, JHEP **0711** (2007) 058 [arXiv:0710.0346]; Comput. Phys. Commun. **185** (2014) 3331 [arXiv:1402.4140].

[53] S. Weinzierl, JHEP **0906** (2009) 041 [arXiv:0904.1077].

[54] S. Catani, L. Cieri, D. de Florian, G. Ferrera and M. Grazzini, Phys. Rev. Lett. **108** (2012) 072001 [arXiv:1110.2375]; J. M. Campbell, R. K. Ellis, Y. Li and C. Williams, JHEP **1607** (2016) 148 [arXiv:1603.02663].

[55] G. Ferrera, M. Grazzini and F. Tramontano, Phys. Rev. Lett. **107** (2011) 152003 [arXiv:1107.1164].

[56] M. Grazzini, S. Kallweit and D. Rathlev, JHEP **1507** (2015) 085 [arXiv:1504.01330].

[57] M. Czakon, P. Fiedler and A. Mitov, Phys. Rev. Lett. **110** (2013) 252004 [arXiv:1303.6254].

[58] M. Czakon, D. Heymes and A. Mitov, Phys. Rev. Lett. **116** (2016) 082003 [arXiv:1511.00549].

[59] R. Boughezal, F. Caola, K. Melnikov, F. Petriello and M. Schulze, Phys. Rev. Lett. **115** (2015) 082003 [arXiv:1504.07922]; F. Caola, K. Melnikov and M. Schulze, Phys. Rev. D **92** (2015) 074032 [arXiv:1508.02684].

[60] X. Chen, J. Cruz-Martinez, T. Gehrmann, E. W. N. Glover and M. Jaquier, JHEP **1610** (2016) 066 [arXiv:1607.08817].

[61] R. Boughezal, C. Focke, X. Liu and F. Petriello, Phys. Rev. Lett. **115** (2015) 062002 [arXiv:1504.02131].

[62] A. Gehrmann-De Ridder, T. Gehrmann, E. W. N. Glover, A. Huss and T. A. Morgan, Phys. Rev. Lett. **117** (2016) 022001 [arXiv:1507.02850]; JHEP **1607** (2016) 133 [arXiv:1605.04295]; JHEP **1611** (2016) 094 [arXiv:1610.01843].

[63] R. Boughezal, J. M. Campbell, R. K. Ellis, C. Focke, W. T. Giele, X. Liu and F. Petriello, Phys. Rev. Lett. **116** (2016) 152001 [arXiv:1512.01291].

[64] J. M. Campbell, R. K. Ellis and C. Williams, [arXiv:1612.04333].

[65] F. Cascioli *et al.*, Phys. Lett. B **735** (2014) 311 [arXiv:1405.2219]; M. Grazzini, S. Kallweit and D. Rathlev, Phys. Lett. B **750** (2015) 407 [arXiv:1507.06257].

[66] T. Gehrmann, M. Grazzini, S. Kallweit, P. Maierher, A. von Manteuffel, S. Pozzorini, D. Rathlev and L. Tancredi, Phys. Rev. Lett. **113** (2014) 212001 [arXiv:1408.5243]; M. Grazzini, S. Kallweit, S. Pozzorini, D. Rathlev and M. Wiesemann, JHEP **1608** (2016) 140 [arXiv:1605.02716].

[67] M. Grazzini, S. Kallweit, D. Rathlev and M. Wiesemann, Phys. Lett. B **761** (2016) 179 [arXiv:1604.08576].

[68] G. Abelof, R. Boughezal, X. Liu and F. Petriello, Phys. Lett. B **763** (2016) 52 [arXiv:1607.04921].

[69] J. Currie, E. W. N. Glover and J. Pires, Phys. Rev. Lett. **118** (2017) 072002 [arXiv:1611.01460]; J. Currie, A. Gehrmann-De Ridder, T. Gehrmann, E. W. N. Glover, A. Huss and J. Pires, [arXiv:1705.10271].

[70] R. Boughezal, J. M. Campbell, R. K. Ellis, C. Focke, W. Giele, X. Liu, F. Petriello and C. Williams, Eur. Phys. J. C **77** (2017) 7 [arXiv:1605.08011].

[71] J. Currie, T. Gehrmann, A. Huss and J. Niehues, [arXiv:1703.05977].

[72] M. Cacciari, F. A. Dreyer, A. Karlberg, G. P. Salam and G. Zanderighi, Phys. Rev. Lett. **115** (2015) no.8, 082002 [arXiv:1506.02660].

[73] S. Moch, J. A. M. Vermaseren and A. Vogt, Nucl. Phys. B **688** (2004) 101 [hep-ph/0403192].

[74] A. Vogt, S. Moch and J. A. M. Vermaseren, Nucl. Phys. B **691** (2004) 129 [hep-ph/0404111].

[75] L. D. Faddeev and V. N. Popov, Phys. Lett. **25B** (1967) 29.

[76] C. Becchi, A. Rouet and R. Stora, Annals Phys. **98** (1976) 287. I. V. Tyutin, [arXiv:0812.0580].

[77] S. Weinberg, "The quantum theory of fields. Vol. 2: Modern applications,"

[78] R. K. Ellis, W. J. Stirling and B. R. Webber, Camb. Monogr. Part. Phys. Nucl. Phys. Cosmol. **8** (1996) 1.

[79] G. 't Hooft and M. J. G. Veltman, Nucl. Phys. B **44** (1972) 189.

[80] C. Gnendiger, A. Signer and A. Visconti, JHEP **1610** (2016) 034 [arXiv:1607.08241]. C. Gnendiger *et al.*, Eur. Phys. J. C **77** (2017) no.7, 471 [arXiv:1705.01827].

[81] T. Muta, Foundations of Quantum Chromodynamics World Scientific Publishing (1998).

[82] J. E. Huth *et al.*, In *Snowmass 1990, Proceedings, Research directions for the decade* 134-136 and Fermilab Batavia - FERMILAB-Conf-90-249 (90/12,rec.Mar.91) 6 p. (105313).

[83] G. P. Salam, Eur. Phys. J. C **67** (2010) 637 [arXiv:0906.1833].

[84] M. E. Peskin and D. V. Schroeder, "An Introduction to quantum field theory," Reading, USA: Addison-Wesley (1995) 842 p.

[85] H. Lehmann, K. Symanzik and W. Zimmermann, Nuovo Cimento **1**, (1955). 3.

[86] J. R. Currie, "Antenna Subtraction for NNLO Calculations at the LHC," Thesis.

[87] A. Gehrmann-De Ridder, T. Gehrmann, E. W. N. Glover and G. Heinrich, JHEP **0711** (2007) 058 [arXiv:0710.0346].

[88] R. K. Ellis, G. Marchesini and B. R. Webber, Nucl. Phys. B **286** (1987) 643 Erratum: [Nucl. Phys. B **294** (1987) 1180].

[89] G. Altarelli and G. Parisi, Nucl. Phys. B **126** (1977) 298.

[90] S. Catani and M. Grazzini, Nucl. Phys. B **570** (2000) 287 [hep-ph/9908523].

[91] J. M. Campbell and E. W. N. Glover, Nucl. Phys. B **527** (1998) 264 [hep-ph/9710255].

[92] A. Gehrmann-De Ridder, T. Gehrmann and E. W. N. Glover, JHEP **0509** (2005) 056 [hep-ph/0505111].

[93] F. A. Berends and W. T. Giele, Nucl. Phys. B **313** (1989) 595.

[94] Z. Bern, V. Del Duca and C. R. Schmidt, Phys. Lett. B **445** (1998) 168 [hep-ph/9810409].

[95] Z. Bern, V. Del Duca, W. B. Kilgore and C. R. Schmidt, Phys. Rev. D **60** (1999) 116001 [hep-ph/9903516].

[96] Z. Bern, L. J. Dixon, D. C. Dunbar and D. A. Kosower, Nucl. Phys. B **425**, 217 (1994) [hep-ph/9403226].

[97] S. Catani, Phys. Lett. B **427** (1998) 161 [hep-ph/9802439].

[98] J. Currie, E. W. N. Glover and S. Wells, JHEP **1304** (2013) 066 [arXiv:1301.4693].

[99] V. N. Gribov and L. N. Lipatov, Sov. J. Nucl. Phys. **15**, 438 (1972) [Yad. Fiz. **15**, 781 (1972)]; Yu. L. Dokshitzer Sov. Phys. JETP **46**, 641 (1972).

[100] R. E. Cutkosky, J. Math. Phys. **1** (1960) 429.

[101] T. Kinoshita, J. Math. Phys. **3** (1962) 650.

[102] T. D. Lee and M. Nauenberg, Phys. Rev. **133** (1964) B1549.

[103] E. B. Zijlstra and W. L. van Neerven, Nucl. Phys. B **383** (1992) 525.

[104] S. Alekhin, J. Blmlein, S. Moch and R. Placakyte, Phys. Rev. D **96** (2017) no.1, 014011 [arXiv:1701.05838].

[105] S. Dulat *et al.*, Phys. Rev. D **93** (2016) no.3, 033006 [arXiv:1506.07443].

[106] R. D. Ball *et al.* [NNPDF Collaboration], [arXiv:1706.00428].

[107] L. A. Harland-Lang, A. D. Martin, P. Motylinski and R. S. Thorne, Eur. Phys. J. C **75** (2015) no.5, 204 [arXiv:1412.3989].

[108] H. Abramowicz *et al.* [H1 and ZEUS Collaborations], Eur. Phys. J. C **75** (2015) no.12, 580 [arXiv:1506.06042].

[109] J. Butterworth *et al.*, J. Phys. G **43** (2016) 023001 [arXiv:1510.03865].

[110] J. C. Collins and D. E. Soper, Ann. Rev. Nucl. Part. Sci. **37** (1987) 383.

[111] G. Altarelli, Phys. Rept. **81** (1982) 1.

[112] S. Frixione, Z. Kunszt and A. Signer, Nucl. Phys. B **467** (1996) 399 [hep-ph/9512328].

[113] K. Fabricius, I. Schmitt, G. Kramer and G. Schierholz, Z. Phys. C **11** (1981) 315.

[114] W. T. Giele and E. W. N. Glover, Phys. Rev. D **46** (1992) 1980.

[115] W. T. Giele, E. W. N. Glover and D. A. Kosower, Nucl. Phys. B **403** (1993) 633 [hep-ph/9302225].

[116] A. Gehrmann-De Ridder and E. W. N. Glover, Nucl. Phys. B **517** (1998) 269 [hep-ph/9707224].

[117] S. Catani and M. H. Seymour, Nucl. Phys. B **485** (1997) 291 Erratum: [Nucl. Phys. B **510** (1998) 503] [hep-ph/9605323].

[118] T. Binoth and G. Heinrich, Nucl. Phys. B **585** (2000) 741 [hep-ph/0004013].

[119] T. Binoth and G. Heinrich, Nucl. Phys. B **680** (2004) 375 [hep-ph/0305234].

[120] T. Binoth and G. Heinrich, Nucl. Phys. B **693** (2004) 134 [hep-ph/0402265].

[121] S. Catani and M. Grazzini, Phys. Rev. Lett. **98** (2007) 222002 [hep-ph/0703012].

[122] J. Gaunt, M. Stahlhofen, F. J. Tackmann and J. R. Walsh, JHEP **1509** (2015) 058 [arXiv:1505.04794].

[123] I. W. Stewart, F. J. Tackmann and W. J. Waalewijn, Phys. Rev. Lett. **105** (2010) 092002 [arXiv:1004.2489].

[124] I. W. Stewart, F. J. Tackmann and W. J. Waalewijn, Phys. Rev. D **81** (2010) 094035 [arXiv:0910.0467].

[125] T. T. Jouttenus, I. W. Stewart, F. J. Tackmann and W. J. Waalewijn, Phys. Rev. D **83** (2011) 114030 [arXiv:1102.4344].

[126] V. Del Duca, C. Duhr, A. Kardos, G. Somogyi and Z. Trocsanyi, Phys. Rev. Lett. **117** (2016) 152004 [arXiv:1603.08927].

[127] A. Gehrmann-De Ridder, T. Gehrmann and E. W. N. Glover, Nucl. Phys. B **691** (2004) 195 [hep-ph/0403057].

[128] A. Gehrmann-De Ridder, T. Gehrmann and E. W. N. Glover, Phys. Lett. B **612** (2005) 36 [hep-ph/0501291].

[129] A. Gehrmann-De Ridder, T. Gehrmann and E. W. N. Glover, Phys. Lett. B **612** (2005) 36 [hep-ph/0501291].

[130] A. Daleo, T. Gehrmann and D. Maitre, JHEP **0704** (2007) 016 [hep-ph/0612257].

[131] A. Gehrmann-De Ridder, T. Gehrmann, E. W. N. Glover and G. Heinrich, JHEP **0711** (2007) 058 [arXiv:0710.0346].

[132] D. A. Kosower, Phys. Rev. D **57** (1998) 5410 [hep-ph/9710213]; D. A. Kosower, Phys. Rev. D **71** (2005) 045016 [hep-ph/0311272].

[133] D. A. Kosower, Phys. Rev. D **67** (2003) 116003 [hep-ph/0212097].

[134] E.W.N. Glover and J. Pires, JHEP **1006** (2010) 096 [arXiv:1003.2824].

[135] X. Chen, "Hadronic Production of Higss Boson in Association with a Jet at Next-to-Next-to-Leading Order," Thesis.

[136] T.A. Morgan, "Precision Z Boson Phenomenology at the LHC," Thesis.

[137] JHEP **1001** (2010) 118 [arXiv:0912.0374].

[138] W. H. Press, S. A. Teukolsky, W. T.Vetterling, B.P.Flannery "Numerical recipes in fortran 77", G. P. Lepage, J. Comput. Phys. **27** (1978) 192.

[139] A. Buckley, J. Ferrando, S. Lloyd, K. Nordstrm, B. Page, M. Rfenacht, M. Schnherr and G. Watt, Eur. Phys. J. C **75** (2015) 132 [arXiv:1412.7420].

[140] K. Hagiwara and D. Zeppenfeld, Nucl. Phys. B **313** (1989) 560; F. A. Berends, W. T. Giele and H. Kuijf, Nucl. Phys. B **321** (1989) 39; N. K. Falck, D. Graudenz and G. Kramer, Nucl. Phys. B **328** (1989) 317.

[141] E. W. N. Glover and D. J. Miller, Phys. Lett. B **396** (1997) 257 [hep-ph/9609474]; Z. Bern, L. J. Dixon, D. A. Kosower and S. Weinzierl, Nucl. Phys. B **489** (1997) 3 [hep-ph/9610370]; J. M. Campbell, E. W. N. Glover and D. J. Miller, Phys. Lett. B **409** (1997) 503 [hep-ph/9706297]; Z. Bern, L. J. Dixon and D. A. Kosower, Nucl. Phys. B **513** (1998) 3 [hep-ph/9708239].

[142] L.W. Garland, T. Gehrmann, E.W.N. Glover, A. Koukoutsakis and E. Remiddi, Nucl. Phys. B **627** (2002) 107 [hep-ph/0112081]; Nucl. Phys. B **642** (2002) 227 [hep-ph/0206067]; T. Gehrmann and L. Tancredi, JHEP **1202** (2012) 004 [arXiv:1112.1531].

[143] T. Gehrmann and E. Remiddi, Nucl. Phys. B **640** (2002) 379 [hep-ph/0207020]; T. Gehrmann and E. W. N. Glover, Phys. Lett. B **676** (2009) 146 [arXiv:0904.2665].

[144] A. Gehrmann-De Ridder, T. Gehrmann, N. Glover, A. Huss and T. A. Morgan, PoS RADCOR **2015** (2016) 075 [arXiv:1601.04569].

[145] M. Derrick *et al.* [ZEUS Collaboration], Phys. Lett. B **363** (1995) 201 [hep-ex/9510001].

[146] I. Abt *et al.* [H1 Collaboration], Z. Phys. C **61** (1994) 59.

[147] T. Gehrmann, E. W. N. Glover, T. Huber, N. Ikizlerli and C. Studerus, JHEP **1006** (2010) 094 [arXiv:1004.3653].

[148] T. Gleisberg, S. Höche, F. Krauss, M. Schönherr, S. Schumann, F. Siegert and J. Winter, JHEP **0902** (2009) 007 [arXiv:0811.4622].

[149] T. Carli, T. Gehrmann and S. Höche, Eur. Phys. J. C **67** (2010) 73 [arXiv:0912.3715].

[150] F. Cascioli, P. Maierhofer and S. Pozzorini, Phys. Rev. Lett. **108** (2012) 111601 [arXiv:1111.5206].

[151] T. Biekötter, M. Klasen and G. Kramer, Phys. Rev. D **92** (2015) 074037 [arXiv:1508.07153].

[152] J. Currie, T. Gehrmann and J. Niehues, Phys. Rev. Lett. **117** (2016) 042001 [arXiv:1606.03991].

[153] J. C. Collins, Phys. Rev. D **57** (1998) 3051 [hep-ph/9709499].

[154] C. Adloff *et al.* [H1 Collaboration], Eur. Phys. J. C **19** (2001) 289 [hep-ex/0010054].

[155] F. D. Aaron *et al.* [H1 Collaboration], Eur. Phys. J. C **67** (2010) 1 [arXiv:0911.5678].

[156] F. Jegerlehner, Nucl. Phys. Proc. Suppl. **181-182** (2008) 135 [arXiv:0807.4206].

[157] I. Antcheva *et al.*, Comput. Phys. Commun. **180** (2009) 2499 [arXiv:1508.07749].

[158] F. James and M. Ross Comput. Phys. Commun. **10** (1975) 343.

[159] W. L. van Neerven and A. Vogt, Nucl. Phys. B **588** (2000) 345 [hep-ph/0006154].

[160] K.H. Streng, T.F. Walsh and P.M. Zerwas, Z. Phys. C **2** (1979) 237; R. D. Peccei and R. Rückl, Nucl. Phys. B **162** (1980) 125; C. Rumpf, G. Kramer and J. Willrodt, Z. Phys. C **7** (1981) 337.

[161] S. Bethke, S. Kluth, C. Pahl and J. Schieck [JADE Collaboration], Eur. Phys. J. C **64** (2009) 351 [arXiv:0810.1389]; C. Pahl, S. Bethke, O. Biebel, S. Kluth and J. Schieck, Eur. Phys. J. C **64** (2009) 533 [arXiv:0904.0786]; J. Schieck *et al.* [JADE Collaboration], Eur. Phys. J. C **73** (2013) 2332 [arXiv:1205.3714]; G. Dissertori, A. Gehrmann-De Ridder, T. Gehrmann, E. W. N. Glover, G. Heinrich, G. Luisoni and H. Stenzel, JHEP **0908** (2009) 036 [arXiv:0906.3436]; G. Dissertori, A. Gehrmann-De Ridder, T. Gehrmann, E. W. N. Glover, G. Heinrich and H. Stenzel, Phys. Rev. Lett. **104** (2010) 072002 [arXiv:0910.4283]; G. Abbiendi *et al.* [OPAL Collaboration], Eur. Phys. J. C **71** (2011) 1733 [arXiv:1101.1470]; T. Gehrmann, M. Jaquier and G. Luisoni, Eur. Phys. J. C **67** (2010) 57 [arXiv:0911.2422]; R. Abbate, M. Fickinger, A. H. Hoang, V. Mateu and I. W. Stewart, Phys. Rev. D **83** (2011) 074021 [arXiv:1006.3080]; Phys. Rev. D **86** (2012) 094002 [arXiv:1204.5746]; A. H. Hoang, D. W. Kolodrubetz, V. Mateu and I. W. Stewart, Phys. Rev. D **91** (2015) 094018 [arXiv:1501.04111]; T. Gehrmann, G. Luisoni and P. F. Monni, Eur. Phys. J. C **73** (2013) 2265 [arXiv:1210.6945]; T. Becher and M. D. Schwartz, JHEP **0807** (2008) 034 [arXiv:0803.0342]; Y. -T. Chien and M. D. Schwartz, JHEP **1008** (2010) 058 [arXiv:1005.1644]; T. Becher and G. Bell, JHEP **1211** (2012) 126 [arXiv:1210.0580]; A. Banfi, H. McAslan, P. F. Monni and G. Zanderighi, Phys. Rev. Lett. **117** (2016) 172001 [arXiv:1607.03111].

[162] A. Gehrmann-De Ridder, T. Gehrmann, E. W. N. Glover and G. Heinrich, JHEP **0711** (2007) 058 [arXiv:0710.0346].

[163] P. Hoyer, P. Osland, H. G. Sander, T. F. Walsh and P. M. Zerwas, Nucl. Phys. B **161** (1979) 349; E. Laermann, K. H. Streng and P. M. Zerwas, Z. Phys. C **3** (1980) 289.

[164] W. Braunschweig *et al.* [TASSO Collaboration], Z. Phys. C **47** (1990) 181.

[165] P. Abreu *et al.* [DELPHI Collaboration], Phys. Lett. B **274** (1992) 498.

[166] B. Adeva *et al.* [L3 Collaboration], Phys. Lett. B **263** (1991) 551.

[167] K. Abe *et al.* [SLD Collaboration], Phys. Rev. D **55** (1997) 2533 [hep-ex/9608016].

[168] G. Marchesini, B. R. Webber, G. Abbiendi, I. G. Knowles, M. H. Seymour and L. Stanco, Comput. Phys. Commun. **67** (1992) 465.

[169] T. Sjostrand, Comput. Phys. Commun. **82** (1994) 74.

[170] J. G. Körner, G. A. Schuler and F. Barreiro, Phys. Lett. B **188** (1987) 272.

[171] W. Bartel *et al.* [JADE Collaboration], Z. Phys. C **33** (1986) 23.

[172] C. Patrignani *et al.* [Particle Data Group], Chin. Phys. C **40** (2016) 100001.

[173] M. Czakon, M. L. Mangano, A. Mitov and J. Rojo, JHEP **1307** (2013) 167 [arXiv:1303.7215].